

THE UNIVERSITY OF HULL

**Development of a Combined DNA and Drug Extraction
Methodology for Forensic Toxicology Application**

being a Thesis submitted for the Degree of Doctor of Philosophy
in the University of Hull

by

Loay M. T. Kashkary

MSc (Jordan University of Science and Technology)

August 2014

Abstract

Biological samples recovered at crime scenes may contain unsuspected and valuable evidence, such as illicit drugs, in addition to nucleic acids. Deoxyribonucleic acid (DNA) analysis provides valuable information to identify a suspect or victim, as well as to exclude an innocent individual as the perpetrator of a crime. Identification of drugs can also be very informative for forensic investigation to determine whether a perpetrator committed a crime under the influence of illicit substances.

In the field of forensic analysis, sample preparation for identifying both DNA and drugs of abuse represents a challenge due to limited sample quantity and only trace levels of target analytes present in the matrices. As a result, an analytical approach has been developed to enable the combined extraction of DNA and four amphetamines (amphetamine [AM], methamphetamine [MA], 3,4-methylenedioxyamphetamine [MDA], and 3,4-methylenedioxymethamphetamine hydrochloride [MDMA]) from a small amount of sample (50 μ l) using a single extraction procedure.

This study has focused on solid-phase extraction (SPE) using inorganic silica-based matrices as sorbents to facilitate such sample processing. The advantages of using inorganic silica-based monoliths are due to the simple fixation of the material in a column or within a microfluidic device, their mechanical stability with organic solvents, the availability of simple surface modifications to enable the desired chemical interaction with the target molecules, and a unique bimodal structure that allows a large surface area with minimum back pressure.

A dual-phase SPE method was developed consisting of silica beads modified with octadecyl groups packed inside a luer lock adapter for amphetamine extraction coupled in series with a silica-based monolith for DNA extraction within a microfluidic system for a fully combined genetic and drug extraction system.

The proposed method was effective for the extraction of the target drugs from a spiked buffer and artificial urine giving an average recovery greater than 70% and 50%, respectively, with high reproducibility ($< 15\%$ RSD). The limits of detection were $0.6 \mu\text{g ml}^{-1}$ for AM and MA, $0.7 \mu\text{g ml}^{-1}$ for MDA, and $0.8 \mu\text{g ml}^{-1}$ for MDMA with linear calibration curves between 0.625 and $20 \mu\text{g ml}^{-1}$. The method was also able to extract DNA from the spiked TE buffer and urine sample with average extraction efficiencies of 36% and 30%, respectively, which were successfully amplified via the polymerase chain reaction (PCR). The proposed method is not only suitable for the combined extraction of DNA and amphetamines from a limited sample size, but also reduces sample handling and potential contamination. This method could, in future, be applied to anti-doping analysis for the detection of doping agents and conducting DNA profiling as evidence to ascertain whether samples belong to the right athletes.

Acknowledgements

My gratitude and praise go to Almighty Allah, for giving me strength, patience and inspiration during every moment in my life.

I am truly and deeply indebted to so many people. Firstly, I would like to express special thanks to my first supervisors, Professor Steve Haswell and Professor Gillian Greenway, for their guidance, support and continuous encouragement during my PhD study. I would also like to thank my second supervisor, Professor Nicole Pamme, for help during my PhD course.

I am very grateful to Dr Kirsty Shaw for her advice and constructive comments on the genetic experimental work throughout this project. My thanks are given also to Dr Steve Clark for microfluidic device manufacture, and Mr Tony Sinclair for production of the monolith SEM images. I would also like to thank all the people in Laboratory F326.

Massive and special thanks to my great mother Khadija and my lovely wife Ayeda, for their continuous support and encouraging words. Also, many thanks and kisses to my children (Alzahraa, Mohammed, Albatool and Mustafa) for the time that I took from them. Thank you very much, and I hope I can make you all proud.

Last but not least, an acknowledgement is extended to the Government of the Kingdom of Saudi Arabia for generous financial support of this work.

Abbreviations

μ SPE	Micro-solid-phase extraction
μ TAS	Micro total analytical system
3SR	Self-sustained sequence replication
AM	Amphetamine
BET	Brunauer-Emmett-Teller
BJH	Barrett-Joyner-Halenda
bp	Base pair
BSA	Bovine serum albumin
C ₁₈	Octadecyl carbon chain
CE	Capillary electrophoresis
CL	Chemiluminescence
CNS	Central nervous system
COC	Cycloolefin copolymer
d	Diameter
D	Diffusion coefficient
DAD	Diode array detector
dATP	Deoxyadenosine triphosphate
dCTP	Deoxycytosine triphosphate
dGTP	Deoxyguanosine triphosphate
DNA	Deoxyribonucleic acid
dNTP	Deoxyribonucleotide triphosphate
dsDNA	Double-stranded DNA
dTTP	Deoxythymidine triphosphate

Abbreviations

EDTA	Ethylenediaminetetraacetic acid
ELISA	Enzyme-linked immunosorbent assays
EMEM	Eagle's minimum essential medium
EOF	Electroosmotic flow
EtBr	Ethidium bromide
ETFE	Ethylene-tetrafluoroethylene
FSS	Forensic Science Service
FT-IR	Fourier transform infrared spectroscopy
GC-MS	Gas chromatography-mass spectrometry
GPTMS	γ - glycidoxypropyltrimethoxysilane
GuHCl	Guanidine hydrochloride
GuSCN	Guanidine thiocyanate
HPLC	High-performance liquid chromatography
HRP	Horseradish peroxidase
IR	Infrared
K	Kelvin
LAMP	Loop-mediated isothermal amplification
LLE	Liquid-liquid extraction
LLOQ	Lower limit of quantification
LOD	Limit of detection
MA	Methamphetamine
MDA	3,4-methylenedioxyamphetamine
MDMA	3,4-methylenedioxymethamphetamine
MES	2-(N-morpholino)ethanesulfonic acid
μm	Micrometre

NASBA	Nucleic acid sequence-based amplification
ng	nanogram
NSB	Non-specific binding
OD	Optical density
PBS	Phosphate buffered saline
PCR	Polymerase chain reaction
PDMS	Polydimethylsiloxane
PEEK	Polyetheretherketone
PEO	Polyethylene oxide
pg	Picogram
PMMA	Polymethyl methacrylate
ppm	Part per million
ProK	Proteinase K
R	Correlation coefficient
R ²	Coefficient of determination
RCA	Rolling circle amplification
R _e	Reynolds number
RFLP	Restriction fragment length polymorphism
RNA	Ribonucleic acid
RSD	Relative standard deviation
SCX	Strong cation-exchanger
SDA	Strand displacement amplification
SDS	Sodium dodecyl sulphate
SEM	Scanning electron microscopy
SGM	Second-Generation Multiplex

SPE	Solid-phase extraction
SPME	Solid-phase micro-extraction
ssDNA	Single-stranded DNA
STR	Short tandem repeat
t	Time
TBE	Tris-borate-EDTA
TE	Tris (hydroxymethyl) aminomethane/ EDTA
TEOS	Tetraethyl orthosilicate
THF	Tetrahydrofuran
TMOS	Tetramethyl orthosilicate
TMSPM	Trimethoxysilyl propylmethacrylate
UNODC	United Nations Office on Drugs and Crime
UV	Ultraviolet
UV-Vis	Ultraviolet-visible spectroscopy
VNTR	Variable number of tandem repeats
WCX	Weak cation-exchanger

Table of Contents

ABSTRACT	II
ACKNOWLEDGEMENTS.....	IV
ABBREVIATIONS	V
TABLE OF CONTENTS.....	IX
LIST OF FIGURES	XIII
LIST OF TABLES	XIX
LIST OF EQUATIONS	XX
1 INTRODUCTION.....	1
1.1 FORENSIC SAMPLE PREPARATION.....	2
1.1.1 <i>Liquid-liquid extraction (LLE)</i>	3
1.1.2 <i>Solid-phase extraction (SPE)</i>	5
1.1.3 <i>SPE mechanisms</i>	7
1.2 SORBENTS IN SPE	10
1.2.1 <i>Silica particles</i>	11
1.2.2 <i>Monolithic materials</i>	13
1.3 MICROFLUIDICS	22
1.3.1 <i>Physical aspects of a microfluidic system</i>	22
1.3.2 <i>On-chip fluid manipulation</i>	25
1.3.3 <i>Microfabrication</i>	27
1.4 DNA ANALYSIS	29
1.4.1 <i>Nomenclature for STR markers</i>	32
1.4.2 <i>DNA structure</i>	32
1.4.3 <i>Conventional DNA sample preparation</i>	34

1.4.4	<i>Cell lysis</i>	34
1.4.5	<i>DNA purification</i>	36
1.4.6	<i>DNA quantification</i>	39
1.4.7	<i>DNA amplification</i>	41
1.4.8	<i>Separation and detection of PCR products</i>	46
1.4.9	<i>Miniaturised solid-phase DNA extraction</i>	46
1.5	ANALYSIS OF DRUGS OF ABUSE	54
1.5.1	<i>Screening test for amphetamine analysis</i>	56
1.5.2	<i>Extraction of amphetamines</i>	58
1.6	AIMS OF THE PHD PROJECT	64
2	METHODOLOGY	66
2.1	CHEMICALS	66
2.2	INSTRUMENTATION AND MATERIALS	68
2.3	MICROFLUIDIC CHIP FABRICATION	69
2.3.1	<i>Microfluidic chip design</i>	71
2.4	DNA ANALYSIS	72
2.4.1	<i>DNA sources and preparation</i>	72
2.4.2	<i>Microfluidic chip-based solid-phase extraction</i>	73
2.4.3	<i>DNA extraction protocol</i>	75
2.4.4	<i>DNA quantification</i>	76
2.4.5	<i>DNA amplification</i>	78
2.4.6	<i>Agarose gel electrophoresis</i>	79
2.5	DRUGS ANALYSIS	81
2.5.1	<i>Modification of the silica monolith surface</i>	81
2.5.2	<i>Preparation of standard solutions of drugs</i>	83
2.5.3	<i>Solid-phase extraction of the drugs of interest</i>	84
2.5.4	<i>Method developed for drug analysis</i>	85
2.5.5	<i>Figures of merit</i>	86

3	RESULTS AND DISCUSSION: DNA SOLID-PHASE EXTRACTION	89
3.1	PHYSICAL CHARACTERISATION OF THE SILICA-BASED MONOLITH	89
3.2	SOLID-PHASE EXTRACTION	96
3.2.1	<i>Optimal extraction conditions</i>	96
3.2.2	<i>Breakthrough curve</i>	98
3.2.3	<i>Figures of merit for the DNA analysis</i>	100
3.2.4	<i>Cell lysis</i>	101
3.2.5	<i>Extraction of mouse DNA</i>	102
3.3	DNA AMPLIFICATION	106
3.4	EFFECT OF MIXED DNA	111
3.5	NEW MICROFLUIDIC DEVICE DESIGNED FOR DNA ANALYSIS	115
3.6	SUMMARY	117
4	RESULTS AND DISCUSSION: COMBINED DNA AND DRUGS EXTRACTION.....	119
4.1	HPLC METHOD DEVELOPMENT.....	120
4.1.1	<i>UV detection wavelength</i>	120
4.1.2	<i>Optimum mobile phase combination</i>	121
4.2	INVESTIGATION OF MONOLITHIC SILICA FOR DRUGS EXTRACTION	125
4.2.1	<i>Drugs extraction using thermally activated monoliths</i>	125
4.2.2	<i>Chemical modification of silica monolith surface with lysine</i>	127
4.2.3	<i>DNA extraction using lysine-bonded monoliths</i>	133
4.2.4	<i>Drugs extraction using lysine-bonded monoliths</i>	138
4.2.5	<i>Chemical modification of silica bead surfaces with C₁₈</i>	143
4.3	COMBINED DNA AND DRUG EXTRACTION	159
4.4	SUMMARY	166
5	CONCLUSIONS	169
5.1	DNA EXTRACTION	170

5.2	DRUGS EXTRACTION	171
5.3	COMBINED DNA AND DRUGS EXTRACTION.....	172
6	FURTHER WORK.....	173
7	REFERENCES.....	174
8	PUBLICATIONS AND PRESENTATIONS.....	199
8.1	JOURNAL ARTICLES.....	199
8.2	ORAL PRESENTATIONS	199
8.3	POSTER PRESENTATIONS	199

List of Figures

Figure 1-1: The main steps of the liquid-liquid extraction (LLE) procedure.....	4
Figure 1-2: Schematic depicting the essential steps for solid-phase extraction	7
Figure 1-3: Interaction between a polar unbounded sorbent (silica) and a polar analyte (phenylamine) via hydrogen bonding (red dotted line).	8
Figure 1-4: Interactions between non-polar analytes and non-polar bonded silica sorbents via van der Waals forces.....	9
Figure 1-5: Ion-exchange interactions: (A) strong cation-exchange sorbent and (B) strong anion-exchange sorbent.....	10
Figure 1-6: Schematic showing the siloxane bridges on the surface of amorphous silica and the three types of silanol groups present on the surface of silica.....	12
Figure 1-7: Scanning electron micrograph of a polymeric (methacrylate) monolith showing macropore (red circle).....	14
Figure 1-8: SEM micrograph showing A) the typical porous structure of a silica-based monolith, B) the macropores or through-pores, and C) the mesoporous structure of the silica skeleton.....	16
Figure 1-9: Scanning electron micrograph of silica rods possessing structures prepared by the sol-gel method. The bar represents 10 μm	17
Figure 1-10: Schematic representation of hydrolysis and condensation reactions of a monomer compound involved in the sol-gel process	18
Figure 1-11: SEM micrograph of the porous structure of a silica xerogel column. The bar represents 1 μm	200
Figure 1-12: A photograph of commercially available monolithic silica gel pipette tips and a spin column showing the optimal sample volume and method of extraction.....	21
Figure 1-13: Diagram showing A) random, turbulent flow and B) well-defined laminar flow.....	24
Figure 1-14: Schematic showing A) a pressure flow profile with fast solution movements in the centre of a channel compared to B) the plug flow profile where the same velocity is exhibited for all molecules except for those very close to the internal surface wall when an electrical field is applied.....	26
Figure 1-15: Example of the allelic ladder using the AmpF/STR [®] SGM Plus [™] kit with all possible alleles for accurate genotyping.....	31
Figure 1-16: Schematic showing the basic components of DNA.....	33
Figure 1-17: Structure of PicoGreen [®]	40
Figure 1-18: Schematic of the PCR principle.....	42

Figure 1-19: Schematic description of the RCA process in which a circular DNA template is continuously amplified to produce long multimeric DNA sequences that can be cleaved into monomer-length oligonucleotides.....	45
Figure 1-20: Different silica materials within microfluidic device chambers: (A) silica beads, (B) silica beads at 10× magnification, (C) silica-based monolith using sol-gel, (D) two-step silica beads and sol-gel, and (E) two-step silica beads and sol-gel at 10× magnification.....	48
Figure 1-21: Dye-filled dual-phase microdevice for integrated protein capture-DNA extraction from 10 µl of human whole blood. The arrows show the direction of flow from stage 1 (green) to stage 2 (red). Chip dimensions: 3 cm (length) x 2.5 cm (width).....	50
Figure 1-22: Amount of DNA recovered from a silica-based monolith during the elution step for samples containing carrier RNA (ratio 10:1, RNA:DNA) and without carrier RNA in comparison with the amount of DNA initially added (<i>error bar</i> = 3).	51
Figure 1-23: A microfluidic extraction chip channel 300 µm in width×100 mm in depth; the diameter of the inlet and outlet holes is 1 mm.....	52
Figure 1-24: Structure of chitosan.....	53
Figure 1-25: Schematic showing the classification of drugs of abuse according to their source.....	55
Figure 1-26: Schematic showing the experimental set-up of the development of a chemiluminescent ELISA technique within a microfluidic environment for the determination of amphetamine in plasma and urine samples. It consists of a syringe pump, microfluidic device, photodiode detector and readout device (Prolight Diagnostics AB, Lund, Sweden). The inset photograph shows the channel configuration of the microfluidic device.....	57
Figure 1-27: Schematic drawing of the extraction stages of methamphetamine using a packed syringe needle with octadecylated monolith	62
Figure 1-28: Schematic diagram showing the procedures for the extraction of amphetamines from urine using a monolithic silica disk in a microtube holder	63
Figure 2-1: Schematic diagram of the process used for the production of glass microfluidic devices using a wet-etching technique.....	70
Figure 2-2: Photograph showing the glass microfluidic device for DNA extraction. The extraction is performed in the hexagonal chamber where the silica monolith is constructed.....	71
Figure 2-3: A) Photograph of the Neubauer improved haemocytometer, B) grid layout of the counting chamber.....	73
Figure 2-4: Photograph showing the hydrodynamic pumping apparatus on the microfluidic device used to perform DNA extraction.....	74
Figure 2-5: Screenshot showing the FLUOstar software and the position of the standards, blank and samples following their positions on a 96-well plate.....	77

Figure 2-6: Quant-iT™ PicoGreen® dsDNA assay calibration curve. The fluorochrome was excited at 480 nm and the fluorescence emission intensity measured at 520 nm using a spectrofluorometer.....	77
Figure 2-7: Photograph showing the components required for gel electrophoresis.....	80
Figure 2-8: Schematic of a female luer lock adaptor from A) a side view, and B) a cross-sectional view showing where the C ₁₈ -modified silica beads were packed.....	83
Figure 2-9: Photograph of the experimental set-up for the extraction of amphetamine, methamphetamine (MA), 3,3-methylenedioxyamphetamine (MDA) and 3,4-methylenedioxymethamphetamine hydrochloride (MDMA) using packed C ₁₈ -modified silica beads.....	85
Figure 3-1: The surface structure of thermally activated potassium silicate monoliths created inside a glass capillary at A) 100 °C, B) 90 °C and C) 80 °C.....	93
Figure 3-2: SEM micrographs of three silica-based monoliths A) to C) prepared at 90 °C. .	95
Figure 3-3: Example of an ideal DNA extraction profile	96
Figure 3-4: Effect of pH and ionic strength on the elution of DNA. Each experiment was carried out in triplicate. Error bars represent the standard deviation (n = 4).	98
Figure 3-5: DNA breakthrough curve providing the continuous loading capacity of 13.72 ng of purified human DNA on a 600 µg monolithic microfluidic device. Error bars shown represent the standard deviation (n = 4).	99
Figure 3-6: Calibration curve of kit DNA standards using PicoGreen® analysed using a FLUOstar Optima Plate Reader over a low concentration range from 2 to 0.0156 ng ml ⁻¹	100
Figure 3-7: Photographs showing the integrity of neuroblastoma cell walls before A) and after B) adding 5 M GuHCl. Bar = 100 µm.	101
Figure 3-8: Average DNA elution profile for DNA extracted from 1,000 mouse cells using a silica-based monolith within a microfluidic device showing binding (1-8), washing (9-15) and elution (16-24) stages (n = 3).	104
Figure 3-9: Graph showing how DNA extraction efficiency is affected by changes in the number of cells. Standard deviations are shown using error bars (n = 3).	105
Figure 3-10: Electropherogram showing PCR products for amplified mouse gene with different MgCl ₂ concentrations.....	109
Figure 3-11: An electropherogram showing successful amplification of the β-actin gene from A) 1,500 and B) 62 mouse cells. Lane 1-8: sequentially eluted samples; (+ve) β-actin positive control; (-ve) negative control.	110
Figure 3-12: Ethidium bromide-stained PCR products amplified from human and mouse DNA after gel electrophoresis.....	113

- Figure 3-13: UV transilluminator image of slab-gel electrophoresis results from DNA eluted from a mixed mouse and human sample using β -actin and D21 S11 gene. Lanes 1-8: sequentially eluted DNA fractions; Lane 9: human positive control; Lane 10: mouse positive control; Lane 11: positive mixed control; and Lane 12: negative control (no DNA).....114
- Figure 3-14: Photograph A) shows the formation of air bubbles and blocked channels with the hexagonal extraction microfluidic device. The problems were solved with the new oval design B). For both microfluidic devices, the access holes in the top plates were 1.5 mm and the base plates were etched to a depth of 100 μm116
- Figure 4-1: Absorption spectra of 20 $\mu\text{g ml}^{-1}$ of AM, MA, MDA and MDMA in highly purified water; 210 nm was selected as λ max for all drugs of interest.121
- Figure 4-2: HPLC chromatograms for the direct injection of 20 $\mu\text{g ml}^{-1}$ of AM, MA, MDA and MDMA showing a non-peak response when A) methanol:water (80:20, v/v) and B) 10 mM sodium acetate:methanol (70:30, v/v, pH 6) mobile solvents were used. Separation was performed on 5 μm Prodigy™ C₁₈ (Phenomenex, 150 x 4.6 mm), under isocratic conditions at a flow rate of 1 ml min⁻¹. UV detection was obtained at 210 nm and injection volume was 20 μl123
- Figure 4-3: Typical chromatogram for a mixed standard of amphetamines (20 ppm) using a 5 μm Prodigy™ C₁₈ (Phenomenex, Torrance, CA, USA) 150 x 4.6 mm column, mobile phase under isocratic conditions: 10% acetonitrile, 90% 50 mM phosphoric acid (pH 4 using triethylamine); a flow rate of 1 ml min⁻¹ with UV detection obtained at 210 nm and the injection volume was 20 μl124
- Figure 4-4: The extraction of ultra-pure water spiked with a 20 $\mu\text{g ml}^{-1}$ mixed drugs standard using a thermally activated monolith. Each experiment was carried out in triplicate.....127
- Figure 4-5: The chemical structure of lysine.....128
- Figure 4-6: Scheme showing the predominant form of an amino acid depending on the pH of the solution.....128
- Figure 4-7: Schematic reaction pathways for the generation of the desired A) epoxy, B) diol and C) lysine monolithic stationary phases129
- Figure 4-8: Electron micrographs showing the silica-based monolith structure (A) before, and (B) after chemical modification of the surface of the monolith with lysine.131
- Figure 4-9: FT-IR spectra of the silica-based monolith (blue spectrum), and the amino-modified silica monolith (red spectrum).....132
- Figure 4-10: Graph showing the average DNA elution profile from 20 ng of purified human DNA using a lysine-bonded silica-based monolith for extraction (n = 3).....134
- Figure 4-11: Agarose gel electropherogram of the PCR products (D21 S11 gene: 223 and 227 bp) from human DNA released from the lysine-modified silica-based monolith.....135
- Figure 4-12: Graph showing DNA extraction efficiency as a function of different elution flow rates.....137

- Figure 4-13: The breakthrough curve provides a loading capacity of 1,042 ng of purified human DNA on a lysine-bonded monolith.....138
- Figure 4-14: HPLC chromatograms of A) a directly injected $20 \mu\text{g ml}^{-1}$ mixed standard of AM, MA, MDA and MDMA and B) loading buffer collected after passing through the lysine-modified silica-based monolith.....140
- Figure 4-15: The effect of phosphate buffer pH on the retention of analytes during the loading stage ($n = 3$).....141
- Figure 4-16: Stationary phase with covalently attached zwitterionic lysine.....142
- Figure 4-17: Schematic representing the chemical reaction between the surface silanol groups on the silica-based monolith and the organosilane compounds, where $R = \text{C}_{18}$144
- Figure 4-18: SEM micrographs of the silica beads A) before and B) after surface modification with octadecyl groups.....144
- Figure 4-19: FT-IR spectra of the silica beads (red spectrum) and the C_{18} -modified silica beads (blue spectrum).....145
- Figure 4-20: Chromatogram of 20 ppm A) directly injected mixed standard of four amphetamines and B) the eluted fraction of the extracted sample using modified C_{18} silica beads. The separation was performed on a $5 \mu\text{m}$ Prodigy™ C_{18} (Phenomenex, Torrance, CA, USA) $150 \times 4.6 \text{ mm}$ column, under isocratic conditions of 10% acetonitrile, 90% 50 mM phosphoric acid mobile phase (at pH 4 using triethylamine) at a flow rate of 1 ml min^{-1} . UV detection was obtained at 210 nm and the injection volume was $20 \mu\text{l}$147
- Figure 4-21: Chromatograms obtained from collected loading solution for the four target amphetamines at flow rates of 100, 50 and $20 \mu\text{l min}^{-1}$ on C_{18} -modified silica beads.....149
- Figure 4-22: Effect of elution flow rate on the extraction recovery of the mixed drugs standard purified with octadecylated silica beads packed inside a female luer lock adaptor.....150
- Figure 4-23: Chromatogram of a directly injected artificial urine sample spiked with four amphetamines and the three collection fractions of the extracted drugs using the C_{18} -modified silica beads. The separation was performed on $5 \mu\text{m}$ Prodigy™ C_{18} ($150 \times 4.6 \text{ mm}$ column), under isocratic conditions of 10% acetonitrile, 90% 50 mM phosphoric acid mobile phase (at pH 4) at a flow rate of 1 ml min^{-1} . UV detection was obtained at 210 nm and the injection volume was $20 \mu\text{l}$151
- Figure 4-24: Calibration curve for the extraction of the mixed amphetamine standard in the range of 0.625 to $20 \mu\text{g ml}^{-1}$ using an HPLC system with UV-visible detection.153
- Figure 4-25: Comparison of chromatograms when 1 ml of $20 \mu\text{g}$ of mixed drugs standard was A) directly injected into the HPLC system and B) extracted using C_{18} -modified silica beads and eluted with a $50 \mu\text{l}$ mobile phase. The HPLC column was a $5 \mu\text{m}$ Prodigy™ C_{18} ($150 \times 4.6 \text{ mm}$); isocratic conditions of 10% acetonitrile:90% 50 mM phosphoric acid mobile phase (pH 4) at a flow rate of 1 ml min^{-1} . UV detection was obtained at 210 nm and the injection volume was $20 \mu\text{l}$158

- Figure 4-26: Photograph of the experimental set-up for combined genetic and drugs extraction. The C₁₈ silica beads were packed inside the luer lock adaptor where the drug extraction takes place. The DNA extraction was carried out within the microfluidic chip device.....159
- Figure 4-27: DNA extraction profile carried out on octadecylated silica beads packed inside a luer lock adaptor.....161
- Figure 4-28: DNA elution profiles of 13 ng of purified DNA extracted from TE buffer (—) and from artificial urine (...) using the tandem silica extraction system (packed C₁₈ silica beads inside a luer lock adaptor and a silica-based monolith within a microfluidic device).....162
- Figure 4-29: UV transilluminator image of slab-gel electrophoresis results from DNA eluted from an artificial urine sample using D21 S11 gene.163
- Figure 4-30: UV chromatogram of 5 µg ml⁻¹ A) directly injected mixed amphetamines standard and B) elution fraction of extracted artificial urine using C₁₈ silica beads after DNA extraction with a silica-based monolith. The chromatographic conditions were: Prodigy™ C₁₈ (150 x 4.6 mm column, 5 µm); isocratic conditions of 10% acetonitrile:90% 50 mM phosphoric acid mobile phase (pH 4); flow rate of 1 ml min⁻¹. UV detection was obtained at 210 nm and the injection volume was 20 µl.164

List of Tables

Table 1.1: Examples of the optimum concentrations required for commonly used reagents in the PCR process.....	43
Table 1.2: Extraction recoveries of methamphetamine (0.5 $\mu\text{g ml}^{-1}$) and amphetamine (0.2 $\mu\text{g ml}^{-1}$) with different pH values using reversed-phase (C_8 and C_{18}), strong cation-exchanger (SCX), and C_8 -SCX mixed-phase sorbents.....	60
Table 2.1: Chemicals, solvents and reagents used.....	66
Table 2.2: Specialised instruments and materials used.....	68
Table 2.3: Primer sequences used in a standard thermal cycler to amplify human Amelogenin, D21 S11 and TH01, and mouse β -actin.....	78
Table 2.4: Concentrations of master mix reagent components.....	78
Table 2.5: Chemical structures of the target drug analytes used in this study.....	84
Table 3.1: DNA extraction efficiencies from different numbers of mouse cells, including relative standard deviation (RSD). ND: not detected (n = 3).	103
Table 3.2: Five different concentrations of magnesium chloride used with the β -actin mouse gene set.....	107
Table 3.3: DNA extraction efficiencies from various levels of mixed DNA, including relative standard deviations (RSDs) (n = 3).....	112
Table 4.1: Recoveries and relative standard deviations (RSDS) for an artificial urine sample spiked with four amphetamines which were then extracted using octadecylated silica beads.....	152
Table 4.2: Analytical figures of merit.....	154
Table 4.3: Intra-day and inter-day recoveries for the drugs of interest and relative standard deviations of the extraction method.....	155
Table 4.4: The average concentrations of 1 ml mixed drugs standard (20 $\mu\text{g ml}^{-1}$) pre-concentrated using C_{18} silica beads and then eluted with various amounts of mobile phase (n = 3).....	156
Table 4.5: The recoveries for the four target amphetamines extracted from TE buffer and artificial urine using octadecylated silica beads in a series silica system (n = 3).	165

List of Equations

Equation 1.1: Reynolds number.....	23
Equation 1.2: Diffusion distance.....	23
Equation 1.3: DNA-silica interaction.....	38
Equation 2.1: Least squares regression.....	87
Equation 2.2: <i>Y</i> -value of limit of detection.....	88
Equation 2.3: Limit of detection.....	88
Equation 2.4: <i>Y</i> -value of the lower limit of quantification.....	88
Equation 2.5: Lower limit of quantification.....	88
Equation 3.1: Reaction scheme for the production of a silica-based monolith.....	91

1 Introduction

Deoxyribonucleic acid (DNA) analysis and the identification of harmful illegal substances are required in many clinical and/or forensic toxicology investigations. Comparison of DNA profiles of suspects or victims (criminal justice samples) with crime scene samples, for example, is considered essential for the inclusion or exclusion of an individual from a criminal case such as sexual assault, burglary, or murder. In addition, toxicology can play a major role in the investigation of the circumstances surrounding forensic and/or clinical cases. For example, sudden or suspicious deaths with no obvious cause may be related to poisoning by harmful substances such as illicit drugs, industrial chemicals, plant poisons, and pollutants. In most forensic cases, the availability of biological samples may be limited in terms of quantity or quality (potentially degraded or contaminated), which can act as an obstacle to DNA analysis and further laboratory investigations where illicit drug identification is required.¹ Sample preparation (including extraction) is, therefore, a crucial step in achieving suitable quantities of target analyte(s) with minimal contamination.

This chapter (chapter one) presents an overview of the literature related to current sample preparation methods which are relevant to this thesis (solid-phase extraction [SPE]) for the extraction of both DNA and the four drugs of interest (four amphetamines). The chemicals, materials, instruments, experimental set-up and methods are detailed in chapter two. The results and discussion are divided into two sections. Section one (chapter three) describes the evaluation of fabricated monolithic materials (silica-based monoliths) within a microscale environment for DNA extraction from decreasing numbers of cells and contaminated samples.

The second section (chapter four) evaluates the use of a chemically modified monolith in the extraction of the drugs of interest (four amphetamines) followed by combined DNA and target drug extraction from a low sample volume. The main findings are then considered in light of the current literature in the conclusion (chapter five). The limitations of the work described in this thesis are reviewed and further research presented in chapter six.

1.1 Forensic Sample Preparation

Biomedical samples and raw materials (such as blood, hair, and plant matter) cannot be directly analysed with most modern analytical instruments, such as chromatography and capillary electrophoresis, due to their complex matrices, the low concentration of target analytes and the presence of potential contaminants that may interfere with the analytical process.^{2, 3} One or more pre-treatment steps are, therefore, required to extract and pre-concentrate the target molecule (s) in addition to removing potential interfering compounds by a process called sample preparation.⁴ This process is very important in the field of forensic analysis, where samples can suffer from low quantity, contamination, or degradation. The pre-treatment stage generally accounts for 80% of total analysis time, can be complicated (involving multiple steps), labour intensive, and time consuming.^{5 6} Accordingly, if possible, sample preparation should be made simple with minimal pre-treatment steps, efficient with high-throughput performance, and show good reproducibility.⁷

The analysis of incorrectly prepared samples is responsible for 30% of total analysis error.⁸ For instance, during some extraction methods, the eluate is evaporated to dryness in order to concentrate the analytes, but this step must be avoided if volatile compounds (such as amphetamines, herbicides and pesticides) need to be detected.^{8,9} Pre-treatment processes depend on the sample and analytes present, and their compatibility with the analytical technique being used. For instance, genetic analysis requires disruption of the cellular membrane to release nucleic acids, and a purification step (extraction) to pre-concentrate the analytes and then remove any contaminants that can interfere with downstream applications.

Extraction is an essential part of any sample preparation technique, and has the specific aim of separating the analyte(s) of interest from a sample matrix using extraction methods based on the chemical and physical properties of the analytes.¹⁰ Liquid-liquid extraction (LLE) and solid-phase extraction (SPE) are the most important and commonly used extraction techniques for various types of forensic samples.^{11,12}

1.1.1 Liquid-liquid extraction (LLE)

Liquid-liquid extraction (LLE), which was developed in the 1950s, is an established sample preparation method in analytical toxicology, particularly for extracting drugs from tissues.¹³⁻¹⁵ The basic principle of LLE is based on the relative solubility of the target analyte between two immiscible phases (the sample as the aqueous phase [polar] and a solvent as the organic phase [non-polar or less polar]) at an appropriate pH at which the analyte is uncharged. For example, amphetamine is a basic drug with a pK_a value of 9.9,¹⁶ therefore the aqueous phase has to be basic to extract

analytes from an aqueous biological fluid into a less polar organic solvent such as ethyl acetate.¹⁷ The LLE procedure is accomplished using a mixing technique at a specific pH for the aqueous phase to increase the solubility of the analyte into the organic layer, so allowing the mixture to separate into two layers (upper and lower) as shown in Figure 1-1. The organic phase (usually the upper layer) is transferred into a clean tube followed by evaporation to dryness, prior to reconstitution for subsequent analysis.¹⁸ The LLE technique is still used in many toxicological laboratories due to its low cost, ease of operation, ability to deal with large volumes, and the possibility of high selectivity towards target analytes with careful selection of the organic solvent.¹⁹ Nevertheless, there are also many disadvantages, such as emulsion formation, a highly manual operation with multiple back extractions (i.e., it is a labour-intensive and time-consuming technique). Potential problems with the use of large volumes of hazardous organic solvents, all of which represent limitations in the use of LLE as a routine extraction procedure, which, in turn, has led to other sample preparation techniques being developed, such as SPE.²⁰⁻²³

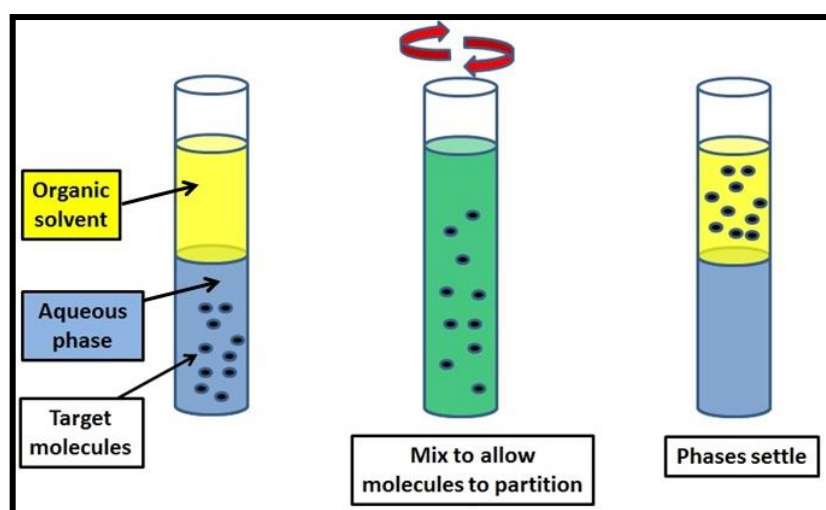


Figure 1-1: The main steps of the liquid-liquid extraction (LLE) procedure.

1.1.2 Solid-phase extraction (SPE)

The concept of SPE had been raised for a long time, but did not become a common scientific technique until 1977 when the Waters Corporation produced disposable cartridges/columns containing bonded silica sorbents.^{24, 25} The term ‘solid-phase extraction’ was first introduced by J.T. Baker[®] Chemical Company employees (Zief *et al.*) in 1982.²⁶ It has become the method of choice for sample preparation in many areas such as clinical, pharmaceutical, environmental, and industrial analysis.²⁷⁻³⁰

The mechanism of SPE is based on the partitioning of analytes between two phases: the liquid phase (the sample that contains the analytes of interest) and the solid-phase (the sorbent).³¹ Purification and pre-concentration are accomplished by adsorption (attraction) of target analytes onto a solid sorbent, followed by a washing step to remove all interfering substances that may affect the analysis of the analytes. Finally, the analytes of interest are eluted (desorbed) from the solid sorbent using a suitable solvent for subsequent analysis.³²

The more common use of SPE in comparison with LLE as a method of extraction is due to a number of inherent advantages, such as low organic solvent consumption, reduction of potential emulsion formation, simplicity, relative speed (fewer steps), better removal of interferents, and good reproducibility.^{33, 34} In addition, SPE can be automated and used for simultaneous extractions of various analytes with different chemical or physical properties.³⁵ There are, however, drawbacks associated with this technique, such as cracks occurring in the SPE structure when allowed to dry during the extraction steps,³⁶ and potential risk of column blockages due to any large particulates in the sample.³⁷

Furthermore, evaporation of the eluate is time consuming due to the use of protic solvents, e.g., methanol, which have low vapour pressure.^{23, 38} Despite these problems, SPE is still used more widely than the LLE pre-treatment technique.¹⁸

1.1.2.1 Solid-phase extraction procedure

The SPE procedure generally consists of a four-step process (see Figure 1-2). Firstly, the solid-phase sorbent is activated using a suitable solvent; for example, polar adsorbents are activated with a non-polar solvent, while non-polar adsorbents can be activated by a polar solvent as this enables solvation of the sorbent functional groups, removal of any impurities present in the sorbent and any air in the void spaces.³⁹ The sorbent then equilibrates with solvent that has the same composition as the loading solvent in order to wet the solid-phase and produce a suitable environment to maximise the adsorption of the analytes of interest onto the sorbent phase. It is important to keep the solid sorbent wet before applying the sample; otherwise, the retention of target analytes will be reduced and the extraction recovery will be low.⁴⁰

In the second step, the sample is applied to the solid-phase (a process called loading) by different techniques such as pumping, aspiration, application of a voltage, or gravitational force.⁴¹ The analytes of interest are then retained and concentrated on the sorbent based on intermolecular interchange between the solid-phase surface and the target analytes. This is followed by a washing step, which entails the removal of any substances that may affect the downstream analysis of the target analytes by using solvents with a similar strength to that of the loading step to avoid displacing the analytes.³¹

Finally, the analytes of interest are desorbed from the sorbent by disrupting the intermolecular interaction between the analytes and the solid-phase sorbent with an appropriate solvent, resulting in elution of the target analytes, which are then ready for further analysis such as one based on a chromatographic technique.⁴²

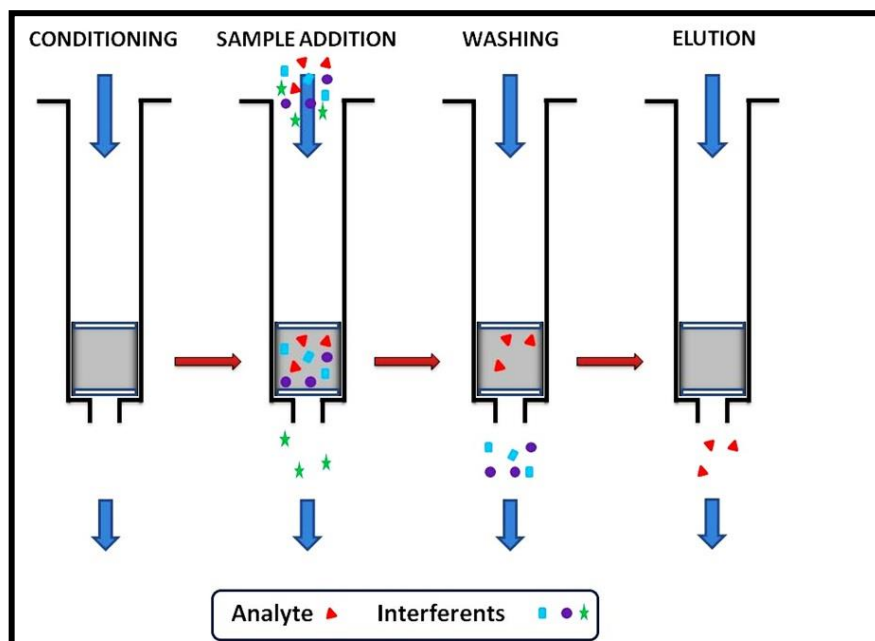


Figure 1-2: Schematic depicting the essential steps for solid-phase extraction.⁴³

1.1.3 SPE mechanisms

There are several mechanisms that are used for the interaction of the analyte of interest with the sorbent in SPE. In general, sorbents are categorised into normal phase, reversed phase, and ion-exchange.²⁰

1.1.3.1 Normal-phase SPE

The solid sorbent (stationary phase) is usually a polar sorbent such as silica (SiO_2), alumina (Al_2O_3), magnesium silicate or Florisil[®] (MgSiO_3), or a silica sorbent chemically modified with polar groups such as amino, cyano or diol groups.

Polar interactions (such as hydrogen bonding, or dipole-dipole interactions) occur between polar groups on the sorbent surface and the polar functional groups of the analyte in a non-polar sample matrix, as shown in Figure 1-3.⁴⁴ Adsorbed analytes are usually desorbed from the solid-phase with a more polar solvent.

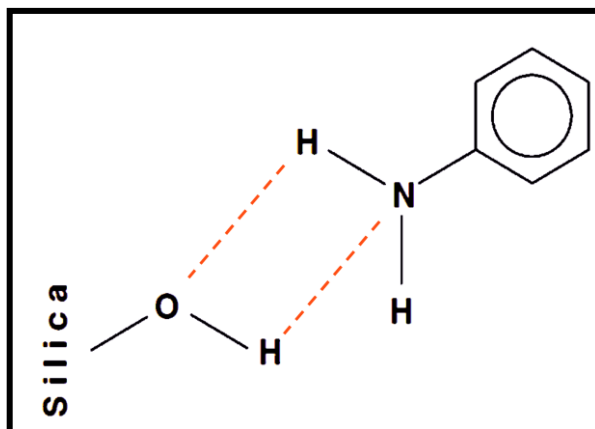


Figure 1-3: Interaction between a polar unbound sorbent (silica) and a polar analyte (phenylamine) via hydrogen bonding (red dotted line).²⁵

1.1.3.2 Reversed-phase SPE

In reversed-phase SPE, the stationary phase has non-polar functional groups (such as octadecyl, octyl, cyclohexyl, phenyl, or butyl) to extract non-polar or moderate polar analytes from a polar sample matrix using van der Waals or dispersion forces (see Figure 1-4).⁴⁴ Non-polar solvents can then disrupt the interaction force between the target analytes and stationary phase, resulting in elution of the adsorbed analytes.

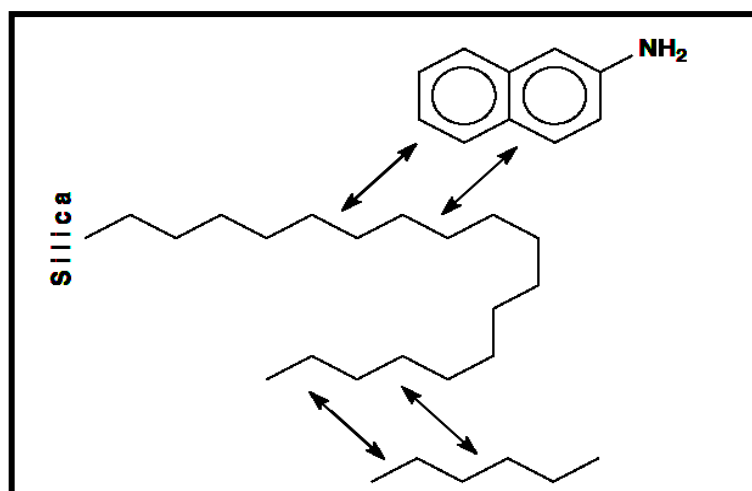


Figure 1-4: Interactions between non-polar analytes and non-polar bonded silica sorbents via van der Waals forces.²⁵

1.1.3.3 Ion-exchange SPE

The surface of the sorbent used for ion-exchange SPE is bonded to ionised functional groups such as an aliphatic quaternary amine group ($-\text{N}^+(\text{CH}_3)_3$) or an aliphatic sulfonic acid ($-\text{SO}_3^-$), or to ionisable functional groups such as primary/secondary amines or carboxylic acids (COOH).²⁵ The ion-exchange mechanism is based on the electrostatic attraction between the charged functional groups on the target analyte and the oppositely charged ion-exchange sorbent, as shown in Figure 1-5. When a negatively charged molecule (anion) exchanges with a sorbent containing a positively charged functional group (e.g., $-\text{N}^+(\text{CH}_3)_3$), the process is called anion exchange. When a positively charged molecule (cation) is present in a sample, a negatively charged functional group (e.g., $-\text{SO}_3^-$) on the solid support attracts the cation in a process known as cation exchange. Desorption of the analyte of interest occurs by either allowing the analyte to be in its neutral form via pH change or by using a solvent with an appropriate ionic strength that contains ions that compete with the target analytes for interaction with the ion-exchange sorbents.⁴⁴

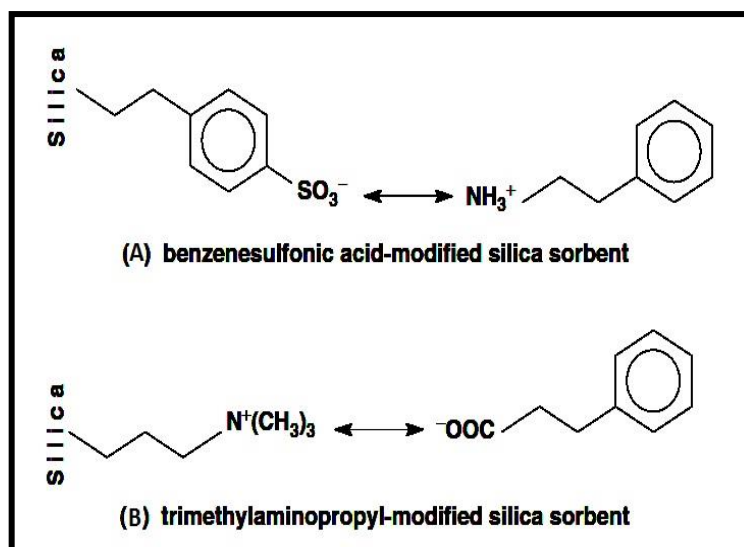


Figure 1-5: Ion-exchange interactions: (A) strong cation-exchange sorbent and (B) strong anion-exchange sorbent.²⁵

1.2 Sorbents in SPE

The selection of SPE sorbents is based upon understanding the mechanism of interaction between the sorbents and the target analytes in the sample matrix, as explained in section 1.1.3. In general, sorbent materials used in SPE need to be reactive towards target analytes for good adsorption and, at the same time, should be reversible for complete elution.⁴⁵ In addition, the solid-phase materials should be thermally and chemically stable and not affected by the sample matrix or solvents used in the extraction process.⁴⁶ Finally, SPE sorbents should have a large surface area for high contact with the analyte(s) of interest and so that their surfaces can be easily modified (chemically) for high selectivity towards target analytes.⁴⁷

The sorbent materials used in SPE are very similar to those employed in high-performance liquid chromatography (HPLC) columns. Historically, calcium carbonate (CaCO_3) was the first sorbent, used by Tswett in 1906 to separate plant pigment using a process he called ‘chromatography’.⁴⁸ In the early 1930s, inorganic-based sorbents (polar sorbents) such as silica, alumina, and Florisil[®] were used to pack chromatographic columns. In 1966, Abel *et al.* introduced non-polar solid stationary phases by chemically modifying silica surfaces with trichlorosilane (HSiCl_3).⁴⁹ Various sorbents were later developed, but the most commonly used material is silica, because it has different structural forms and the surface can be easily modified to increase its selectivity towards target analytes.^{50, 51} Therefore, the focus here is on silica, which can exist in two forms: silica particles (beads) and silica monoliths. The application of silica to extract DNA and drugs of interest will be discussed in later sections.

1.2.1 Silica particles

Silicon dioxide (SiO_2), also known as silica, is an inorganic polymer which is solid, porous and granular and exists naturally in some materials such as quartz or can be synthesised from sodium silicate or silicon tetrachloride.⁵² Silica consists of a network of siloxane backbone bridges ($\equiv\text{Si-O-Si}\equiv$) with silanol groups ($\equiv\text{Si-OH}$) on the surface. The silanol groups exist in three forms: isolated (single hydroxyl groups), geminal (two hydroxyl groups on the same silicon atom), and vicinal (two hydroxyl groups on adjacent silicon atoms), as shown in Figure 1-6.⁵³ These hydroxyl groups can form hydrogen bonds with basic compounds, such as those containing an amino group.

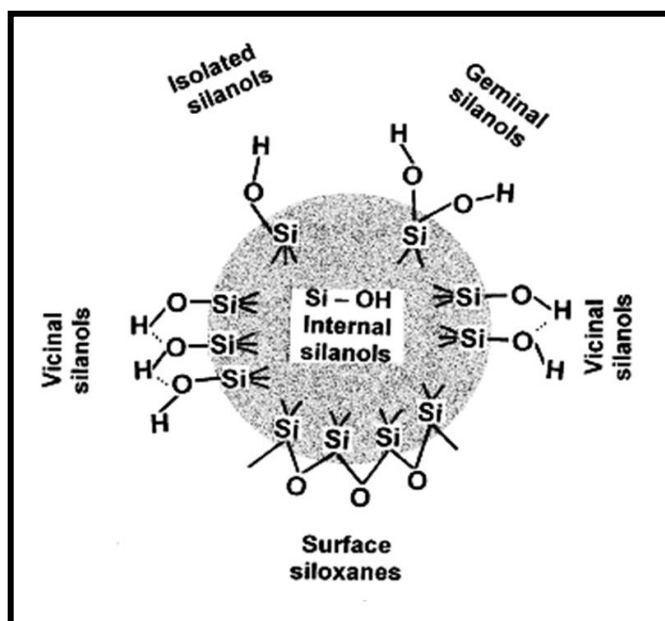


Figure 1-6: Schematic showing the siloxane bridges on the surface of amorphous silica and the three types of silanol groups present on the surface of silica.⁵⁴

By consideration of the pK_a of silanol (from 4.5 to 8.5),⁵⁵ silica is stable over a narrow range of pH values between 2 and 8.⁵⁶ However, silica particles do not swell or shrink when exposed to organic solvents and their surface can be easily modified with a variety of functional groups for appropriate extraction mechanisms (e.g., from hydrophobic to hydrophilic interactions or ion exchange).³¹

The silica particles used in SPE are spherical or irregular in shape (size: 40-60 μm in diameter; pore size 6-12 nm; and an average surface area of 500 $\text{m}^2 \text{g}^{-1}$).^{57, 58} To increase the surface area, a small particle size is required but this can generate high back pressures, particularly in tightly packed devices when a hydrodynamic pump is applied.⁵⁸ To overcome this problem, low flow rates with short diffusion lengths are used.^{59, 60}

1.2.2 Monolithic materials

A new structural material has been developed over the last 25 years to overcome the problem of high back pressures caused by the small silica particles used in packed columns for liquid chromatography (LC) separation. This material is known as a ‘monolith’. In chromatography, the term ‘monolith’ is used to describe a single continuous mass of highly porous material typically created by the *in situ* polymerisation of monomers.⁶¹ Depending on the preparation material, monoliths can be divided into organic polymer-based monoliths and inorganic silica-based monoliths.

In 1989, Hjerten *et al.* prepared, *in situ*, what they called “continuous beds” from poly(acrylic acid-co-methylenebisacrylamide) within an LC column (30 mm long and 6 mm in diameter) for chromatographic separation.⁶² Later, Svec and Frechet in the early 1990s fabricated what was called “continuous polymer rods”, characterised by a large pore size to overcome the back pressure generated by the solvent-swollen acrylic-based material used by Hjerten.⁶³ Several organic polymers have been used for monolithic fabrication, such as methacrylate, polystyrene and acrylamide.⁶⁴ Polymeric materials have several advantages e.g., they are easy to prepare in a single *in situ* polymerisation step, and the desired length and shape of the continuous beds can be achieved by using masks to control exposure to an ultra-violet light source.⁶⁵ In addition, polymeric beds are successfully used for chromatographic separation due to their biocompatibility, and a wide pH range from 1 to 14.^{66, 67}

However, organic polymers have some drawbacks, such as low mechanical strength due to swelling or shrinking with organic solvents.⁶⁸ Therefore, to overcome some of these drawbacks, inorganic silica-based materials were introduced in 1996 by

Nakanishi and Soga in a “porous silica rod” and by Fields as “continuous column support”.^{69, 70} The term ‘monolith’ first emerged in 1993 to describe the cellulose sponge used for protein separation, and later for many other materials such as agarose and cryogels.^{65, 71} Inorganic silica-based monoliths will be described in the following section.

Monoliths can be categorised, depending on their pore size, as microporous (< 2 nm), mesoporous (2-50 nm), or macroporous (> 50 nm).⁷² Organic polymer monoliths contain only macroporous structures (see Figure 1-7), which are effective for the extraction and separation of large molecules such as proteins and nucleic acid, but not recommended for small molecules such as drugs due to poor extraction and separation efficiency.⁷³ In general, extraction of small molecules requires monoliths with pore sizes ranging from 8 to 10 nm (mesopores), whereas macromolecules need pore sizes greater than 50 nm (macropores).⁷⁴

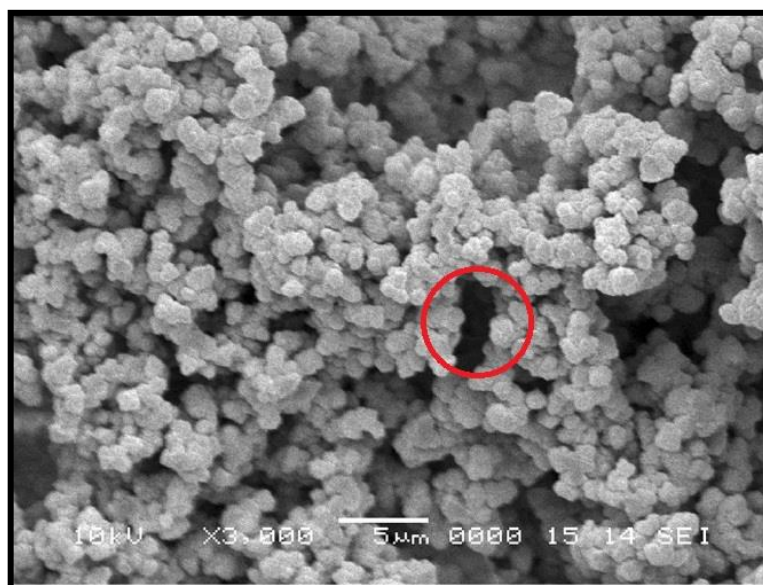


Figure 1-7: Scanning electron micrograph of a polymeric (methacrylate) monolith showing macropore (red circle).⁷⁵

However, the internal structure of inorganic silica-based monoliths is characterised by bimodal pore size distribution consisting of large flow-through pores (macropores) for high permeability and small diffusion pores (mesopores) for the desired high surface area, as shown in Figure 1-8.⁷⁶ The bimodal pore structure of a silica monolith allows for small and large molecules to interact with the internal surface of the monolith through the mesopores and macropores, respectively. In addition, the high surface area of a monolith maximises analyte retention and results in increased extraction efficiency.⁶⁴ The possibility of controlling the size of the macropores (or through-pores) enables the maintenance of the required flow velocity of the mobile phase through the pores, which reduces the column back pressure and increases the mass transfer kinetics.⁷⁷⁻⁷⁹ In respect of the bimodal structure of inorganic silica-based materials and their mechanical stability with organic solvents, the work presented in this study will focus on the solid-phase extraction of a large molecule e.g., DNA and small molecules, such as amphetamines.

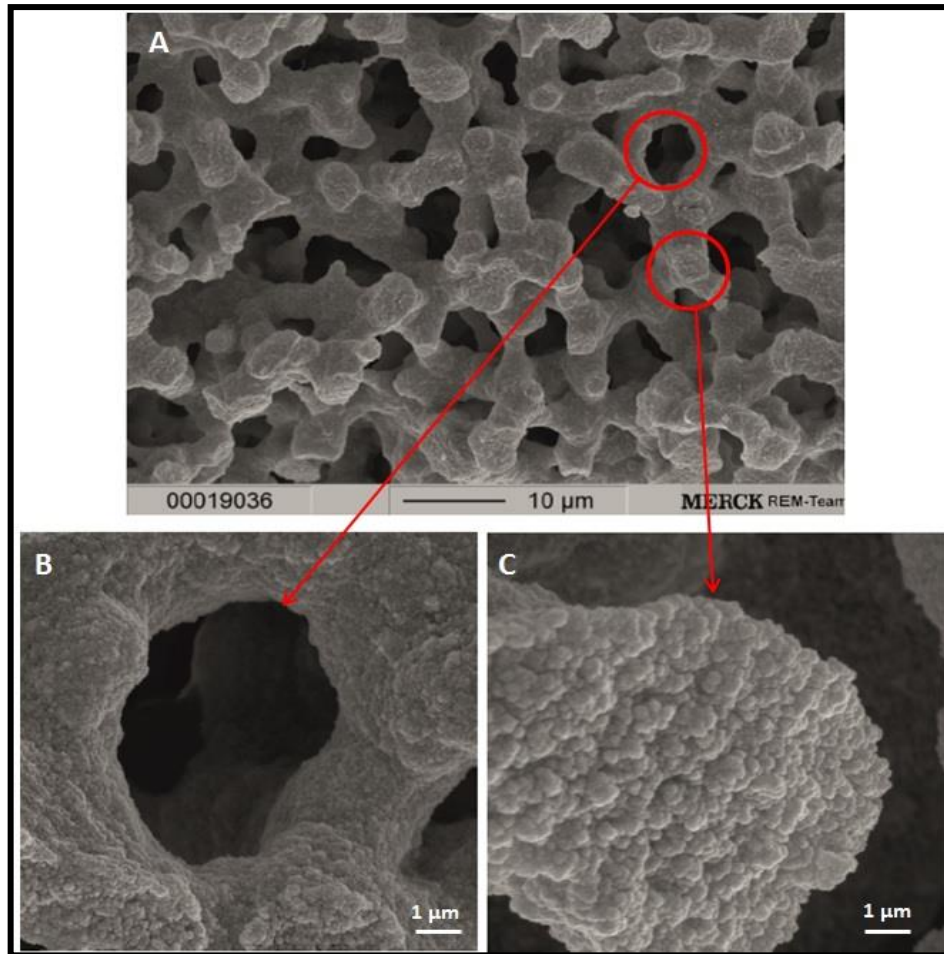


Figure 1-8: SEM micrograph showing A) the typical porous structure of a silica-based monolith, B) the macropores or through-pores, and C) the mesoporous structure of the silica skeleton.⁸⁰

1.2.2.1 Inorganic silica-based monoliths

Two different methods have been used to produce inorganic silica-based monoliths in order to generate a single continuous rigid porous structure. The first method was introduced by Minakuchi *et al.*⁶⁹ to fabricate three-dimensional network structures with a bimodal pore size distribution of mesopores and macropores based on the sol-gel approach reported by Nakanishi *et al.*⁸¹⁻⁸³ Fabrication of a sol-gel monolith by this method showed a homogeneous internal structure with a high purity (Figure 1-9).

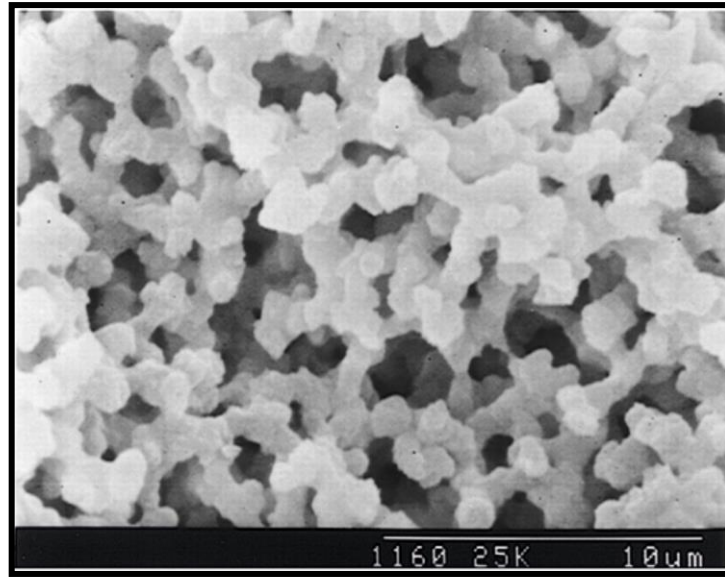


Figure 1-9: Scanning electron micrograph of silica rods possessing structures prepared by the sol-gel method. The bar represents 10 μm .⁶⁹

In the first method, silica gel monoliths are prepared from metal-organic silicon alkoxides by simultaneous hydrolysis and polycondensation in order to convert liquid colloidal suspensions (a sol)⁸⁴ into a wet gel. The most widely used alkoxy silane precursors for sol-gel preparation are: tetramethyl orthosilicate (TMOS, $\text{Si}(\text{OCH}_3)_4$), tetraethyl orthosilicate (TEOS, $\text{Si}(\text{OC}_2\text{H}_5)_4$), and methyltrimethoxysilane (MTMS, $\text{CH}_3\text{Si}(\text{OCH}_3)_3$).^{67, 84} These precursors have an organic group attached to a negatively charged oxygen linked to a metal atom.^{85, 86}

The sol-gel procedure consists of four steps: hydrolysis of precursors (sol formation), polycondensation of hydrolysed precursors (gelation), aging, and drying.^{84, 87} Figure 1-10 shows the schematic reaction pathways involved in the formation of a silica gel monolith. In the first reaction, a liquid alkoxide is catalytically hydrolysed, resulting in the formation of alcohol and highly reactive silanol groups ($\equiv\text{Si}-\text{OH}$), which undergo a subsequent step in a process known as condensation to produce siloxane linkage ($\equiv\text{Si}-\text{O}-\text{Si}\equiv$) and water.⁷⁹

Successive hydrolysis and condensation reactions lead to the growth of cyclic oligomers, which subsequently link together to form a three-dimensional network as a sol-gel polymer, due to polycondensation behaviour.^{88, 89}

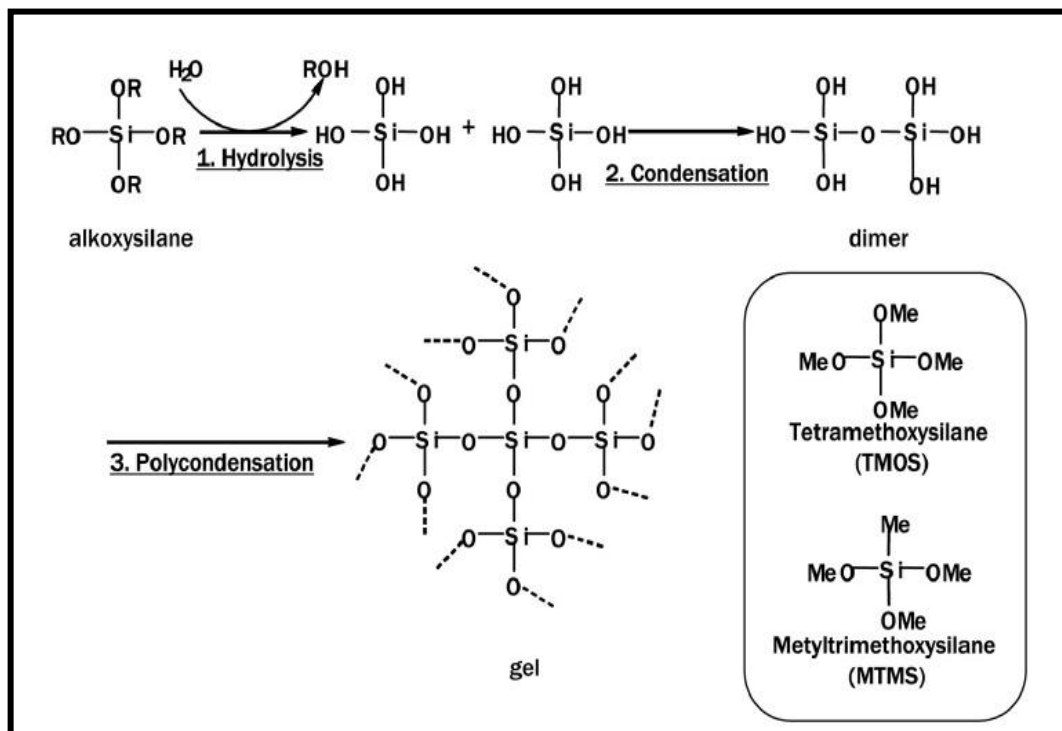


Figure 1-10: Schematic representation of hydrolysis and condensation reactions of a monomer compound involved in the sol-gel process.⁸⁷

A catalyst is required to promote the reaction due to the slow hydrolysis and kinetics of polycondensation. This catalyst can be an acid, such as acetic acid (CH_3COOH) or nitric acid (HNO_3),⁹⁰ or a base, such as N-methylimidazole ($\text{CH}_3\text{C}_3\text{H}_3\text{N}_2$).^{91, 89} Alkoxide precursors are also insoluble in water and, therefore, the presence of a water-soluble polymer such as polyethylene oxide (PEO) is necessary to act as a solubilising agent to form a homogeneous, single-phase aqueous solution.⁶⁷ Additionally, PEO acts as a porogen to form a through-pore template in the silica gel.⁸⁷

The homogeneous solution can be transformed by fabrication into any desired shape during the aging step by placing it in a mould, which allows the formation of a rigid three-dimensional network over a period of days at 40 °C, followed by washing with distilled water and then treatment with ammonium hydroxide solution in order to create the mesopore structure.^{92, 93} Finally, all the solvents and organic material are decomposed by heat treatment at high temperature (550-650 °C).^{94, 95} The major drawback associated with this type of monolith is the multi-step process, which means it is time consuming (five days) and difficult to fabricate a monolith in a reproducible manner.^{96, 97}

The second method for producing inorganic silica-based monoliths was developed in 1996 by Fields. He reported a continuous xerogel silica monolithic column prepared from a potassium silicate solution to analyse polycyclic aromatic hydrocarbons.^{70, 90} A fused silica column (0.32 mm i.d.) was filled with a dispersed solution of 10 w/w of formamide (HCONH₂) in potassium silicate (K₂SiO₃) solution and placed in an oven at 100 °C for 1 hour to allow gelation formation. The column was then washed and dried with helium for 24 hours at 120 °C.

The surface of the fabricated monolith was functionalised with a 10% solution of dimethyloctadecylchlorosilane (ODS) in dried toluene and heated at 70 °C for 5 hours. This early work had a relatively low surface area (62 m² g⁻¹) due to the lack of mesopores on the skeleton structure of the macropores.⁹⁶ In addition, the structural morphology of this monolith was less homogeneous than the sol-gel monolith, which adversely affected the HPLC separation efficiency (see Figure 1-11).^{80, 98-100}

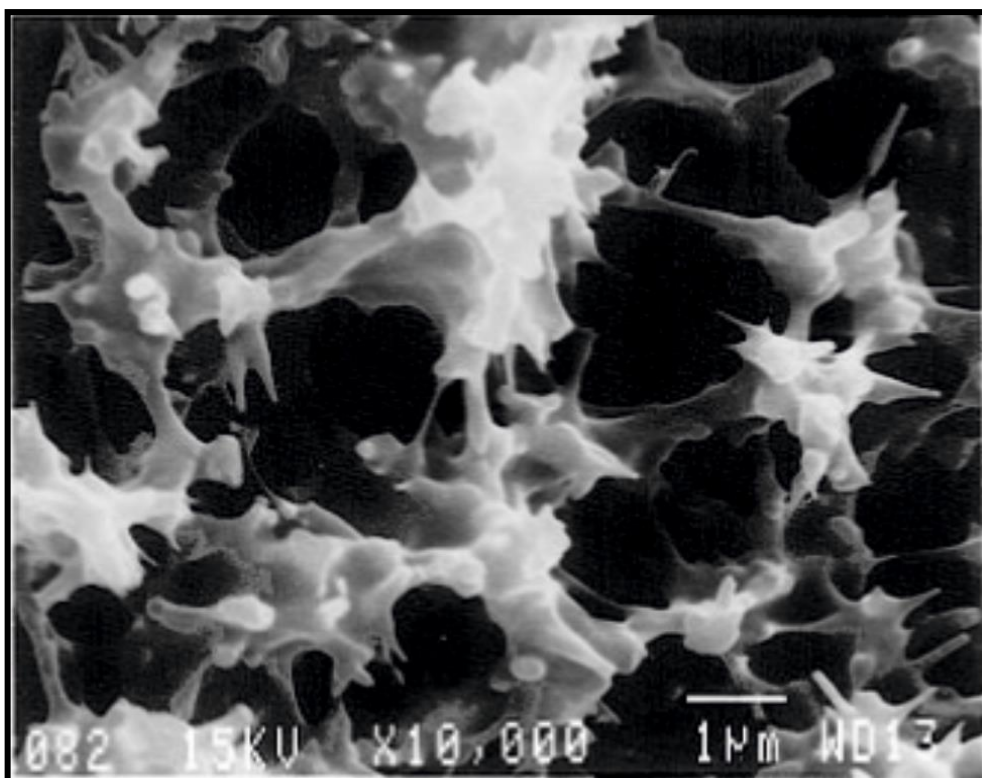


Figure 1-11: SEM micrograph of the porous structure of a silica xerogel column. The bar represents 1 μm .⁷⁰

Despite the above-mentioned problems, the advantages of the simpler preparation of this silica-xerogel monolith within a short time (less than 30 hours)¹⁰¹ with good preparation reproducibility and less observed cracking compared to monoliths generated by the sol-gel process inspired researchers to generate a silica monolith that contains a bimodal pore structure and high surface area using this method.^{51, 96} The analytical group at the University of Hull has been using this type of monolith for the development of micro-reactor technology¹⁰² and for DNA extraction purposes.¹⁰³ The work in this thesis, therefore, continued to use a thermally activated potassium silicate monolith for further investigation.

The surface of this type of monolith can be functionalised with the desired moieties in order to enhance the selectivity of the sorbents for separation or extraction.¹⁰⁴ For example, introducing amino groups or octadecyl moieties produces sorbents with ion-exchange or reversed-phase mechanisms, respectively.¹⁰⁵ Simultaneous extraction of analytes can be performed by using zwitterionic stationary phases or multifunctionalised sorbents.^{106, 107} A silica-based monolith can be fabricated inside cartridges, spin columns,¹⁰⁸ discs,¹⁰⁹ or pipette tips.¹¹⁰ Figure 1-12 shows an example of commercially available SPE formats where each unit has a different sample capacity and exhibits various mechanisms of interaction with the analyte(s) of interest. However, advanced techniques have been developed to miniaturise SPE in an attempt to deal with very limited sample volumes, by introducing solid-phase sorbents inside a microfluidic device using a silica monolith or small-diameter silica particles in the range 50-60 μm .¹¹¹

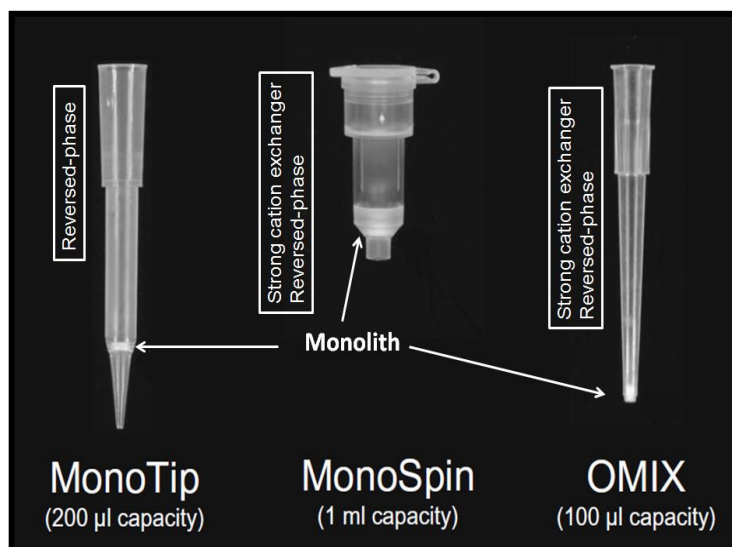


Figure 1-12: A photograph of commercially available monolithic silica gel pipette tips and a spin column showing the optimal sample volume and method of extraction.¹¹²

1.3 Microfluidics

Microfluidics refers to the manipulation of small volumes of fluid (10^{-6} to 10^{-15} L) in a network of channels with micrometer dimensions.^{113, 114} As a result of the numerous advantages associated with microfluidics, it has been applied in many research areas such as chemical and biological analysis, medical diagnostics, and environmental testing.¹¹⁵ The benefits of miniaturising analytical tools include a reduction in sample and reagent consumption, low analytical cost, portability, low risk of sample loss or contamination, and rapid analysis time.^{116, 117} The integration of multiple analytical processes such as sample pre-treatment, separation and detection on a single miniaturised device (a few square centimetres) has led to the concept of a ‘lab-on-a-chip’ or a ‘micro total analytical system’ (μ TAS).¹¹⁸ The μ TAS term was first introduced in the early 1990s by Manz *et al.*¹¹⁹

1.3.1 Physical aspects of a microfluidic system

There are some important features that characterise a microfluidic environment as a result of scaling down the dimensions.¹²⁰ Firstly, the surface-area-to-volume ratio is significantly increased, which can, in some cases, be beneficial (e.g., increasing the surface area for DNA binding)¹²¹ or in others can be detrimental (e.g., inhibition of PCR due to the adsorption of DNA polymerase onto the internal surfaces of the silicon microfluidic device).¹²² Secondly, the transfer time of heat and mass is greatly reduced, which can be a major advantage for biochemical reactions (e.g., PCR).¹²³ Finally, the movement of reagents within the microchannel dimension using electrokinetic (electroosmotic and electrophoretic) or hydrodynamic pumping follows the laminar flow regime, which provides precise spatial and temporal control

of a chemical reaction by allowing the reagents to mix in a controlled region and at a specific time.¹²⁴ Within micron dimension channels, viscous forces acting on the fluid become dominant, whereas inertial forces are diminished.¹²⁵ The Reynolds number (R_e) is a dimensionless number that describes the characteristics of fluid flow as being laminar (well-defined streamlines flowing side-by-side) or turbulent (unstable) based on the ratio of inertial to viscous forces (Equation 1.1):¹²⁶

$$R_e = \frac{\rho \cdot v \cdot d}{\eta} \quad \text{Equation 1.1}$$

Where ρ is the density of the fluid (kg m^{-3}), v is the average velocity of the moving fluid (m s^{-1}), d is the diameter of the channel (m), and η is the viscosity of the fluid (Ns m^{-2}).

At a high Reynolds number ($R_e > 2,000$), inertial forces are dominant and turbulent flow will be observed, whereas at a low Reynolds number ($R_e < 10$) the flow is laminar (reagent streams flow with a smooth and constant motion), as shown in Figure 1-13.¹²⁷ In microfluidic systems where the diameters of the channels are very small, laminar flow should be expected. Consequently, in the presence of a concentration gradient between adjacent parallel laminar streams, molecules are transported across their common interface only by the mechanism of diffusion.¹²⁸ The Einstein-Smoluchowski equation (Equation 1.2)¹²³ can be used to estimate the extent of diffusion of a molecule:

$$x = \sqrt{2Dt} \quad \text{Equation 1.2}$$

Where x is the distance (m) travelled by a diffused molecule, D is the diffusion coefficient ($\text{m}^2 \text{s}^{-1}$), and t is time (s).

Equation 1.2 shows that a rapid diffusion time can be achieved when the diffusion coefficient is large (i.e., with a small molecule). For the same molecular size (the same diffusion coefficient), a reduction in the channel dimensions can also decrease the time required for diffusive mixing. For example, scaling down the channel width from 1 mm to 50 μm significantly reduces the time taken for a water molecule to mix fully by 400 times (from 200 s to 500 ms).¹²⁰

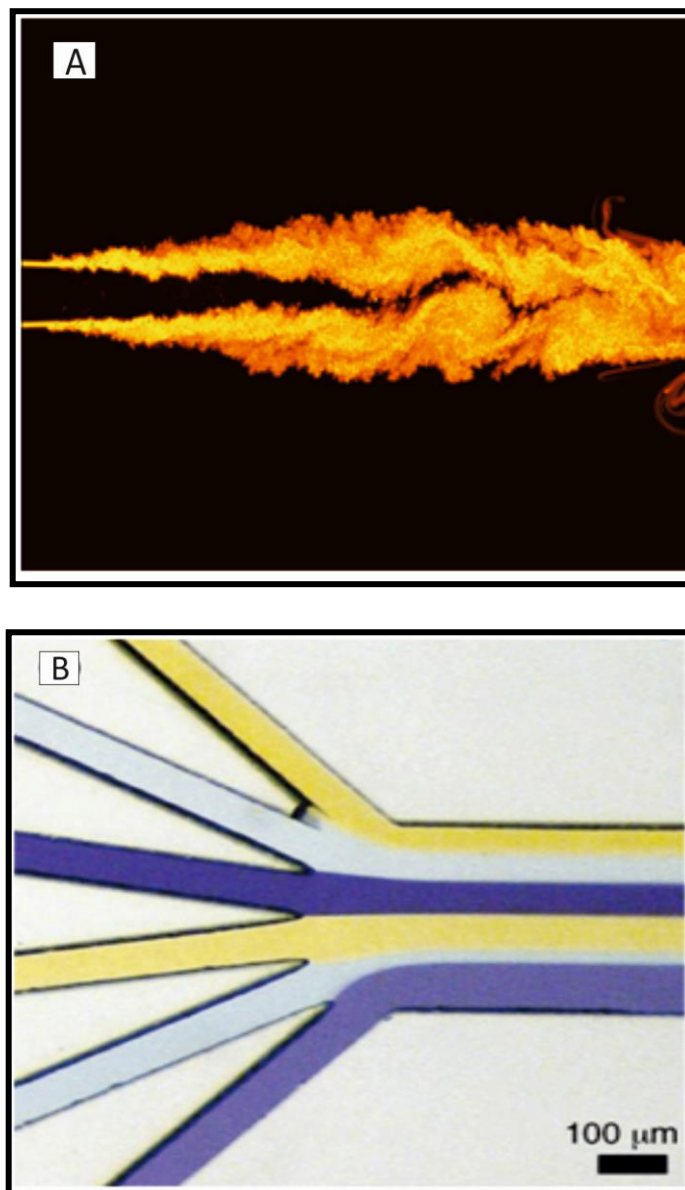


Figure 1-13: Diagram showing A) random, turbulent flow and B) well-defined laminar flow.¹¹³

1.3.2 On-chip fluid manipulation

The two most commonly used methods of generating flow movement within microfluidic chip-based systems are through hydrodynamic and electrokinetic (electroosmotic and/or electrophoretic) forces.^{129, 130} Hydrodynamic flow can be created as the result of off-chip pressure (e.g., syringe pumps connected to a microfluidic device via tubing and connectors) to mobilise aqueous and non-aqueous solutions within a channel network.¹³¹ The flow profile within a channel is parabolic due to frictional forces at the channel walls (Figure 1-14 A). The direction of flow is dependent on the channel geometry and the presence/absence of valves. In comparison, electroosmotic flow (EOF) is a common technique that is characterised by bulk fluid movement in the presence of an applied electrical field. All ions and non-charged species are moved towards the cathode at a different rate, depending on their charge and size.¹³²

Microfluidic devices manufactured from glass or silica have a negatively charged surface at a $\text{pH} > 4$ due to deprotonation of the silanol groups ($\equiv\text{Si-O}^-$). Positive ions in the solution are aligned into a double layer, where an inner layer is formed from cations attracted to the negatively charged internal surface forming the rigid Stern layer. These cations do not completely neutralise the negative charges at the inner surface and, therefore, a diffuse layer is also produced which extends towards the bulk of the solution.¹³³ When an electric current is applied, the cations that form the diffuse layer migrate towards the negative electrode, dragging with them the bulk solution.

The above motion creates a flat flow profile characterised by homogeneous velocity across the width of the channel with slow movement very close to the internal surface wall, as shown in Figure 1-14 B. This technique has the disadvantage of generating a Joule heating that may lead to band broadening and loss of separation resolution. Another disadvantage associated with electrokinetic movement is the generation of gas bubbles in the system as the result of electrolysis at the electrodes, which leads to a break in the flow and electrical heating.¹³⁴ In this study, hydrodynamic force was selected for precise control of the flow rate and to avoid the EOF drawbacks.

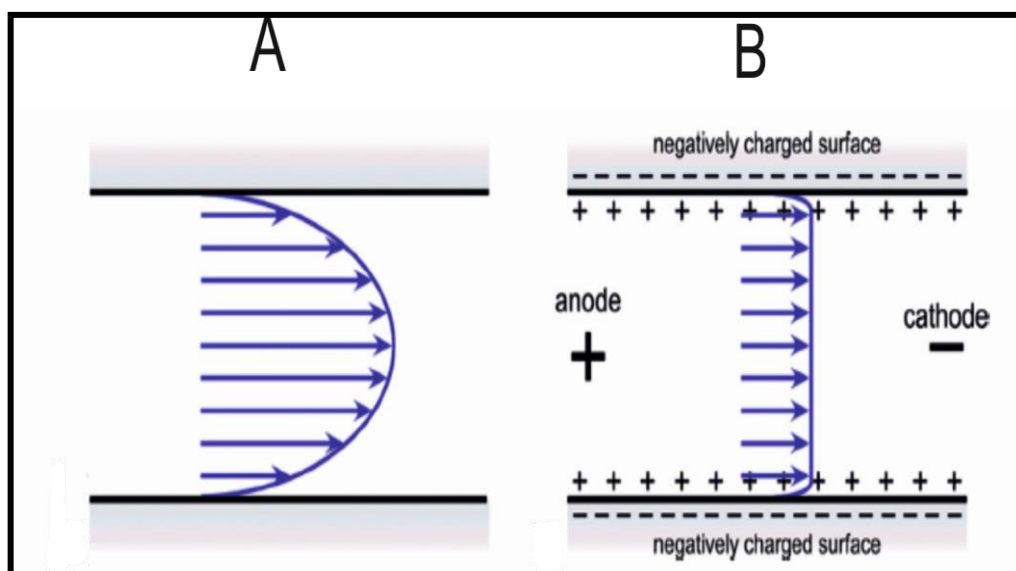


Figure 1-14: Schematic showing A) a pressure flow profile with fast solution movements in the centre of a channel compared to B) the plug flow profile where the same velocity is exhibited for all molecules except for those very close to the internal surface wall when an electrical field is applied.¹³⁵

1.3.3 Microfabrication

A wide range of diverse technologies such as film deposition, patterning, etching, and bonding are required for the fabrication of microfluidic structures. There are many factors to consider when choosing the most appropriate technique for microfluidic device fabrication. These include the availability of fabrication equipment, suitable substrate materials, process costs and time, and reproducibility of the fabrication technique.^{131, 132}

Since microfluidic systems have been applied to a wide range of applications, the properties of the substrate material can be both diverse and important for the success of the application, which has led to a wide variety of substrate materials being developed. The earliest manufactured microfluidic devices were fabricated from either silicon or glass/quartz materials for their good physiochemical properties, as well as easy micromachining.¹³⁶ Silicon has high thermal conductivity, allowing fast temperature ramping which is ideal for performing PCR. However, surface coating is required, for example with polypropylene, prior to use because bare silicon inhibits PCR amplification due to adsorption of DNA polymerase onto the internal surfaces of the microfluidic device.^{122, 137} Silicon substrates are also limited by non-optical transparency and incompatibility with EOF.¹³⁷

In order to overcome the disadvantages of silicon substrates, glass is employed as a substrate material. Glass has good optical transparency, excellent thermal stability, EOF compatibility, and high resistance to many chemical solvents.^{117, 122} Therefore, it has been successfully used as a substrate material for the miniaturisation of PCR and capillary electrophoresis (CE).

However, glass microdevices also have disadvantages, such as a high cost of fabrication and the requirement of a high temperature for binding (650 °C).¹¹⁷ Photolithography with wet etching is a widely used technique for manufacturing glass or silicon chips due to the inexpensive mass production of the devices and availability of the apparatus required for substrate fabrication.¹³²

With advances in the lab-on-a-chip field, new fabrication methods are emerging due to the diversity of the substrate materials that have been used and a requirement for low production costs and fast machining processes. Polymers have been developed as an alternative to silicon and glass substrates due to ease of fabrication, lower cost compared to glass, disposability, biocompatibility and optical transparency.¹²² To date, widely used polymer substrates for microfluidic applications are polydimethylsiloxane (PDMS), polymethyl methacrylate (PMMA), polyetheretherketone (PEEK), and cycloolefin copolymer (COC).^{138, 139} Examples of the most common polymer fabrication techniques include soft lithography with rigid photomasking for PDMS microfluidic devices¹⁴⁰ or an injection moulding method to fabricate microfluidic channels with PMMA material.¹⁴¹

There are, however, problems with using polymers for specific applications. During real-time PCR, for example, PDMS and PMMA generate some background fluorescence when excited with a halogen lamp, which can lead to decreased sensitivity to the target fluorescence to be detected.¹⁴² In addition, the permeable nature of PDMS can lead to loss of samples during PCR thermal cycling.¹⁴³

As no single material can be preferable over others for all microfluidic applications, hybrid substrates have also been developed in order to exploit their comparative advantages to the full, for instance polymer/glass.¹²³

However, for single techniques on a chip such as DNA extraction, it can be easy to select a substrate based on the most suitable properties. Therefore, in this work, glass microfluidic devices were used and the method of fabrication is discussed in detail in the methodology chapter.

1.4 DNA Analysis

The simple forensic serological method (ABO blood typing) for excluding individuals is not a very useful technique for most forensic cases. Developments in molecular biology have opened up the field of analysing the chemical composition of a person's genetic material, a process known as DNA profiling. This started in 1985, when Sir Alec Jeffreys developed a highly discriminatory method, later termed 'DNA fingerprinting'.¹⁴⁴ The tandem-repetitive 'minisatellite' regions (10-15 base pairs in length) that Jeffreys had been studying became known as the variable number of tandem repeats (VNTR). Restriction fragment length polymorphism (RFLP) analysis is used to study these regions. The technique entails cutting DNA at sites that surround the VNTRs using a restriction enzyme to provide different-length fragments which are then separated by gel electrophoresis.

Although the RFLP method is a powerful tool in the field of paternity testing and forensic analysis, it suffers from several limitations. First, the method requires large amounts of DNA in a sample ($6 \mu\text{g}$)¹⁴⁵ and cannot be successfully carried out with degraded DNA molecules.¹⁴⁶

In addition, analysis with RFLP is not ideal for large numbers of biological samples because it is time consuming and difficult to automate,¹⁴⁷ especially when a mixture of biological materials requires serial analysis of a single RFLP locus.¹⁴⁸

More recently, PCR-based methods and markers have rapidly overtaken the RFLP method in improving the speed, sensitivity and power of discrimination from a low-quantity or poor-quality sample. Short tandem repeats (STRs), of unit ranges of 2-6 base pairs in length, have become commonly used DNA repeat markers in forensic laboratories because they are PCR-based and provide a high degree of discrimination, even from biological material containing mixed or degraded DNA molecules. In addition, STR typing methods are ideally suited to automation and involve sensitive fluorescent detection, which enables the simultaneous analysis of multiple loci.¹⁴⁸

Forensic scientists have now demonstrated STR loci in the form of commercial kits to amplify multiplexes simultaneously. The Forensic Science Service (FSS) went on to develop the so-called 'First-Generation Multiplex' profiling system that amplified four loci (vWA, TH01, F13A1, and FES/FPS)¹⁴⁹ with a probability of discrimination of 1 in 10,000.¹⁴⁸ The Second-Generation Multiplex (SGM) that followed was able to evaluate six STR loci (vWA, TH01, FGA, D8 S1179, D18 S51, and D21 S11) plus the Amelogenin (gender marker).¹⁵⁰ With this system the chance of matching probability is 1 in 10⁸. To decrease the matching possibility to 1 in 1 billion individuals, the AmpF/STR[®] SGM Plus[™] kit (Applied Biosystems, UK) was produced to analyse 10 common STR loci (vWA, TH01, FGA, D8 S1179, D18 S51, D21 S11, D3 S1358, D16 S539, D2 S1338, and D19 S433), along with the Amelogenin sex marker.¹⁵¹

An artificial DNA size standard and allelic ladder are also included in the AmpF/STR[®] SGM Plus[™] kit to provide accurate genotyping for individuals (see Figure 1-15). The figure shows the number of alleles at each of the amplified loci and Amelogenin locus and their corresponding fluorescent marker dyes (blue, green, black and red; the internal size standard is labelled in orange). This type of forensic DNA profiling represents a powerful method for paternity determination and identification of individuals.¹⁵²

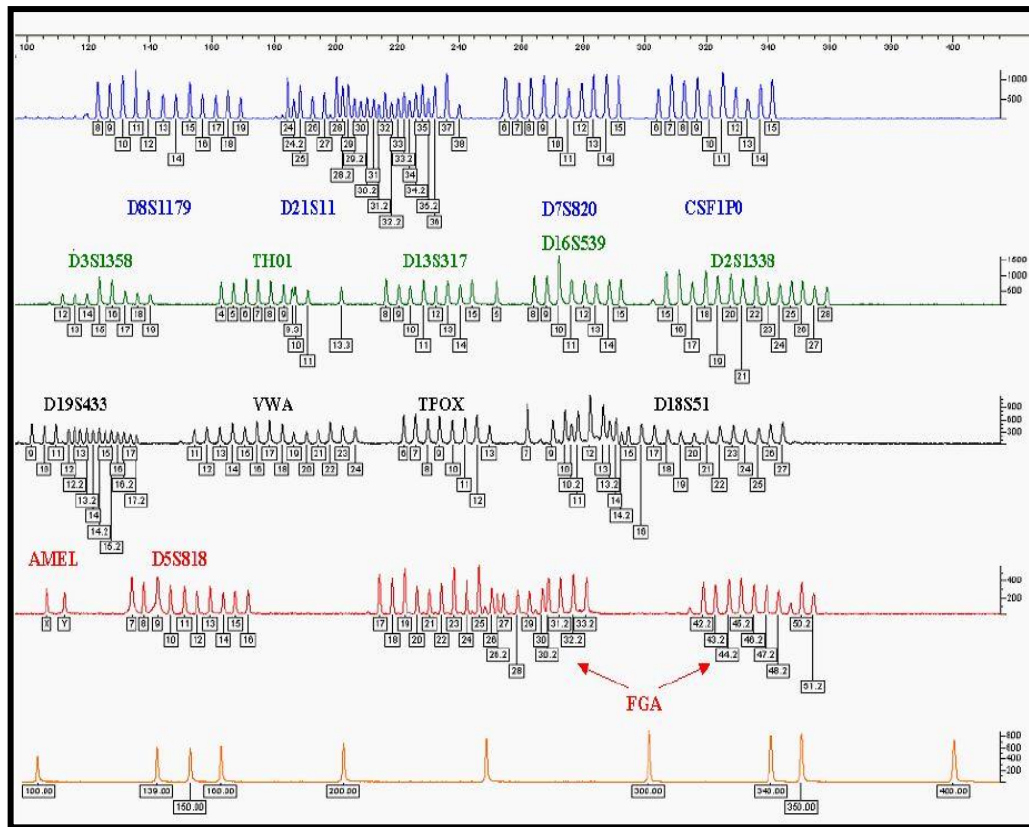


Figure 1-15: Example of the allelic ladder using the AmpF/STR[®] SGM Plus[™] kit with all possible alleles for accurate genotyping.¹⁵³

1.4.1 Nomenclature for STR markers

Nomenclature gives information about locus and is dependent upon whether it is located within or outside a gene. A locus that is part of a protein-coding gene is given the abbreviated name of this gene. For example, vWA is found in intron 40 of the von Willebrand factor gene; FGA is found in the third intron of the human alpha fibrinogen locus on the long arm of chromosome 4 and the TH01 is located within the tyrosine hydroxylase gene in intron 01.¹⁴⁸ Those STR markers located outside a gene are designated based on chromosomal location. For example, the 'D' in STR locus D5 S818 stands for DNA, and the '5' for chromosome number 5. The 'S' means it is a single copy sequence and is the 818th locus discovered on that chromosome.

1.4.2 DNA structure

DNA contains all the genetic information needed for an organism to function and replicate and is mainly found in the nucleus of a cell, but small amounts also exist in the mitochondria. Each human nucleated cell contains approximately 6 pg of genomic DNA.¹⁴⁶ In the middle of the 20th century, Watson and Crick elucidated the structure of DNA as a double-stranded helix based on X-ray diffraction data.¹⁵⁴ Watson and Crick's proposed structure is composed of two 'anti-parallel' strands, each consisting of a deoxyribose sugar, a phosphate group and a nitrogenous base to form what is called a deoxyribonucleotide.¹⁴⁶ Deoxyribonucleotides are linked by covalent phosphodiester bonds. A triphosphate group and a deoxyribose sugar compose the DNA backbone structure.¹⁵⁵

The nitrogen bases consist of two pyrimidines, thymine (T) and cytosine (C), and two purines: guanine (G) and adenine (A).¹⁴⁵ The two DNA strands are held together by hydrogen bonding between complementary pairings of nitrogenous bases on opposing strands. A hybridises with T by two hydrogen bonds and C hybridises with G by three hydrogen bonds (Figure 1-16). The nucleotide has a phosphate group on the 5' carbon atom of the deoxyribose sugar and a hydroxyl group on the 3' position.¹⁵⁵ The sequence order of the nucleotide bases is normally directional from 5' to 3'.

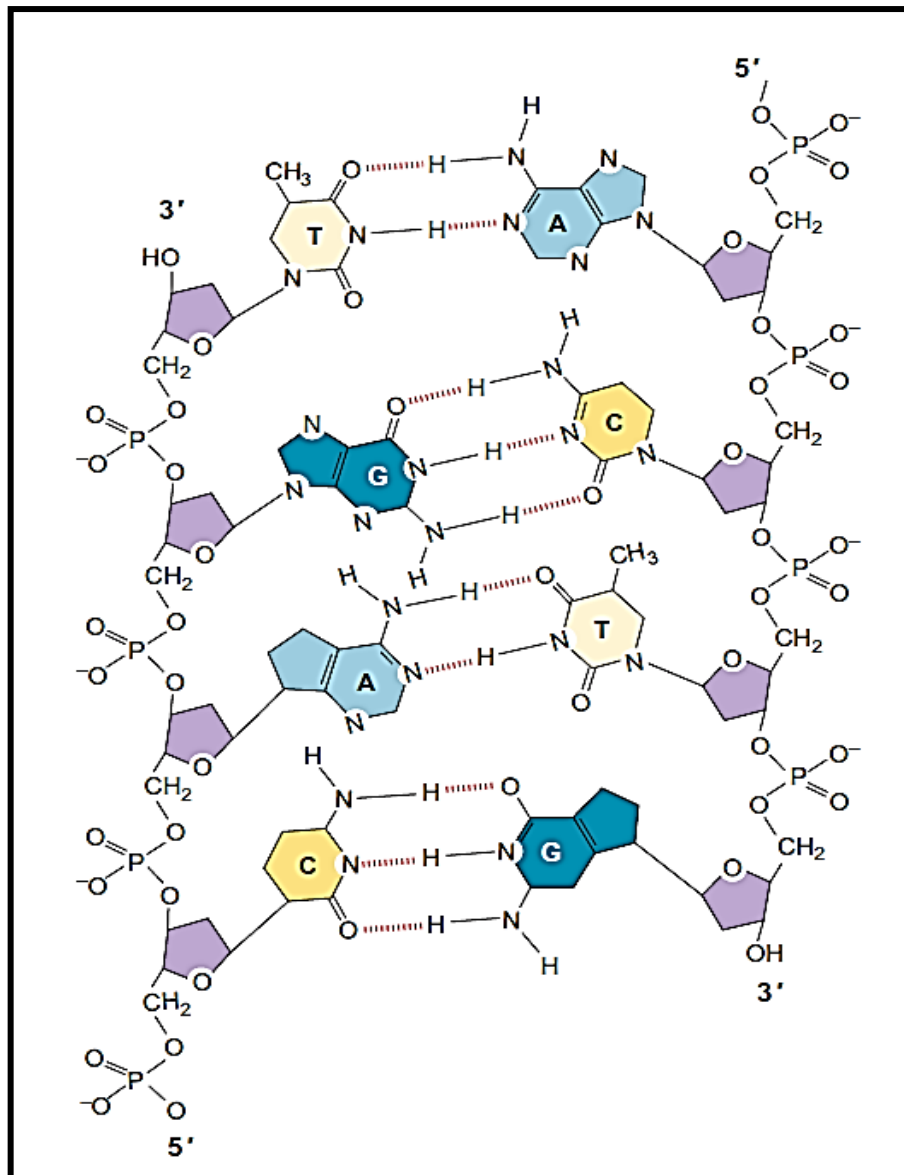


Figure 1-16: Schematic showing the basic components of DNA.¹⁵⁶

1.4.3 Conventional DNA sample preparation

A wide variety of biological materials can be used as a source of nucleic acids, such as blood, urine, semen, saliva, hair, and bone.¹⁴⁸ In the field of genetic analysis, the isolation and purification of nucleic acids (DNA or ribonucleic acid [RNA]) from biological samples is an essential requirement for successful downstream analysis. For example, the presence of contaminants such as cellular debris and haem proteins in the sample can inhibit PCR.¹⁵⁷

In addition, pre-concentration of nucleic acids from samples of limited quantity is a crucial step in most clinical and forensic applications.¹⁵⁸ Although each type of biological specimen may have a different sample preparation technique for DNA profiling, the general process following biological sample collection involves four steps: cell lysis and DNA purification, DNA amplification, electrophoretic separation and fluorescence detection of amplified products.¹⁵⁹

1.4.4 Cell lysis

Cell lysis is the process in which cellular and nuclear membranes are disrupted to release the nuclear components as a result of external forces, namely mechanical and non-mechanical.

Mechanical or physical lysis methods include using sonication (high-frequency sound waves resulting in breakage of the cellular membrane), bead mills (the grinding action of minute glass, ceramic, or steel beads due to vigorous mixing), and applying high pressures.¹⁶⁰ Mechanical lysis methods also include exposing cells to

extracellular osmotic pressure, thermal change either by increasing the temperature or repeated freezing and thawing, or the application of an electrical field.¹⁶¹

However, the most common methods used for cellular membrane disruption are based on non-mechanical techniques (chemical and/or enzymatic).¹⁶² Methods employed in chemical lysis involve using detergents such as Triton X-100 and/or sodium dodecyl sulphate (SDS) or high concentrations of chaotropic salts such as guanidine hydrochloride (GuHCl).¹⁶³ In protein analysis, for example, ionic detergents such as SDS effectively break open cell walls, resulting in cell lysis, due to their ability to solubilise cellular lipids and disrupt non-covalent bonds in proteins in an alkaline medium.¹⁶⁴ In addition to solubilising phospholipid membranes, non-ionic detergents such as Triton X-100 have an effective haemolytic action.¹⁶⁵

However, some applications, such as PCR, can be inhibited by the detergent itself or the tandem addition of Proteinase K (ProK), which enzymatically denatures proteins. Chemical cell lysis can also be achieved through the addition of chaotropic salts such as GuHCl or urea. Chaotropic agents not only increase the solubility of proteins by disrupting hydrogen bonds and enhancing the hydrophobic effect between and within proteins,¹⁶⁶ but can also be exploited to inactivate endogenous nucleases that catalyse the hydrolysis of nucleic acids. Cell lysis can be achieved by enzymatic methods for organisms that have cell walls in addition to a cell membrane. For instance, lysozyme can efficiently lyse Gram-positive bacteria, whereas the zymolase enzyme disrupts the polysaccharide cell wall of yeasts.¹⁶⁷

1.4.5 DNA purification

Following the release of nucleic acids from a cell, a purification step is required to increase the concentration of DNA and minimise contaminants, such as proteins, haemoglobin and heparin, that can potentially inhibit subsequent analysis such as PCR.¹⁶⁸ Liquid-liquid (e.g., phenol-chloroform) and solid-phase extraction (e.g., chelating resin and silica) are examples of DNA purification techniques used for most biological samples.

In organic solvent (phenol-chloroform) extraction, double-stranded DNA molecules are separated from denatured proteins, lipids, and cell debris following vigorous mixing and centrifugation. DNA is collected from the upper hydrophilic layer because it is more soluble in the aqueous phase. Although phenol-chloroform is effective for DNA extraction, the protocol is time consuming due to the multiple steps of mixing and centrifugation, and requires special precautions (e.g., use of a hood) due to the hazardous substances involved.^{117, 169}

SPE techniques using ion-exchange resins, sol-gels, or silica monoliths provide a reliable standard method for DNA purification in clinical and forensic laboratories.^{162, 170} Chelex[®] is a cation-exchange chelating resin where positively charged cellular components have a high affinity with and bind to the negatively charged resin, whereas negatively charged DNA remains free in the aqueous supernatant after centrifugation.

Chelex[®] is composed of a styrene-divinylbenzene copolymer containing paired iminodiacetate ions, which act as chelating groups due to a strong affinity to polyvalent metals, such as Mg^{2+} , therefore preventing DNA damage by nucleases. Unlike organic extraction, the Chelex[®] method is rapid and easy to carry out in a

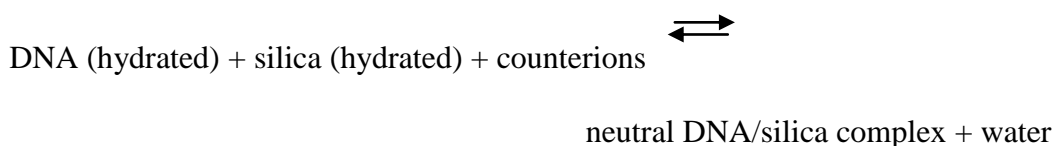
single tube, which minimises the possibility of cross-contamination. However, it has a disadvantage: it yields only single-stranded DNA (ssDNA) due to high incubation temperatures.^{117, 148}

Adsorption of nucleic acids onto a solid support such as silica or glass represents the most widely used extraction method due to the robust and efficient mechanism of DNA purification from PCR inhibitors.¹⁷¹ The extraction method using solid support involves four major steps: (i) conditioning the solid-phase surface with a buffer at a particular pH, (ii) adsorption of DNA onto a solid support surface with the aid of a high concentration of chaotropic salt (e.g., guanidine hydrochloride), (iii) removing impurities that may inhibit subsequent analysis (e.g., PCR) with buffer or organic solution (e.g., ethanol), and finally (iv) elution of the adsorbed DNA with water or a low ionic strength solution suitable for PCR amplification.¹⁷² The mechanism for DNA adsorption onto silica surfaces was investigated by Melzak *et al.*¹⁷³ and was found to be the result of three factors: the shielding of intermolecular electrostatic forces, dehydration of both DNA and silica surfaces, and the formation of intermolecular hydrogen bonds in the DNA-silica contact layer.

Across a wide pH range, DNA carries two negative charges per base pair, which results from the phosphate diester groups on its backbone.¹⁷⁴ At basic or near-neutral pH, the surface of silica is negatively charged due to weakly acidic silanol groups, with an average pK_a ranging from 5 to 7.¹⁷⁴ Therefore, electrostatic repulsion occurs between the negatively charged DNA molecule and the silica surface. A high ionic strength solution containing a high concentration of chaotropic agent, such as GuHCl or guanidine thiocyanate (GuSCN), dehydrates both the DNA molecule and silica surface due to the ability of one GuHCl molecule to bind to 10 molecules of water.¹⁷⁵

The result is a reduction in electrostatic repulsion between the DNA and the sorbent, positioning DNA adjacent to the silica surfaces. Guanidine hydrochloride also denatures the hydrogen bonding between the bases of double-stranded DNA, yielding a single-stranded structure.

Using a high ionic strength solution with a pH < 7,¹⁷³ below the p*K*_a of silica, protonation of the silanol groups on the silica surface increases and the result is the formation of hydrogen bonds between the DNA and silica surfaces that contain more free and/or vicinal silanol groups.⁵⁸ Chaotropic agents have also been utilised to denature cellular membranes and prevent DNA degradation by inhibiting nuclease activity.¹⁷³ A summary of the driving forces for DNA adsorption on silica surfaces is shown in Equation 1.3.



Equation 1.3¹⁷³

Following nucleic acid adsorption to the solid-phase matrix, a washing step is required to remove co-adsorbed cellular debris and unbound contaminants from the solid-phase. Proteins are removed which may also have bound to the silica support by means of reversed-phase action with hydrophobic siloxane groups ($\equiv\text{Si-O-Si}\equiv$).¹⁵⁹ Finally, purified DNA can be eluted from the solid-phase using a low ionic strength buffer or water. It should be noted that the presence of any chaotropic salt solution or alcohol in the elution fractions can inhibit downstream applications (e.g., PCR) and thus needs to be avoided.⁶¹

1.4.6 DNA quantification

Accurate quantification of extracted DNA is desirable for successful PCR amplification. For example, in a 50 μl reaction volume, the amount of template DNA needs to be in the range between 0.5 ng and 2 ng.¹⁷⁶ Stochastic fluctuation occurs when insufficient template DNA is added, resulting in 'allele drop out'. However, when a large amount of template DNA is added, split peaks (also known as minus A or n-1 peaks) will result due to the high concentration of amplification products.¹⁴⁸

Ultraviolet (UV) and fluorescence spectroscopy are the most commonly used techniques for measuring the total amount of DNA in a sample when species origin is not important, because they determine both human and non-human DNA (animal, bacterial, or foodstuff).¹⁷⁶ Double-stranded DNA (dsDNA) absorbs UV light at 260 nm compared with 280 nm for proteins. UV absorption analysis can also provide information about the purity of DNA in a sample by measuring the optical density (OD) ratio at 260/280 nm.

A sample is considered to be free of inhibitors and contaminants if the OD 260/280 nm ratio is between 1.8 and 2.¹⁷⁷ The limitations of the UV method are due to its inability to distinguish between nucleic acids (i.e., it is a non-specific DNA quantitation method as RNA and proteins absorb UV light at the same wavelength), and it cannot detect low concentrations of DNA ($< 5 \mu\text{g ml}^{-1}$ DNA solution) such as those obtained from forensic cases.¹⁷⁶

Fluorescence spectroscopy methods require an intercalating fluorochrome dye, such as PicoGreen[®], which, when bound to double-stranded DNA, gives a maximum fluorescence emission peak at 520 nm following excitation at 480 nm.

Very low background fluorescence levels are seen in the absence of dsDNA. The main advantage of the PicoGreen[®] assay is its high sensitivity to very low concentrations of dsDNA, down to 25 pg ml⁻¹.¹⁷⁸ The total dsDNA quantity is determined from a standard curve using known concentrations of calibration standards, unlike the UV method in which DNA concentration is determined by the direct measurement of optical density. However, fluorescence spectroscopy assay requires a greater number of preparatory steps and longer incubation time compared with the UV method. PicoGreen[®] (Figure 1-17) is also not selective for human DNA because it detects dsDNA from any other species that may be present in a sample.¹⁴⁸

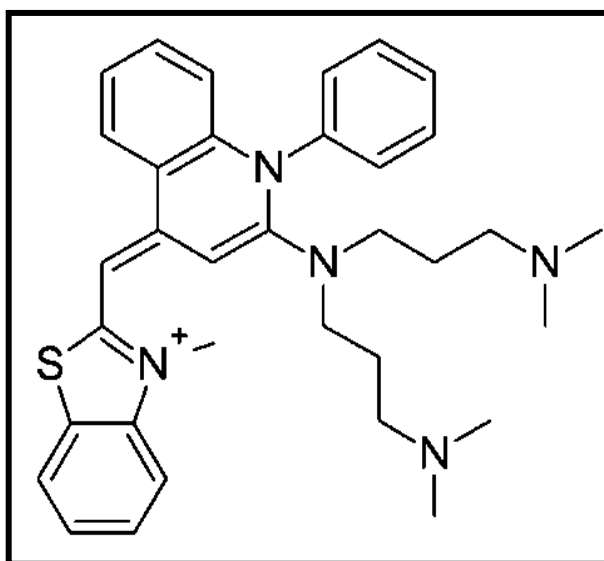


Figure 1-17: Structure of PicoGreen[®].¹⁷⁹

1.4.7 DNA amplification

PCR is an enzymatic-based technique developed in 1985 by Kary Mullis to amplify specific regions of DNA *in vitro*,¹⁸⁰ where a small amount of a particular sequence of DNA or even a single copy of a sequence can be amplified to billions of copies based on thermal cycling that involves three critical temperatures.^{148, 181}

First, by increasing the sample temperature to 90-95 °C, the hydrogen bonds between the DNA double helix are broken, yielding two single strands (two templates) in a process called ‘denaturation’ (Figure 1-18 A). The sample is then cooled to 50-65 °C, depending upon the specific primer sequences, which is the optimal temperature for two oligonucleotide primers to bind or ‘anneal’ to each single strand on a specific DNA template (Figure 1-18 B).¹⁸² The two primers have different sequences - one for the forward strand and another for the reverse one - so the limits of the amplified DNA template are defined by the 5’ end of the primers.¹⁴⁸

When fluorescence detection is being used, a fluorophore is attached to the 5’ end of the forward primers. Finally, the temperature of the reaction rises slightly to 72 °C, at which the *Taq* polymerase, isolated from *Thermus aquaticus*, catalyses the addition of deoxyribonucleotide triphosphates (dNTPs) to form a complementary sequence to the template DNA sequence through a process known as ‘extension’ (Figure 1-18 C).

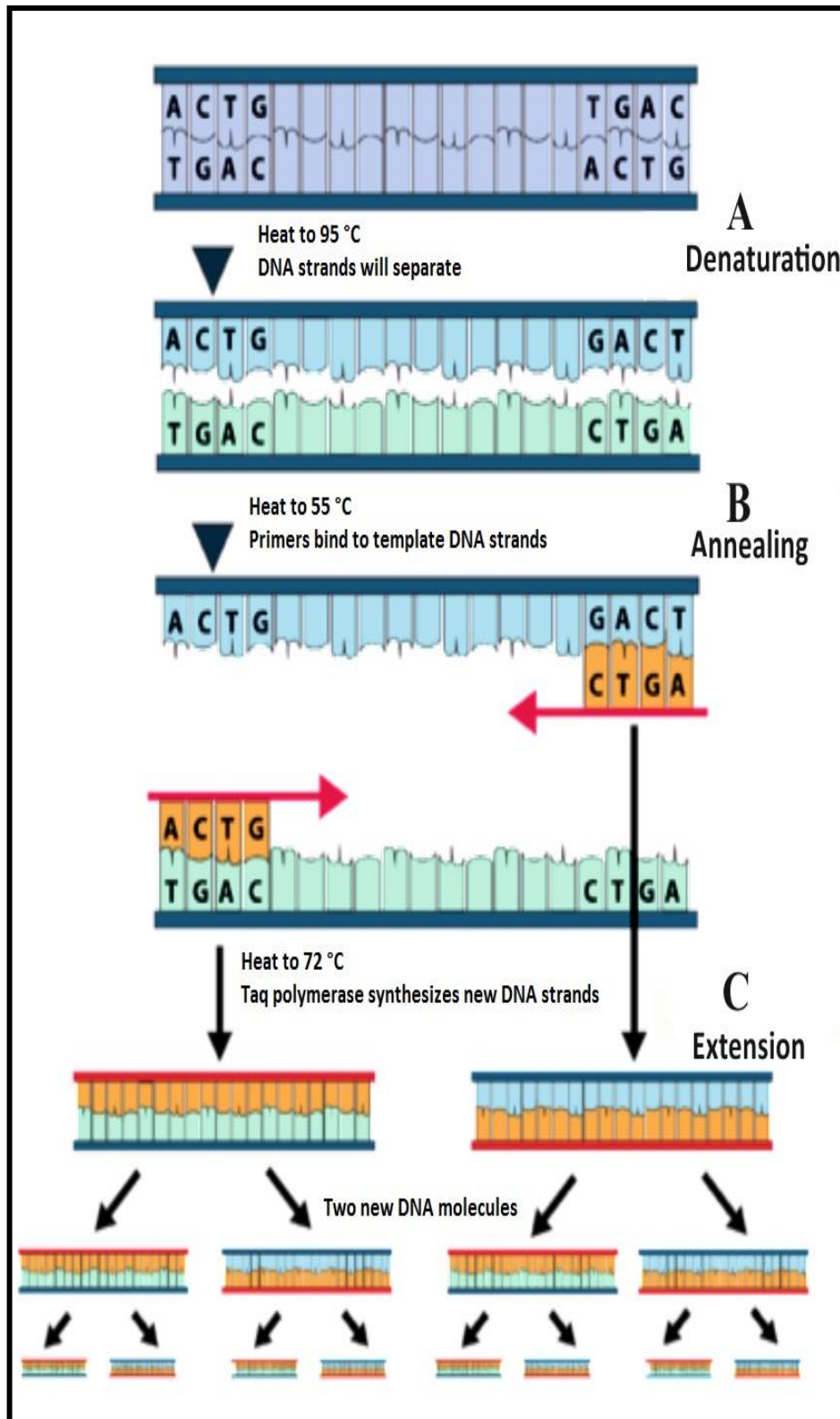


Figure 1-18: Schematic of the PCR principle.¹⁸³

Common PCR components include template DNA, buffer solution, salts (MgCl_2), four nucleotides, primers and a thermostable DNA polymerase such as the *Taq* polymerase (Table 1.1).

Table 1.1: Examples of the optimum concentrations required for commonly used reagents in the PCR process.

PCR component	Information
Template DNA	Most commercial kits optimally require between 0.5 and 2.5 ng of template DNA. ¹⁴⁶
Magnesium chloride	Acts as a co-factor for <i>Taq</i> polymerase activity. Also functions to stabilise hybridisation between the primer and the template DNA. Typical concentrations are between 0.5 and 2.5 mM. ¹⁸⁴
Primers	At least two short synthesised oligonucleotides are required (18 to 30 nucleotides) in a concentration range of between 0.1 and 1 μM . ¹⁴⁸
dNTPs	Consists of four nucleotides (dATP, dTTP, dGTP, and dCTP), which are sequentially added to form the complementary strand for the target DNA. In addition, they provide the energy for the PCR reaction. ¹⁸⁴ The optimal concentration of each nucleotide is 200 μM . ¹⁴⁶
<i>Taq</i> polymerase	A heat-stable enzyme isolated from the thermophilic bacterium <i>Thermus aquaticus</i> . The usual concentration is between 0.1 and 5 units. ¹⁴⁶

Samples collected may contain different PCR inhibitors, such as haemoglobin (blood), bile salts and complex polysaccharides (faeces), urea (urine), humic acids (soil), RNA, lipids, bacterial proteases, or high concentrations of some anticoagulants (e.g., ethylenediaminetetraacetic acid [EDTA] or heparin).¹⁶⁹ The inhibitors can act on *Taq* polymerase by different modes of action, such as inactivation (high concentrations of calcium and magnesium), denaturation (by phenol or detergents), or by blocking the active site (by haem).¹⁸⁵ Thus, PCR inhibitors need to be removed or their effects reduced, either by increasing the concentration of DNA polymerase or by dilution of the sample using proteins such as bovine serum albumin (BSA).¹⁸⁶

Although the main PCR amplification technique used in this study focuses on the conventional thermocycling method, it is useful in this introduction to mention that there are several techniques that have used constant temperature (isothermal) for DNA amplification and these have also been successfully applied in a microfluidic environment. Rolling circle amplification (RCA),¹⁸⁷ loop-mediated isothermal amplification (LAMP),¹⁸⁸ nucleic acid sequence-based amplification (NASBA),¹⁸⁹ self-sustained sequence replication (3SR)¹⁹⁰ and strand displacement amplification (SDA)^{191, 192} are examples of isothermal amplification techniques with their own method of amplification. In this section, RCA is used as an example of an isothermal amplification mechanism. As demonstrated in Figure 1-19, DNA polymerase extends a circular DNA template by continuous amplification of an annealed primer (at 37 °C) around the circular DNA to form a long DNA replicate of the circular template, which can be cleaved into monomer-length oligonucleotides using a restriction enzyme.¹⁹³

As there is no need for thermal cycling, isothermal amplification methods can be simply designed for battery-operated portable detection systems.¹⁹⁴ Isothermal methods suffer, however, from several disadvantages that limit their application. For example, SDA is not suitable for amplifying long target sequences,¹⁸⁷ LAMP requires the complex design of four primers,¹⁹⁵ and RCA is more suitable for circular templates including viruses and plasmids.¹⁹⁶

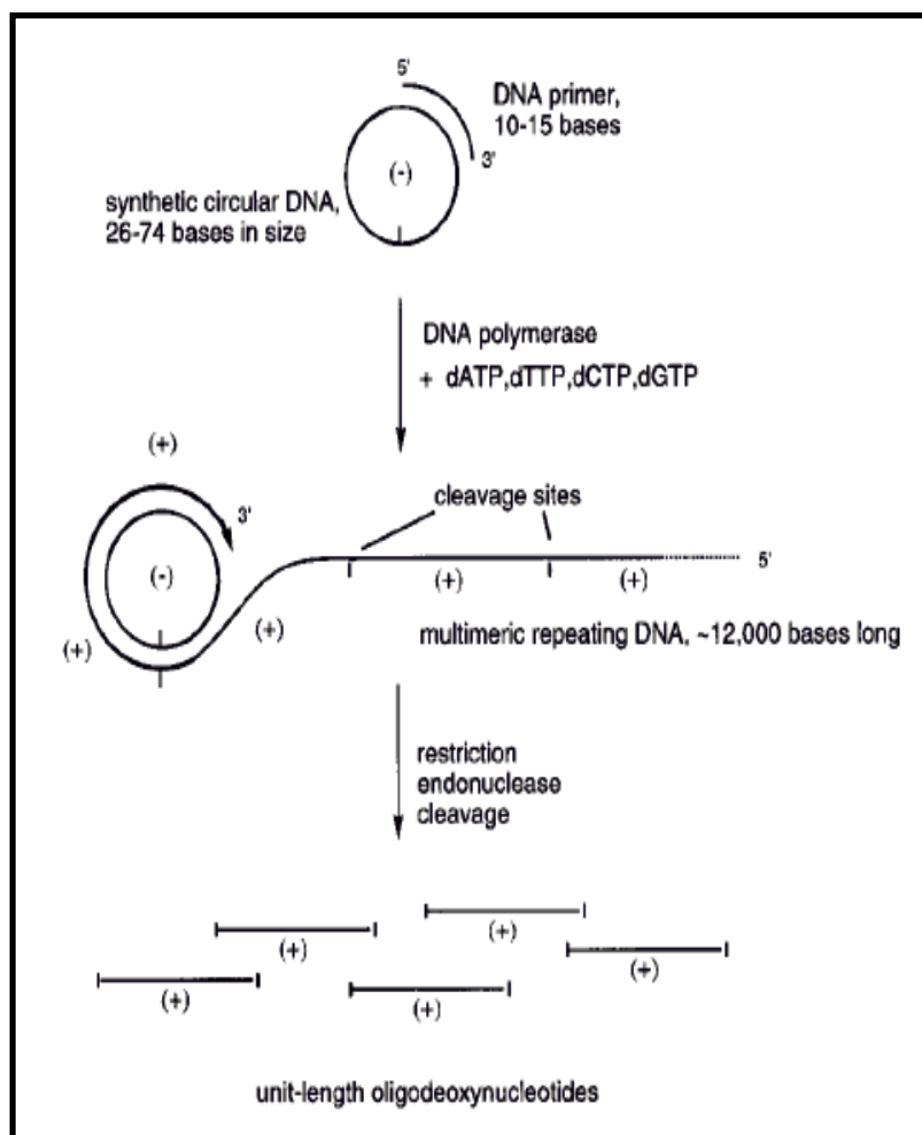


Figure 1-19: Schematic description of the RCA process in which a circular DNA template is continuously amplified to produce long multimeric DNA sequences that can be cleaved into monomer-length oligonucleotides.¹⁹³

1.4.8 Separation and detection of PCR products

The separation of PCR products is performed using electrophoresis, in which DNA molecules are distinguished from one another according to size using either slab-gel or capillary methodology. Under the influence of an electrical field, PCR products migrate through a gel matrix from the cathode to the anode, where DNA molecules with a low molecular weight move faster than higher molecular weight fractions.¹⁷⁶ PCR products can either be detected using intercalating dyes, such as ethidium bromide (EtBr), an intercalating agent used to visualise DNA products using short-wavelength UV light, or by the incorporation of fluorescently labelled primers.

Capillary electrophoresis is a fully automated technique, requiring only a small amount of sample and reagents and simple sample preparation.¹⁴⁸ However, slab-gel electrophoresis is more commonly used for the analysis of PCR products in molecular biology and forensic DNA laboratories because capillary electrophoresis instruments and reagents are expensive and this restricts their use in some laboratories.

1.4.9 Miniaturised solid-phase DNA extraction

The incorporation of genetic analysis into a microfluidic device has many advantages: for example, the ability of these devices to process low quantities of sample, minimum contamination effects due to a closed system, the integration of multiple processes on single microfluidic devices, and automation.^{197, 198} Therefore, a variety of methods have been developed for nucleic acid analysis from simple to complicated biological starting samples, such as urine, saliva, blood, and tissue.

Scaling down conventional SPE techniques for DNA purification has led to the successful creation and development of silica-based SPE beds within microfluidic systems.¹⁷⁴

Monolithic materials are particularly useful for DNA purification because of the advantages of a large surface area, controllable pore size, and high mass transfer from the porous structure.¹⁹⁹ The silica-based forms introduced in micro-solid-phase extraction (μ SPE) can be the packing for silica-based monoliths, silica beads, or immobilised silica beads for sol-gel monoliths.

The effectiveness of miniaturising a silica particle-based (beads) methodology for DNA purification from a variety of complex biological matrices (white blood cells, cultured cells and whole blood) was first evaluated in 2000 by Tian *et al.* using a capillary-based chamber.⁵⁸ They demonstrated that DNA extraction efficiency is affected by the size, shape and porosity of the silica beads. Three different types of silica bead (irregular-shaped particles, spherical-shaped silica resins with 6 nm pores, and spherical-shaped silica resins with 12 nm pores) were evaluated for DNA extraction efficiency.

It was shown that irregular-shaped silica beads, followed by 6 nm pore spherical-shaped silica resins, demonstrated more reproducible DNA extraction efficiency due to their ease of packing within a μ SPE device. However, smaller or more porous particles (6 nm pores), which offered a larger surface-area-to-volume ratio for optimal DNA binding, suffered from high back pressures due to their high packing density. In addition, applying silica beads to microfluidic systems as a solid support for DNA extraction suffered from poor inter-chip reproducibility.⁵⁸

Incorporating silica-based monolith into a microfluidic device that serves as the solid-phase for DNA purification was further extrapolated in 2002 by Wolfe *et al.*¹⁷² The work examined the extraction efficiency, stability and reproducibility of silica beads (15 μm), continuous silica networks produced by sol-gel chemistry, and combination silica beads/sol-gel matrices by adding silica beads to the sol-gel precursor mixture prior to the condensation reaction (see Figure 1-20).

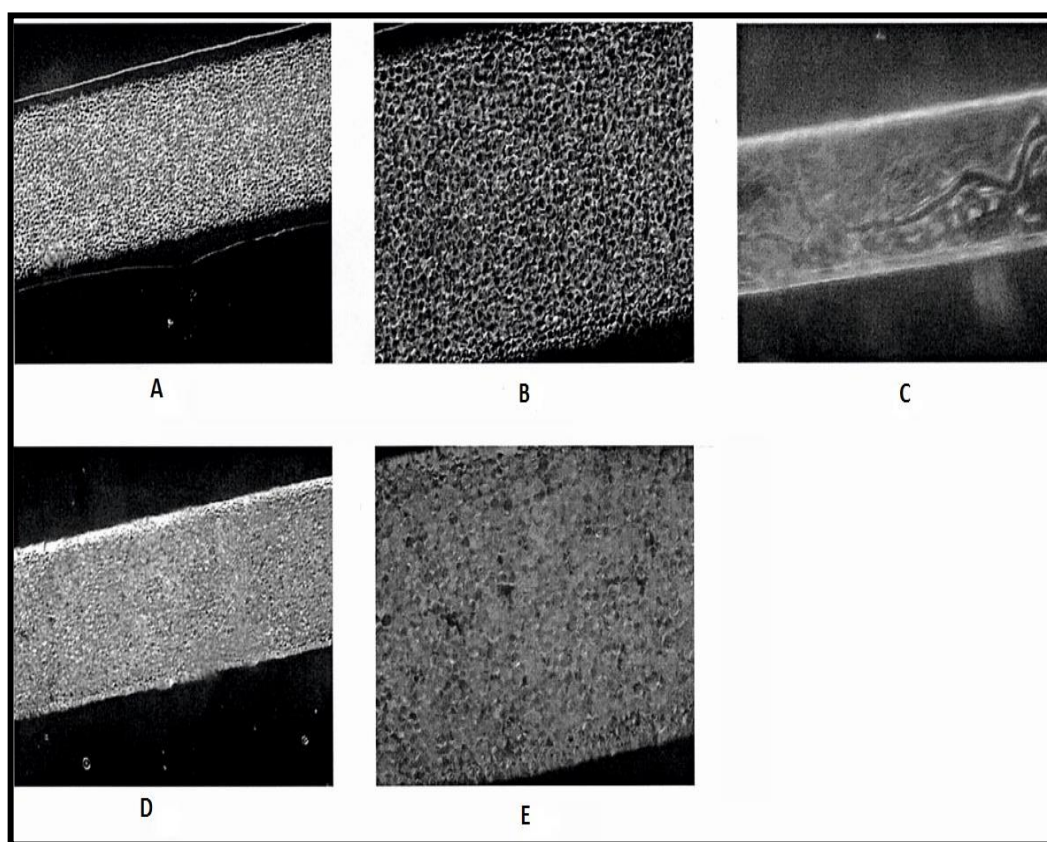


Figure 1-20: Different silica materials within microfluidic device chambers: (A) silica beads, (B) silica beads at 10 \times magnification, (C) silica-based monolith using sol-gel, (D) two-step silica beads and sol-gel, and (E) two-step silica beads and sol-gel at 10 \times magnification.¹⁷²

Figure 1-20 (A) and (B) show images of a microfluidic chamber packed with silica beads. Silica beads alone showed high DNA extraction efficiency (57.1%), but decreased reproducibility (standard deviation 43.1%) resulting from compression of

the particles under flow as multiple extractions proceeded. The alternative approach of using a sol-gel monolith (TEOS) demonstrated low extraction efficiency (33.2%) and poor extraction reproducibility due to inadequate mechanical stability (crack formation in the structure), as shown in Figure 1-20 (C). Sol-gels are defined as “liquid colloidal suspensions of silica-based materials that can be acid or base catalysed to gel in place to create a silica network”.¹¹⁷ A combination of silica beads with sol-gel achieved the highest DNA extraction efficiency (70.6%), with high reproducibility (standard deviation 3.05%) and good structural stability compared with using silica beads alone (see Figure 1-20 D and E). However, the use of bead/sol-gel methodology is a sophisticated multi-step process that requires packing and restraining silica beads inside a microfluidic device followed by the sol-gel solution flowed over prior to catalysis.

A two-stage, dual-phase microchip-based system for DNA extraction was reported in 2007 by Wen *et al.* from the Landers group¹⁹⁹ to overcome the limited capacity of a monolith for whole blood DNA extraction due to the proclivity of proteins to undergo non-specific adsorption on silica surfaces. The system consisted of four parallel columns (2 mm wide, 385 μm deep) packed with reversed-phase commercial octadecyl (C_{18})-coated silica beads used for hydrophobic protein capture (stage 1) connected in a series with (stage 2) a DNA extraction channel (20 μm wide, 200 μm deep) filled with a photopolymerised monolith using 3-(trimethoxysilyl) propylmethacrylate (TMSPM) and derivatised with TMOS solution to increase the DNA binding capacity (Figure 1-21).¹⁹⁹ The two-phase system completely eliminates the need for a washing step, which usually requires an isopropanol reagent that may inhibit PCR, and prevents any potential sample contamination that may

occur from switching syringes or tubing. While the combined methodology enabled DNA extraction from 10 μl whole blood with an efficiency of 69%, the amount of DNA introduced was high (350 ng) and the system required special instruments to fabricate a weir (30 μm deep) in each chamber of the reversed-phase stage to retain the silica beads, which is a restriction in some laboratories.

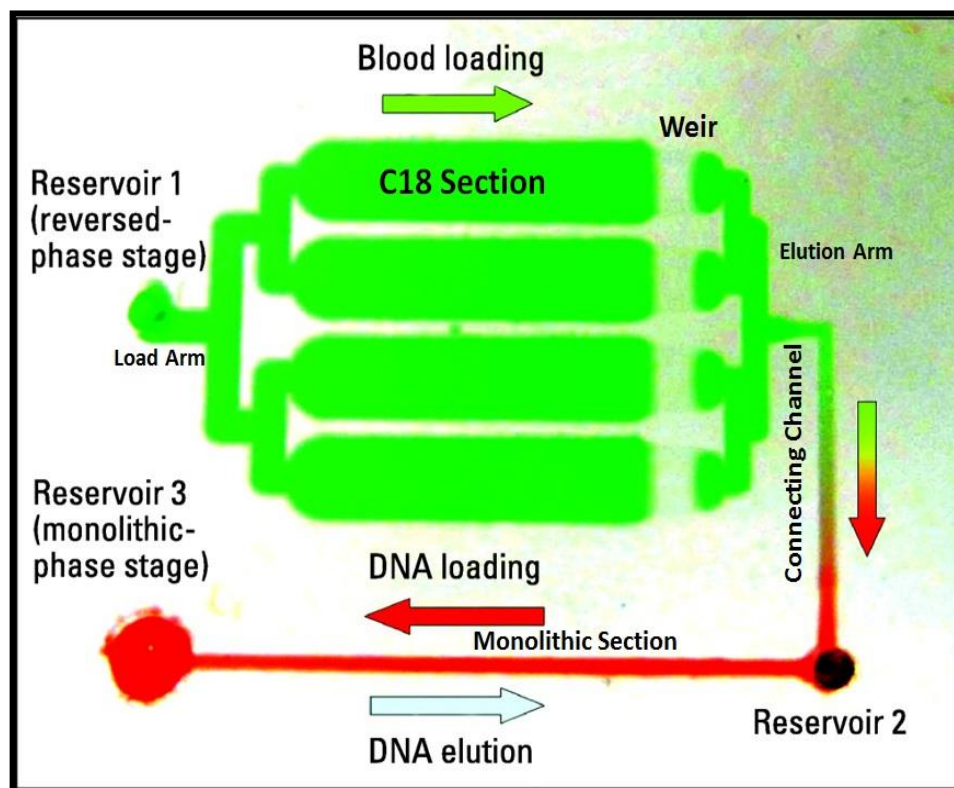


Figure 1-21: Dye-filled dual-phase microdevice for integrated protein capture-DNA extraction from 10 μl of human whole blood. The arrows show the direction of flow from stage 1 (green) to stage 2 (red). Chip dimensions: 3 cm (length) x 2.5 cm (width).^{174, 199}

In 2009, Shaw *et al.* from the Haswell group at the University of Hull, investigated the effects of utilising nucleic acid carrier molecules to extract smaller amounts of pre-purified DNA (25 ng) within a microfluidic environment using silica-based monoliths prepared *in situ* from a mixture of potassium silicate (9% K₂O, 21% SiO₂) and formamide in a 10:1 ratio.¹⁵⁸ Figure 1-22 demonstrates that the addition of carrier RNA (ratio 10:1; RNA:DNA) to a limited concentration of DNA during the loading step markedly increases DNA extraction efficiency in comparison with those to which no carrier RNA was added. Whilst the use of carrier RNA methodology shows high DNA recovery from pre-extracted DNA, the use of biological samples (cells) as starting material can be associated with competition for non-specific binding sites by other endogenous compounds such as proteins.

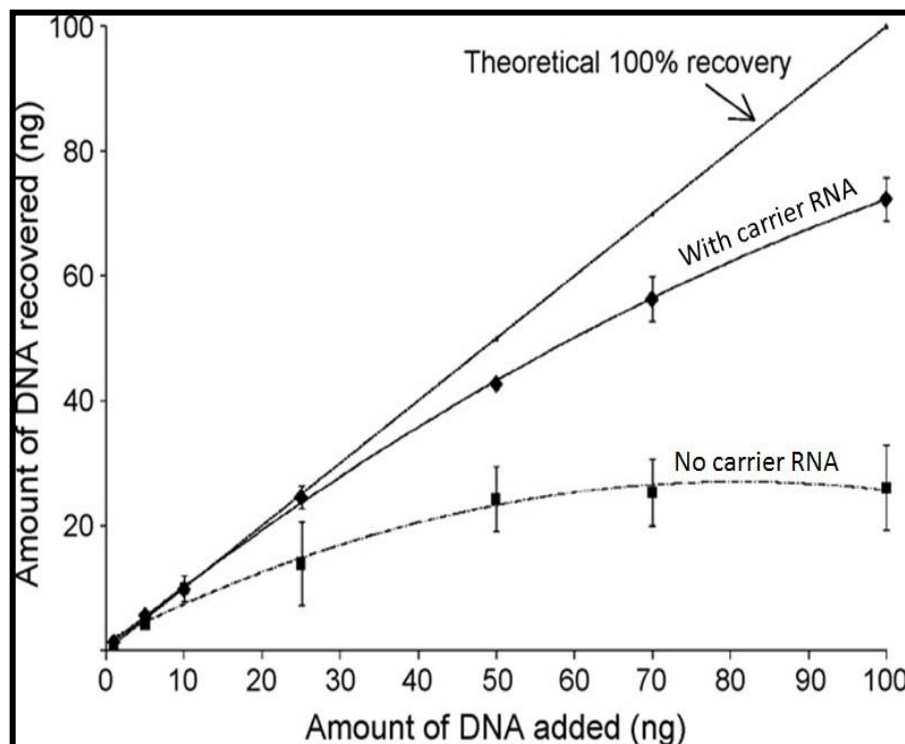


Figure 1-22: Amount of DNA recovered from a silica-based monolith during the elution step for samples containing carrier RNA (ratio 10:1, RNA:DNA) and without carrier RNA in comparison with the amount of DNA initially added (error bar = 3).¹⁵⁸

Modification of monolithic surfaces with chemical functional groups that possess a high affinity to DNA has been considered as an alternative mechanism to adsorb DNA on the surfaces of monolithic supports without the aid of a chaotropic agent that acts as a PCR-inhibitory reagent.²⁰⁰ DNA is a highly negatively charged polymer over a wide pH range due to the presence of two negatively charged phosphate groups per base pair.¹⁷⁴ Therefore, an electrostatic interaction between a positively charged ion (such as an amino group or chitosan) and negatively charged DNA can be exploited as a method of DNA extraction. Nakagawa *et al.* introduced an amine-coated microfluidic channel for capturing DNA through electrostatic interaction at an optimised pH 7.5 by coating the internal surface of a silicon microfluidic chip with 3-aminopropyltriethoxysilane (APTES) or 3-[2-(2-aminoethylamino)-ethylamino]-propyltrimethoxysilane (AEEA), as shown in Figure 1-23.²⁰¹

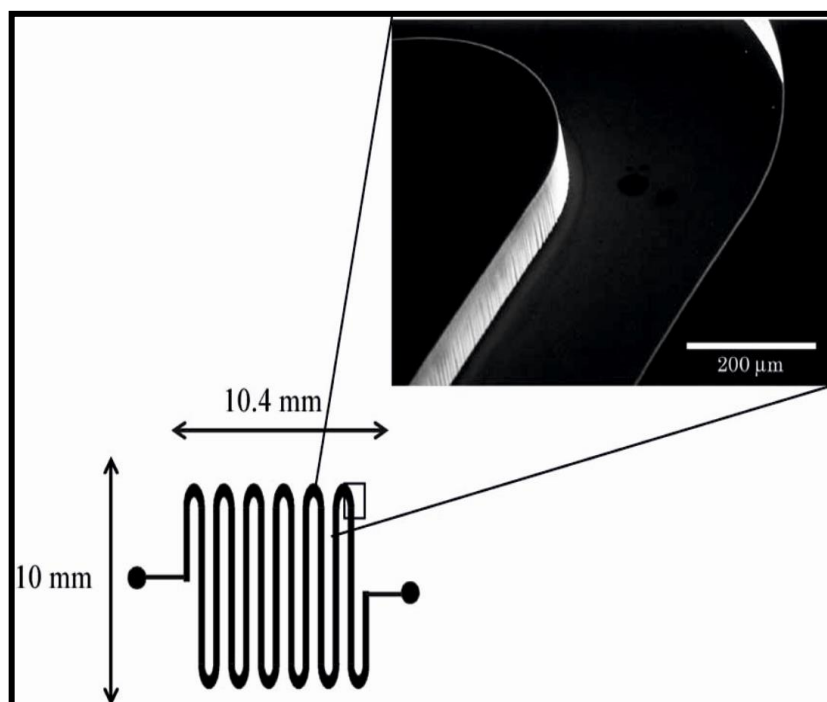


Figure 1-23: A microfluidic extraction chip channel 300 μm in width × 100 mm in depth; the diameter of the inlet and outlet holes is 1 mm.²⁰¹

After washing the channels with ultra-pure water to remove the proteins, the DNA was eluted by increasing the alkalinity of the elution buffer to pH 10.6 in order to neutralise the charge on the amine group and release the DNA. The extraction recovery of DNA using covalently bonded amine on the solid supports was 45% with AEEA and only 10% with APTES, because AEEA contains more amine groups than APTES. Although this was the first approach that avoided the use of chaotropic salts and organic solvents, the elution of DNA into a highly salted environment is problematic for subsequent PCR. More recently, in a similar approach, the bioactive polymer chitosan (obtained by the partial deacetylation of chitin) was covalently bound to silica surfaces to exploit an anion-exchange mechanism enabling DNA extraction.²⁰² The capture and release of DNA were controlled by protonation and deprotonation of the amino group on the chitosan (pK_a 6.3).²⁰³ At pH 5, the amino groups are in a protonated form which is more suitable for DNA binding, but at pH 9 (a suitable medium for subsequent PCR) the deprotonation form is dominant and hence DNA is released.^{204, 205} The chitosan method is ideal for extraction of a negatively charged molecule such as DNA (with 63% extraction recovery)²⁰² due to its hydrophilic nature and the presence of only one protonatable functional moiety (amino group), as shown in Figure 1-24. However, it is not ideal for positively charged molecules (such as drugs) when simultaneous extraction is required.

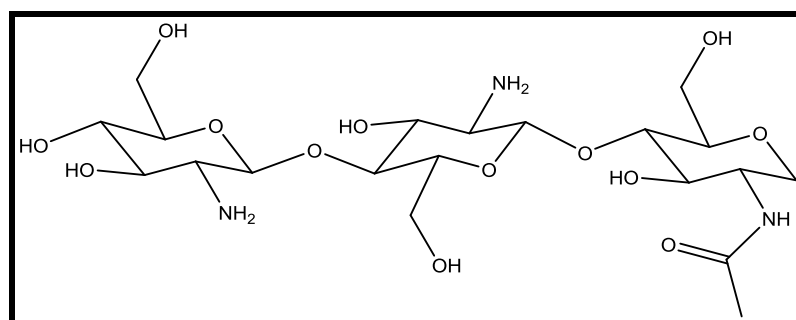


Figure 1-24: Structure of chitosan.²⁰⁶

In addition to DNA analysis, illicit drug investigations in relation to biological samples have become important tests following most forensic crimes. Therefore, the next section will focus on the extraction of amphetamines as one of the most commonly abused drugs.

1.5 Analysis of Drugs of Abuse

Drugs of abuse are a serious problem all over the world due to their risk to human health and security.²⁰⁷ In 2012, the United Nations Office on Drugs and Crime (UNODC) reported that more than 150 million people in the 15 to 64 age range consumed illicit drugs at least once during 2009 worldwide, with associated problems of drug dependency and drug-use disorders.²⁰⁸ Kintz *et al.*²⁰⁹ and Trujols *et al.*²¹⁰ have described drugs (both licit and illicit) as “chemical weapons” which can cure or kill based on the taken dose. According to a United Nations report on drug control, illicit drugs are those under international control (Schedule I and II) that are illegally produced and/or consumed.²¹¹ Drugs of abuse can be classified based on their pharmacological effects or their origin (see Figure 1-25). However, in forensic drug analysis, there are four pharmacological effect classifications which are encountered most frequently: hypnotics, such as benzodiazepines; stimulants, such as amphetamines; analgesics, such as opioids; and hallucinogens, such as cannabis.²¹²

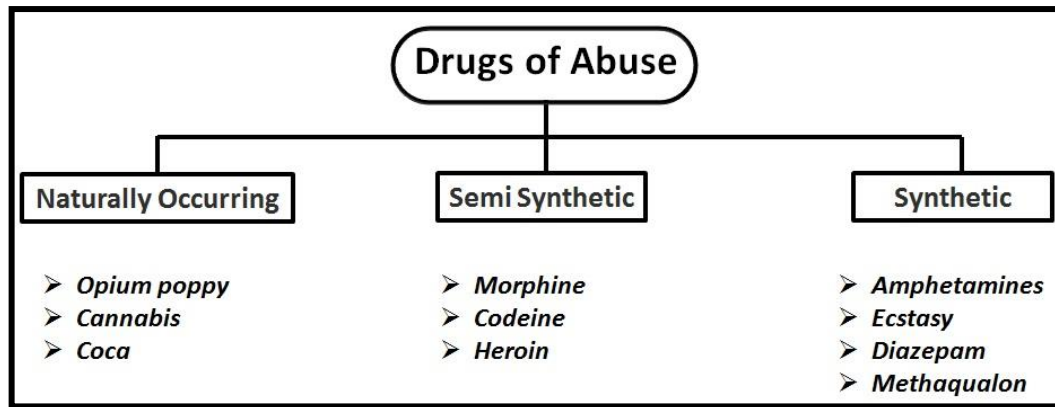


Figure 1-25: Schematic showing the classification of drugs of abuse according to their source.

Since the end of the Second World War (1945),²¹³ amphetamine-type stimulants have been abused across the world, with a dramatic increase in addiction among the young and are, therefore, considered to be one of the most trafficked illicit drugs in the world.^{214, 215} As well as common amphetamine (AM), there are derivatives such as methamphetamine (MA), 3,4-methylenedioxyamphetamine (MDA), and 3,4-methylenedioxymethamphetamine (MDMA, or ‘ecstasy’).²¹⁶ According to the 2013 Annual Report of the European Monitoring Centre for Drugs and Drug Addiction (EMCDDA), an estimated 2.5 million young adults used amphetamine and/or its related derivatives, such as ‘ecstasy’, during 2012.²¹⁷

Amphetamines are central nervous system (CNS) stimulants used illegally for their psychotropic effects (such as euphoria and increased alertness) and as doping agents in sports due to their sympathomimetic effects.^{13, 215} The general intoxication symptoms of amphetamines are as follows: dependence, hallucinations, depression, anxiety, hyperthermia, and cardiac arrhythmia, and may also cause death.^{218, 219}

Amphetamines are also frequently associated with violence and crime.²²⁰ Therefore, the presence of amphetamine and its related derivatives has become an important test in forensic investigation.²²¹ Twenty-four hours following oral consumption, about 30% of amphetamines are excreted with alkaline urine (pH 6-8) as a parent form of the drug, whereas in acidic urine (pH 5) this amount increases up to 74%.^{222, 223}

1.5.1 Screening test for amphetamine analysis

Immunoassays are the initial technique for detecting target molecules directly from different matrices based on antibody-antigen interaction.^{224, 225} Among several kinds of detection, including chromatographic techniques, these methods are rapid, simple, portable, and sensitive.²²⁶ The selectivity of immunochemical techniques depends on the specificity of the antibodies towards the target compound. In recent years, chemiluminescence (CL) reactions have been used to improve the detection sensitivity of conventional immunoassays such as enzyme-linked immunosorbent assays (ELISA) by up to three times.²²⁷

Since 2000, when Greenway *et al.*²²⁸ at the University of Hull introduced a microfluidic device for detecting codeine from an acetate buffer using CL, many efforts have been concerned with detecting amphetamines from biological samples within a microfluidic environment. In 2005, Far *et al.*²²⁹ reported the first use of ELISA with a chemiluminescent detection technique for the rapid and sensitive detection of amphetamine in urine and plasma using a disposable plastic microfluidic device with a total volume capacity of 7 μ l, as shown in Figure 1-26.

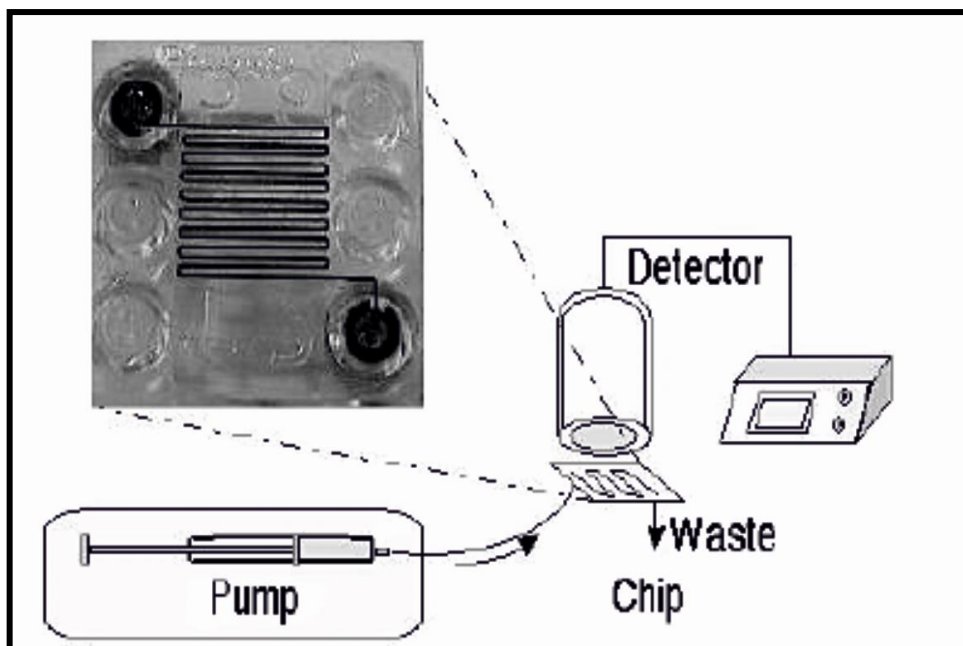


Figure 1-26: Schematic showing the experimental set-up of the development of a chemiluminescent ELISA technique within a microfluidic environment for the determination of amphetamine in plasma and urine samples. It consists of a syringe pump, microfluidic device, photodiode detector and readout device (Prolight Diagnostics AB, Lund, Sweden). The inset photograph shows the channel configuration of the microfluidic device.²²⁹

Briefly, samples (urine or plasma) that contained amphetamines (antigens) were mixed with a buffered solution of horseradish peroxidase-labelled amphetamine (amphetamine-HRP) and then flushed through microfluidic channels coated with anti-amphetamine monoclonal antibodies to allow antibody-antigen interaction. One of the advantages of microfluidics over a conventional set-up is that it reduces the antibody-antigen incubation time (competition phase) from a few hours to 10 minutes due to the small diffusion distances. The channels were washed to remove the unbound amphetamine and amphetamine-HRP. Finally, hydrogen peroxide and luminol were injected to produce a chemiluminescent reaction and determine the amounts of bonded amphetamine-HRP. The concentration of amphetamine was inversely proportional to the intensity of the emitted light signal that was identified

using a photodiode detector. Although the assay detection limits for urine and plasma are 20 and 6 $\mu\text{g l}^{-1}$, respectively, immunoassay reagents are expensive and the method cannot differentiate between the target drug and its derivatives. In addition, individual sample optimisation is required, e.g., urine samples need to be diluted 1:10 with phosphate buffered saline (PBS) at a high alkalinity (pH 9.2), whereas plasma requires a 1:4 dilution at pH 7.4 in order to reduce the effect of non-specific binding (NSB) of matrix components to the target antibodies.

1.5.2 Extraction of amphetamines

The detection of amphetamines in biological samples such as blood, urine, hair, stomach contents, and oral fluid is important for clinical treatments in the case of overdose toxicities or for forensic cases as evidence in court. Generally, urine is the most commonly used sample for drugs of abuse, such as amphetamines, because it can be obtained in larger volumes compared to other types of biological matrix.

Unlike blood withdrawal, urine is a non-invasive method of sample collection with a concentration of drugs generally higher than other types of sample; for example, relatively large amounts of amphetamine have been found in urine (200 times) compared to those in blood.²³⁰

An immunoassay is usually applied as a preliminary screening method for the rapid detection of drugs of abuse in urine without any requirement for sample pre-treatment. However, chromatographic techniques such as gas chromatography coupled with mass spectrometry (GC-MS) or HPLC coupled with UV or diode array detectors (DAD) have been employed as confirmatory methods for positive

immunoassay results in most forensic toxicology laboratories.²³¹ These chromatographic technologies require a sample preparation step in order to remove undesirable sample components that may block the system and to aid pre-concentration of the target analytes. The two main conventional techniques used for sample preparation are LLE and SPE. The formation of emulsion, the toxicity of the organic solvents used, and the inability of the method to be fully automated are, however, the most likely disadvantages associated with the LLE procedure, and, therefore, it has become less commonly used in forensic laboratories.²³²

SPE is, however, a widely used extraction method in different fields, including clinical and forensic toxicology.²³³ SPE overcomes the drawbacks of LLE as it requires low solvent volume, there is no emulsion formation, it can show high selectivity for analytes of interest, it is suitable for simultaneous extraction, and it can be automated.^{234, 235} As stated earlier in this chapter, polymer- and silica-based monoliths can be used as solid-phase materials. However, a silica-based monolith is the most suitable for the extraction of drugs of abuse. This is because it is more mechanically stable with organic solvents and more resistant to swelling or shrinking.²³⁶

Amphetamines are partially hydrophobic basic drugs with a pK_a value of almost 10; therefore, two mechanisms of interaction contribute to retaining analytes on a solid support.²³⁷ With alkaline urine or solvent (pH from 6 to 8), amphetamines are in a molecular (non-ionised) form and then adsorb to the hydrophobic moiety by Van der Waals interaction, whilst in an acidic medium (pH < 6) amphetamines are ionised and interact with the cationic-exchanger moiety by ion-exchange interaction.

In 1997, Lee *et al.* evaluated the extraction recoveries of commercial adsorbent cartridges using reversed-phase (C_8 and C_{18}), strong cation-exchanger (SCX), and C_8 -SCX mixed, to extract AM and MA from urine samples at different pHs.²³⁷ The highest extraction recoveries for both analytes ($> 85\%$) were obtained with a mixed-mode sorbent (C_8 -SCX) at pH 6, as shown in Table 1.2. With all types of sorbents, no AM or MA were recovered with strong acid (pH 3) or strong basic (pH 10) conditions due to the possibility of very tight adsorption. The optimum pH for both C_{18} and SCX was 7 to obtain high recovery for the target analytes (about 40%). Although high extraction recoveries were achieved using a mixed mode, the amount of urine sample required was high (5 ml), which is not applicable for limited forensic samples.

Table 1.2: Extraction recoveries of methamphetamine ($0.5 \mu\text{g ml}^{-1}$) and amphetamine ($0.2 \mu\text{g ml}^{-1}$) with different pH values using reversed-phase (C_8 and C_{18}), strong cation-exchanger (SCX), and C_8 -SCX mixed-phase sorbents.²³⁷

	C_8 -SCX mixture		SCX		C_8		C_{18}	
pH	MA% (RSD)	AM% (RSD)	MA% (RSD)	AM% (RSD)	MA% (RSD)	AM% (RSD)	MA% (RSD)	AM% (RSD)
5	76.7 (3.3)	74.8 (4.2)	10.8 (0.1)	11.5 (0.6)	61.4 (0.5)	63.7 (1.3)	16.3 (0.2)	18.1 (0.3)
6	86.8 (0.2)	88.1 (1.1)	20.3 (0.5)	21.4 (1.3)	19.7 (1.0)	21.3 (2.7)	31.5 (0.1)	32.8 (0.4)
7	61.5 (0.7)	63.2 (0.9)	48.7 (2.3)	40.2 (3.1)	10.2 (0.2)	13.4 (0.8)	40.9 (0.1)	40.2 (0.4)
9	40.7 (0.2)	43.1 (0.6)	12.8 (2.2)	15.4 (3.4)	ND	ND	ND	ND
10	ND	ND	ND	ND	ND	ND	ND	ND
11	ND	ND	ND	ND	ND	ND	ND	ND

MA: methamphetamine; RSD: relative standard deviation; AM: amphetamine; ND: not detected

Since solid-phase micro-extraction (SPME) was introduced by Pawliszyn *et al.* in 1989,²³⁸ more concern has been focused in the last 15 years to developing micro-sample preparation techniques using silica materials for forensic samples with special emphasis on drugs of abuse extraction (including amphetamines). In 2004, Namera *et al.* illustrated the use of an octadecylated silica-based monolith column (TMOS) mounted inside a syringe needle for the extraction of MA from a urine sample (see Figure 1-27).²³⁹ In the loading step, a mixture of urine (150 μ l) and buffer (300 μ l, pH 10.2) was introduced into a monolithic column by pulling the syringe plunger and holding for 30 minutes to allow contact between the aqueous sample and the surface of the solid-phase. The monolithic column was then removed from the connector to dry under a vacuum pump for 10 seconds. Finally, the target analyte was desorbed by pushing 10 μ l of organic solvent through using a new syringe. This approach extracted the MA with a high recovery rate (90%). However, the process was time consuming due to the sample filtration step to avoid blockage within the tube and the requirement for incubation. In addition, the use of a high alkaline buffer (pH 10.2) can dissolve a silica-based monolith.

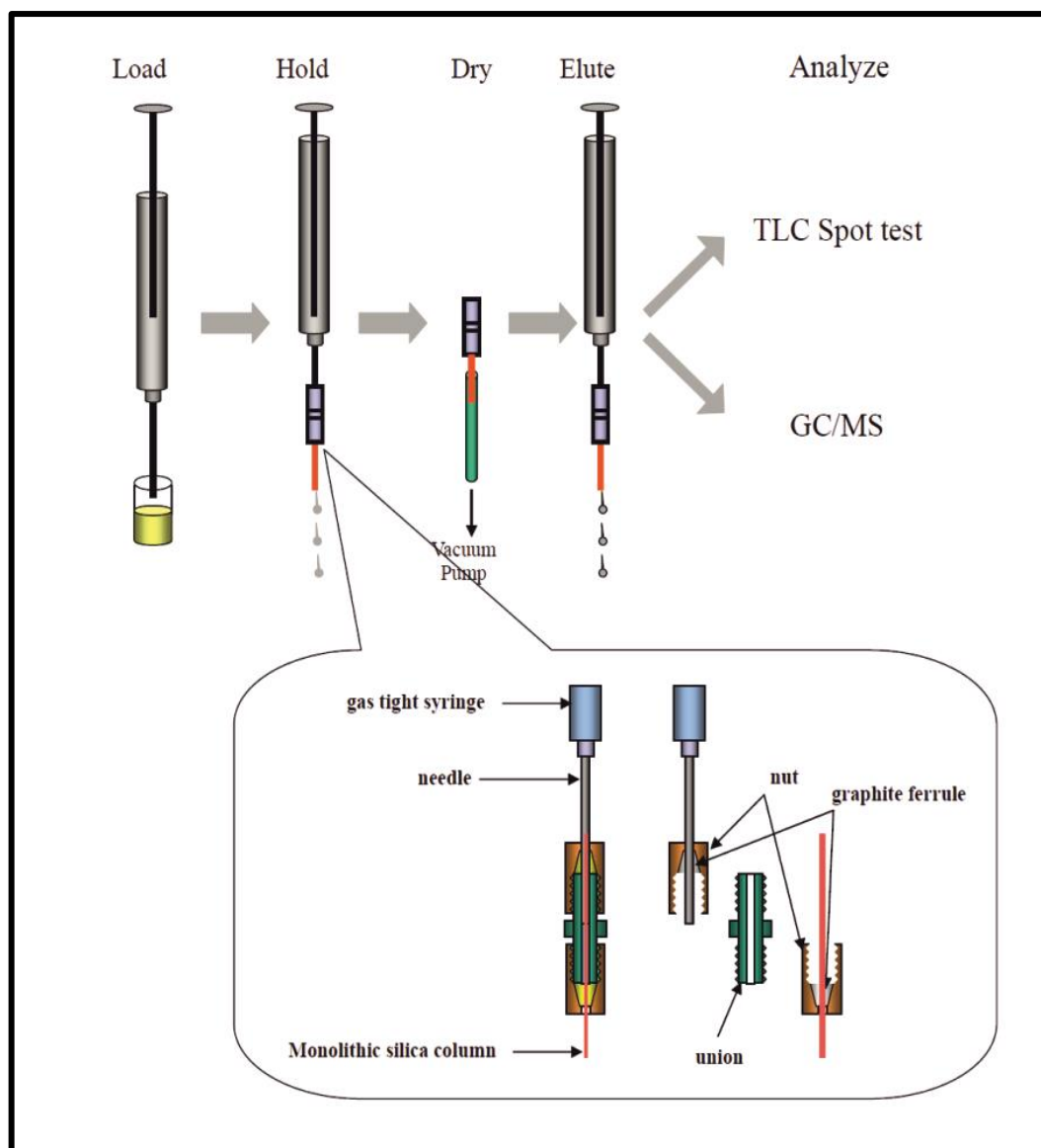


Figure 1-27: Schematic drawing of the extraction stages of methamphetamine using a packed syringe needle with octadecylated monolith.²³⁹

Kumazawa *et al.*²⁴⁰ developed a monolithic silica extraction pipette tip for the simultaneous determination of AM and MA. In this device, a fabricated TEOS monolithic silica bar was cut and fixed inside the end of 200 μ l pipette tips using supersonic adhesion and the monolithic silica surface was then chemically modified with an octadecyl group to give a reversed-phase interaction.

The results showed that the pipette tips containing the C₁₈-bonded monolithic silica had the ability to purify AM and MA from a urine sample (500 µl) containing 1 M sodium hydroxide with an extraction recovery of 82.2 and 82.9%, respectively. Although the SPE pipette tips are simpler than conventional SPE cartridges, 25 aspirating/dispensing cycles are required to reach equilibrium between the sample and the extraction phase, rendering this procedure a time-consuming process.

A spin column packed with a C₁₈-bonded monolithic silica disk column (TEOS) was developed by Namera *et al.*¹⁰⁸ for the extraction of amphetamines from urine samples (500 µl), as shown in Figure 1-28. The proposed method was used for extracting AM, MA, MDA, and MDMA by adjusting the urine to pH 10 to achieve recoveries of 92%, 93%, 99%, and 83%, respectively. Multi-step centrifugations (conditioning of the solid-phase, sample loading, washing, and elution of target drugs) and a large sample volume were required with a high alkalinity medium, which represented the major drawbacks of this method.

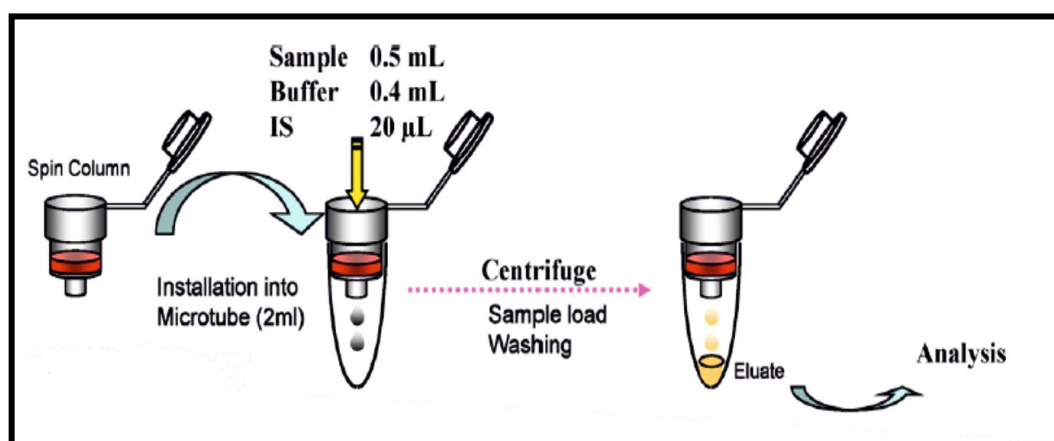


Figure 1-28: Schematic diagram showing the procedures for the extraction of amphetamines from urine using a monolithic silica disk in a microtube holder.¹⁰⁸

1.6 Aims of the PhD Project

A limited sample volume is a potential problem associated with most of the biological samples recovered at the scene of a crime in order to perform genetic analysis and drugs of abuse investigation. While much literature is available on the miniaturisation of each of the individual extraction techniques for DNA and illicit drugs analysis, no combined extraction has been reported at any level of sample volume. The overall aim of the present study was to develop a reliable solid-phase extraction method for the combined analysis of DNA and four amphetamines in a limited sample volume using a single experimental process. The specific aims of this project can be summarised as follows:

- An evaluation of a microfluidic system containing an inorganic silica-based monolith (potassium silicate) for the extraction of DNA from a small number of cells without the use of carrier RNA.
- An assessment of silica-based monolith selectivity when a mixture of human and mouse DNA at varying ratios is extracted.
- Development and validation of a simultaneous extraction method for four amphetamines of interest from low-volume samples (50 µl) using silica material followed by HPLC with UV-detector analysis.
- Development of a combined method for the independent purification of four amphetamines and DNA from a low-volume sample.

The work presented in this thesis is divided into different sections. Firstly, the materials, instrumentation and methods used are described in the Methodology chapter. Secondly, the two Results chapters, which are divided into two main sections presenting and discussing results obtained during the experimental work

performed for the DNA extraction, followed by combined DNA and drug extraction. The Conclusions chapter summarises the main results findings with regard to other research. The strengths and limitations of this thesis are considered and suggested under Future work. All literature sources used in this thesis are listed in the References section. Finally, the Publications and Presentations containing scientific publications related to the work described here.

2 Methodology

This chapter describes the experimental techniques and procedures used for the work described in this thesis, detailing (2.1) the chemicals, (2.2) instrumentation and materials, (2.3) microfluidic chip fabrication, (2.4) DNA analysis and (2.5) drugs analysis.

2.1 Chemicals

The solvents and reagents used were purchased from the suppliers as shown in Table 2.1. All chemicals were of analytical grade and used as supplied, without any further purification.

Table 2.1: Chemicals, solvents and reagents used.

Chemical	Supplier
<i>Photolithography and wet etching</i>	
Ammonium fluoride (40%)	Fisher Scientific, Leicestershire, UK
Chrome Etch 18	Chestech Ltd, Warwickshire, UK
Hydrofluoric acid (4%)	Fisher Scientific, Leicestershire, UK
Microposit Developer Concentrate	Chestech Ltd, Warwickshire, UK
Microposit Remover 1165	Chestech Ltd, Warwickshire, UK
<i>DNA analysis</i>	
2-(N-morpholino) ethanesulfonic acid (MES)	Sigma-Aldrich, UK
Agarose multipurpose	Bioline, UK
Bovine serum albumin (BSA)	NEB Inc., UK
Deoxyribonucleotide triphosphates (dNTPs)	Bioline, UK
Endorsing ink	Niceday, USA
Epoxy resin	National Adhesives, Eastleigh, UK
Ethidium bromide (EtBr)	Fisher Scientific, UK
Ethylenediaminetetraacetic acid (EDTA)	Sigma-Aldrich, UK
Formamide	Avocado Research Chemicals Ltd, UK

Glycerol	Sigma-Aldrich, UK
GoTaq [®] Hot Start Polymerase	Promega, UK
Guanidine hydrochloride (GuHCl)	Promega Corporation, USA
HyperLadder [™]	Bioline, UK
Loading dye	MBI Fermentas, Canada
<i>Mus musculus</i> cells	LGC Promochem, Middlesex, UK
Potassium silicate solution	VWR International, UK
Primers	Eurofins MWG Operon, Germany
QIAamp [®] DNA Blood Mini Kit	Qiagen, UK
Quant-iT [™] dsDNA High Sensitivity	Invitrogen, UK
Sodium bicarbonate	Fisher Scientific, UK
Sodium carbonate	Fisher Scientific, UK
Tris (hydroxymethyl) aminomethane	Fisher Scientific, UK
Trypan blue	Sigma-Aldrich, UK
Ultra-pure water	Elga Ltd, High Wycombe, UK
<i>Drugs analysis</i>	
(+)-methamphetamine hydrochloride	Sigma-Aldrich, UK
2,6-lutidine	Sigma-Aldrich, UK
3,4-methylenedioxyamphetamine hydrochloride (MDMA)	Sigma-Aldrich, UK
3,4-methylenedioxy-N-ethylamphetamine hydrochloride (MDA)	Sigma-Aldrich, UK
3-glycidioxypropylmethylsilane	Sigma-Aldrich, UK
Acetonitrile	Fisher Scientific, UK
Chloro(dimethyl)octadecylsilane	Sigma-Aldrich, UK
DL-amphetamine hydrochloride	Sigma-Aldrich, UK
Hydrochloric acid	Fisher Scientific, UK
Lysine	Sigma-Aldrich, UK
Methanol	Sigma-Aldrich, UK
Phosphoric acid	Sigma-Aldrich, UK
Silica beads	Sigma-Aldrich, UK
Sodium acetate	Sigma-Aldrich, UK
Sodium hydroxide	Merck, UK
Sodium phosphate dibasic	Sigma-Aldrich, UK
Sodium phosphate monobasic	Sigma-Aldrich, UK
Tetrahydrofuran	Fisher Scientific, UK
Toluene anhydrous (99.8%)	Sigma-Aldrich, UK
Triethylamine	Fisher Scientific, UK

2.2 Instrumentation and Materials

The instrumentation and materials used for all experiments are listed in Table 2.2.

The instrumental set-up and procedures are described in the subsequent sections.

Table 2.2: Specialised instruments and materials used.

Instrument/material	Supplier
<i>Photolithography and wet etching</i>	
B-270 glass	Telic Co., USA
Diamond drill	Drill Service Ltd, Horley, Surrey, UK
Furnace	EF3, Vecstar Furnaces, Chesterfield, UK
Photomask	JD Photo-Tools Printer, Lancashire, UK
Ultraviolet lamp	Mega Electronics, Cambridge, UK
<i>DNA analysis</i>	
BabyBee™ syringe drivers	Bioanalytical Systems Inc., UK
Disposable plastic syringe	BD Plastipak™, Spain
Eppendorf tube	VWR, Leicestershire, UK
EVO 60 scanning electron microscope (SEM)	EVO 60, Carl Zeiss Ltd, UK
Ethylene-tetrafluoroethylene	Upchurch Scientific, UK
Female luer lock adapter	Kinesis, UK
FLUOstar Optima Plate Reader	BMG Labtech, UK
Gas-tight luer lock syringe	Supelco, Sigma-Aldrich, UK
Gilson™ GVLab Fixed-Speed Vortex Mixer	Fisher Scientific, UK
Glass capillary (0.6 ± 0.05 mm ID)	Brand GMBH, Germany
Hettich EBA 21 centrifuge	DJB Labcare Ltd, UK
HU15 horizontal electrophoresis tank	Scie-Plas, UK
Micropipettes	Eppendorf, UK
Microtiter plate	Scientific Laboratory Supplies Ltd, UK
Neubauer haemocytometer	Weber Scientific International Ltd, UK
Omni Swab™	Whatman, UK
Oven	Scientific Laboratory Supplies Ltd, UK

pH meter	Fisherman Hydrus 300, Thermo Orion, USA
SEMPRP 2 sputter coater	Nanotechnology Ltd, UK
Spectrafuge™ mini-centrifuge	Sigma-Aldrich, UK
Surface area and porosity analyser	Micromeritics Ltd, UK
Techne® Endurance TC-312 Thermal Cycler	TC-312 benchtop thermal cycler, Techne, UK
Two-piece fingertight fitting	Upchurch Scientific, UK
Ultraviolet light transilluminator	Syngene, UK
<i>Drugs analysis</i>	
785A UV/Visible Detector for HPLC	PerkinElmer, California, USA
Fused quartz cuvette	Fisher Scientific, UK
Hot plate-stirrer	VWR International, USA
LC 200 series binary pump	PerkinElmer, California, USA
Prodigy™ 5 µm ODS-2 150 Å, LC Column (150 x 4.6 mm)	Phenomenex Inc. (Torrance, CA, USA)
Ultraviolet-visible (UV-Vis) spectroscopy	PerkinElmer, California, USA

2.3 Microfluidic Chip Fabrication

The glass microfluidic devices used were fabricated at the University of Hull by Dr Steve Clark using photolithography and wet-etching processes, as described previously.¹³² A schematic of the fabrication process used is shown in Figure 2-1. AutoCAD software was used to design the geometry of the microfluidic chip channels required and the design was then printed as a photomask film using JD Photo-Tools. The mask was then placed over the top of a 1 mm thick piece of B-270 glass pre-coated with photoresist and chrome layers (total thickness of 120 nm). The design pattern was transferred by exposing the photoresist layer to UV light for 1 minute in a dark room. The wafer was then submerged in Microposit® Developer Concentrate diluted in a 1:1 ratio with purified water for 1 minute, followed by immersion in Chrome Etch 18 solution for a further 1 minute to remove the exposed photoresist layer and etched away uncovered chrome.

A glass etching solution consisting of 1% hydrofluoric acid/5% ammonium fluoride at 65 °C was then used to etch the exposed glass isotropically to the required depth (etch rate was approximately $5 \mu\text{m min}^{-1}$). The remaining photoresist and chrome layers were then removed using Microposit[®] Remover 1165 and Chrome Etch 18 solution, respectively. Access holes were drilled into the top glass cover plate using diamond drill bits. The etched base and drilled glass cover plates were thermally bonded together at 595 °C for 3 hours to complete the fabrication process.

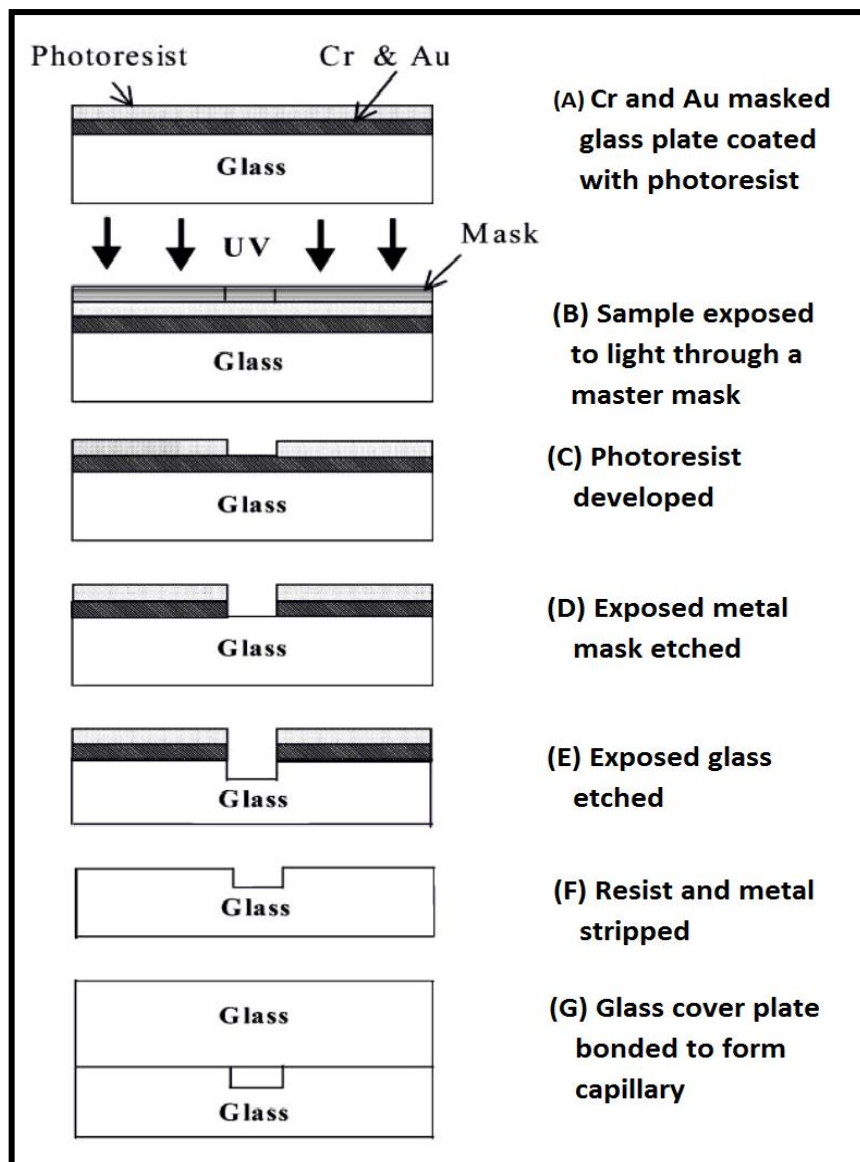


Figure 2-1: Schematic diagram of the process used for the production of glass microfluidic devices using a wet-etching technique.²⁴¹

2.3.1 Microfluidic chip design

The microfluidic device designs used were obtained from a previous project carried out at the University of Hull.¹⁵⁹ Hexagonal DNA extraction chambers (4 mm wide, 8 mm long and 100 μm deep) were fabricated in glass using the method described in section 2.3 with channel dimensions of 230 μm wide, 8-12 mm long and 100 μm deep (Figure 2-2). The volume of the extraction chamber was 2.4 μl . Access holes 1.5 mm in diameter were drilled in the glass top plate in order to allow the microfluidic device to be connected to a hydrodynamic syringe pump.

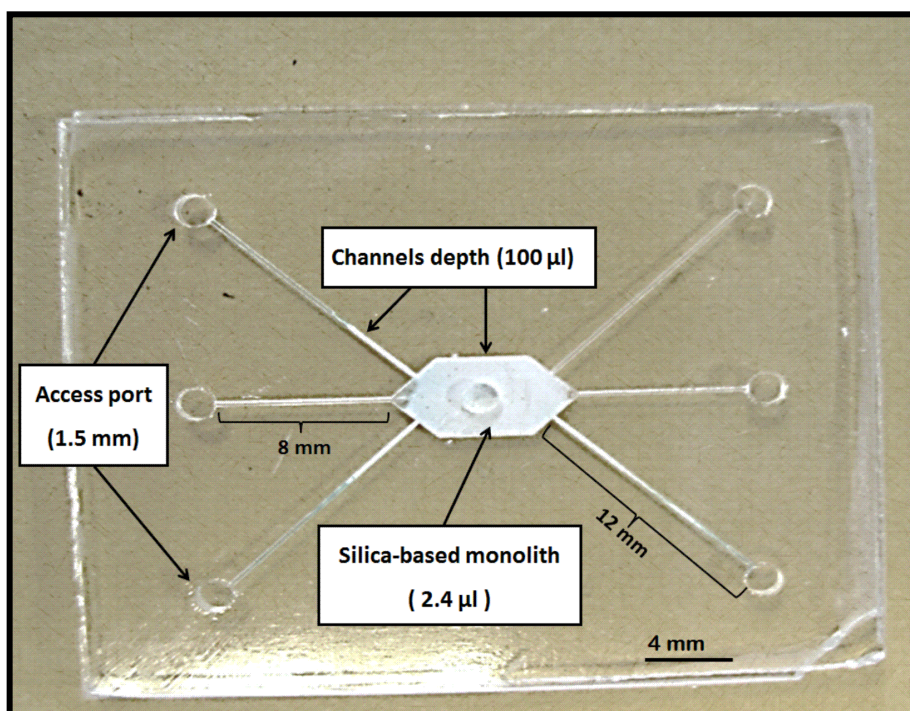


Figure 2-2: Photograph showing the glass microfluidic device for DNA extraction. The extraction is performed in the hexagonal chamber where the silica monolith is constructed.

2.4 DNA Analysis

2.4.1 DNA sources and preparation

Two types of cell were used in this work to represent the kind of biological sample that may be found at a crime scene: human cells and animal (mouse) cells.

2.4.1.1 Human cells

Omni Swab™ was used to collect human DNA from buccal cells by lightly scraping the inside cheek of a volunteer. Genomic DNA was isolated using a QIAamp® DNA Blood Mini Kit.²⁴² The sampling end of the Omni Swab™ was placed into a 2 ml microcentrifuge tube and 600 µl phosphate buffered saline (PBS) was added to the sample; 20 µl Proteinase K (> 600 mAU ml⁻¹) and 600 µl AL (lysis buffer) aliquots were added to the sample prior to incubation at 56 °C for 10 minutes. Next, 600 µl of ethanol (96-100%) was added and all the components were mixed together by vortexing. The lysate was then transferred into a QIAamp Mini spin™ column and centrifuged to remove the filtrate. The column was then washed sequentially with AW1 (containing alcohol and chaotropic salt) and AW2 (containing alcohol and sodium azide) buffers before the DNA was eluted in water.

2.4.1.2 Mouse cells

Mus musculus cells grown in American Type Culture Collection (ATCC)-formulated Eagle's minimum essential medium (EMEM) were provided by the Department of Biology at the University of Hull. Cell populations were counted using an improved Neubauer haemocytometer (Figure 2-3) and then diluted in EMEM to produce a range of cell numbers (diluted down from a maximum working concentration of

1500 cells mL^{-1}). The cells were then pelleted and the supernatant removed prior to the cells being frozen at $-20\text{ }^{\circ}\text{C}$ until required.

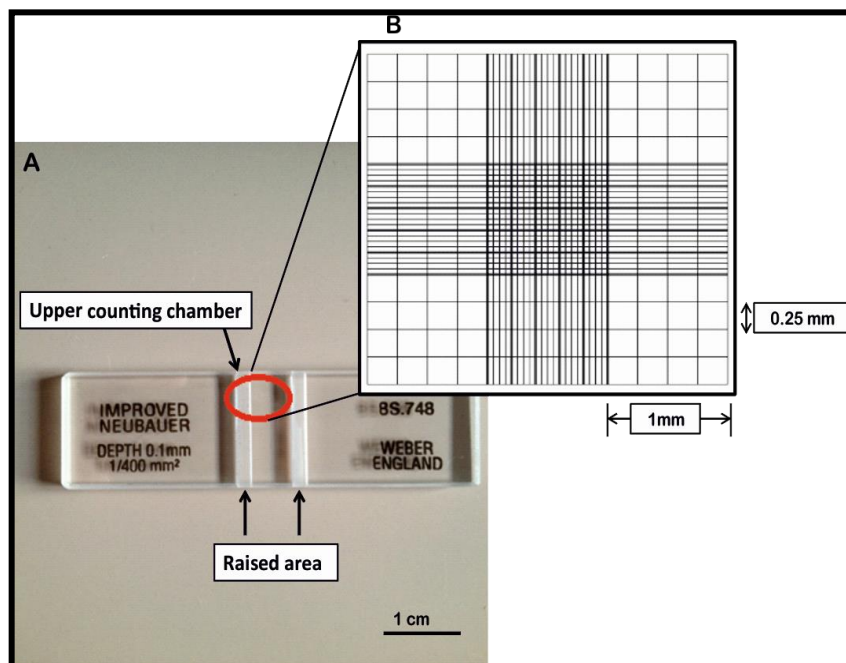


Figure 2-3: A) Photograph of the Neubauer improved haemocytometer, B) grid layout of the counting chamber.

2.4.2 Microfluidic chip-based solid-phase extraction

2.4.2.1 Preparation of the silica monoliths

Thermally activated silica-based monoliths were fabricated within the microfluidic device following the procedure described by Shaw *et al.*¹⁰³ A thick mixture of potassium silicate and formamide solutions was prepared in a 10:1 (v/v) ratio by continuous mixing at room temperature. The device was then filled with glycerol coloured with endorsing ink for visualisation and the extraction chamber was slowly filled with the monolith solution until the glycerol had been displaced from the hexagonal cavity into the attached channels.

The monolith was cured in an oven at different temperatures (100, 90 and 80 °C) for 15 minutes and then the glycerol was flushed from the channels using an empty 1 ml plastic syringe.

The microfluidic device was then returned to the oven for overnight incubation to complete the formation of the solid monolith. The entire device was cleaned and prepared for extraction by flushing with deionised water and then drying for 15 minutes at 40 °C. A 50 μ l gas-tight luer lock syringe was connected to a two-piece finger-tight fitting and ethylene-tetrafluoroethylene (ETFE 1/16 inch OD x 0.17 mm ID) tubing to the inlet reservoir on one side of the microfluidic device. The outlet on the opposite side of the device was used to collect the sample. Epoxy resin was used to hold the ETFE tubing in the drilled holes and to block the other holes. Hydrodynamic pumping was carried out using BabyBee™ syringe drivers to control the flow rate injection as shown in Figure 2-4.

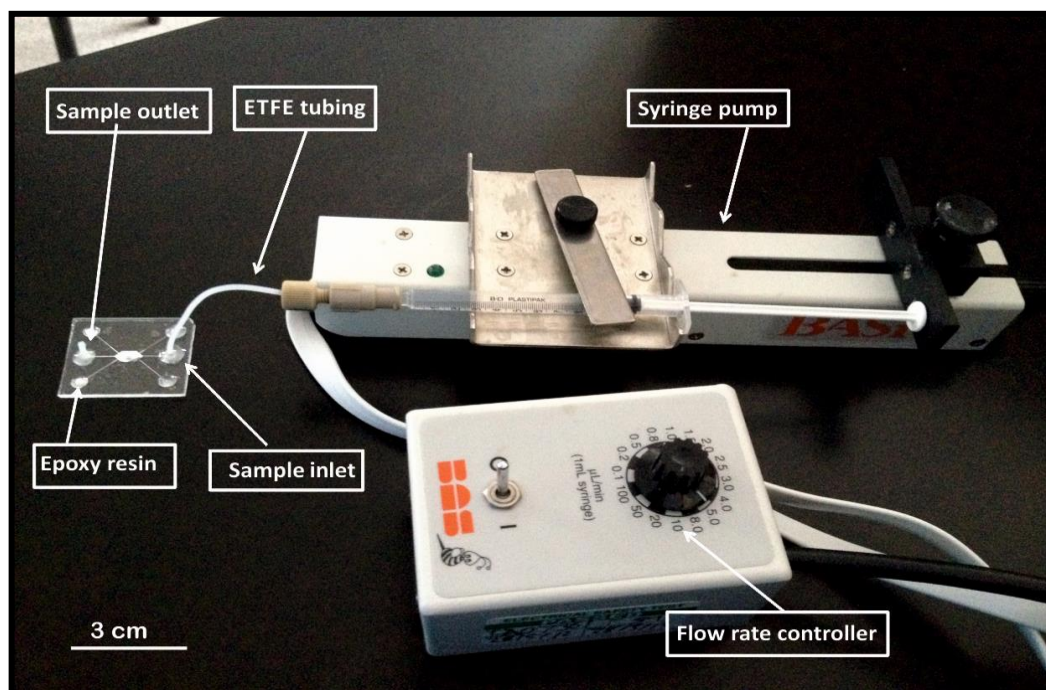


Figure 2-4: Photograph showing the hydrodynamic pumping apparatus on the microfluidic device used to perform DNA extraction.

2.4.2.2 Physical characterisation of the silica-based monolith

Scanning electron microscopy (SEM) was used to observe the morphology of the monoliths. Prior to analysis, a monolith was coated with a 2 nm gold-platinum layer using a SEMPREP 2 sputter coater to provide conductivity and protect the sample from beam damage, and then images were taken using a fixed voltage of 20 kV. In addition, a Brunauer-Emmett-Teller (BET) model using a surface area and porosity analyser was used to study the physical properties of the monoliths. The surface area was calculated using BET isotherms of nitrogen adsorption and desorption at 77 K (Kelvin). The pore volume and pore size distribution were calculated on a nanometre scale from nitrogen adsorption isotherms using the BJH (Barrett-Joyner-Halenda) model.

2.4.3 DNA extraction protocol

DNA extraction was performed following the previous work procedure but with optimised elution solutions.¹⁵⁸ The surface of the monolith was activated with 5 M GuHCl in TE buffer (10 mM Tris, 1 mM EDTA; pH 6.7) for 30 minutes at a flow rate of 5 $\mu\text{l min}^{-1}$. Biological samples (human DNA, mouse DNA, or mixed human and mouse DNA) were diluted with 5 M GuHCl in a 1:9 ratio (v/v) and the mixture was pumped through the microfluidic device using a 50 μl glass syringe at a flow rate of 2.5 $\mu\text{l min}^{-1}$ to achieve DNA adsorption onto the silica surface. Cellular and proteinaceous debris that would inhibit the PCR amplification was removed using 80% ethanol at a flow rate of 5 $\mu\text{l min}^{-1}$. Finally, deionised water or a low ionic strength buffer (10 mM TE at pH 8.5)²⁴³ was pumped through the device at a flow rate of 1 $\mu\text{l min}^{-1}$ to elute the adsorbed DNA off the monolith.¹⁵⁹

All analyte fractions from loading, washing and elution were collected in 2 μl aliquots and quantified for DNA.

2.4.4 DNA quantification

A Quant-iT™ dsDNA High Sensitivity Assay Kit was used to quantify the DNA that had been extracted. PicoGreen® is a fluorochrome with maximum excitation at 480 nm and emission at 520 nm when intercalated with double-stranded DNA.²⁴⁴ A working solution of PicoGreen® dye was prepared by mixing Quant-iT™ reagent with Quant-iT™ buffer in a 1:200 ratio (v/v). The reaction was carried out in a 96-well microtiter plate by adding 100 μl of working solution to 2 μl of extracted DNA. After 5-minute incubation in the dark, the fluorescence emission at 520 nm was measured using a FLUOstar Optima Plate Reader, the output from which is shown in Figure 2-5. A calibration curve was constructed using the different DNA standard concentrations supplied with the kit (10, 8, 6, 4, 2, 1, and 0.5 $\text{ng } \mu\text{l}^{-1}$) along with a blank (0.0 $\text{ng } \mu\text{l}^{-1}$) to quantify the DNA present (Figure 2-6). The DNA extraction efficiency was calculated as the percentage of DNA recovered during the elution step over the total amount of DNA introduced into the device.

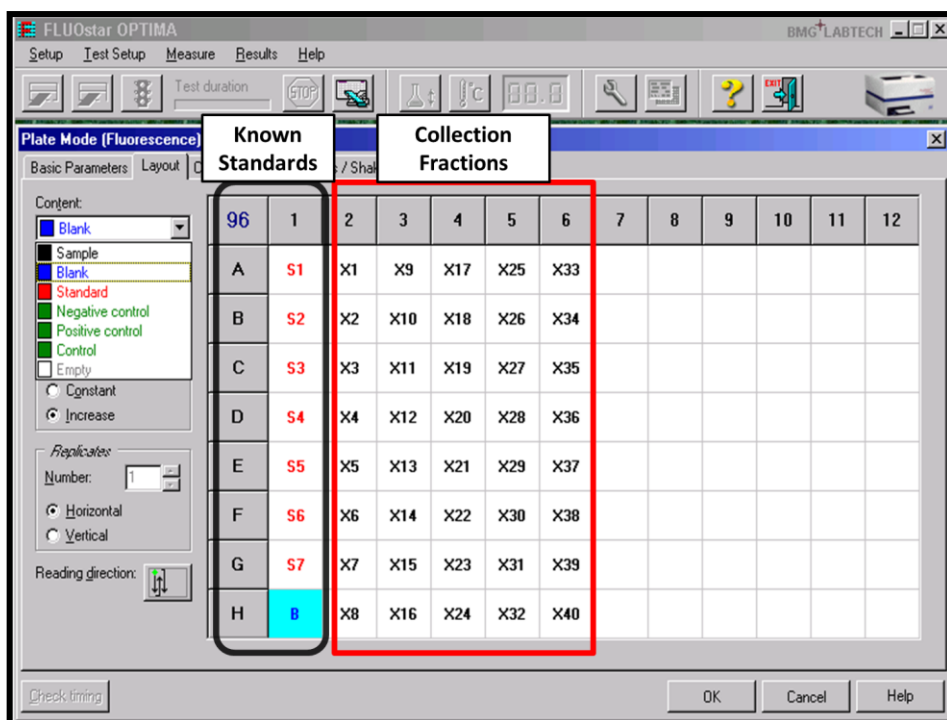


Figure 2-5: Screenshot showing the FLUOstar software and the position of the standards, blank and samples following their positions on a 96-well plate.

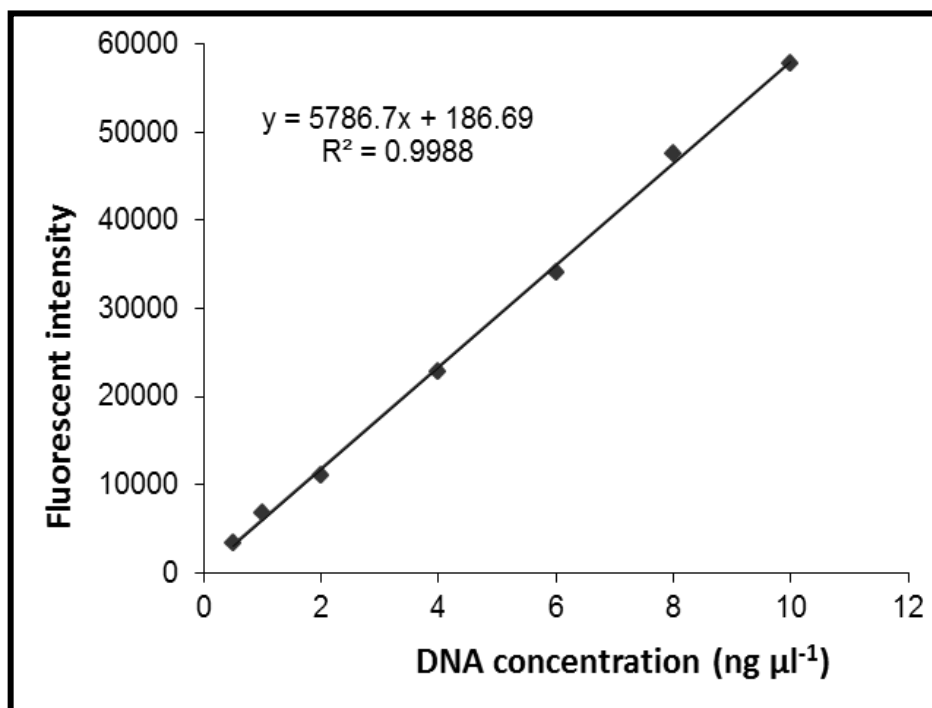


Figure 2-6: Quant-iT™ PicoGreen® dsDNA assay calibration curve. The fluorochrome was excited at 480 nm and the fluorescence emission intensity measured at 520 nm using a spectrofluorometer.

2.4.5 DNA amplification

Following DNA quantitation, PCR amplification was carried out (off chip) using a Techne[®] Endurance TC-312 Thermal Cycler to evaluate the quantity and integrity of the extracted DNA. Forward and reverse primers were designed to amplify four loci: the human Amelogenin gender marker, D21 S11 and TH01, and mouse β -actin (Table 2.3).

Table 2.3: Primer sequences used in a standard thermal cycler to amplify human Amelogenin, D21 S11 and TH01, and mouse β -actin.

Oligonucleotide	Sequence (5`-3`)
Human Amelogenin	Forward: CCCTGGGCTCTGTAAAGAA (19) Reverse : ATCAGAGCTTAAACTGGGAAGCTG (24)
Human D21 S11	Forward: TGTATTAGTCAATGTTCTCCAGAGAC (26) Reverse : ATATGTGAGTCAATTCCCAAG (22)
Human TH01	Forward: GTGATTCCCATTTGGCCTGTTTC (21) Reverse : ATTCCTGTGGGCTGAAAAGCTC (22)
Mouse β -actin	Forward: GCAGCTCCTTCGTTGCCGGT (20) Reverse : CCCGCCCATGGTGTCCGTTTC (20)

The following concentrations were used over ice to prepare the PCR master mix that was used for each separate experiment (Table 2.4).

Table 2.4: Concentrations of master mix reagent components.

PCR component	Stock concentration	Final concentration in 10 μ l reaction component
GoTaq [®] buffer (pH 8.6)	5 X	1 X
GoTaq [®] Hot Start Polymerase	5 U μ l ⁻¹	0.1 U μ l ⁻¹
MgCl ₂	25 mM	1 mM
Bovine serum albumin (BSA)	2 μ g μ l ⁻¹	0.2 μ g μ l ⁻¹
Deoxyribonucleotide triphosphates (dNTPs)	10 mM each of ATP, CTP, GTP and TTP	200 μ M each of ATP, CTP, GTP and TTP
Primers: forward and reverse	10 μ M	0.5 μ M

The total volume of each reaction was made up to 10 μl using purified water. An initial PCR experiment was performed on a conventional PCR instrument (TC-312 Benchtop Thermal Cycler) set at the following programmed temperatures:

Initial denaturation: 95 °C for 2 min

PCR: 95 °C for 1 min
60 °C for 1 min
72 °C for 1 min } for 35 cycles

Final extension: 60 °C for 7 min

DNA amplifications were confirmed by gel electrophoresis.

2.4.6 Agarose gel electrophoresis

Gel electrophoresis was used to separate and visualise the PCR products as described in a previous project carried out at the University of Hull.¹⁵⁹ An agarose gel was prepared by dissolving 2% agarose powder (w/v) in 0.5 X TBE buffer (45 mM Tris, 45 mM borate, 1 mM EDTA buffer; pH 8.3) and heating the mixture in a microwave oven for 2 minutes to produce a clear solution. The solidified gel was placed in an HU15 standard horizontal electrophoresis tank filled with sufficient 0.5 X TBE buffer to cover the gel (Figure 2-7). A loading solution of PCR products along with positive and negative controls was prepared by mixing 3 μl of sample with 3 μl of loading dye solution. A 5 μl HyperLadder™ II DNA molecular weight marker with bands ranging from 1000 bp to 100 bp was also loaded for size determination.

The DNA molecules were separated under an electrical field at 100 V until adequate separation had been achieved and then the gel was stained with ethidium bromide (50 μ l in 100 ml 0.5 X TBE buffer) for 20 minutes and then visualised by a UV light transilluminator.

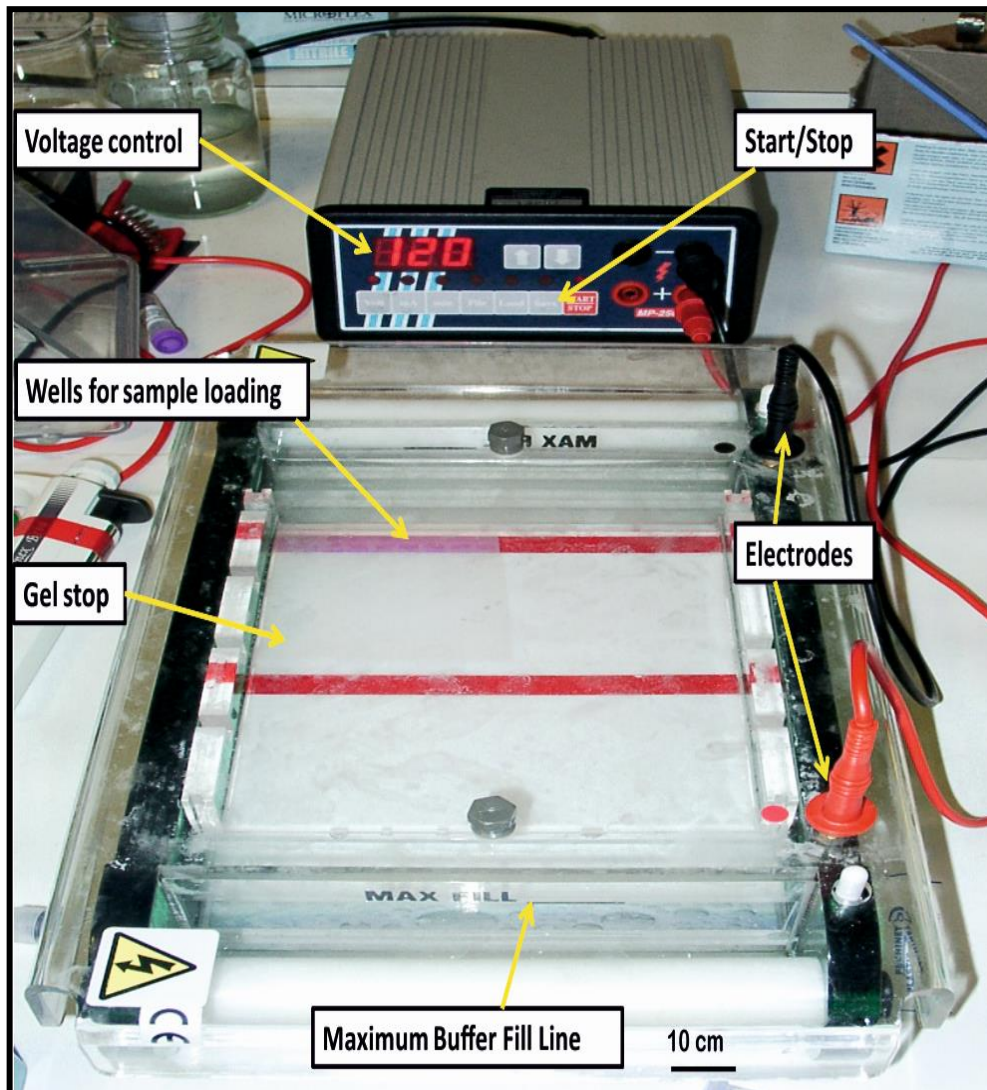


Figure 2-7: Photograph showing the components required for gel electrophoresis.

2.5 Drugs Analysis

2.5.1 Modification of the silica monolith surface

2.5.1.1 Chemical modification with lysine groups

A 1 cm thermally activated silica-based monolith was produced in a glass capillary (0.6 ± 0.05 mm ID) and chemically modified *in situ* with lysine. This was achieved by first modifying the monolith with γ -glycidoxypropyltrimethoxysilane (GPTMS) to add epoxy groups to the silica surface and then lysine was covalently incorporated into the silica skeleton via an epoxy ring-opening reaction (the reaction scheme is showing on page 129). The procedure of the monolithic surface modification was carried out as follows:²⁴⁵

1. A mixture of 1 ml of GPTMS and 50 μ l of 2,6-lutidine (catalyst; 99%) was added to 20 ml of dried toluene (99.8%) and pushed through the monolith using a syringe pump at a flow rate of 2 μ l min^{-1} for 1 hour. The monolith was then placed in an oven at 110 °C for 1 hour; this step was repeated three times and the final reaction took 15 hours. The epoxy monolith was cooled at room temperature and rinsed with 1 ml toluene and methanol, respectively, to remove any residue.
2. To convert the epoxy groups to diols, the monolith was pumped with 0.1 mol l^{-1} hydrochloric acid at 2 μ l min^{-1} for 15 hours and then placed in an oven at 60 °C for 2 hours. The modified monolith was then washed with 1 ml of water and 1 ml of methanol at a 2 μ l min^{-1} flow rate in order to remove any excess acid.
3. The modification of the monolith surface with lysine was performed by continuously flowing a mixture of 1 M lysine solution through the monolith at

$2 \mu\text{l min}^{-1}$ for 2 hours and was then placed in an oven at $75 \text{ }^\circ\text{C}$ for a further 2 hours. This step was repeated three times with the final reaction being carried out for 15 hours at room temperature. The 1 M lysine solution was prepared by dissolving 4.38 g of lysine ($> 98\%$) in 30 ml of 50 mmol l^{-1} phosphate buffer (0.1 ml of 1 M NaH_2PO_4 was added to 1.4 ml of 1 M Na_2HPO_4 ; pH 8).

4. The resulting lysine-bonded phase was rinsed with water and methanol prior to use.

2.5.1.2 Chemical modification with C_{18} groups

In order to obtain the reversed phase, silica beads and silica-based monolith were chemically modified using octadecyl groups (see reaction scheme on page 144), as described previously.²⁴⁶ The surfaces of the silica beads were chemically modified with C_{18} ligands by continuous stirring of a mixture of 1 g chloro(dimethyl)octadecylsilane and 10 ml dried toluene at $80 \text{ }^\circ\text{C}$ for 6 hours using a hot plate-stirrer. The silica beads were then washed with dried toluene, tetrahydrofuran (THF; 99.9%), methanol (100%), 50/50 (v/v) methanol/water, and methanol (100%) in sequence and dried in an oven at $40 \text{ }^\circ\text{C}$ for 15 hours. The C_{18} -modified silica beads (0.01 g) were packed inside a female luer lock adaptor and held in place using a glass fibre frit, as shown in Figure 2-8. In addition, the derivatisation of the surface of the silica-based monolith inside the glass capillary ($0.6 \pm 0.05 \text{ mm ID}$) with octadecyl groups was performed as described above using a syringe pump at a low flow rate ($1 \mu\text{l min}^{-1}$).

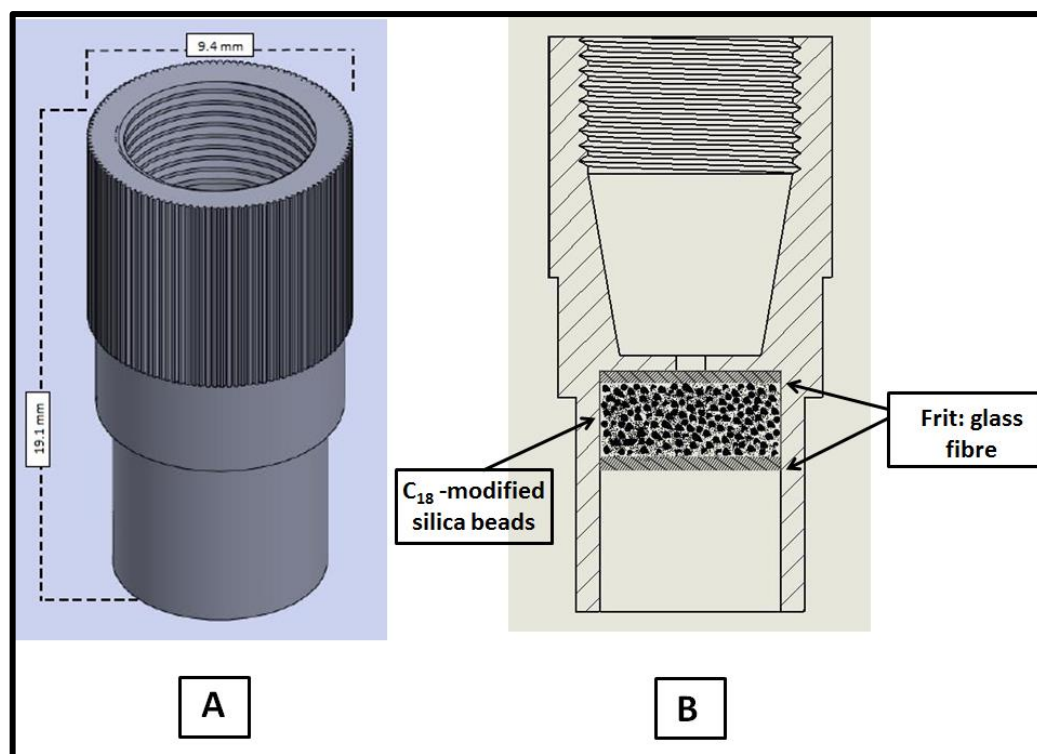
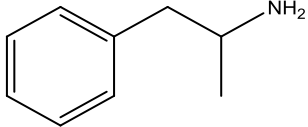
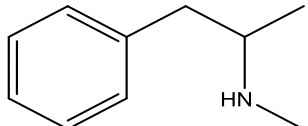
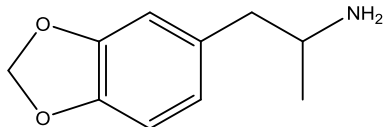
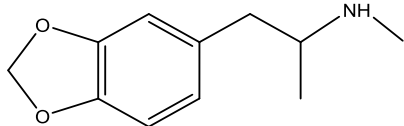


Figure 2-8: Schematic of a female luer lock adaptor from A) a side view, and B) a cross-sectional view showing where the C₁₈-modified silica beads were packed.

2.5.2 Preparation of standard solutions of drugs

Stock standard solutions of the four target drugs - amphetamine (AM), methamphetamine (MA), 3,4-methylenedioxyamphetamine (MDA) and 3,4-methylenedioxymethamphetamine hydrochloride (MDMA) - were prepared separately by dissolving 5 mg of each compound in 50 ml of ultra-pure water to achieve a concentration of 0.1 mg ml⁻¹ (100 ppm). All stock solutions were divided into small 2 ml aliquots and stored at -20 °C until required. Working standard solutions of the four drugs were prepared by diluting the stock standard solutions with ultra-pure water to the desired concentrations, which were then stored at 4 °C. The chemical structures of all four target drugs are shown in Table 2.5.

Table 2.5: Chemical structures of the target drug analytes used in this study.

Analyte	Chemical structure
Amphetamine	
Methamphetamine	
3,4-methylenedioxyamphetamine (MDA)	
3,4-methylenedioxymethamphetamine (MDMA)	

2.5.3 Solid-phase extraction of the drugs of interest

The steps commonly involved in the SPE procedure are as follows: conditioning and equilibration of the adsorbent, loading of the sample, removing the impurities (washing), and eluting the target analyte. All these steps were carried out using a hydrodynamic syringe pump running at a flow rate of $10 \mu\text{l min}^{-1}$ (Figure 2-9).

The modified silica beads were activated with methanol for 5 minutes, and then equilibrated with ultra-pure water for 10 minutes. A mix of the four drugs ($50 \mu\text{l}$) with a final concentration of $20 \mu\text{g ml}^{-1}$ (for each drug) was then adsorbed onto the bead surface and washed with $50 \mu\text{l}$ ultra-pure water. Finally, $50 \mu\text{l}$ of mobile phase was used to elute the analytes and $20 \mu\text{l}$ of the eluent was injected directly into the HPLC system.

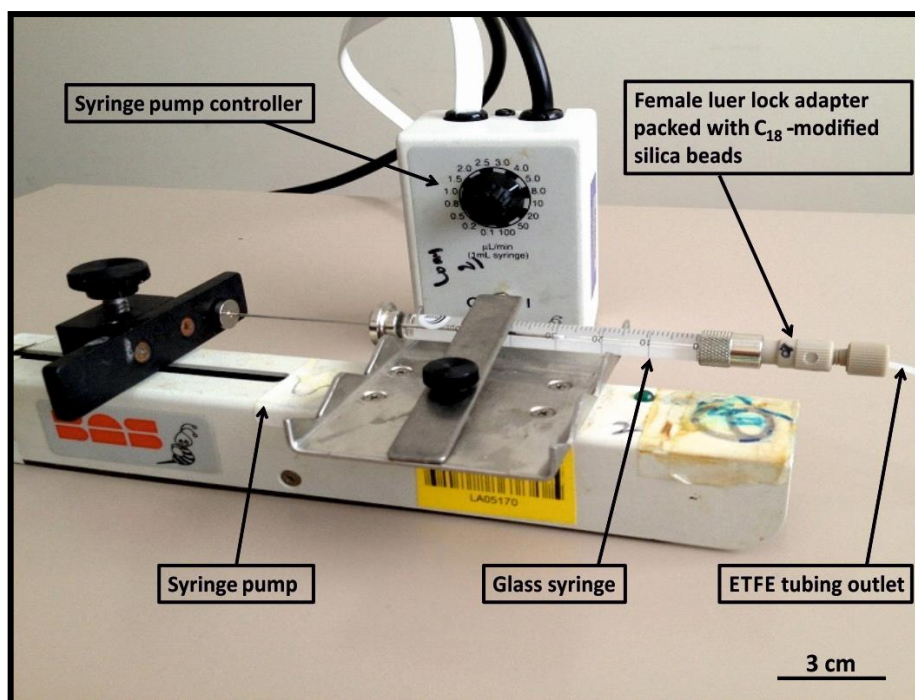


Figure 2-9: Photograph of the experimental set-up for the extraction of amphetamine, methamphetamine (MA), 3,3-methylenedioxyamphetamine (MDA) and 3,4-methylenedioxymethamphetamine hydrochloride (MDMA) using packed C₁₈-modified silica beads

2.5.4 Method developed for drug analysis

2.5.4.1 Optimum wavelength

A UV-visible (UV-Vis) spectrometer was used to determine the λ max of each drug. A fused quartz cuvette was used with an optical path length of 1 cm filled with $20 \mu\text{g ml}^{-1}$ of a working solution of each drug. These solutions were then scanned between 200 nm to 400 nm to select the λ max.

2.5.4.2 Optimum HPLC conditions and mobile phase combination

Chromatographic analysis was performed using HPLC with a UV detector consisting of an LC 200 series binary pump, a PerkinElmer 785A UV/Visible Detector and a Prodigy™ C₁₈ column. In order to obtain the optimal conditions for separation for the four drugs, a range of mobile phases were investigated, which included the following: methanol:ultra-pure water (80:20, v/v); 10 mM sodium acetate (pK_a 4.75): methanol (70:30, v/v) at pH 6; and 50 mM phosphoric acid (at pH 4 using triethylamine):acetonitrile (9:1) under isocratic conditions at ambient temperature (around 23 °C). The sample injection volume was 20 µl and the flow rate was set at 1 ml min⁻¹.

2.5.5 Figures of merit

Method validation parameters, including linearity, limit of detection (LOD), lower limit of quantification (LLOQ) and precision, were evaluated to ensure that the results of the method were suitable and reliable for the analysis required.

2.5.5.1 Linearity

For a good method of analysis, the measured signal of analyte should be directly proportional to the concentration of analyte in the sample within a given range. Linearity was evaluated using a standard linear calibration curve to establish the range of concentrations over which a linear response was obtained. This range for the calibration curve was chosen in accordance with the concentrations of the target analytes that can be found in the human body. Calibration curve points were

obtained in triplicate from working standard solutions of AM, MA, MDA, and MDMA at concentrations of 0.625, 1.25, 2.5, 5, 10, and 20 $\mu\text{g ml}^{-1}$ for each analyte.

Calibration curves were constructed by plotting the concentration of each drug on the x -axis against its peak area for response on the y -axis.²⁴⁷ Linearity was evaluated statistically by the least squares regression method (Equation 2.1) using Microsoft Excel 2010.

$$y = b + mx \qquad \text{Equation 2.1}^{248}$$

Where y is the signal response (peak area), b is the intercept on the y -axis of the best fit line for the data, m is the slope, and x is the concentration. Good linearity is obtained when the correlation coefficient (R) is close to 1.²⁴⁹

2.5.5.2 Limit of detection (LOD) and lower limit of quantification (LLOQ)

The lowest concentration of an analyte in a sample that can be detected with the optimised method and which gives an instrument signal three times greater than the matrix background (noise) is defined as the limit of detection (LOD).²⁵⁰ The lower limit of quantification (LLOQ) is the lowest amount of an analyte in a sample that can be quantitatively determined with acceptable ($\pm 20\%$) precision and accuracy.²⁵¹ Usually, the LLOQ is determined as a signal-to-noise ratio of 10:1.²⁵² LOD and LLOQ were calculated statistically during the evaluation of the linear range of the calibration curve. In this study, the LOD was calculated using Equations 2.2 and 2.3, whereas the LLOQ values were calculated using Equations 2.4 and 2.5.^{251, 253}

$$y_{LOD} = y_B + 3 S_B \quad \text{Equation 2.2}$$

$$LOD = (y_{LOD} - y_B)/m \quad \text{Equation 2.3}$$

$$y_{LLOQ} = y_B + 10 S_B \quad \text{Equation 2.4}$$

$$LLOQ = (y_{LLOQ} - y_B)/m \quad \text{Equation 2.5}$$

Where y_B is the intercept, S_B is the standard error of the predicted y -value for each x concentration in a regression, and m is the slope of the calibration curve.

2.5.5.3 Precision

In order to measure the consistency of the extraction procedure of the silica, its precision was investigated. Precision is represented by the closeness of the analytical results (degree of scatter) obtained from multiple measurements of the same homogeneous samples for the same measure under prescribed conditions.^{248, 254}

Precision is usually expressed as relative standard deviation (RSD) under two main condition aspects, referred to as repeatability and reproducibility, which are also known as intra-day and inter-day assay precision, respectively.²⁵⁵ Repeatability expresses precision by analysing analytes of interest over a short interval of time, on the same day, using the same extraction and analytical methods; reproducibility expresses precision in a similar manner to repeatability, but over longer interval times (days).²⁵⁴ In this study, the intra-day and inter-day precisions were evaluated by triple extraction and detection of mixed samples containing low, medium and high levels (3, 10 and 20 $\mu\text{g ml}^{-1}$) of AM, MA, MDA, and MDMA on the same day and over five consecutive days, respectively. The RSD for method validation is required to be within $\pm 15\%$, except at the LLOQ value where $\pm 20\%$ is acceptable.^{248, 254, 255}

3 Results and Discussion: DNA Solid-phase Extraction

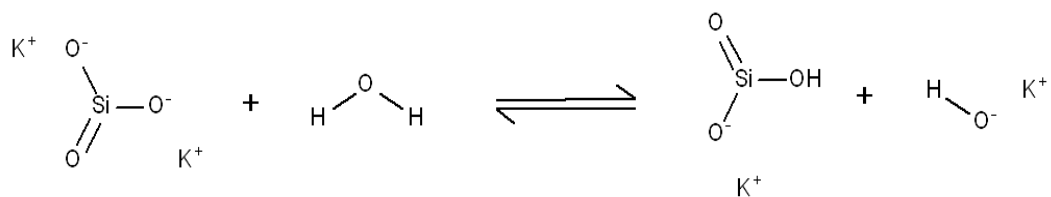
In this chapter, the effectiveness of thermally activated silica-based monoliths for the adsorption of DNA from biological matrices at different levels of volume/concentration is investigated. The results obtained from different experiments are presented in the following order: optimising the curing temperature of a thermally activated monolith and its physical characterisation, solid-phase extraction using a silica-based monolith in a microfluidic device, DNA extraction and subsequent elution, and PCR amplification of human DNA contaminated with animal (mouse) DNA.

3.1 Physical Characterisation of the Silica-based Monolith

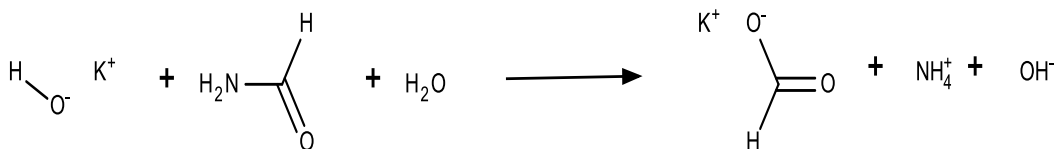
Solid-phase extraction (SPE) is one of the most efficient methods in forensic DNA investigations where a biological sample may be limited in terms of both quantity and quality.^{152, 157} Solid-phase silica in the presence of chaotropic agents, such as GuHCl, has been widely used to bind DNA to the silica surface followed by washing to remove potential interferents, and elution of the purified sample using water or a low ionic strength buffer. Previous work at the University of Hull for DNA extraction purposes using thermally activated porous silica monoliths was shown to give good extraction efficiency (about 80%) when carrier RNA was included in the binding solution.¹⁵⁸ The same type of monolith was used in this work but without the need for the addition of carrier RNA to evaluate situations where biological samples are limited or contaminated.

Compared with other procedures for monolith formation, such as polymer-based monoliths or sol-gel types, potassium silicate thermally activated monoliths are simple to fabricate. For this study, formamide was added drop by drop into the potassium silicate solution (21% SiO₂, 9% K₂O) at a ratio of 1:9 (v/v) with continuous mixing at room temperature until the formamide was completely dispersed, and the mixture was then introduced into a glass capillary or a microfluidic chip and placed in a drying oven for 15 hours. In this procedure, potassium silicate was disassociated in water to potassium bisilicate and potassium hydroxide of pH 11.8. The basic solution then hydrolysed the formamide to form potassium formate and ammonium hydroxide resulting in a gradual reduction of pH to 10.8. This reduction in pH initiated the disassociated potassium bisilicate to undergo polycondensation and form the silica monolith backbone.²⁵⁶ The reaction scheme is shown in Equation 3.1.

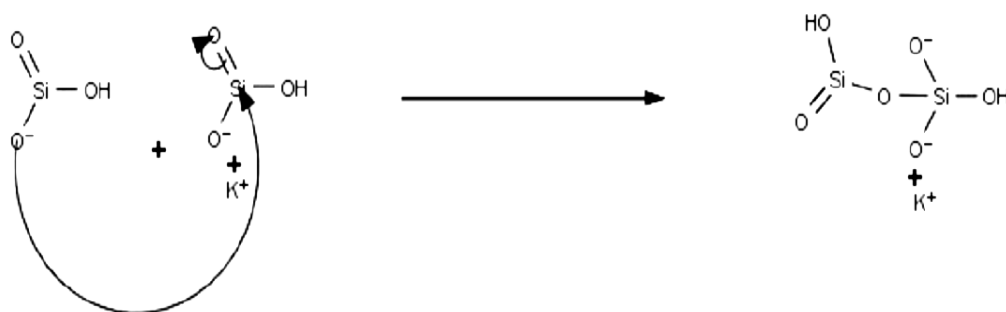
A) Disassociation



B) Hydrolysis



C) Condensation



Equation 3.1: Reaction scheme showing a series of disassociation, hydrolysis and condensation reactions required to produce a silica-based monolith.^{256, 257}

As the result of formamide hydrolysis, ammonium hydroxide (NH_4OH) is generated and this will result in the formation of mesopores throughout the monolith structures. The characteristic features of the monolith were examined based on the change in temperature of the monolith generation. In this study, three different temperatures (80, 90 and 100 °C) were investigated to identify the optimal temperature for silica polymerisation. Figure 3-1 shows the characteristics of silica-based monoliths prepared inside glass capillary tubes at different temperatures.

As can be seen from Figure 3-1 A, at high temperatures (100 °C), the skeleton of the silica-based monolith was weak, producing cracks which caused splitting of the continuous bed of the monolith structure that resulted in a non-homogeneous silica structure. A very low surface area interaction for adsorption is expected due to solution passing through the cracks rather than the fine monolith structure. However, decreasing the temperature of the monolith formation to 90 °C produced a continuous network in the silica skeleton with a high homogeneity and sponge-like structure characterised by a different macropore size, as shown in Figure 3-1 B. With further reduction in the temperature to 80 °C, as shown in Figure 3-1 C, a continuous structure in the silica skeleton was fabricated but this lacked homogeneity with small macropore size. Such structures generate a high back pressure when solutions pass through these small pores.

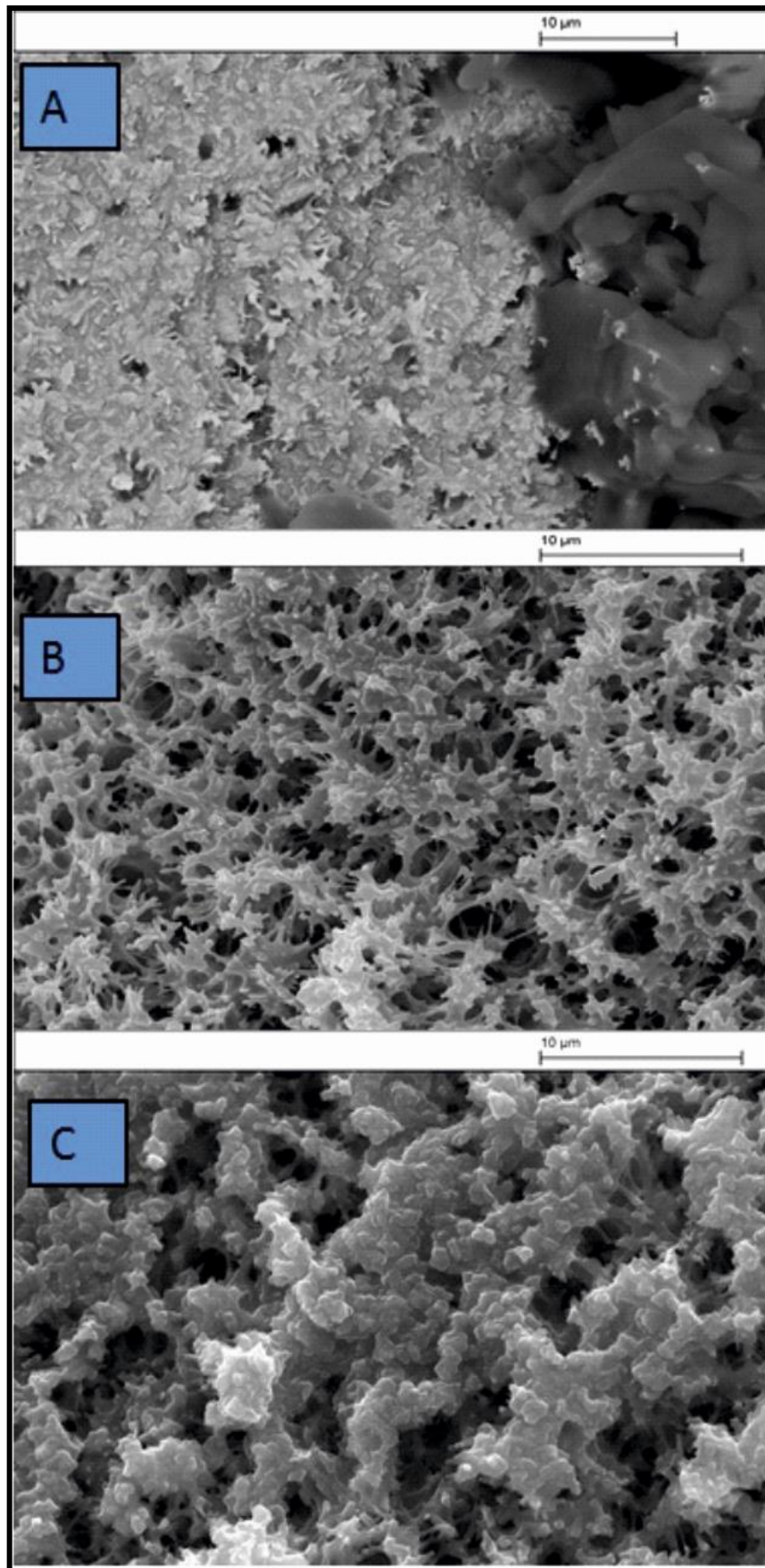


Figure 3-1: The surface structure of thermally activated potassium silicate monoliths created inside a glass capillary at A) 100 °C, B) 90 °C and C) 80 °C.

BET analysis was used to confirm an appropriate temperature that would produce the overall highest surface area. BET surface areas were determined for thermally activated potassium silicate monoliths prepared at 80 °C and 90 °C, but not 100 °C because of the cracking observed. It was found that the average surface area for silica-based monoliths prepared at 90 °C was higher ($297 \text{ m}^2 \text{ g}^{-1}$) than for those prepared at 80 °C ($176 \text{ m}^2 \text{ g}^{-1}$).

BJH adsorption analysis was used to determine the overall pore size distributions of the silica-based monoliths. The average pore size of silica monoliths prepared at 90 °C was 18 nm (mesopores), and the average pore volume of these monoliths was $0.79 \text{ cm}^3 \text{ g}^{-1}$. These results can be compared with monoliths prepared at 80 °C, for which the average pore size and pore volume were much lower (10 nm and $0.37 \text{ cm}^3 \text{ g}^{-1}$ respectively), which explains the generation of back pressure when the solutions were forced through the porous monolithic media. As the monolith had cracked at 100 °C, BJH adsorption was not performed for this structure at this temperature.

Since monolith formation at 90 °C offered a silica-based monolith with suitable macropores and a high total surface area, this was selected as the temperature for the formation of thermally activated potassium silicate monoliths.

In terms of reproducibility, three different batches for monolith fabrication at 90 °C were examined. The results appeared to be very similar in terms of general morphology under SEM, as shown in Figure 3-2, with acceptable RSDs (< 10%) for the physical properties (specific surface area, pore size, and pore volume), which indicated the reproducibility of the preparation procedure for the potassium silicate monolith.

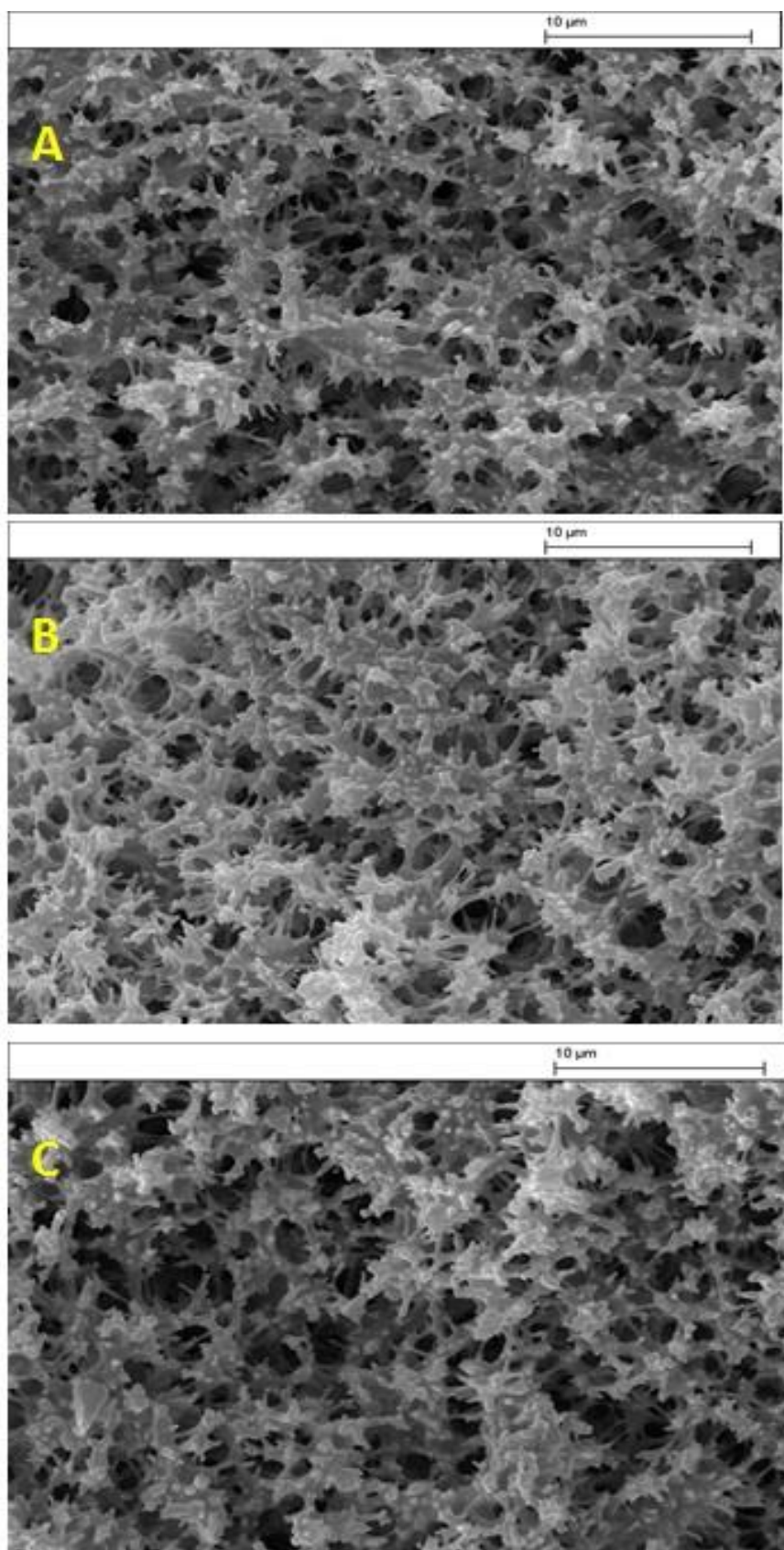


Figure 3-2: SEM micrographs of three silica-based monoliths A) to C) prepared at 90 °C.

3.2 Solid-phase Extraction

This section evaluates the performance of the thermally activated potassium silicate monoliths fabricated at 90 °C for the isolation and detection of low copy numbers of mouse DNA within glass microfluidic devices using hydrodynamic pumping, as shown in Figure 2-4. In addition, a selectivity study was also performed using mixed biological samples containing both human and mouse DNA at different concentrations.

3.2.1 Optimal extraction conditions

Under ideal optimal conditions, an extraction profile would see the entire DNA retained during the loading and washing steps and then fully recovered at the elution step (the distinct peak), as shown in Figure 3-3. Preliminary experiments were carried out by placing a potassium silicate monolith within a glass capillary and using 5 μl purified human DNA (at an average concentration of 4.8 $\text{ng } \mu\text{l}^{-1}$).

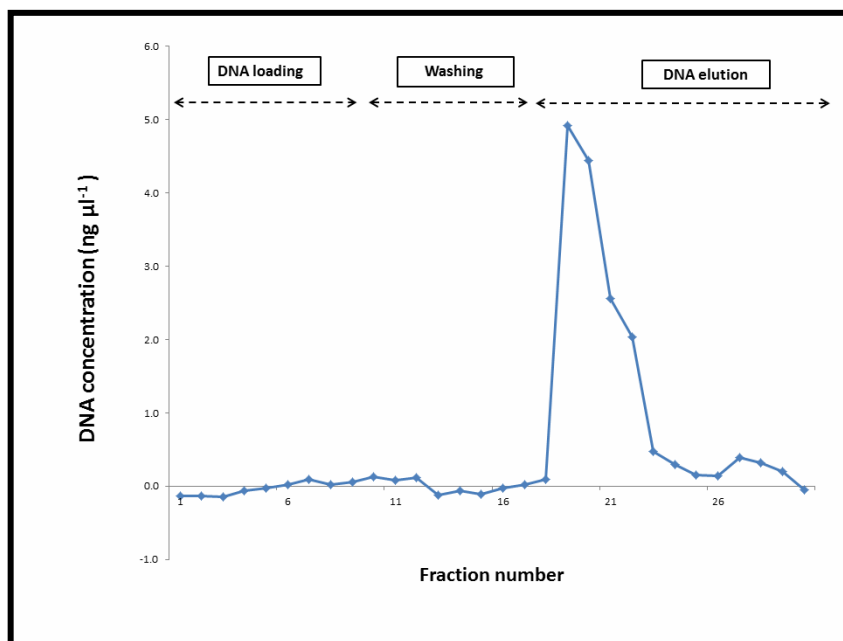


Figure 3-3: Example of an ideal DNA extraction profile

Initial results showed that the DNA extraction efficiency was low ($22.6 \pm 6\%$) with minimal DNA being lost during the loading and washing phases using experimental conditions previously identified in a project carried out at the University of Hull for a thermally activated monolith (as described in section 2.4.3).¹⁵⁹ Evidence from this work indicated that DNA was retained on the monolith surface during the elution step. This result pointed, therefore, to the need to optimise the elution conditions, which can be one of the crucial steps in obtaining high DNA yields.

The adsorption of DNA onto silica via hydrogen bonds is achieved by reducing the electrostatic repulsion between the negatively charged DNA and the negatively charged silanol groups on the silica surfaces using a buffer with a pH (6.7) lower than the theoretical pK_a of the surface silanol groups (7)¹⁷⁴ to increase the protonation of the silanol groups on the silica surface in the presence of a chaotropic agent.⁵⁸ Contrary to adsorption, DNA can be eluted efficiently using a low salt concentration buffer in alkaline media at a pH not higher than 9.²⁴² Water or an elution buffer that contains a sufficient amount of counter ions would, therefore, be able to break the hydrogen bonding between the DNA and the silica surfaces for DNA recovery due to deprotonation of the silanol groups. It was found that a low ionic strength buffer consisting of 10 mM TE at pH 8.4 was able to elute 45.6% of the adsorbed DNA compared to 22.6% DNA extraction efficiency when purified water (pH 5.5) was used, as shown in Figure 3-4. The TE buffer was composed of Tris (to maintain the pH) and EDTA (as a chelating agent). EDTA chelated Mg^{2+} which is essential for nuclease function and prevented DNA from degradation. In addition, TE at pH 8.5 did not require any further steps such as precipitation and the eluted DNA could be used directly for PCR processing and subsequent analysis.

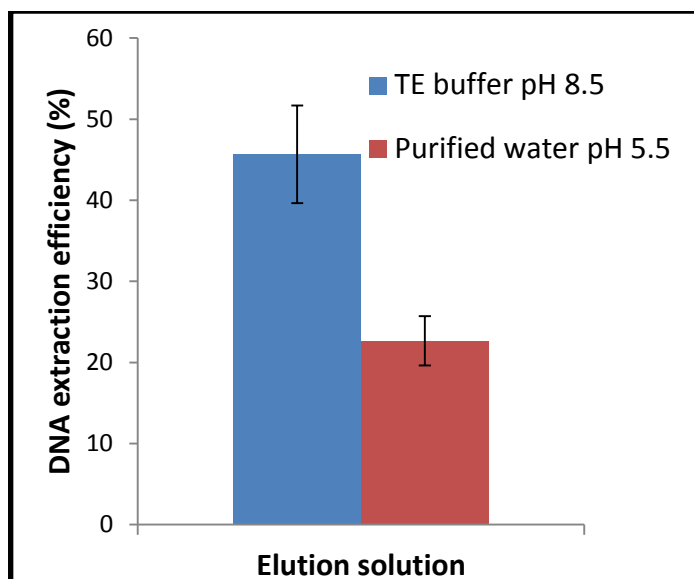


Figure 3-4: Effect of pH and ionic strength on the elution of DNA. Each experiment was carried out in triplicate. Error bars represent the standard deviation ($n = 4$).

3.2.2 Breakthrough curve

While the surface area available on the potassium silicate monoliths for DNA binding is high ($297 \text{ m}^2 \text{ g}^{-1}$), the presence of proteins in a biological sample can decrease the binding sites available for DNA capture and eventually decrease the DNA extraction efficiency. Therefore, it is important for a DNA extraction method to provide a reasonably high DNA binding capacity to cope with the competition from proteins for DNA binding sites. The thermally activated potassium silicate monolith cured within the microfluidic device shown in Figure 2-2 was, therefore, investigated for DNA binding capacity using human DNA. A pre-conditioned monolith was loaded with $3.43 \text{ ng } \mu\text{l}^{-1}$ of purified human DNA prepared in an equilibration buffer (5 M GuHCl in TE buffer; pH 6.7) at a flow rate of $2.5 \text{ } \mu\text{l min}^{-1}$ and then fractions of $4 \text{ } \mu\text{l}$ of the extract (corresponding to 13.72 ng) were collected from the outlet of the device.

The collected fractions were quantified using PicoGreen[®] assay to identify the breakthrough profile. The breakthrough point, the point at which the amount of DNA in the collected fractions gradually increases, was calculated using a breakthrough curve, as shown in Figure 3-5. Breakthrough occurred after 144 μl (494 ng of DNA) of continuous sample loading within a microfluidic chip device that contained 600 μg of potassium silicate monolith, which corresponded to 823 μg DNA g^{-1} of monolith weight. As can be seen from the curve, no plateauing (13.72 ng) of the DNA recovered was achieved even with 344 μl (about 1.18 μg) of purified DNA being continuously loaded. This high binding capacity result will be applicable for most biological samples, including forensic cases which typically contain less DNA than the capacity of this monolith.

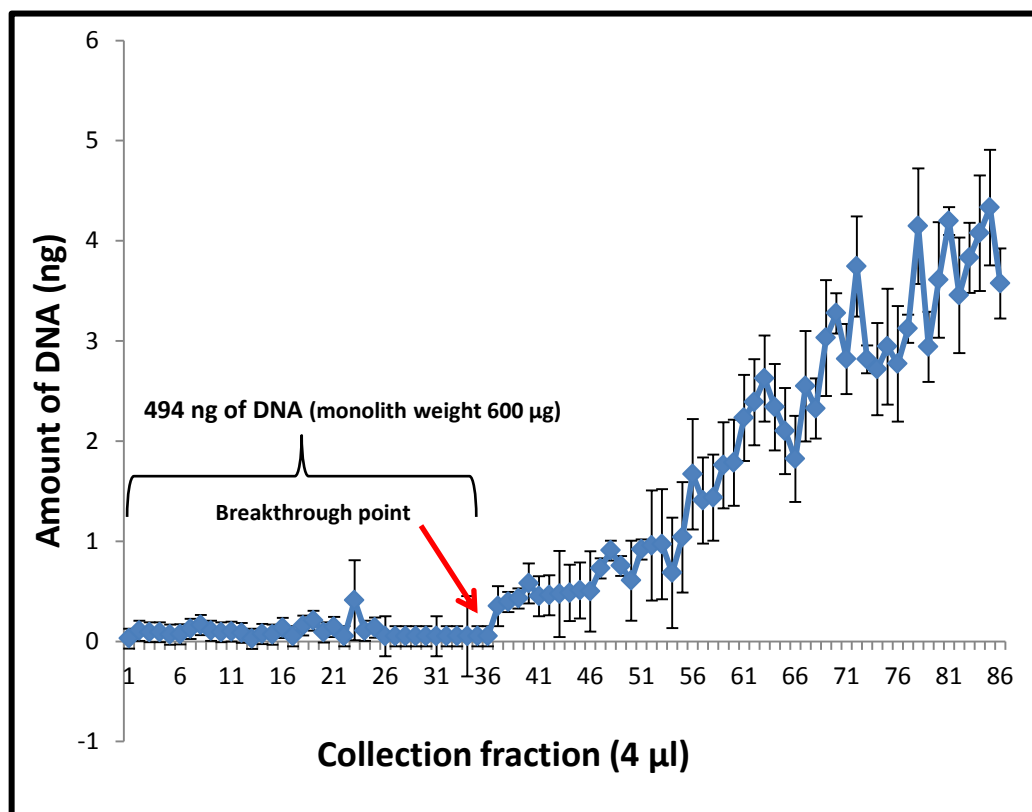


Figure 3-5: DNA breakthrough curve providing the continuous loading capacity of 13.72 ng of purified human DNA on a 600 μg monolithic microfluidic device. Error bars shown represent the standard deviation (n = 4).

3.2.3 Figures of merit for the DNA analysis

The validity of the DNA assay using PicoGreen[®] dye was investigated in order to determine the ability of the FLUOstar Optima Plate Reader to detect low quantities of DNA as compared to Figure 2-6. A calibration plot using the DNA standards kit at the following concentrations: 2, 1, 0.5, 0.25, 0.125, 0.0625, 0.03125 and 0.0156 ng μl^{-1} against fluorescent intensity was constructed (see Figure 3-6). LOD and LLOQ were calculated using Equations 2.2, 2.3 and 2.4, 2.5, respectively. It was found that the assay could detect (LOD) down to 0.18 ng with a confidence quantification (LLOQ) of 0.59 ng of DNA.

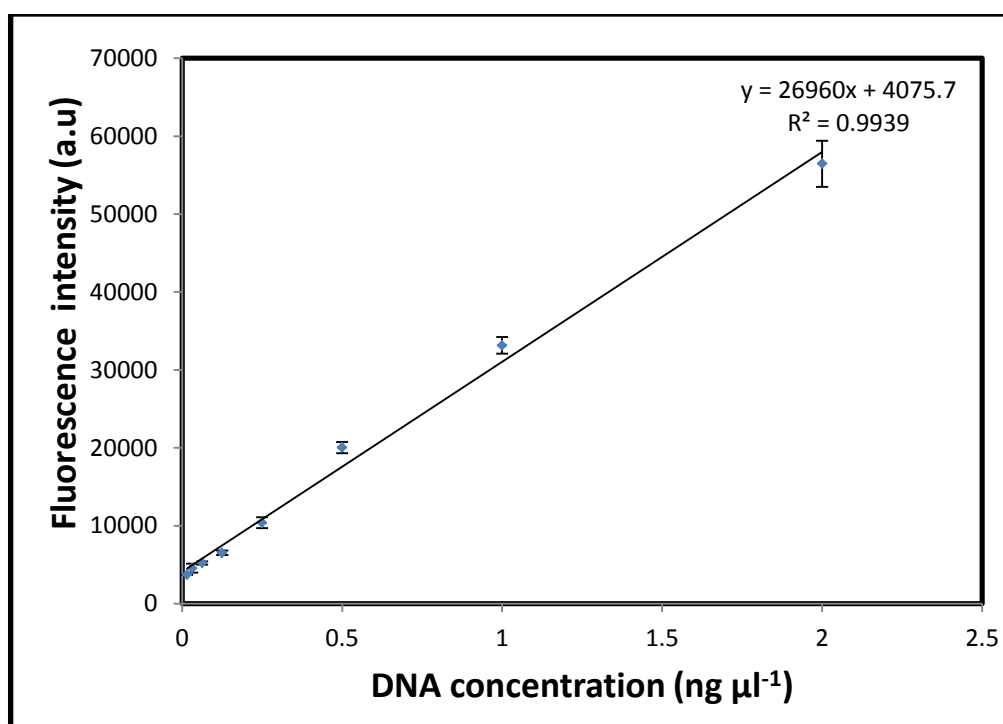


Figure 3-6: Calibration curve of kit DNA standards using PicoGreen[®] analysed using a FLUOstar Optima Plate Reader over a low concentration range from 2 to 0.0156 ng μl^{-1} .

3.2.4 Cell lysis

To promote DNA adsorption to the silica surface of the monolith, a chaotropic salt (GuHCl) was added which also enhanced cell lysis. The addition of a chaotropic salt commonly eliminates the requirement for additional complex cell membrane disruption techniques such as mechanical cell lysis.²⁵⁸⁻²⁶⁰ In this study, mouse neuroblastoma cells (tumours that develop from nerve tissue) were added directly to GuHCl in order to rupture the cellular membrane structure and release nucleic acids. The suitability of GuHCl for achieving lysis of cell membranes was investigated by a trypan viability assay using a standard haemocytometer and transmission microscope.²⁶¹ The results showed that the chaotropic salt was a highly effective method for disruption of a mouse neuroblastoma cell membrane (as shown in Figure 3-7) because the intact cell membranes did not absorb trypan blue and appeared colourless (Figure 3-7 A), whereas the dye was absorbed by the lysed cells and cellular debris after adding 5 M GuHCl and easily distinguished by their blue colour under the microscope (Figure 3-7 B).

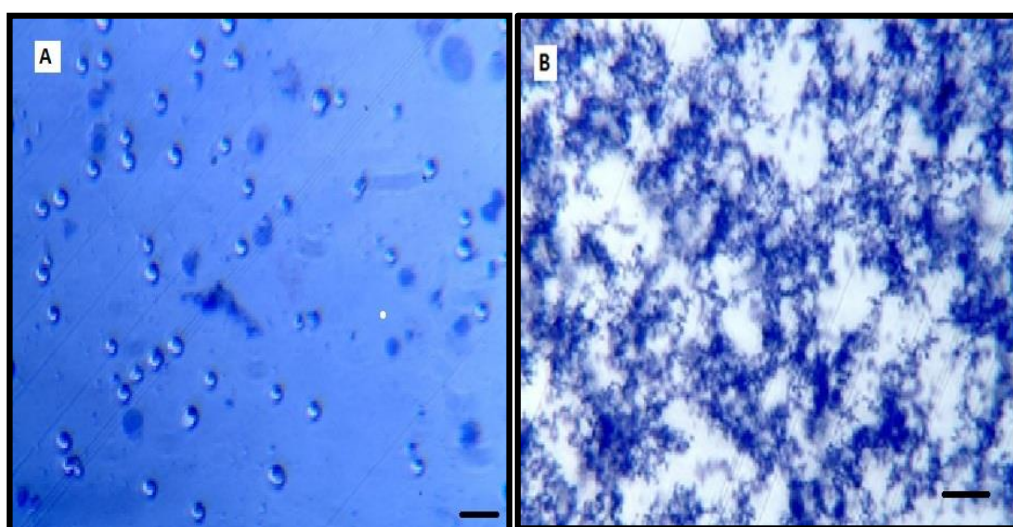


Figure 3-7: Photographs showing the integrity of neuroblastoma cell walls before A) and after B) adding 5 M GuHCl. Bar = 100 µm.

3.2.5 Extraction of mouse DNA

Biological samples recovered for forensic analysis or clinical diagnostic applications can be limited in terms of the amount and quality of DNA present. The use of monoliths within a microscale environment offers an increased surface area available for achieving maximum DNA adsorption and resulting in efficient DNA extraction. Carrier molecules such as ribonucleic acid (RNA),¹⁵⁸ salmon sperm DNA²⁶² or glycogen²⁶³ have been shown to enhance DNA yield during extraction. The ultimate aim of this chapter is, however, to evaluate a microfluidic system containing an integrated silica monolith for the extraction of minimal cell samples without the need for the addition of carrier molecules.

An initial study was required to determine the typical amount of DNA present in a cell. In order to enable calculation of DNA extraction efficiencies, it was necessary to determine the total amount of DNA initially added to the system. Five diluted cell populations of 1,000 mouse cells were lysed by 5 M GuHCl and the total amount of DNA released was quantified using a Quant-iT™ PicoGreen® dsDNA Assay Kit. The mean amount of DNA per *Mus musculus* cell was found to be 50 pg. DNA extraction was then performed using decreasing numbers of mouse cells (from 1,500 to 62 cells) in order to evaluate the performance of the potassium silicate monolithic fabricated within a microfluidic chip to deal with limited sample size or DNA concentration. The extraction procedure was described in section 2.4.3. Table 3.1 summarises the resulting data for DNA extraction for different numbers of cells during the loading, washing and elution stages. The values represent the mean of three measurements and the RSDs.

However, although the fabricated monolith offered reasonable DNA extraction recovery during the elution steps ranging from 14.81% to 84.31%, it exhibited a lack of reproducibility as the RSDs were more than 15%. This can be attributed to difficulty in positioning the monolith within the microfluidic device and the likelihood of air bubble formation between silica network structures of different sizes. The presence of bubbles within the monolithic structure represented a major problem, as the surface area for DNA capture varied from one microfluidic device to another and this resulted in poor extraction reproducibility.

Table 3.1: DNA extraction efficiencies from different numbers of mouse cells, including relative standard deviation (RSD). ND: not detected (n = 3).

Number of cells (amount of DNA)	Average DNA detected during:		
	Loading (RSD)	Washing (RSD)	Elution (RSD)
1,500 (76.70 ng)	3.60% (6.50)	4.05% (8.21)	16.26% (13.57)
1,000 (49.79 ng)	4.53% (3.34)	7.47% (14.43)	14.81% (19.3)
500 (28.96 ng)	6.58% (3.65)	7.10% (5.41)	18.50% (16.1)
250 (14.48 ng)	3.08% (3.74)	13.90% (4.91)	43.10% (15.28)
125 (7.24 ng)	4.30% (5.55)	15.24% (6.2)	47.99% (6.22)
62 (3.62 ng)	ND	ND	84.31% (15.12)

An elution profile of 1,000 mouse cells is shown in Figure 3-8.²⁶⁴ From the figure it can be seen that a minimal amount of DNA passed through the system during the binding and wash phases, indicating successful adsorption. A distinct peak, showing release of DNA, is present during the elution step, which was used to calculate the efficiency of the extraction process. DNA extraction efficiencies were then expressed as a percentage of the amount of DNA recovered during the elution step compared to the initial amount of DNA added to the system.

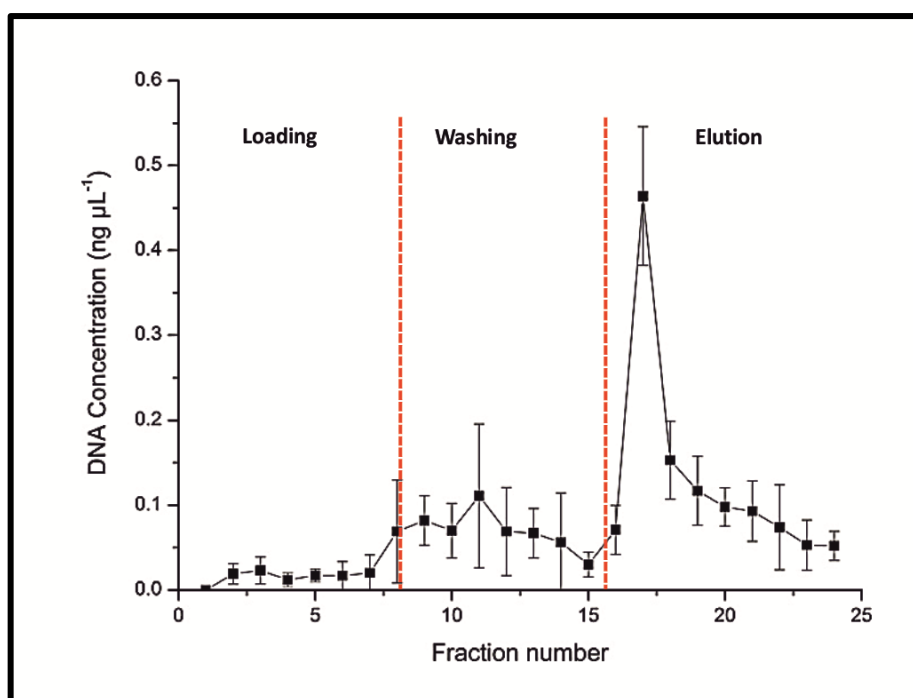


Figure 3-8: Average DNA elution profile for DNA extracted from 1,000 mouse cells using a silica-based monolith within a microfluidic device showing binding (1-8), washing (9-15) and elution (16-24) stages (n = 3).²⁶⁴

Previous research using microfluidic devices containing silica-coated paramagnetic particles had shown a linear relationship between DNA loaded onto the system and DNA recovered in the range of 25-400 ng when a large volume (500 μl) was introduced to the system.²⁶⁵

The work presented here is in concordance with these data but goes further in showing that as little as 4 ng of DNA, equivalent to 62 cells, can be trapped and released from such a system. At reduced cell numbers in the range between 1,500 and 62 cells, the efficiency of the DNA extraction process was shown to increase, particularly at 250 cells or fewer, as shown in Figure 3-9.²⁶⁴

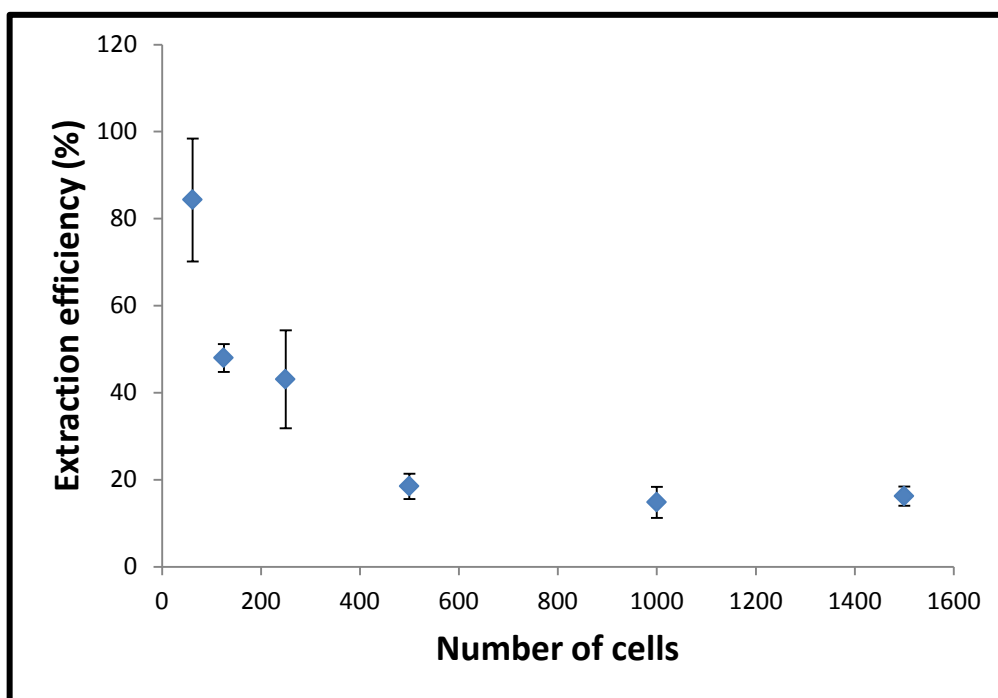


Figure 3-9: Graph showing how DNA extraction efficiency is affected by changes in the number of cells. Standard deviations are shown using error bars ($n = 3$).²⁶⁴

The results indicated that both the amount of cells loaded and DNA extraction efficiencies followed an inverse relationship. As low cell numbers were used, the amount of DNA that was recovered during the elution phase increased. Hence, the methodology was demonstrated to be effective at dealing with limited DNA samples.

This trend is thought to be due to the presence of large molecules in the sample, such as proteins binding irreversibly to sites on the surface walls of the microfluidic device or monolith. At high cell numbers, the amounts of proteins are also high and compete for most of the binding sites available, resulting in a reduced number of sites available for DNA capture. However, at low cell numbers, more binding sites are available for DNA. In addition, the observed trend may be due to the presence of reversible and irreversible binding sites for DNA adsorption. The low levels of DNA binding are carried out by reversible rather than irreversible binding sites on the silica,²⁶⁶ a trend which diminishes with increasing amounts of DNA as the reversible sites preferentially fill. Accordingly, with low DNA concentrations, more reversible binding sites are involved, giving correspondingly higher release efficiency. As shown in Table 3.1, at high numbers of cells, total DNA recovery during the three phases of the extraction process was not equal to the amount of DNA initially added to the system. This hypothesis is in good agreement with the observation that in the presence of carrier RNA, DNA extraction efficiency increases due to selective irreversible binding of the RNA, which in turn improves the elution efficiency of DNA.¹⁵⁸

3.3 DNA Amplification

Prior to DNA amplification, optimisation of PCR components such as magnesium chloride, buffer, dNTPs, enzyme and template was required. An initial study was carried out to optimise the concentration of MgCl₂ as it is an essential co-factor of DNA polymerase in PCR; the concentrations of the other components were fixed.

Optimisation of PCR was carried out on the β -actin mouse gene (135 bp; chosen using the NCBI Probe database) using varying concentrations of MgCl_2 (1.75, 1.50, 1.25, 1 mM and 0.75 mM) prepared from a concentrated stock solution (25 mM) to achieve a total volume of 10 μl per reaction. Table 3.2 shows the concentrations of PCR reaction components.

Table 3.2: Five different concentrations of magnesium chloride used with the β -actin mouse gene set.

Reaction component	PCR 1	PCR 2	PCR 3	PCR 4	PCR 5
MgCl_2	1.75 mM (0.7 μl)	1.5 mM (0.6 μl)	1.25 mM (0.5 μl)	1 mM (0.4 μl)	0.75 mM (0.3 μl)
dNTPs (200 μM)	0.2 μl	0.2 μl	0.2 μl	0.2 μl	0.2 μl
BSA (0.2 $\mu\text{g } \mu\text{l}^{-1}$)	1 μl	1 μl	1 μl	1 μl	1 μl
GoTaq enzyme (0.1 U μl^{-1})	0.2 μl	0.2 μl	0.2 μl	0.2 μl	0.2 μl
GoTaq buffer (1 X)	2 μl	2 μl	2 μl	2 μl	2 μl
Forward β-actin (0.5 μM)	0.5 μl	0.5 μl	0.5 μl	0.5 μl	0.5 μl
Reverse β-actin (0.5 μM)	0.5 μl	0.5 μl	0.5 μl	0.5 μl	0.5 μl
Mouse DNA (3 ng μl^{-1})	1.3 μl	1.3 μl	1.3 μl	1.3 μl	1.3 μl
Water	3.6 μl	3.7 μl	3.8 μl	3.9 μl	4 μl

The PCR was then performed on a Techne[®] Endurance TC-312 Thermal Cycler set as described in section 2.4.5. The results, following slab-gel electrophoresis, showed successful amplification of the size ladder (at the far left lane of the gel) and some of the β -actin genes at different concentrations of MgCl_2 (see Figure 3-10). As expected with the negative control (far right lane of the gel), there was no amplification because no DNA was present for the ethidium bromide to intercalate with and, therefore, no bright band was seen under UV light.

The gel analysis indicated that the amplification of β -actin gene (135 bp) decreased as the concentration of MgCl_2 decreased. This trend is probably due to the low number of free magnesium ions present at 0.75 mM and 1 mM, which is insufficient to activate the *Taq* polymerase enzyme. The optimum concentration of MgCl_2 for the β -actin gene was found to be 1.25 mM for the best band intensity, compared with 1.5 mM and 1.75 mM (Figure 3-10). With high MgCl_2 concentrations (i.e., 1.5 mM and 1.75 mM), the base pairing becomes too strong and that may prevent complete denaturation of double-stranded DNA during the denaturation step. In addition, concentrations that are too high allow the primer in non-specific binding and result in multi-band amplification when visualised on an agarose gel. However, with insufficient MgCl_2 concentration, the primers failed to anneal to the target DNA and resulted in a lack of PCR products or no product bands observed on electropherogram.

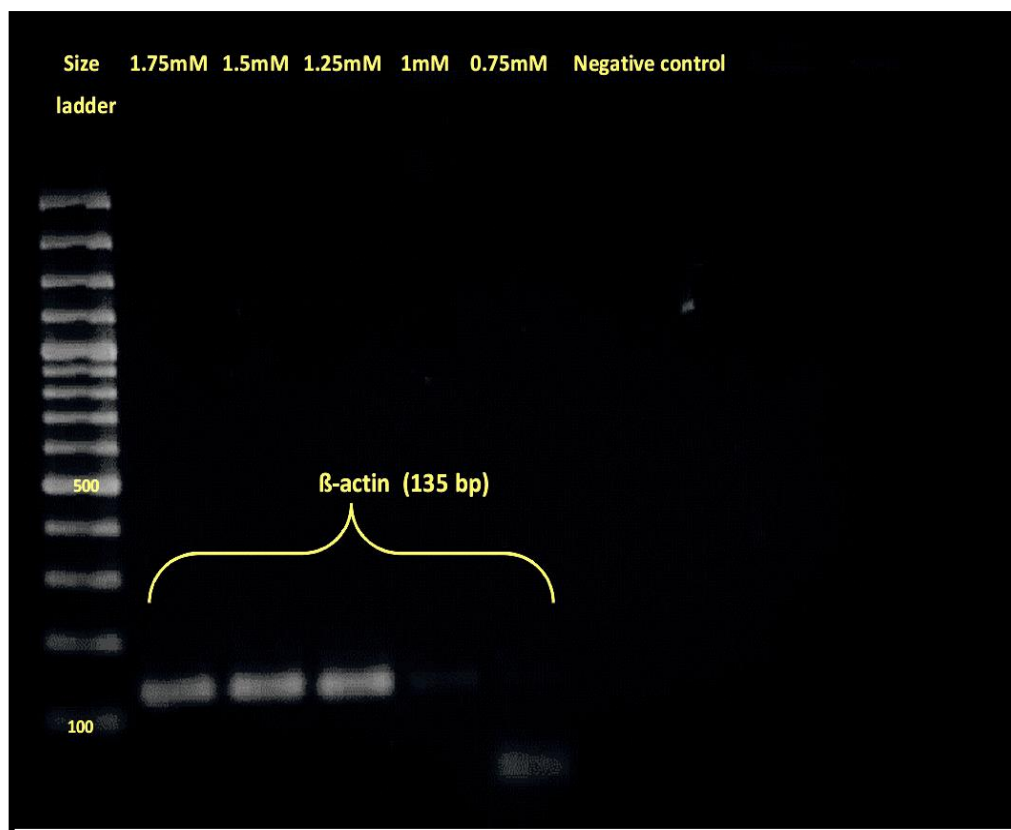


Figure 3-10: Electropherogram showing PCR products for amplified mouse gene with different MgCl_2 concentrations.

Once the PCR components were optimised, 2 μl aliquots of extracted DNA for different numbers of mouse cells (1,500-62 cells) were collected and then added to 8 μl of PCR reagent mixture for thermocycling amplification. The amplified PCR products were then separated according to their size, using gel electrophoresis. Figure 3-11 shows the successful amplification of the β -actin gene (135 bp) from both low (16%; Figure 3-11 A) and high (84%; Figure 3-11 B) extraction efficiencies. This indicates that the use of a potassium silicate monolith was efficient at removing PCR inhibitors and eluted DNA in sufficient quantity and quality for amplification even from low DNA recovery (16%).

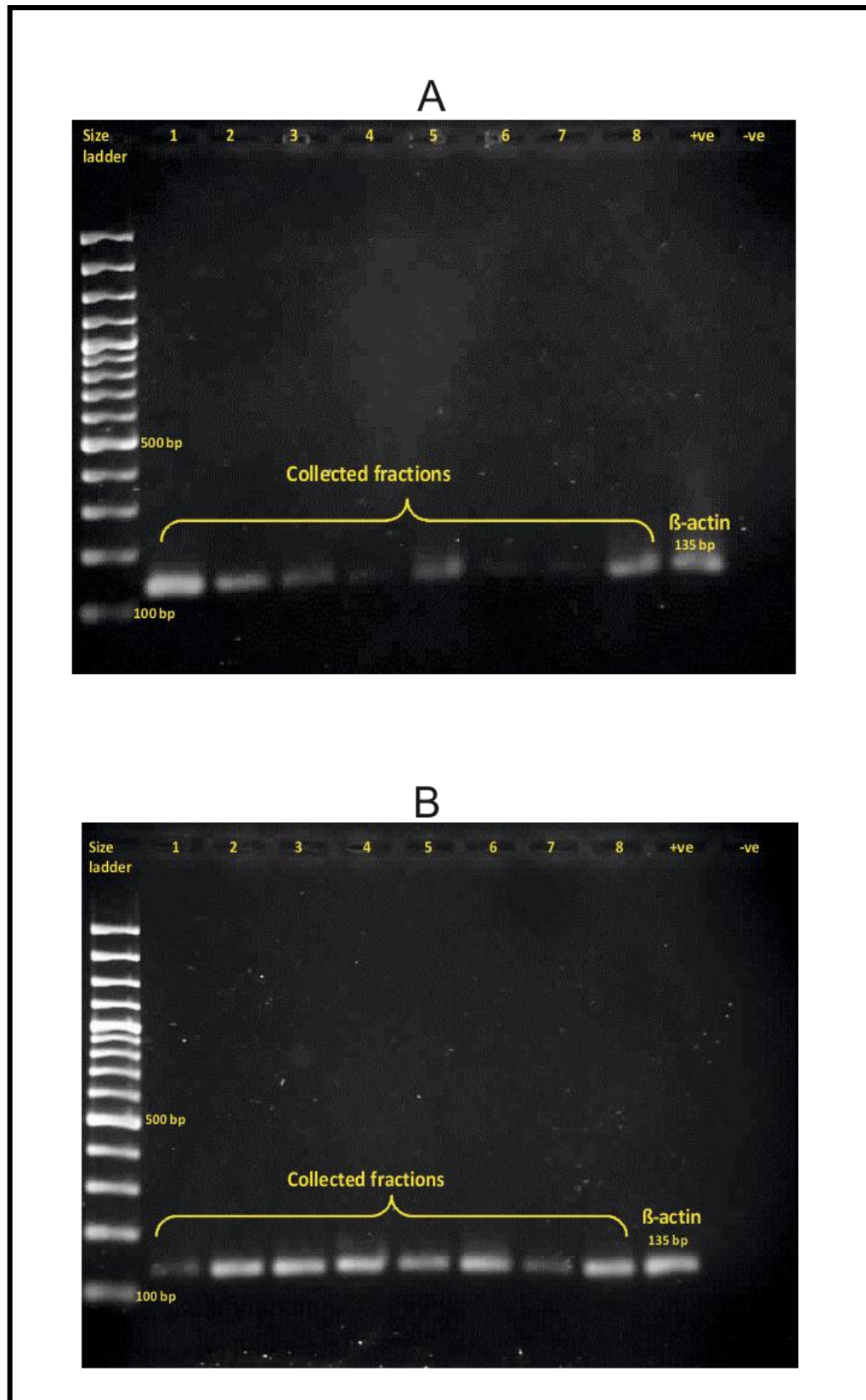


Figure 3-11: An electropherogram showing successful amplification of the β -actin gene from A) 1,500 and B) 62 mouse cells. Lane 1-8: sequentially eluted samples; (+ve) β -actin positive control; (-ve) negative control.

3.4 Effect of Mixed DNA

In complex forensic cases where blends of biological samples from different mixed species occur, such as in mass disasters where human DNA is contaminated with animal DNA, it is important to investigate the efficiency of thermally activated potassium silicate monoliths within the micro-scale environment in extracting target DNA. These types of samples are also particularly relevant in forensic applications where human remains are in the soil and can be contaminated with those of other species.

In this study, the contamination of human DNA with mouse (*Mus musculus*) DNA at different ratios was evaluated: for instance, high concentrations of human DNA in the presence of low concentrations of mouse DNA, an almost equal amount of both species of DNA mixed together, and, finally, a low amount of human DNA added to a high amount of mouse DNA. DNA extractions were performed as described in section 2.4.3 and the DNA eluted at different ratios was collected for PCR amplification.

The results of DNA extraction from the three different ratios of mix during the loading, washing and elution stages are shown in Table 3.3. The values represent the mean of three measurements and the RSDs. Interestingly, it was found that the addition of human DNA to mouse cells was in the same manner of extraction as mouse DNA alone (section 3.2.5), and this supports our previous hypothesis on page 106, which are that on a silica solid-phase matrix, there are always a certain number of reversible sites preferentially filled by nucleic acids before the irreversible ones and with the presence of proteins most of these binding sites that available for DNA capture are reduced.

Table 3.3: DNA extraction efficiencies from various levels of mixed DNA, including relative standard deviations (RSDs) (n = 3).

	Loading (average % ± RSD)	Washing (average % ± RSD)	Elution (average % ± RSD)
24 ng human DNA + 3.62 ng mouse DNA (62 cells)	2 ± 6.77	2.48 ± 8.42	22.64 ± 14.25
24 ng human DNA + 28.9 ng mouse DNA (500 cells)	3.82 ± 6.80	2.37 ± 7.60	18.62 ± 13.93
24 ng human DNA + 76.7 ng mouse DNA (1,500 cells)	3.77 ± 6.72	4.38 ± 10.13	11.54 ± 15.97

In order to enable the production of a DNA profile for mixed DNA, multiplex PCR is required. The development of multiplex PCR assays requires the screening of mouse gene (β -actin) and selected human gene (Amelogenin, D21 S11, and TH01) for any potential cross-reactivity. A preliminary investigation into cross-reactivity for all genes were performed by amplifying human and mouse DNA gene, the results for which are shown in Figure 3-12.

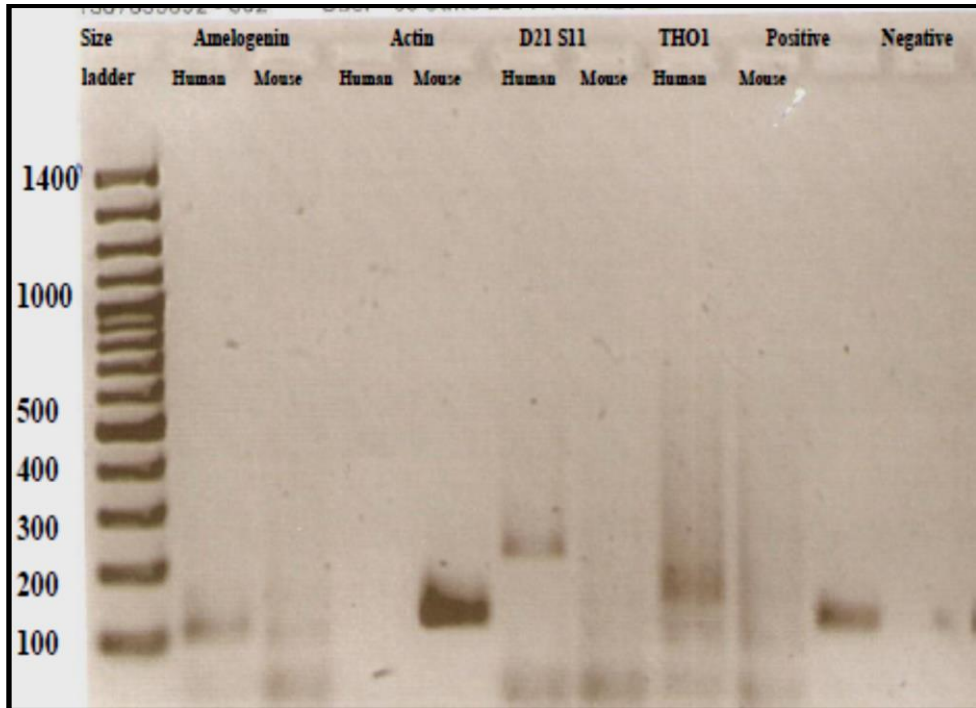


Figure 3-12: Ethidium bromide-stained PCR products amplified from human and mouse DNA after gel electrophoresis.

The agarose gel shows that the PCR amplification is working efficiently with the separation of the expected size of all products: Amelogenin (106 bp), β -actin (135 bp), D21 S11 (223 bp and 227 bp), and TH01 (166 bp), with no amplification in the negative control lane (no contamination). The size ladder was included in the analysis for accurate sizing of PCR products. Figure 3-12 shows no cross-reactivity between the β -actin (mouse gene) and D21 S11 (human gene) loci, as no amplification of human D21 S11 with β -actin or of mouse DNA with the human gene (D21 S11) was observed. However, cross-reactivity was detected between β -actin (mouse gene) and both Amelogenin and TH01 loci (human gene).

Once the multiplex PCR had been optimised, 2 µl fractions of sequentially eluted mixed DNA were collected and the human and mouse genes of interest (D21 S11 and β-actin, respectively) were amplified using a conventional PCR instrument in accordance with the conditions given in section 2.4.5. Following slab-gel electrophoresis, successful multiplex amplification of D21 S11 (223 bp and 227 bp) and β-actin (135 bp) loci from sequentially eluted DNA-containing fractions were observed at different ratios of mixed DNA. These results indicate that the thermally activated potassium silicate monolith method is not a species-specific extraction method, and this is valuable for forensic investigations such as sexual assault case samples. Figure 3-13 shows an example of PCR amplification when an equal amount of human and mouse DNA was extracted. Figure 3-13 shows an example of PCR amplification when an equal amount of human and mouse DNA was extracted.



Figure 3-13: UV transilluminator image of slab-gel electrophoresis results from DNA eluted from a mixed mouse and human sample using β-actin and D21 S11 gene. Lanes 1-8: sequentially eluted DNA fractions; Lane 9: human positive control; Lane 10: mouse positive control; Lane 11: positive mixed control; and Lane 12: negative control (no DNA).

3.5 New Microfluidic Device Designed for DNA Analysis

As described in chapter 2, a glycerol solution was used to ensure that a potassium silicate monolith could be placed within a DNA extraction chamber (hexagonal geometry) and so prevent the monolith filling the small channels (where the reagents move). Even with considerable care, at least one or two of the linked channels was obstructed by the cured monolith, and this is why the chip was designed with six channels (to increase the chance of open channels at each side since one channel is required for the inlet and one for the outlet), as shown in Figure 3-14 A. In addition, air bubbles also formed gradually when the remaining glycerol was removed following the initial monolith curing for 15 minutes at 90 °C. These effects resulted in a general lack of reproducibility with the monolith formation within the hexagonal chamber, which can affect the reproducibility of DNA extraction efficiency. To overcome these problems, a new design was used to fabricate the microfluidic chips (see Figure 3-14 B) using standard photolithography and wet-etching techniques (as described in section 2.3). The new design had only one inlet and one outlet connected directly to an oval geometry 4 mm wide, 8 mm long, and 100 μ l deep (similar to hexagonal geometry). The monolith solution was injected slowly into the DNA extraction chamber from the inlet until it filled the chamber completely and excess solution emerged from the outlet. The monolith was then cured at 90 °C for 18 hours. ETFE tubing was fixed into the holes using epoxy resin and then connected to the syringe via a microtight adapter. The outlet on the opposite side of the monolith was used to collect the sample.

The initial extraction recovery of 24 ng purified human DNA using the new design was found to be similar to the extraction efficiency obtained by the hexagonal design but was more reproducible: $42\% \pm 7\%$ and $46\% \pm 18\%$, respectively. Therefore, the new design was used in all subsequent experiments.

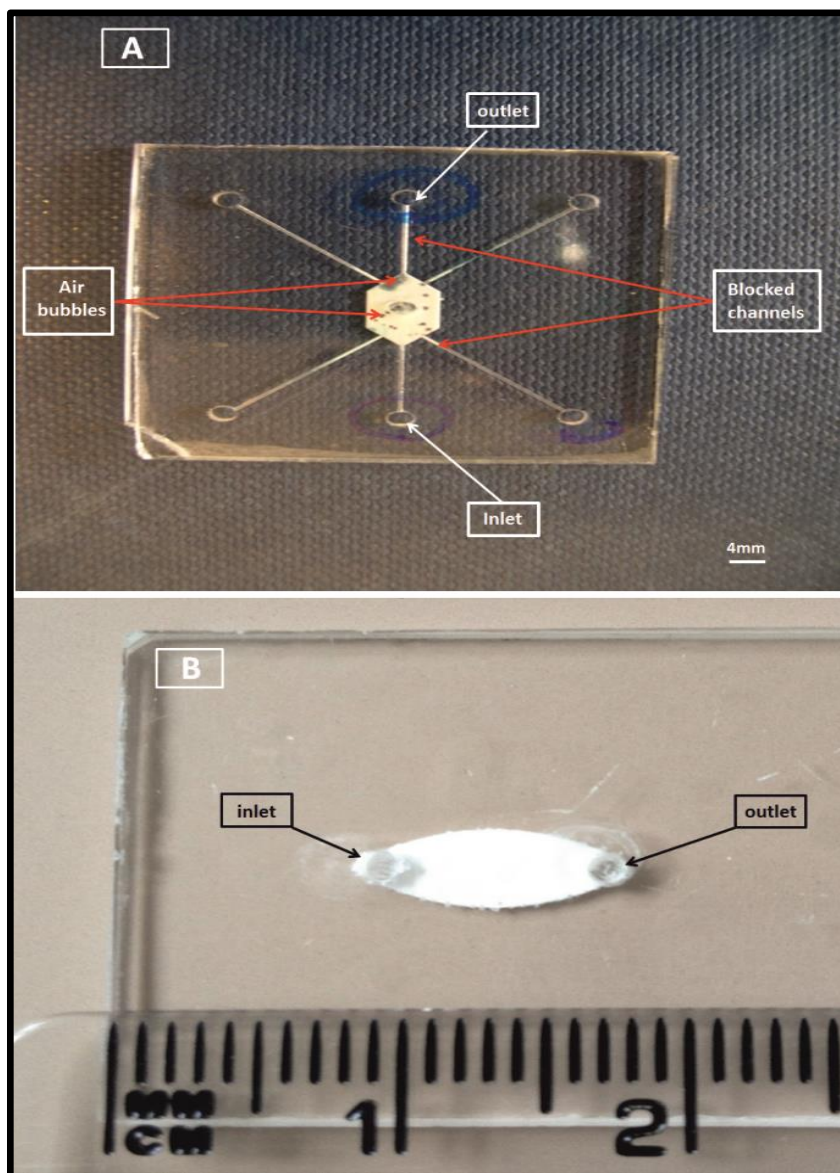


Figure 3-14: Photograph A) shows the formation of air bubbles and blocked channels with the hexagonal extraction microfluidic device. The problems were solved with the new oval design B). For both microfluidic devices, the access holes in the top plates were 1.5 mm and the base plates were etched to a depth of 100 μm .

3.6 Summary

Solid-phase extraction is an ideal technique used in most forensic laboratories for the pre-concentration and purification of DNA. The silica-based monolith has a large surface area available for DNA adsorption, which has a substantial effect on the efficiency of the DNA extraction process. Silica-based SPE methods rely on the adsorption of DNA to the silica surface in the presence of concentrated chaotropic salt solutions, GuHCl, followed by a washing step to remove potential interferents, then by elution of the purified sample using water or a low ionic strength buffer. In this study, it has been demonstrated that DNA can be successfully extracted using a microfluidic device containing thermally activated potassium silicate monoliths cured at 90 °C, which provides a high surface area (297 m² g⁻¹) for DNA adsorption whilst producing low back pressure during extraction. DNA extraction was carried out using hydrodynamic pumping by pre-conditioning the monolith with 10 mM TE buffer (pH 6.7) for 30 minutes at 5 µl min⁻¹ and then loading the DNA continuously in 5 M GuHCl (10 mM TE buffer, pH 6.7) at a flow rate of 2.5 µl min⁻¹. PCR inhibitors were removed using 80% ethanol at a flow rate of 5 µl min⁻¹. To elute the adsorbed DNA off the monolith, a low ionic strength buffer (10 mM TE at pH 8.5) was pumped through the device at a flow rate of 1 µl min⁻¹. A low salt concentration buffer (TE, pH 8.5) was able to elute around 45.6% purified human DNA with no further processing for subsequent analysis. It was found that the PicoGreen[®] assay could detect (LOD) down to 0.18 ng with a confidence quantification (LLOQ) of 0.59 ng of DNA using a FLUOstar Optima Plate Reader. GuHCl was a highly effective method for cell membrane disruption with enhanced DNA binding to the monolith (DNA binding capacity was 823 µg DNA g⁻¹ monolith).

Using the optimal DNA extraction conditions obtained for thermally activated monoliths in the microfluidic device, the extraction efficiency was increased for biological samples containing < 15 ng of total DNA without the need to add carrier nucleic acids. All extracted DNA showed successful amplification via PCR, demonstrating both the effectiveness of the proposed system at removing potential inhibitors and in yielding good-quality DNA.

The DNA extraction method developed was also evaluated in terms of selectivity. In this case, DNA contamination (human DNA contaminated with animal DNA) was found not to influence the extraction method. In addition, pre-concentration studies indicated that DNA from as few as 62 cells could be pre-concentrated and subsequently eluted and detected using the methodology developed. Microfluidic devices with an oval geometry were fabricated and selected to solve the problems of extraction reproducibility with the hexagonal design for future work.

4 Results and Discussion: Combined DNA and Drugs Extraction

The previous chapter (chapter 3) described the extraction and pre-concentration of DNA for identification purposes. In this chapter, a combined approach has been developed that builds on the earlier work of chapter 3 to include the isolation of drugs from the same sample in order to look, uniquely, for the isolation and identification of DNA and drugs of abuse. Whilst the literature has given substantial attention to DNA²⁶⁷⁻²⁷¹ and drugs²⁷²⁻²⁷⁵ extraction/pre-concentration, there does not appear to have been any report on their combined extraction from a single sample analysis.

The extraction of DNA and drugs of abuse for most forensic toxicology is time consuming, as the two methods involved may require a sample to be separated into at least two with enough volume in each to perform extractions. The possibility of using one sample for both DNA and drugs analysis is, therefore, attractive and highly suited to forensic cases where sample sizes are often limited. Accordingly, the ability to perform genetic and drug analysis on the same sample using SPE methodology is the aim of this section of the project. Amphetamine (AM), methamphetamine (MA), 3,4-methylenedioxyamphetamine (MDA) and 3,4-methylenedioxymethamphetamine hydrochloride (MDMA) were used in this study because they are widely abused among young people.^{276, 277}

This chapter is divided into three main sections. The first section (4.1) concerns the development of a chromatographic method for analysis of the drugs of interest. The second section (4.2) describes the performance of different forms of silica monolith in extracting the drugs of interest. The final section (4.3) investigates the

development of a new SPE application for integrated DNA and drugs identification from a single sample.

4.1 HPLC Method Development

HPLC is the most commonly used measurement technique in forensic and clinical toxicology applications.²⁷⁸ In this study, all solutions that passed through the monolith during the extraction of drugs of interest (the loading, washing and elution steps) were collected and injected directly into an HPLC system to identify and quantify the drug. In order to obtain the best chromatographic conditions for the HPLC system, different detection wavelengths and mobile phases were examined. A working solution of a mixture of the drugs was prepared from a stock standard solution of 0.1 mg ml^{-1} (100 ppm) of each drug.

4.1.1 UV detection wavelength

A UV-visible detector was used as the detection method for the HPLC system and the maximum absorption wavelength for each of the drugs of interest was determined. Spectral scanning was performed in the range from 200 to 400 nm for $20 \text{ } \mu\text{g ml}^{-1}$ of each individual drug. The UV-spectra of the four amphetamines are shown in Figure 4-1. AM and MA, as do MDA and MDMA, have almost the same UV spectrum due to their similar structures. The spectral scan indicated that the maximum UV absorbance for the HPLC detector for the four drugs occurs at 210 nm.

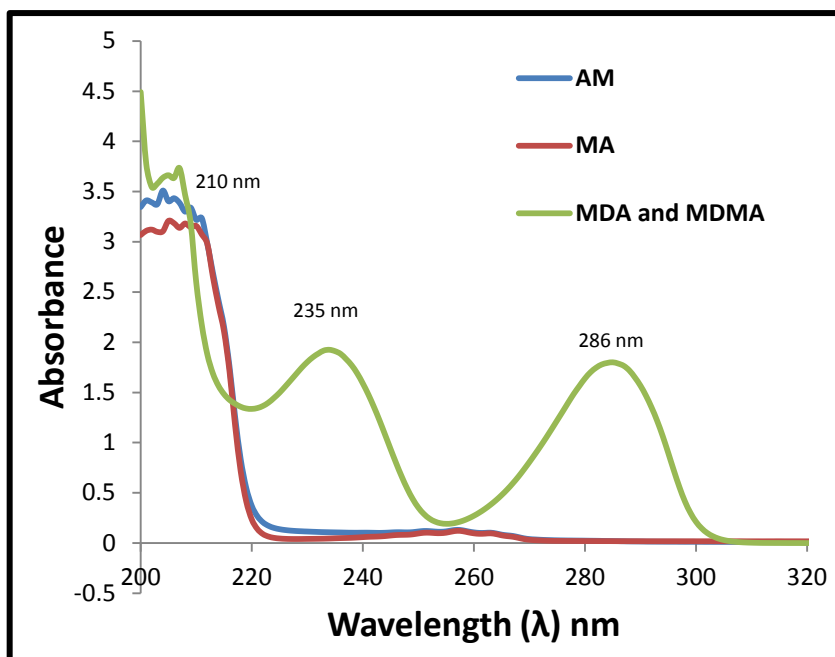


Figure 4-1: Absorption spectra of $20 \mu\text{g ml}^{-1}$ of AM, MA, MDA and MDMA in highly purified water; 210 nm was selected as λ max for all drugs of interest.

4.1.2 Optimum mobile phase combination

Chromatographic analysis was performed using a reversed-phase HPLC system with UV detection consisting of an LC 200 series binary pump, a UV-visible detector and a Prodigy™ C₁₈ column (150 x 4.6 mm), as described in section 2.5.4.2. Based on the analytes to be separated and their solubility, three different mobile phases (methanol:ultra-pure water [80:20, v/v], 10 mM sodium acetate:methanol [70:30, v/v] at pH 6, and 50 mM phosphoric acid [pH 4 using triethylamine]:acetonitrile [9:1])²⁷⁹ were investigated under isocratic conditions at ambient temperature around 23 °C. The analytes of interest were retained on the C₁₈ column by a hydrophobic interaction due to their low polarity.²⁸⁰ Separation depends on the polarities of the analytes, with more polar compounds being eluted early while less polar and non-polar analytes (such as amphetamines) are strongly retained and often require a high percentage of organic solvents to be eluted.

For the direct injection of the mixed drugs standard using a methanol:water (80:20, v/v) mobile phase, no peaks were seen for the drugs of interest (Figure 4-2 A). This is because the strength of the methanol:water mobile phase was not enough to reduce the hydrophobic interactions between the adsorbent and the analytes, and, as a result, the drugs did not pass through the column but were retained on the stationary phase and were not detected. Therefore, a less polar mobile phase than methanol:water was required, such as 10 mM sodium acetate:methanol (70:30, v/v). Although the sodium acetate buffer has less polarity than water, it absorbs light below 220 nm, which may be a problem when using a UV detector at 210 nm.²⁸¹ This explains the absence of peaks for the four amphetamines when a 10 mM sodium acetate:methanol (70:30, v/v) mobile phase was used, as shown in Figure 4.2 B.

Amphetamines contain nitrogen atoms which can interact strongly with the residual silanol groups on a packed column (C₁₈), resulting in low analytical recoveries with tailing peaks. This phenomenon can be reduced by the addition of silanol blockers such as triethylamine (TEA) to the mobile phase which compete with the amphetamines for residual silanol sites on the support.²⁸¹⁻²⁸³ TEA was used with 50 mM phosphoric acid:acetonitrile (9:1) to evaluate the influence of a silanol blocking agent in solving this problem.²⁸⁴ Figure 4-3 shows a successful elution of mixed standards of amphetamine from the HPLC packed column with good chromatographic resolution when TEA was added to the 50 mM phosphoric acid:acetonitrile (9:1, pH 4) mobile phase under isocratic conditions. The peaks in the mixture were identified by comparison with the retention time of the peak for each individual drug. The first peak to elute from the mixture was the most polar compound (AM), followed by the less polar MA, MDA, and MDMA, respectively.

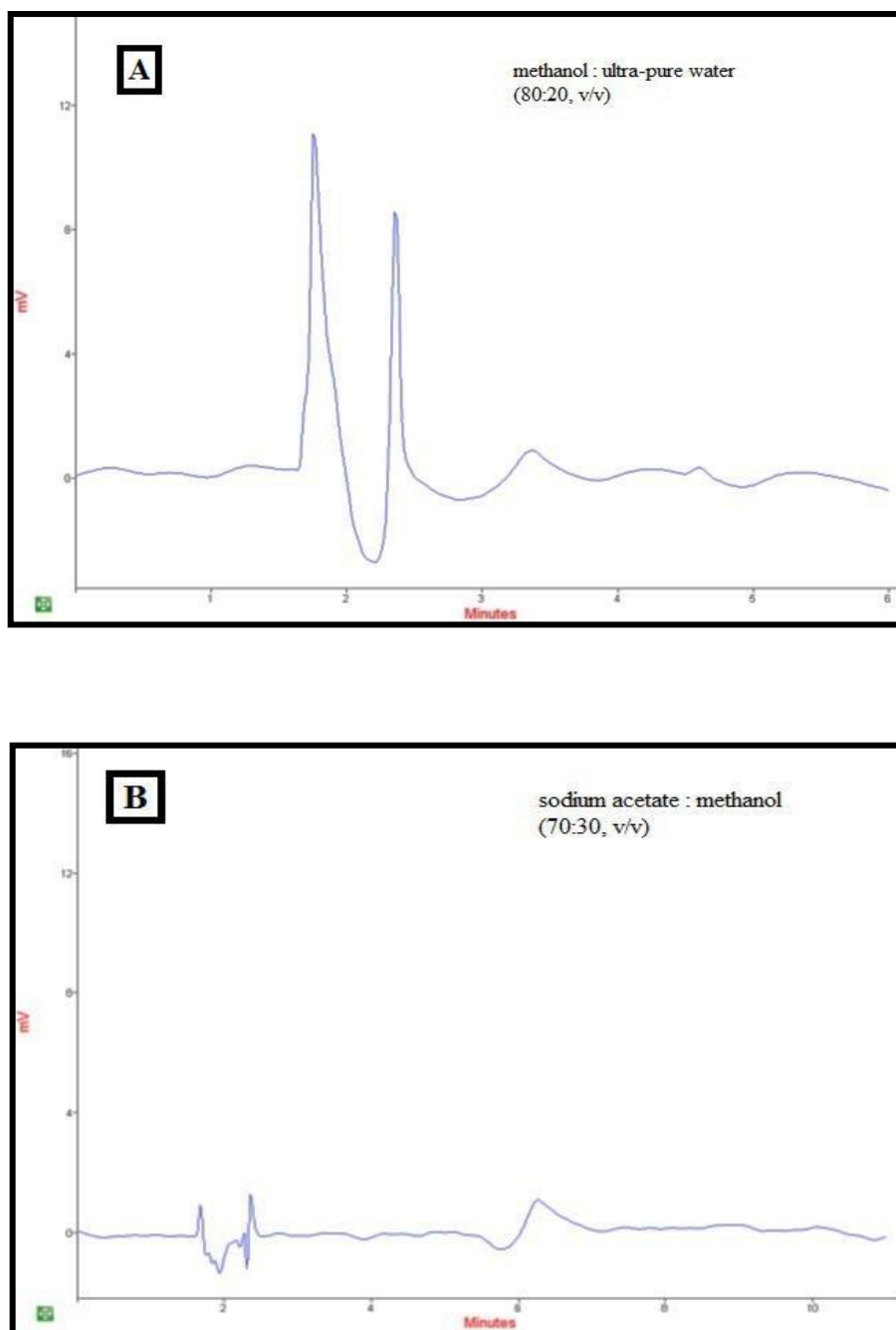


Figure 4-2: HPLC chromatograms for the direct injection of $20 \mu\text{g ml}^{-1}$ of AM, MA, MDA and MDMA showing a non-peak response when A) methanol:water (80:20, v/v) and B) 10 mM sodium acetate:methanol (70:30, v/v, pH 6) mobile solvents were used. Separation was performed on $5 \mu\text{m}$ ProdigyTM C₁₈ (Phenomenex, 150 x 4.6 mm), under isocratic conditions at a flow rate of 1 ml min^{-1} . UV detection was obtained at 210 nm and injection volume was $20 \mu\text{l}$.

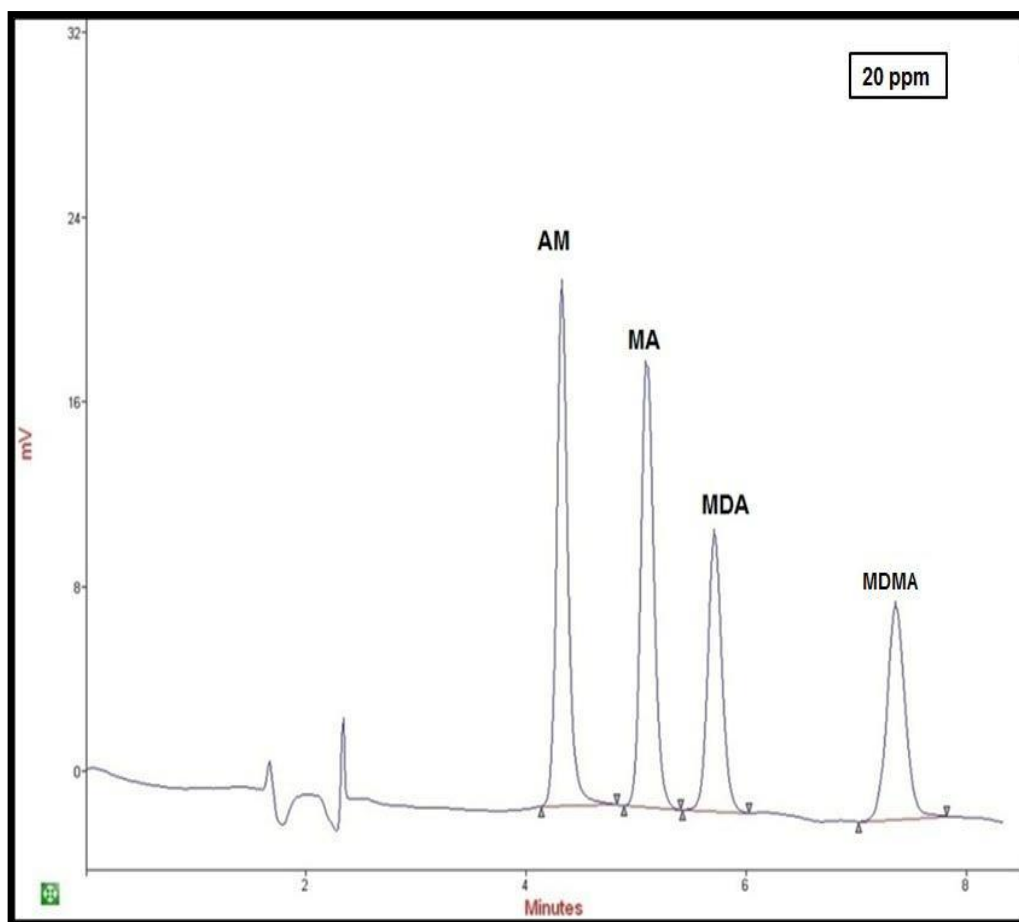


Figure 4-3: Typical chromatogram for a mixed standard of amphetamines (20 ppm) using a 5 μm ProdigyTM C₁₈ (Phenomenex, Torrance, CA, USA) 150 x 4.6 mm column, mobile phase under isocratic conditions: 10% acetonitrile, 90% 50 mM phosphoric acid (pH 4 using triethylamine); a flow rate of 1 ml min⁻¹ with UV detection obtained at 210 nm and the injection volume was 20 μl .

4.2 Investigation of Monolithic Silica for Drugs Extraction

4.2.1 Drugs extraction using thermally activated monoliths

In chapter 3, a thermally activated potassium silicate monolith was shown to be a suitable solid support for higher DNA extraction efficiency. In this section, the performance of the same silica monolith is evaluated for the extraction of AM, MA, MDA and MDMA. A fundamental prerequisite for analyte extraction is knowledge of the chemistry and nature of the sorbent and analyte(s) of interest. The surfaces of the silica-based monolith consist of two functional groups: silanols ($\equiv\text{Si-OH}$) and siloxanes ($\equiv\text{Si-O-Si}\equiv$).⁷⁶ Theoretically, the mechanism of extraction for the drugs of interest on a silica monolith is based on the ionic interaction (weak cation-exchange) between the positively charged analytes and negatively charged silanol groups ($\equiv\text{Si-O}^-$) in a medium with a pH above 4.²⁸⁵ In addition, siloxane groups ($\equiv\text{Si-O-Si}\equiv$) provide a very weak hydrophobic interaction for the non-polar functional groups associated with the drugs of interest.²⁸⁶

The compounds of interest were extracted using a thermally activated potassium silicate monolith placed within a glass capillary, as described in section 2.4.3 for DNA extraction. Hydrodynamic pumping was used to move the eluent during the extraction steps at different flow rates. The silica-based monolith was equilibrated with a 200 μl solution similar to the sample loading conditions, which was either ultra-pure water or 10 mM TE buffer at a flow rate of 5 $\mu\text{l min}^{-1}$ in order to maximise the binding of the analyte of interest to the stationary phase. Ultra-pure water (pH 5.5) was used as a relevant solvent for most of the drugs, whereas the 10 mM TE buffer (pH 6.7) was examined for compatibility with the DNA extraction buffer for the future combination of drugs and DNA analysis.

A mixed drugs standard of 50 μl of 20 $\mu\text{g ml}^{-1}$ was pumped through the potassium silicate monolith at a flow rate of 2.5 $\mu\text{l min}^{-1}$ followed by 100 μl of either ultra-pure water or 10 mM TE buffer (similar to the load solution) to remove any interferents at a flow rate of 5 $\mu\text{l min}^{-1}$. Finally, the retained compounds were eluted with 50 μl of the optimised mobile phase (10% acetonitrile, 90% 50 mM phosphoric acid at pH 4 adjusted by triethylamine) at a flow rate of 1 $\mu\text{l min}^{-1}$. The extract was directly injected into the HPLC with UV detection to evaluate the percentage of analyte recovery. The recovery calculated was obtained from the peak area ratio of the extracted mixed drug standard divided by the relevant peak area of the non-extracted standard (directly injected), multiplied by 100.

The thermally activated monolith did not, however, retain the drugs of interest efficiently and the majority of analytes were lost during the loading and washing steps, with only a low extraction recovery obtained during the elution step (this did not exceed 12%) from analytes prepared in ultra-pure water or 10 mM TE buffer. Figure 4-4 shows an example of the percentage recovery of the four analytes prepared in ultra-pure water. These results indicate that under the conditions used the normal phase monolith shows poor selectivity towards the target analytes. Therefore, functionalising the surface of the monolith with a high selectivity functional group towards the drugs of interest is desired for maximum extraction recovery.

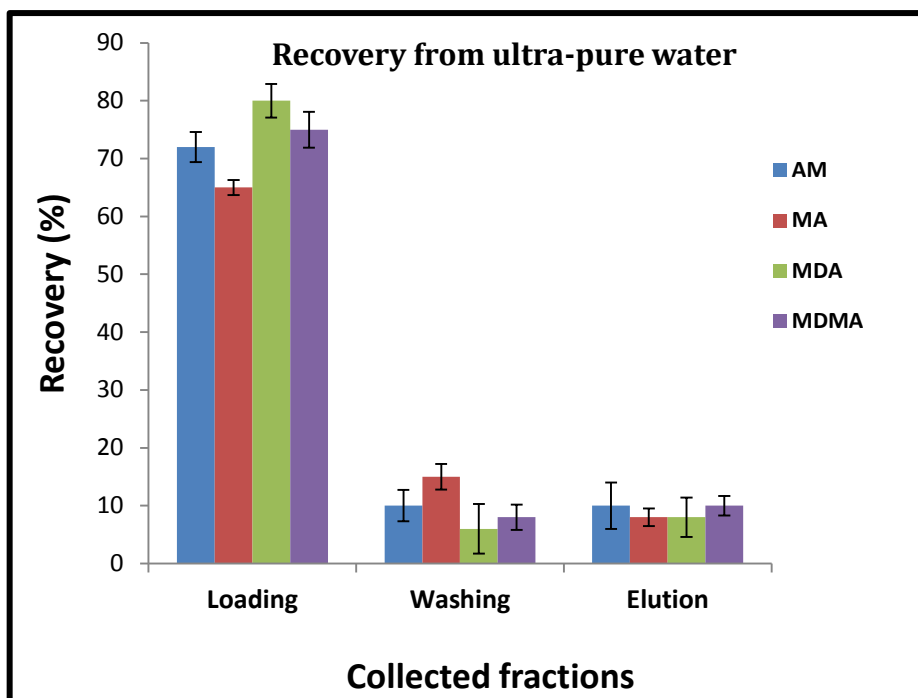


Figure 4-4: The extraction of ultra-pure water spiked with a $20 \mu\text{g ml}^{-1}$ mixed drugs standard using a thermally activated monolith. Each experiment was carried out in triplicate.

4.2.2 Chemical modification of silica monolith surface with lysine

Modification of the silica surface with a functional group plays a significant role in establishing the selectivity required to capture analytes of interest. Choosing the functional group requires consideration of the properties of the analytes, such as lipophilicity and pK_a . For instance, DNA is highly negatively charged over a wide range of pH due to the presence of a phosphate group, whereas basic drugs such as amphetamine (pK_a 9.9) are transformed into an ionised form (positive charge) when the pH is below 9.^{174, 287} Introducing oppositely charged groups on the surface of a solid-phase will exhibit ion selectivity to both anion and cation molecules. These types of stationary phases are known as zwitterionic ion-exchangers.²⁸⁸

A wide variety of amino acid structures can be immobilised on a matrix surface to provide zwitterion-exchange properties.²⁸⁹ In this work, lysine was evaluated as a zwitterionic stationary phase (see Figure 4-5) for DNA (anion) and amphetamine (cation) extraction.

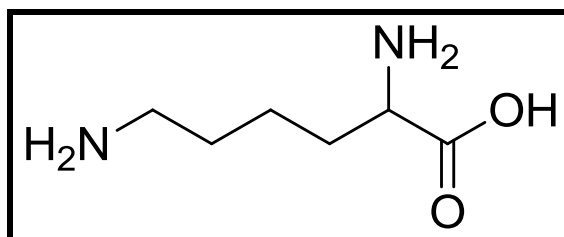


Figure 4-5: The chemical structure of lysine.

Lysine was chosen for a number of reasons. Firstly, the isoelectric point (*pI*) for lysine-bonded silica, where both the negatively charged carboxylic groups and the positively charged amine groups are equal to zero at pH 7.25.²⁹⁰ This pH value is suitable for the simultaneous extraction of negatively charged DNA (binding to positively charged amine groups) and positively charged drugs (binding to negatively charged carboxylic groups), as shown in Figure 4-6.

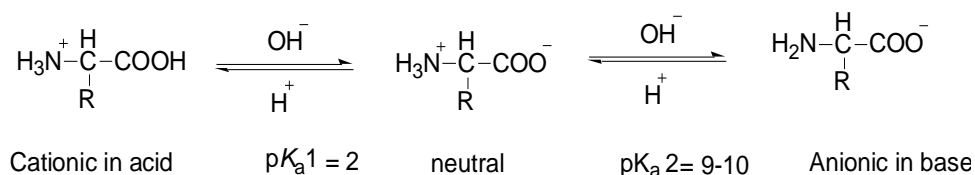


Figure 4-6: Scheme showing the predominant form of an amino acid depending on the pH of the solution.²⁹¹

In addition, lysine can be readily bonded to a silica surface, as shown in Figure 4-7. First, γ -glycidoxypropyltrimethoxysilane (GPTMS) was covalently bonded onto the surface of a silica monolith (2,6-lutidine acts as a catalyser) to generate an epoxy surface monolith. The surface was then treated with hydrochloric acid in order to open the epoxy ring to prepare a diol monolith. Finally, lysine was introduced onto the silica skeleton structure via a covalent bond with the diol monolith; accordingly, one of the primary amino groups in the lysine became a secondary amino group.²⁴⁵

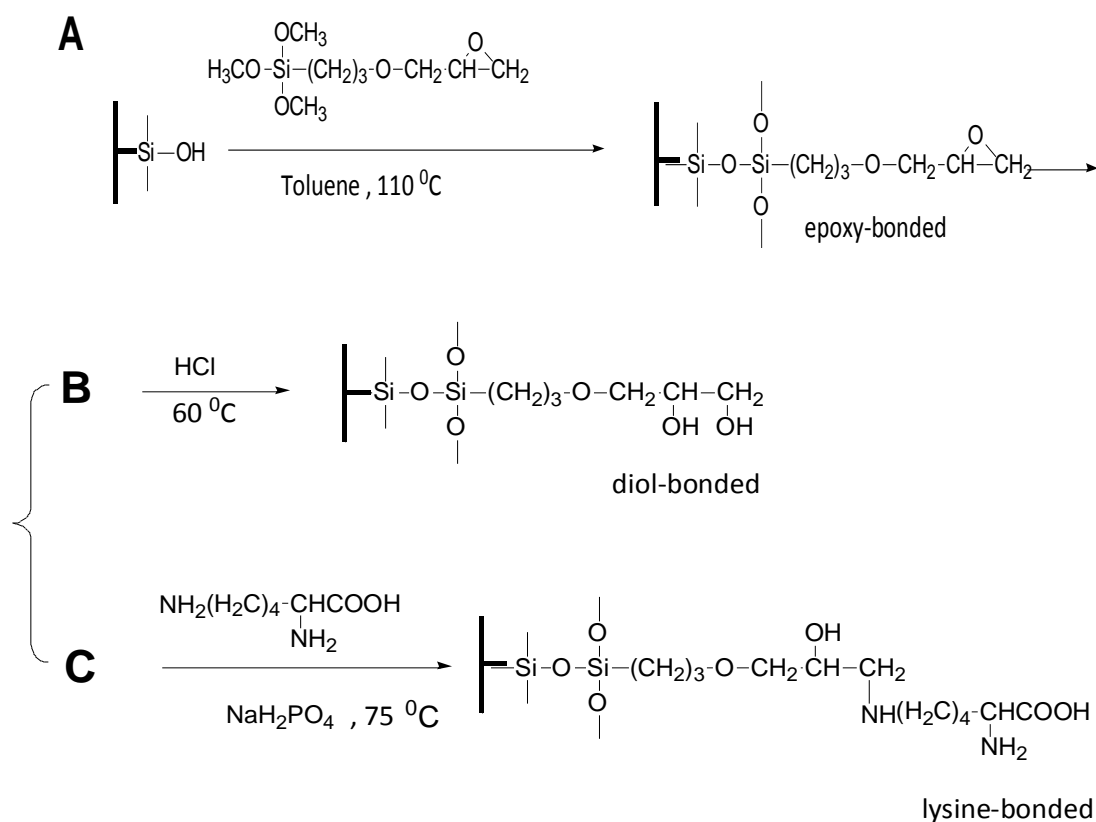


Figure 4-7: Schematic reaction pathways for the generation of the desired A) epoxy, B) diol and C) lysine monolithic stationary phases.²⁴⁵

4.2.2.1 Physical characterisation of the modified lysine stationary phase

The chemically modified lysine-bonded silica-based monolith was produced in a glass capillary following the reaction outlined above in Figure 4-7 and as described in section 2.5.1.1. The modified stationary phase was characterised by SEM, BET and Fourier transform infrared (FT-IR) analysis to identify the differences between the modified and non-modified silica-based monoliths.

Figure 4-8 shows the SEM micrographs of the surface of the silica-based monolith before (A) and after (B) modification with lysine and they are characterised by a bimodal pore structure with continuous macropores and mesopores. The SEM image indicates no marked differences in the structural morphology of the two monoliths even at high resolution (1 μm), and there was also no significant difference between them in the size of macropores.

However, when performing BET analysis, the surface area of the lysine-modified silica-based monolith was found to have decreased from 297 $\text{m}^2 \text{g}^{-1}$ (non-modified silica-based monolith) to 141 $\text{m}^2 \text{g}^{-1}$. The pore sizes had also decreased from 18 nm (non-modified silica-based monolith) to 11 nm for the amino-functionalised silica monolith due to the anchoring of organic moieties (lysine) on the inner surface of the pores. This indicates that some changes had taken place with the silica monolith which could be due to the successful modification of the silica-based surface with lysine.

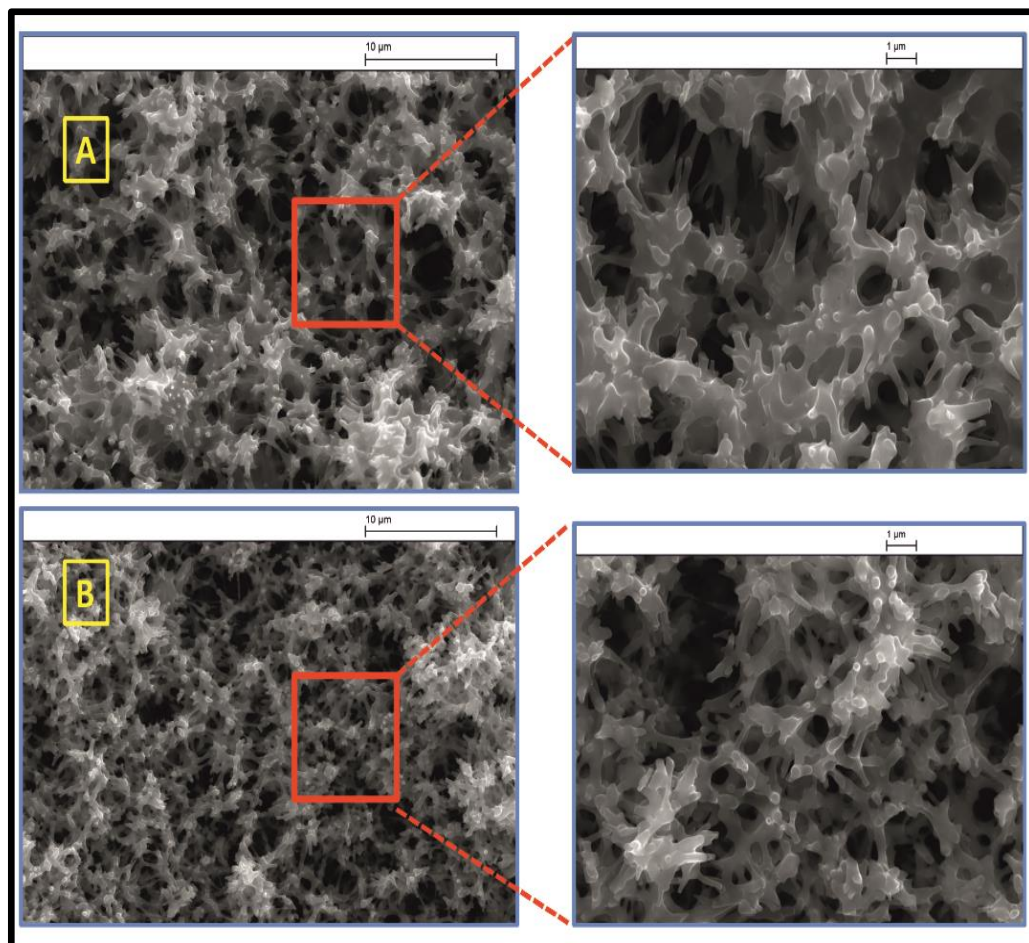


Figure 4-8: Electron micrographs showing the silica-based monolith structure (A) before, and (B) after chemical modification of the surface of the monolith with lysine.

FT-IR spectroscopy was also used to study the changes in chemical structure between the non-modified and modified monoliths in the region between 400 and 4000 cm^{-1} .²⁹² Figure 4-9 shows the FT-IR spectra of the non-modified silica-based monolith (blue spectrum) and the lysine-modified silica-based monolith (red spectrum). As seen in Figure 4-9, the strong peak observed at 1130 cm^{-1} and the narrow peak at 808 cm^{-1} are associated with the $\equiv\text{Si-O-Si}\equiv$ vibration for the modified and the non-modified silica surface.²⁹²

The FT-IR spectrum of the lysine-bonded silica shows some differences compared with the silica-based spectrum. The broad band at 3462 cm^{-1} corresponded to the N-H stretching vibration.²⁹³ After modification, the band at 2740 cm^{-1} for $\equiv\text{Si-OH}$ disappeared and the bending vibration of the CH_2 functional group was found at a wavelength of 2980 cm^{-1} .²⁹² The bending vibration band of the free NH_2 group was also observed at 1630 cm^{-1} .^{293, 294} These observed changes between the two spectra suggest that the lysine had been successfully grafted onto the surface of the silica-based skeleton.

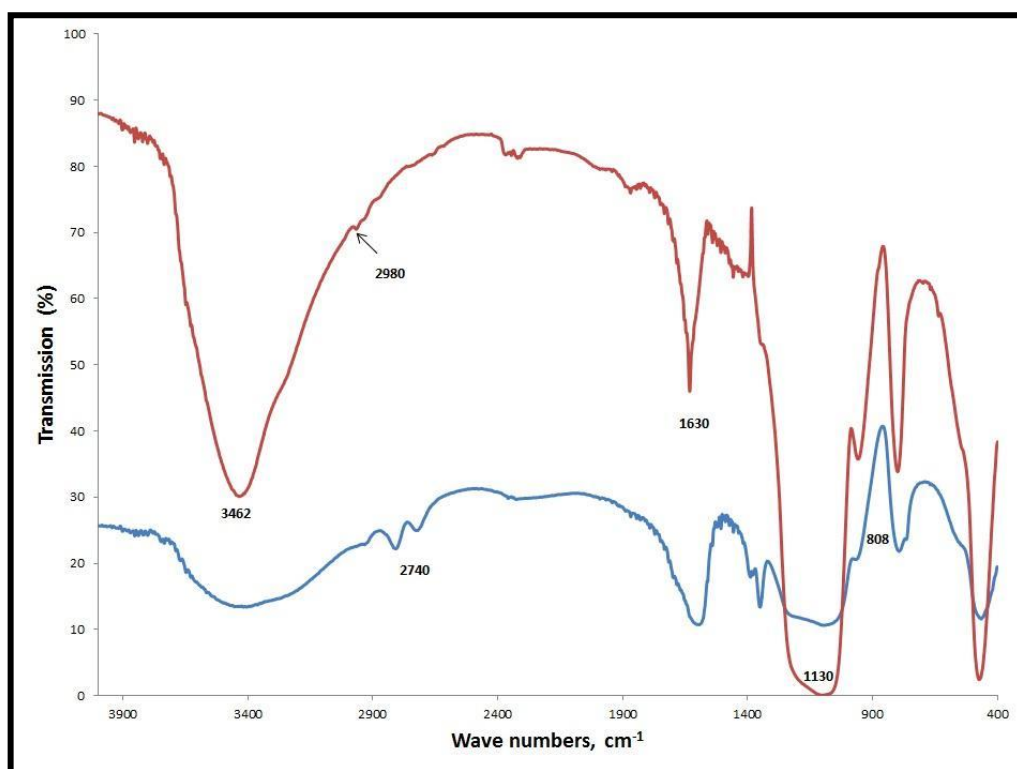


Figure 4-9: FT-IR spectra of the silica-based monolith (blue spectrum), and the amino-modified silica monolith (red spectrum).

4.2.3 DNA extraction using lysine-bonded monoliths

Amine-coated solid supports have been widely used for DNA extraction.²⁹⁵⁻²⁹⁷ The presence of oppositely charged groups on a lysine-modified silica-based monolith surface provides cation, anion and zwitter-exchange properties. The aim of this section is to evaluate a 15 mm (corresponding to 600 μg) modified silica-based monolith within a glass capillary (0.6 ± 0.05 mm ID) for DNA extraction using hydrodynamic pumping. With non-modified silica-based SPE, DNA adsorbs onto the monolith surface through hydrogen bonding in the presence of a chaotropic solution such as guanidine hydrochloride, as described in section 3.2.1.

The mechanism of DNA capture with an anion-exchanger is, however, different. The DNA purification process depends on the pH of the solution. The $\text{p}K_{\text{a}}$ of the amino group in the lysine is about 9,²⁹⁸ which can exploit a cationic charge below its $\text{p}K_{\text{a}}$. At pH 5, the amino group is, therefore, positively charged and electrostatic interaction with the negatively charged phosphate backbone of the DNA can occur. In order to achieve DNA extraction using a silica-based lysine anion-exchanger, three general SPE steps are required: loading of the sample, removing the impurities (washing), and eluting the target analyte. In this work, the surface of the monolith was activated with 10 mM 2-(N-morpholino) ethanesulfonic acid (MES) buffered at pH 5 for 30 minutes at a flow rate of $5 \mu\text{l min}^{-1}$.²⁰³ Human genomic DNA samples were prepared to a final concentration of $0.4 \text{ ng } \mu\text{l}^{-1}$ in MES buffer (total loaded volume was $50 \mu\text{l}$). The samples were then loaded at a flow rate of $5 \mu\text{l min}^{-1}$ to achieve DNA adsorption onto the modified silica surface. Cellular and proteinaceous debris that inhibit PCR amplification were removed using the loading buffer at a flow rate of $5 \mu\text{l min}^{-1}$.

Finally, increasing the basicity of the buffer (50 mM sodium carbonate, 50 mM sodium bicarbonate) from pH 5 to 9 was used to promote the adsorbed DNA to be released from the monolith due to the deprotonation of amino groups.^{201, 295} All solutions which passed through the modified solid-phase matrix were collected in 4 μ l aliquots and then divided into two equal fractions. The first 2 μ l fraction was analysed for DNA quantification using PicoGreen[®] assay and the second fraction was used for DNA amplification (PCR) as described in chapter 2. Initial experiment results found that the positively charged amino group was effective for DNA absorption with minimal loss during the loading and washing steps and then promoted DNA dissociation from the monolith as the amino group became neutral at pH 9 (Figure 4-10). DNA extraction efficiency was calculated as the amount of DNA recovered during elution expressed as a percentage of the initial amount loaded on the monolith. Preliminary results obtained from average DNA extraction efficiency was 29.8% using an elution flow rate at 5 μ l min⁻¹.

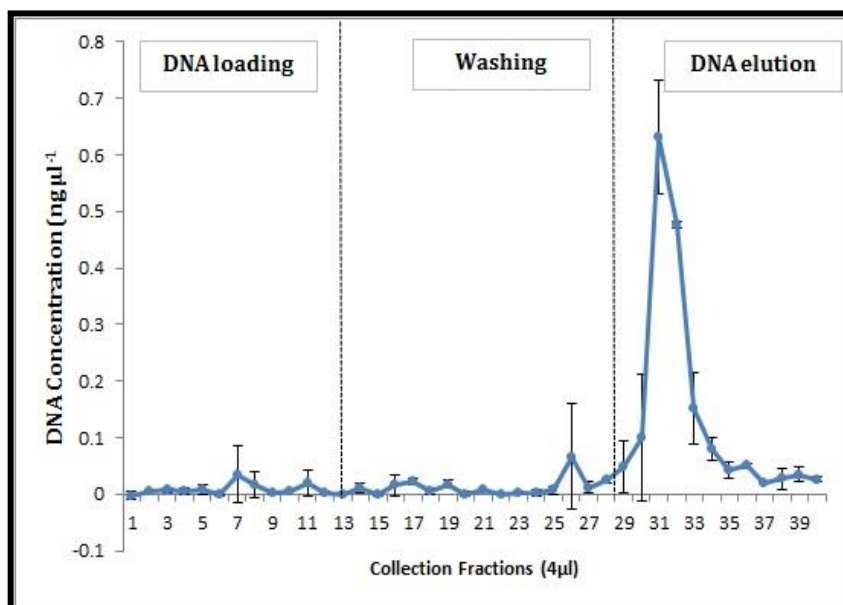


Figure 4-10: Graph showing the average DNA elution profile from 20 ng of purified human DNA using a lysine-bonded silica-based monolith for extraction ($n = 3$).

PCR analysis was carried out on the eluted DNA to confirm that there were no adverse effects from the elution buffer (pH 9) on downstream applications and the efficiency of the extraction method using a lysine-coated monolith to remove PCR inhibitors. The PCR products were analysed using conventional slab-gel electrophoresis. The results (Figure 4-11) showed successful amplification of the target D21 S11 (223 bp and 227 bp) locus, indicating that the concentration of elution buffer, set at 50 mM with pH 9, was efficient in releasing DNA and did not substantially hinder PCR amplification.

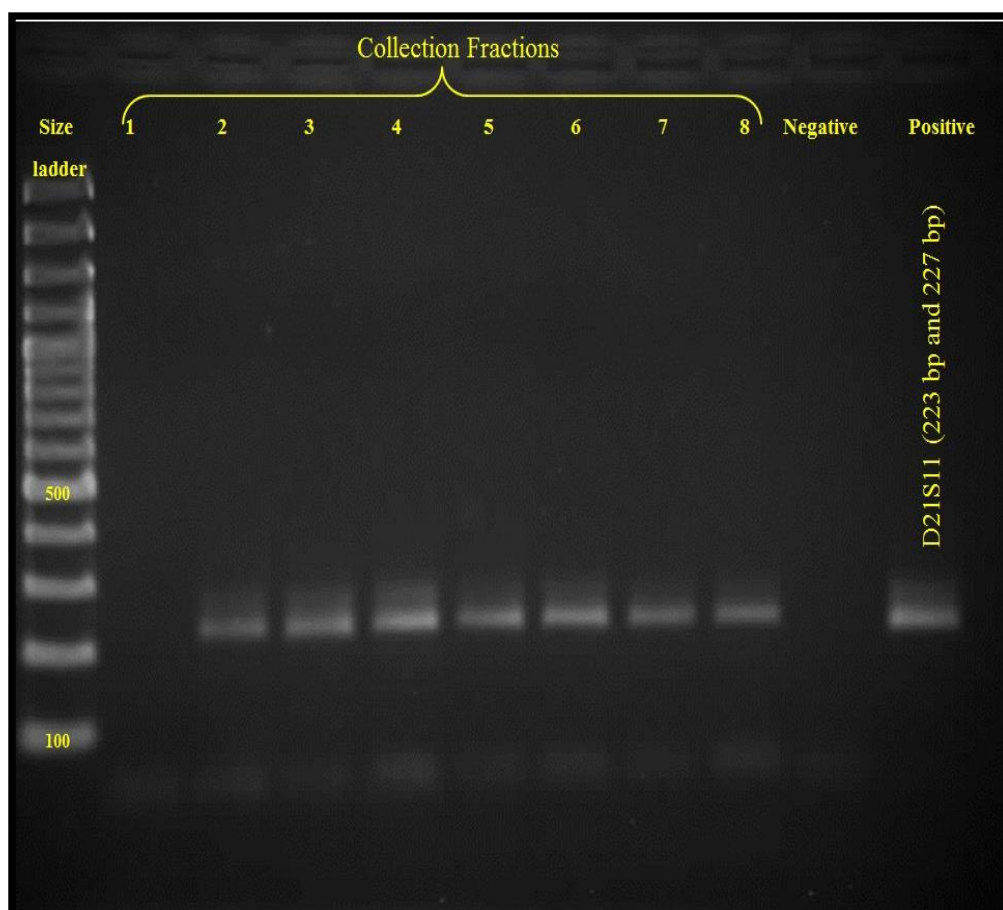


Figure 4-11: Agarose gel electropherogram of the PCR products (D21 S11 gene: 223 and 227 bp) from human DNA released from the lysine-modified silica-based monolith.

In an attempt to increase DNA extraction efficiency, different elution flow rates were used over the range from 1 to 10 $\mu\text{l min}^{-1}$. As expected, an inverse relationship between elution flow rate and extraction efficiency was observed (see Figure 4-12).

It was found that the highest DNA yield during the elution phase was obtained when the elution flow rate was decreased. As mentioned previously, the pK_a of the amino groups in the lysine is about 9 and these are expected to be protonated at pH 5 so that the lysine can capture the negatively charged molecule such as DNA. In contrast, the deprotonation of amino groups occurs at pH 9, and this will promote DNA release. The amino groups will, however, require time to equilibrate and change to facilitate DNA release. Increasing the flow rate (10 $\mu\text{l min}^{-1}$) decreases the contact time between the amino groups and elution buffer, which resulted in low DNA extraction efficiency (30%) with lack of reproducibility (22% RSD). However, at lower flow rates (1 $\mu\text{l min}^{-1}$), the time needed for equilibration of the amino groups with the elution buffer solution (pH 9) is greater, which led to high DNA release (77%) with superior reproducibility (4% RSD).

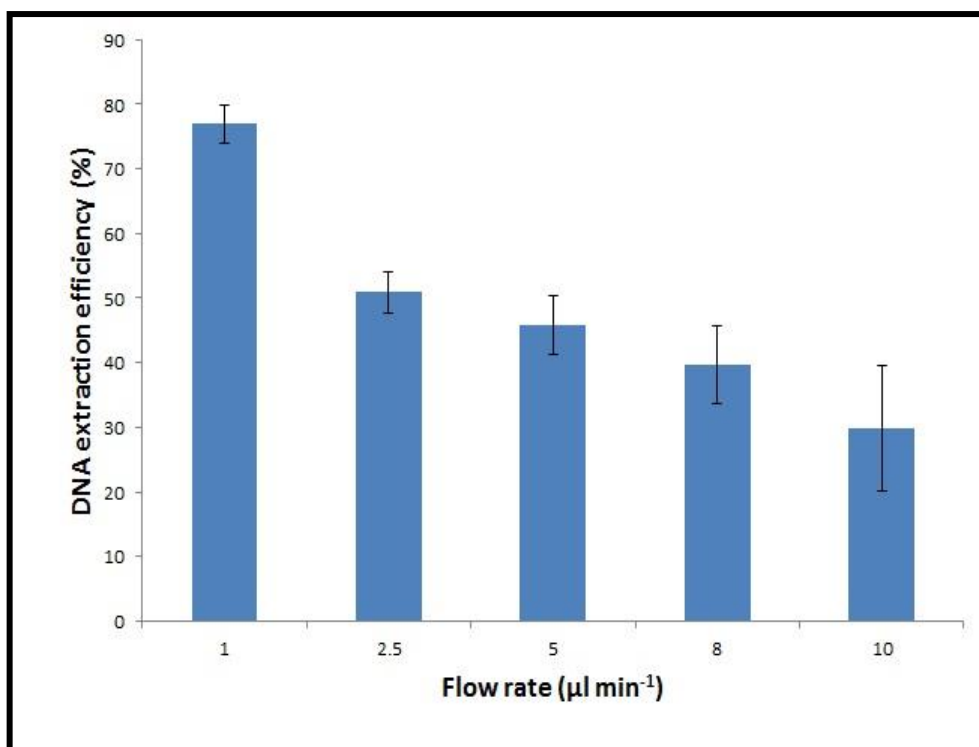


Figure 4-12: Graph showing DNA extraction efficiency as a function of different elution flow rates.

4.2.3.1 DNA binding capacity

Previous results (section 3.2.2) indicated that the amount of DNA adsorbed onto a monolith was $823 \mu\text{g DNA g}^{-1}$ when a non-modified silica surface was used. The DNA binding capacity of the $600 \mu\text{g}$ lysine-modified monolith was calculated in order to evaluate the amount of DNA that saturated the binding sites after modification. To determine the DNA capacity of the modified monolith, a buffer solution (10 mM MES) containing purified human DNA ($3.95 \text{ ng } \mu\text{l}^{-1}$) was continuously loaded and all fraction volumes ($4 \mu\text{l}$) that passed through the modified monolith were collected and quantified for the amount of DNA using a fluorescence assay (PicoGreen[®]). Using the same breakthrough method as described in chapter 3, it was found that the average loading capacity was $1.7 \text{ mg DNA g}^{-1}$ for the modified monolith (see Figure 4-13).

These results indicate that a DNA-capturing method using a lysine-modified monolith is highly effective in terms of DNA adsorption compared to a non-modified monolith ($0.823 \text{ mg DNA g}^{-1}$).

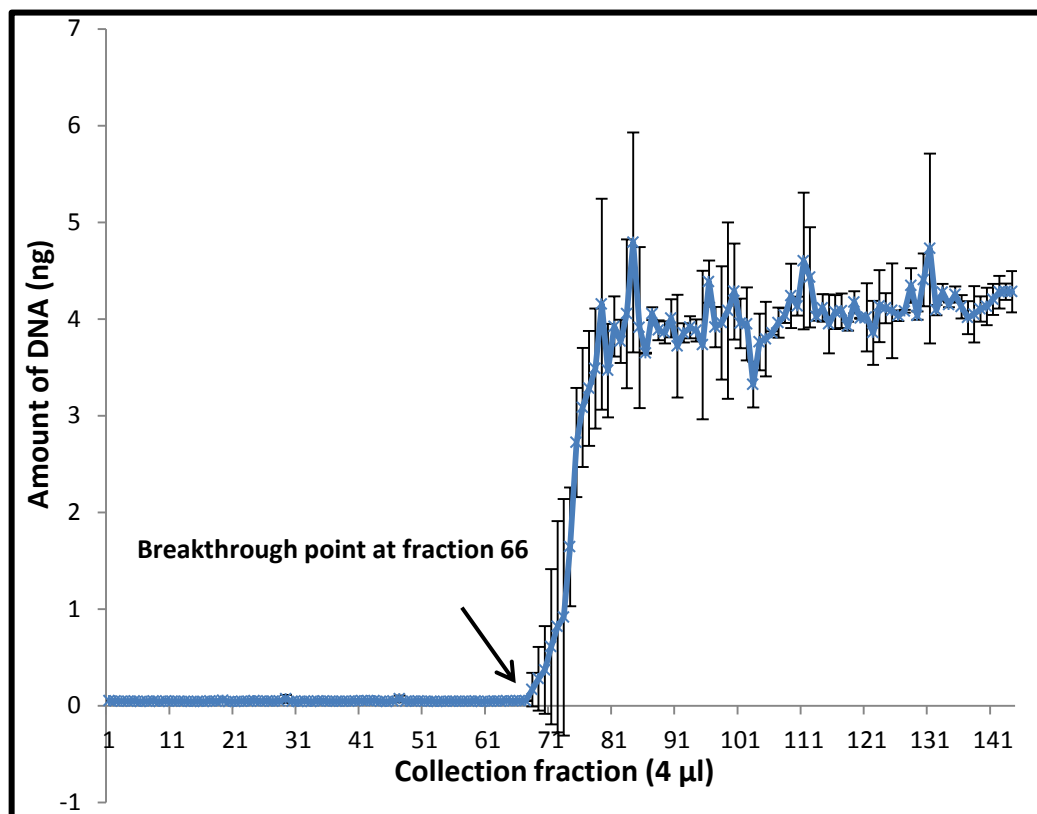


Figure 4-13: The breakthrough curve provides a loading capacity of 1,042 ng of purified human DNA on a lysine-bonded monolith.

4.2.4 Drugs extraction using lysine-bonded monoliths

In the previous section, the DNA capture and release method was based on electrostatic interaction between positively charged amino groups on the surface of a lysine-modified monolith and negatively charged DNA. The lysine-bonded monolith exhibited zwitterionic characteristics due to the presence of oppositely charged groups on the surface.

The pK_a of the carboxylic acid group in the lysine is about 2.18,²⁸⁹ and can exploit cationic-exchange properties above its pK_a . Therefore, at pH 5, the carboxylic group is negatively charged and electrostatic interaction with positively charged molecules can occur.

The adsorption selectivity of the lysine-modified phase for the four amphetamines was investigated because they can exist in ionised form (positively charged) at pH 5 (their pK_a range is between 9.8 and 10.1).¹⁶ The extraction steps were carried out using a hydrodynamic syringe pump and optimised extraction conditions identified for DNA extraction (see section 2.4.3). The modified adsorbent was conditioned and equilibrated using a 10 mM MES buffer at pH 5 for 30 minutes at a flow rate of 5 $\mu\text{l min}^{-1}$. A mixture of drugs was added directly to the 10 mM MES loading solution to give a final concentration of 20 $\mu\text{g ml}^{-1}$ and then loaded at a flow rate of 2.5 $\mu\text{l min}^{-1}$ (the total loaded volume was 50 μl). Contaminants were removed using the loading buffer at a flow rate of 5 $\mu\text{l min}^{-1}$. Finally, the target analytes were released from the monolith at a flow rate of 1 $\mu\text{l min}^{-1}$ using an optimised mobile phase. All of the solution was collected after passing through the lysine-modified silica-based monolith. Initial drugs extraction results using the modified monolith (lysine-bonded monolith), however, found that the carboxylic acids (negatively charged) were unable to interact with the four drugs of interest (positively charged) when 10 mM MES (pH 5) was used, as the chromatogram obtained from the loading step showed a strong similarity in the peak areas and retention times for those with a directly injected mixed standard of amphetamines (see Figure 4-14). These results indicate that the majority of analytes were lost during the loading step.

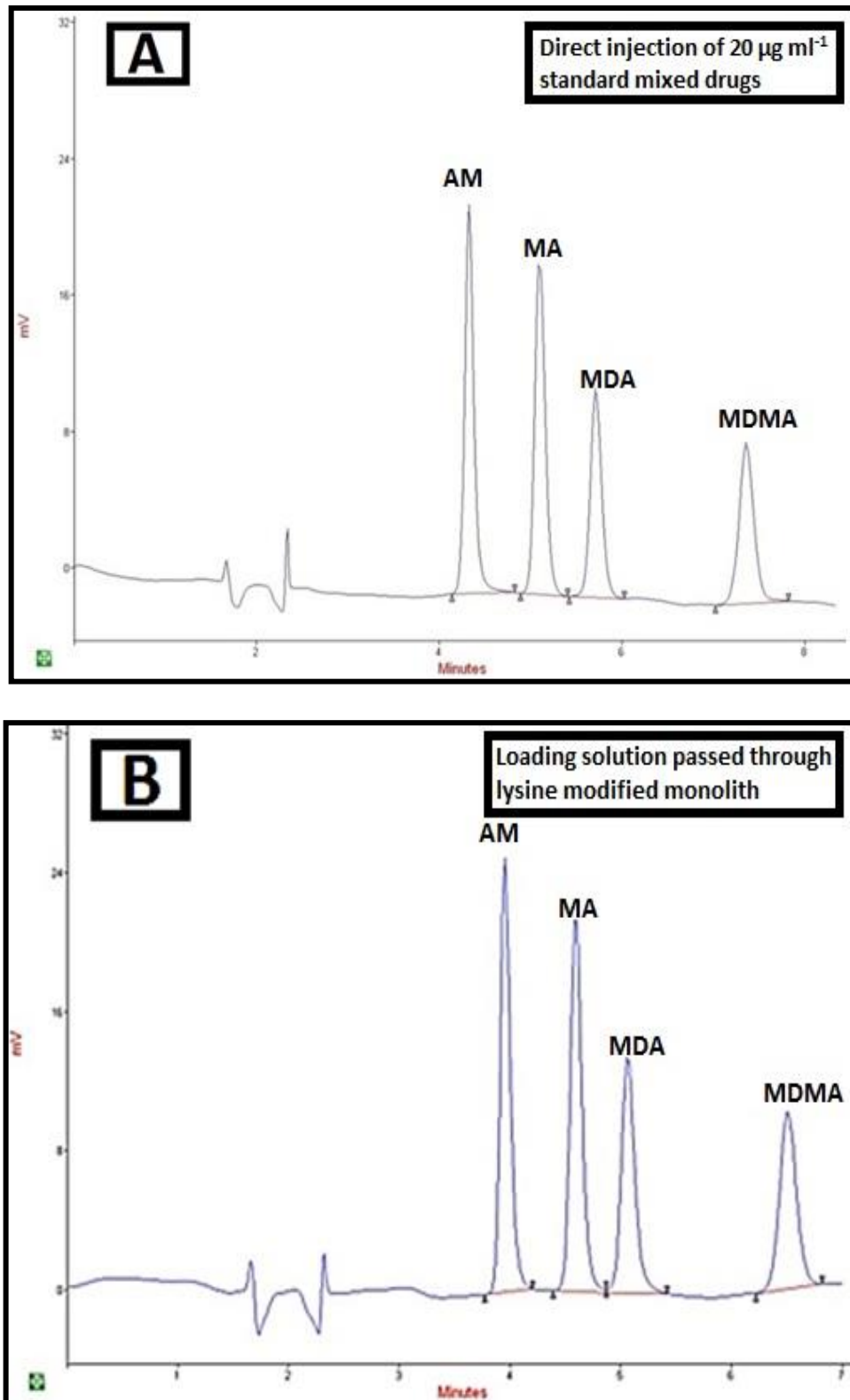


Figure 4-14: HPLC chromatograms of A) a directly injected 20 µg ml⁻¹ mixed standard of AM, MA, MDA and MDMA and B) loading buffer collected after passing through the lysine-modified silica-based monolith.

As indicated previously, the pK_a of a carboxylic acid group is about 2.18 and deprotonated (ionised) when the pH is increased. The active pH range of the MES buffer is from 4 to 5; therefore, it was necessary to change to another loading buffer with a higher pH value to ensure that the carboxylic acid groups were changed to the cationic-exchanger form for efficient analyte retention. A phosphate buffer offers a pH range of 5 to 8 and low UV absorbance (less than 205 nm), which will not interfere with the drugs of interest.^{281, 299} Different pH values (5, 6, 7 and 8) of phosphate buffer were examined as a loading buffer for the target analytes. There was no reason to increase the pH of the loading buffer beyond 8 because the four amphetamines would then transform to a non-ionised form and no ionic-exchange would occur. The loading solution that passed through the modified monolith was collected and then injected directly into the HPLC system to evaluate the effectiveness of the sorbent in retaining the drugs of interest. Figure 4-15 shows the percentage of analyte recovery during the loading stage and this is compared with the resulting peak areas for a direct injection of a $20 \mu\text{g ml}^{-1}$ mixed standard.

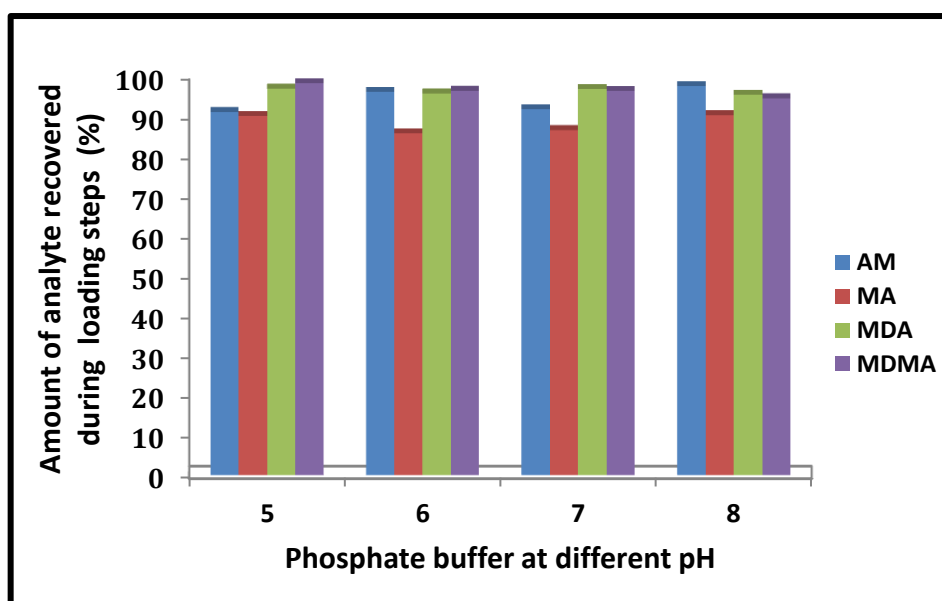


Figure 4-15: The effect of phosphate buffer pH on the retention of analytes during the loading stage (n = 3).

As can be seen from Figure 4-15, more than 90% of the target analytes were lost during the loading step at all pH ranges, which suggests that this method is not effective for amphetamines. Weak retention of the four drugs can be due to repulsion from the positively charged layer of protonated secondary amino groups and also to the location of carboxyl groups at the inner side of the lysine-bonded chain after reaction with the epoxy ring, as indicated in Figure 4-16. The results presented here fit well with those in the published literature where a lysine-modified monolith showed limited cation-exchange properties to Na^+ , NH_4^+ , and K^+ .³⁰⁰

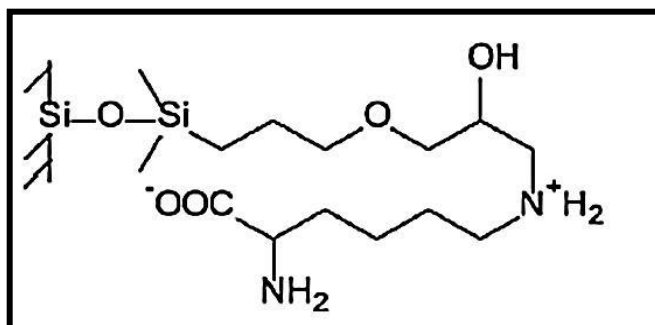


Figure 4-16: Stationary phase with covalently attached zwitterionic lysine.²⁸⁸

4.2.5 Chemical modification of silica bead surfaces with C₁₈

The results in the previous section found that the four drugs of interest were weakly retained to the silica-based monolith covalently bonded with lysine. Therefore, an alternative modification method was required. Octadecyl (C₁₈) as a pre-concentration/extraction matrix has been used in many applications.³⁰¹⁻³⁰⁴ An octadecyl group has a high affinity with hydrophobic molecules such as some drugs and proteins.¹⁹⁹ Purification techniques have, in general, been performed using silica beads and/or monolithic media packed in a cartridge or column.^{168, 305} The use of packed modified C₁₈ monolithic silica for drug extraction and purification is not new and requires multiple stages, such as centrifugation (spin column),¹⁰⁸ filtration (capillary tube),^{239, 305} or several aspiration and dispensing steps (pipette tip).^{240, 306} The surface of the thermally activated silica-based monolith inside a glass capillary was, therefore, modified with octadecyl groups as described in detail in section 2.5.1.2. Unfortunately, a high back pressure was generated during the modification of the thermally activated monolith. The reason for the increased back pressure may have been the blockage of the pores by the attached large organic moieties (octadecyl groups). The silica-based monolith was, therefore, substituted with silica beads chemically modified with octadecyl (C₁₈) groups as described in section 2.5.1.2. The modified octadecyl (C₁₈) silica beads were then packed inside a female luer lock adaptor (Figure 2-8) to perform drug purification under the influence of a hydrodynamic pump, as shown in Figure 2-9. The chemical reaction between the silanols on the monolith surface and the chloro(dimethyl)octadecylsilane compounds is shown in Figure 4-17.

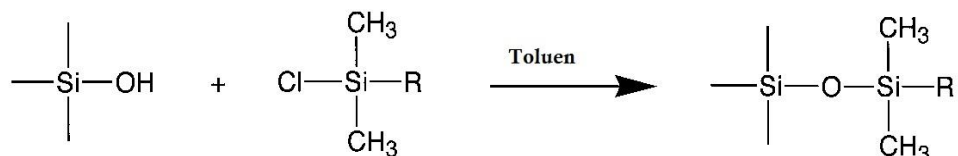


Figure 4-17: Schematic representing the chemical reaction between the surface silanol groups on the silica-based monolith and the organosilane compounds, where R = C₁₈.³⁰⁷

4.2.5.1 Physical characterisation of the modified C₁₈ silica beads

The structural morphology of the silica beads was examined by SEM before and after surface modification. As shown in Figure 4-18 A, the SEM image of the non-modified surface showed that the silica beads have an irregular shape with a diameter ranging between 40 and 100 μm. After modification of the silica beads with octadecyl groups, no significant changes to the size and surface of the silica beads were observed (see Figure 4-18 B).

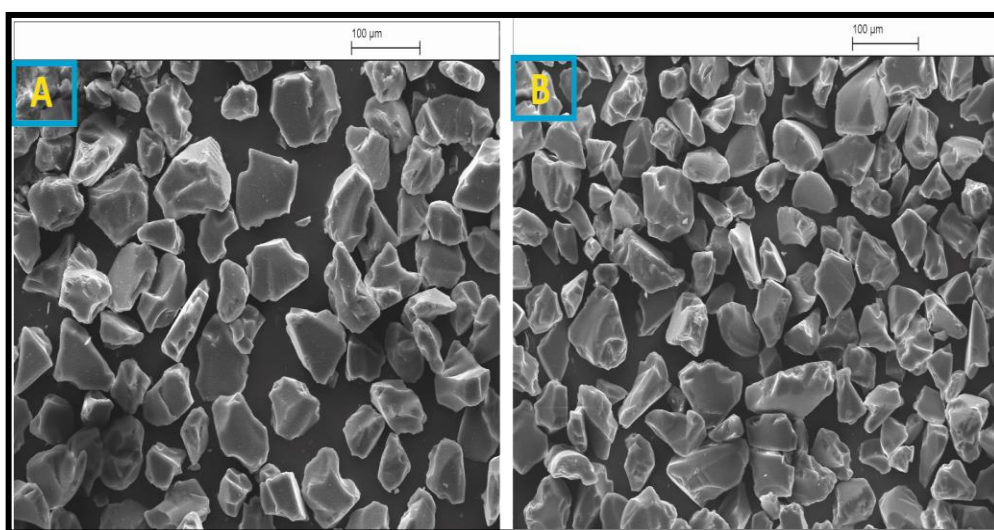


Figure 4-18: SEM micrographs of the silica beads A) before and B) after surface modification with octadecyl groups.

The C₁₈ silica beads were further characterised by FT-IR spectroscopy in order to monitor the chemical attachment of the chloro(dimethyl)octadecylsilane with the surface silanol groups on the silica beads.

The region between 400 and 4000 cm^{-1} was used to study the surface characterisations of the modified and non-modified silica bead samples (see Figure 4-19). Both samples showed a strong absorption peak at 1115 cm^{-1} , which is attributed to the asymmetric stretching vibration of $\equiv\text{Si-O-Si}\equiv$ (1130 to 1000 cm^{-1}).³⁰⁸ Moreover, the band at 812 cm^{-1} corresponded to a symmetric stretching vibration of $\equiv\text{Si-O-Si}\equiv$ (860 to 730 cm^{-1}).²⁹² A new band was observed at around 2860 cm^{-1} for the modified beads spectra, which is a characteristic band for C-H vibration.⁵² In addition, the modified surface showed absorption peaks at around 2960 cm^{-1} arising from C-H₂ on the alkyl chain groups, suggesting successful modification of the silica bead surfaces.⁵² The broad band from 3000 to 4000 cm^{-1} for the non-modified surface represented vibrations of $\equiv\text{Si-OH}$ or absorbed water which disappeared with hydrophobic silica beads as an indication of successful modification with C₁₈.^{292, 309}

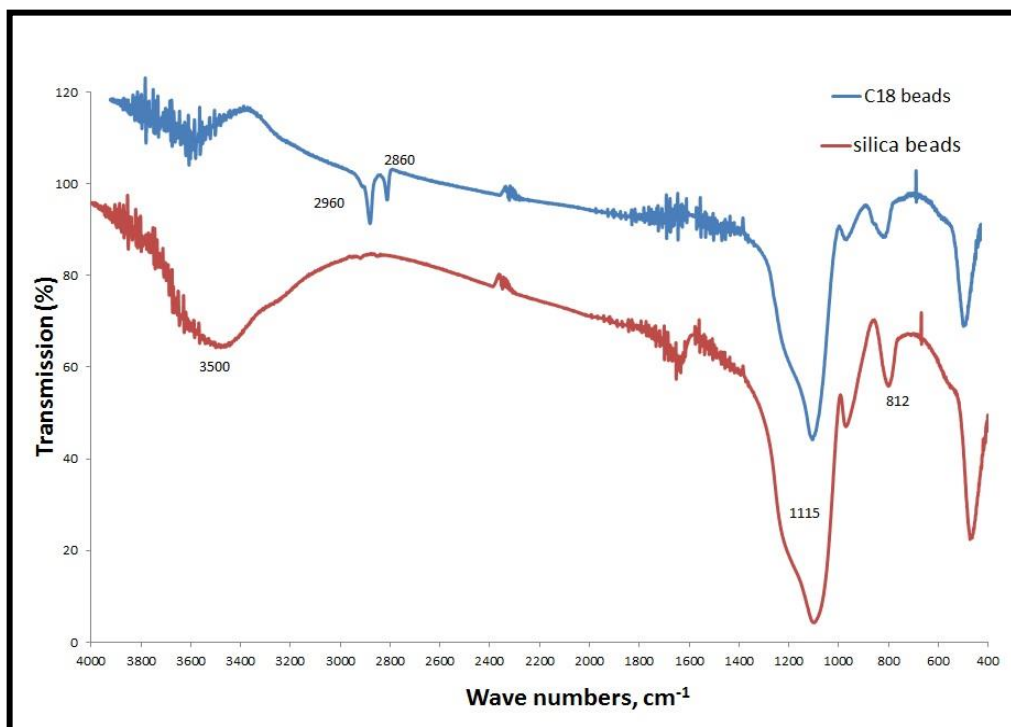


Figure 4-19: FT-IR spectra of the silica beads (red spectrum) and the C₁₈-modified silica beads (blue spectrum).

4.2.5.2 Extraction of the drugs of interest using modified silica beads

In order to evaluate the extraction efficiency of the AM, MA, MDA and MDMA using packed C₁₈-modified silica beads, 50 µl of the final concentration of 20 µg ml⁻¹ for the mixed drugs standard was loaded onto pre-activated C₁₈ silica beads, followed by 50 µl ultra-pure water to wash out any impurities. Finally, the retained drugs were eluted with 50 µl of the mobile phase used for the HPLC analysis (10% acetonitrile, 90% 50 mM phosphoric acid at pH 4 adjusted by triethylamine). Hydrodynamic pumping at a flow rate of 10 µl min⁻¹ was used for all extraction steps. Packing the beads within a microfluidic system could generate high back pressure,⁵⁸ but these beads had a large surface area (non-modified at 550 m² g⁻¹ and an irregular shape) and minimal back pressure was seen as the syringe pump did not stop. There was no leaking around the connector at the flow rates used because the modified beads were packed inside a 9.4 mm diameter female luer lock adaptor which allowed the solution to pass in different directions around the irregularly shaped beads. Figure 4-20 shows two chromatograms: the first (A) corresponds to the directly injected 20 µg ml⁻¹ mixed drugs standard, and the second (B) was obtained from the eluted fraction of the same extracted concentration using octadecylated silica beads. The recovery percentage of the extraction was calculated as a peak area ratio of extracted drugs to those directly injected as a mixed drugs standard under the optimised conditions of the HPLC system. It was found that the average recovery for the four drugs in the mixed standard after triplicate extraction using C₁₈ silica beads was high (90%) with good reproducibility (< 15% RSD). This indicates the effectiveness of the modified silica beads, as the target analytes retained during the loading step were then eluted in significant amounts using the optimised HPLC mobile phase (10% acetonitrile, 90% 50 mM phosphoric acid; pH 4 adjusted by triethylamine).

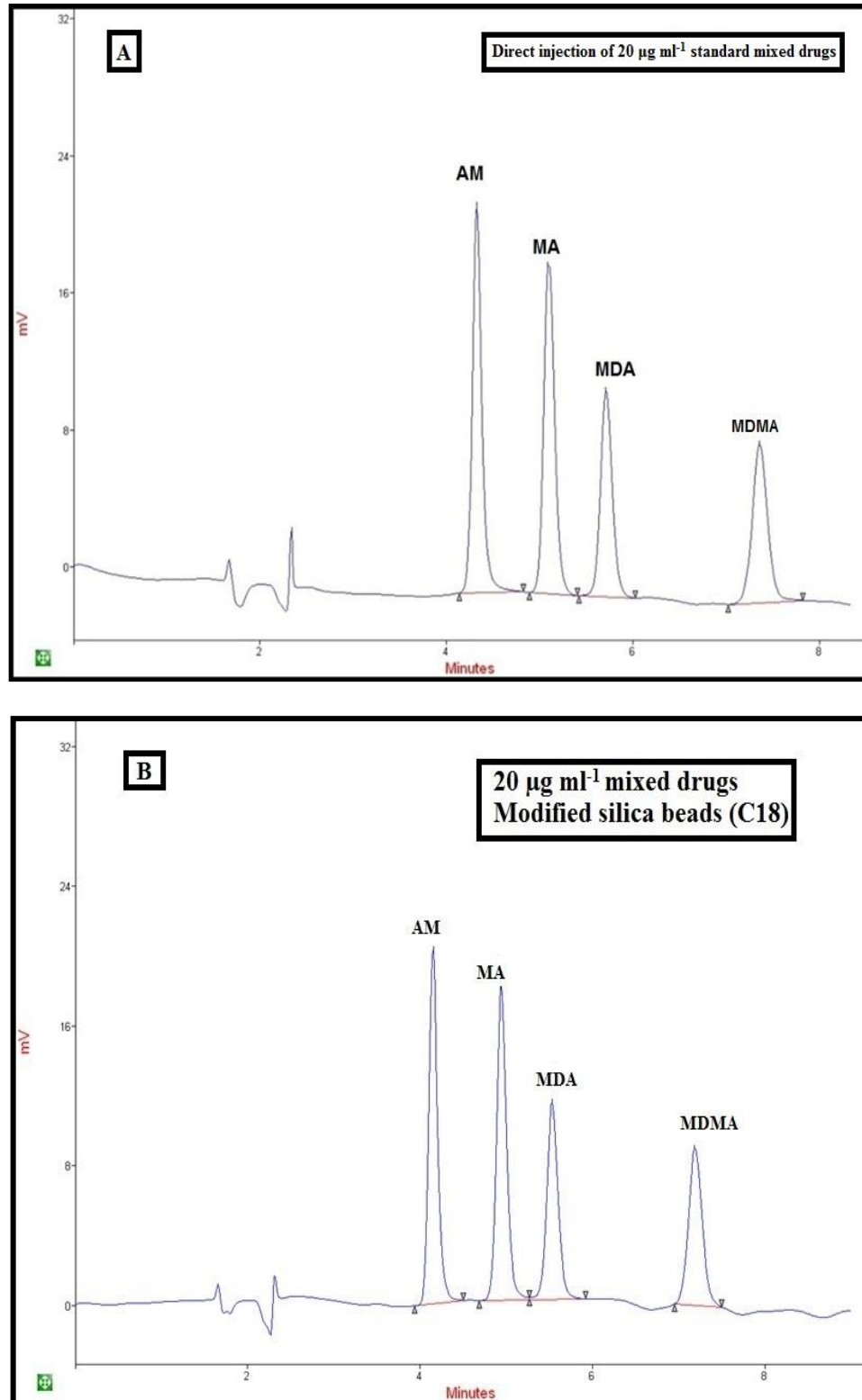


Figure 4-20: Chromatogram of 20 ppm A) directly injected mixed standard of four amphetamines and B) the eluted fraction of the extracted sample using modified C₁₈ silica beads. The separation was performed on a 5 µm ProdigyTM C₁₈ (Phenomenex, Torrance, CA, USA) 150 x 4.6 mm column, under isocratic conditions of 10% acetonitrile, 90% 50 mM phosphoric acid mobile phase (at pH 4 using triethylamine) at a flow rate of 1 ml min⁻¹. UV detection was obtained at 210 nm and the injection volume was 20 µl.

4.2.5.3 Optimisation of the extraction flow rate

Flow rate is an important factor to optimise when carrying out extraction using a hydrodynamic pump. A conventional SPE cartridge requires 25 to 30 minutes to perform drugs extraction and uses large sample volumes (2 ml).²⁴⁰ High flow rates were applied as a simple technique to reduce the extraction time in this study. Since adsorption of drugs to the sorbent and desorption from it are considered important in the extraction process, different flow rates were examined for the loading and elution steps.

Firstly, to evaluate the effect of flow rate on the adsorption of the drugs of interest onto the modified solid-phase, three different flow rates (100, 50, and 20 $\mu\text{l min}^{-1}$) were applied to load 50 μl of the ultra-pure water spiked with the target drugs to give a final concentration of 20 $\mu\text{g ml}^{-1}$. The eluted solution during the loading step was collected and injected into HPLC. Theoretically, no peaks belonging to the analytes should be observed at this stage due to hydrophobic interaction between the drugs and the modified beads. Unexpectedly, the chromatograms of the collected solutions during the loading steps at 100 and 50 $\mu\text{l min}^{-1}$ showed four peaks corresponding to the target analytes, as shown in Figure 4-21. However, when the flow rate was decreased to 20 $\mu\text{l min}^{-1}$, peaks for the target drugs were not detected in the loading solution as shown in the HPLC chromatogram (Figure 4-21). This result indicates that sample loading at 100 and 50 $\mu\text{l min}^{-1}$ reduces the interaction time between the analytes and the packed beads and, therefore, the analytes were recovered in the collected loading solution. Decreasing the flow rate to 20 $\mu\text{l min}^{-1}$ increased the interaction time for analytes binding to the surface of the modified sorbent and this resulted in greater adsorption of the target analytes to the surface of the C₁₈-modified silica beads.

Secondly, as expected, similar results were found when the four flow rates (100, 50, 20 and 10 $\mu\text{l min}^{-1}$) were examined for drugs desorption. At 100, 50 and 20 $\mu\text{l min}^{-1}$, the extraction recovery during the elution steps was lower (55%) than at 10 $\mu\text{l min}^{-1}$ (90%) due to the low interaction time between the target analytes and elution solution (mobile phase) flowing through the system (Figure 4-22). Moreover, high back pressure was observed at higher flow rates (100 and 50 $\mu\text{l min}^{-1}$) during the loading and elution steps but was not apparent with the lower flow rates (20 and 10 $\mu\text{l min}^{-1}$).

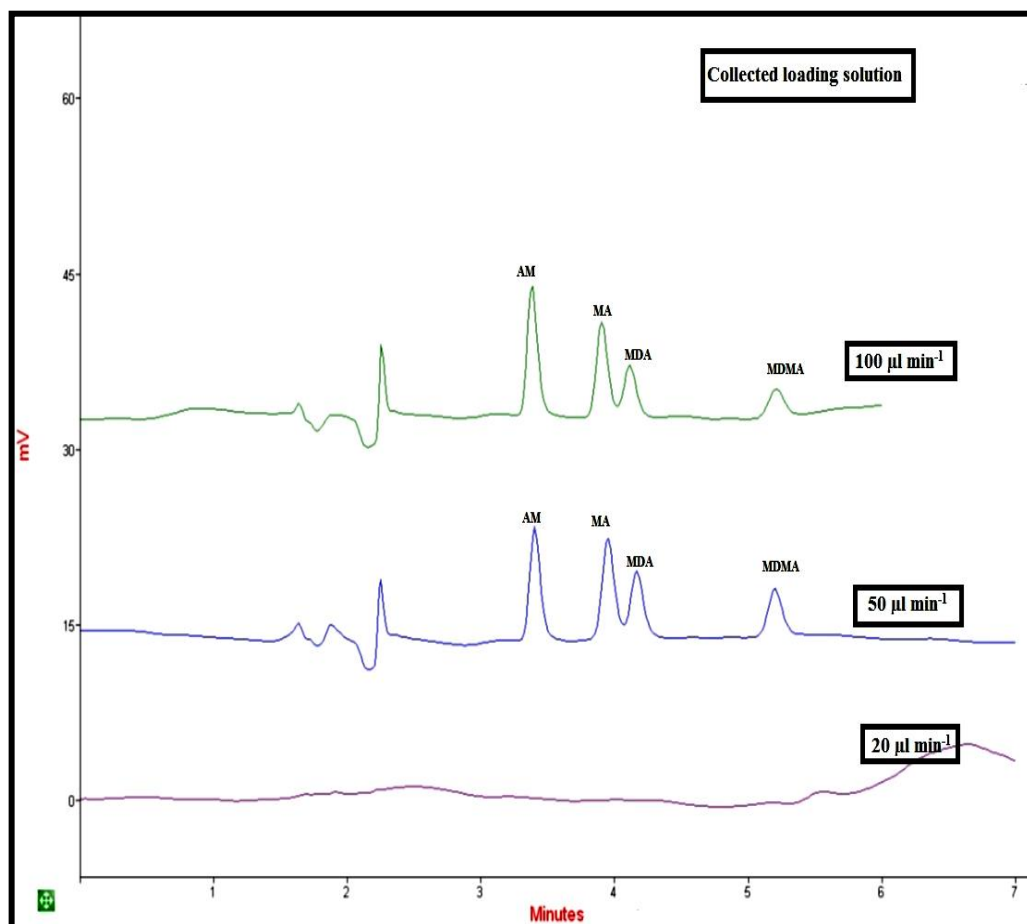


Figure 4-21: Chromatograms obtained from collected loading solution for the four target amphetamines at flow rates of 100, 50 and 20 $\mu\text{l min}^{-1}$ on C_{18} -modified silica beads.

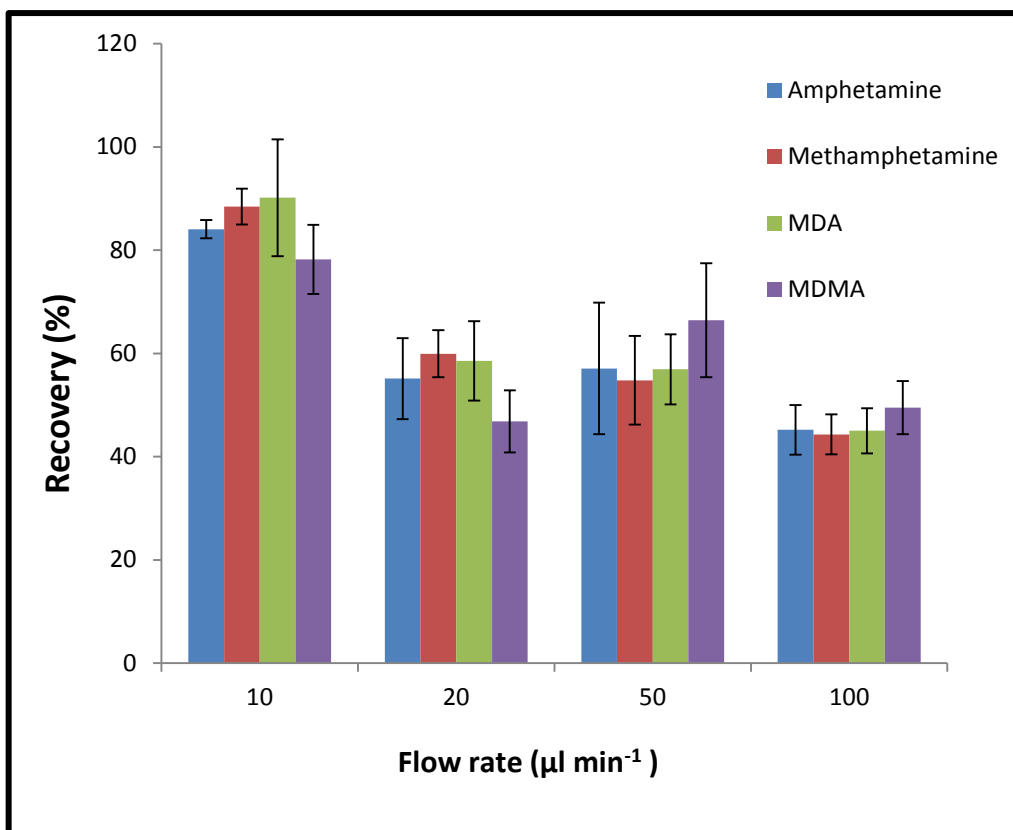


Figure 4-22: Effect of elution flow rate on the extraction recovery of the mixed drugs standard purified with octadecylated silica beads packed inside a female luer lock adaptor.

4.2.5.4 Recovery from artificial urine

Since the octadecylated silica beads showed an ability to extract the drugs of interest from ultra-pure water, it was important to investigate the performance of the modified silica in extracting the mixed standard from a realistic sample. A 10 ml volume of artificial urine medium was spiked with 200 μg of each target analyte to achieve a final concentration of 20 $\mu\text{g ml}^{-1}$. The artificial urine sample contained most of the components of real urine (such as urea, uric acid, creatinine and water) but was less complex and spiked with a high concentration of amphetamines for direct injection.

A 50 μl sample of the spiked artificial urine was extracted using the optimised condition indicated in section 4.2.5.3. All solutions that were passed through the outlet were collected and directly injected into the HPLC system. Figure 4-23 shows no peaks of the drugs of interest during the loading step, which indicates successful hydrophobic interaction between the analytes in the sample and the modified sorbent surface. The octadecylated beads enabled reduction in the impurity of the artificial urine during the washing stage, as the intensity at the first minute in the chromatogram decreased with elution fractions.

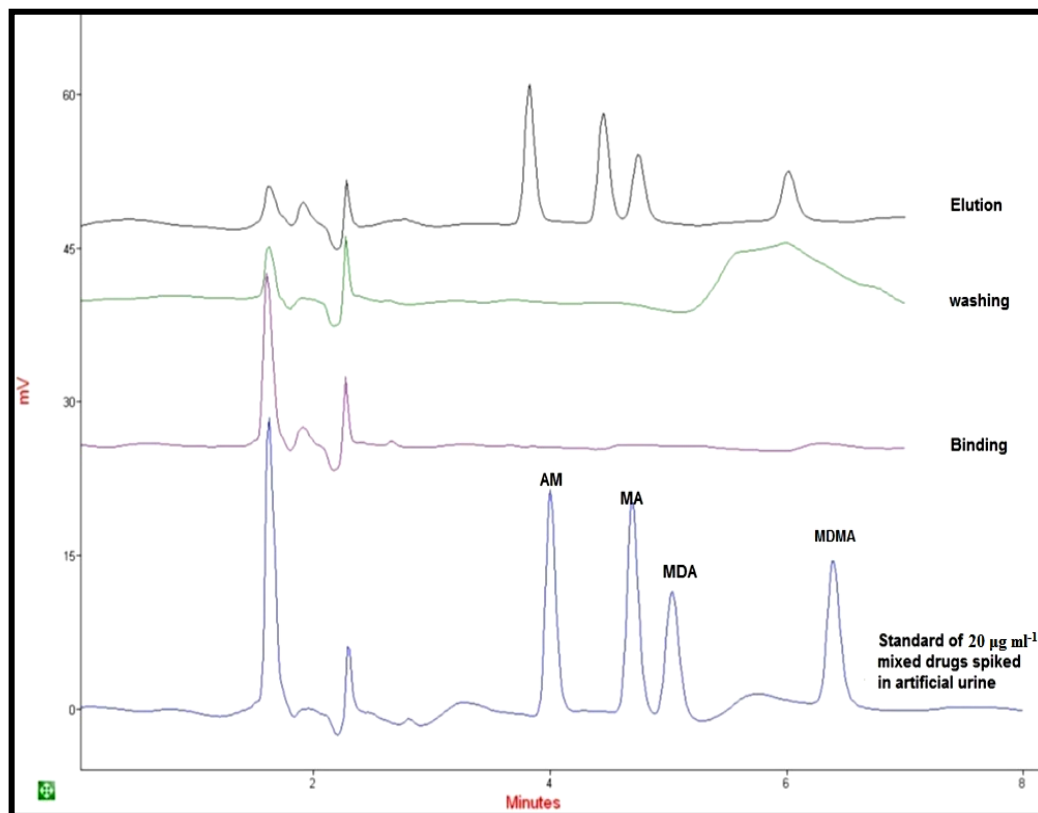


Figure 4-23: Chromatogram of a directly injected artificial urine sample spiked with four amphetamines and the three collection fractions of the extracted drugs using the C_{18} -modified silica beads. The separation was performed on 5 μm ProdigyTM C_{18} (150 x 4.6 mm column), under isocratic conditions of 10% acetonitrile, 90% 50 mM phosphoric acid mobile phase (at pH 4) at a flow rate of 1 ml min^{-1} . UV detection was obtained at 210 nm and the injection volume was 20 μl .

The recovery of the four amphetamines after extraction was between 50 and 75% with an acceptable RSD below 15% (see Table 4.1). The recoveries of the four spiked compounds from the artificial urine sample were lower than that extracted from the mixed drugs standard (in spiked ultra-pure water), as reported in section 4.2.5.2, but they were still acceptable values for forensic and clinical toxicology application²⁵⁴ compared with about 65% extraction recoveries for the amphetamines using a commercial cartridge.³¹⁰ These differences in recovery may be due to the composition of the artificial urine medium, which contains some hydrophobic compounds which compete with the target analytes for binding sites.

Table 4.1: Recoveries and relative standard deviations (RSDS) for an artificial urine sample spiked with four amphetamines which were then extracted using octadecylated silica beads.

Spiked drugs (20 µg ml ⁻¹)	Mean recovery (%, n = 3)	RSD (%)
AM	75	12.5
MA	64	8.6
MDA	60	7.8
MDMA	50	9.7

4.2.5.5 Figures of merit

The method was evaluated in terms of linearity, limit of detection (LOD), lower limit of quantification (LLOQ) and precision to verify the reliability and applicability of the modified octadecylated silica beads in extracting the four amphetamines of interest when analysed using HPLC with UV detection. Stock solutions of the four drugs of interest were used to provide a calibration curve at the following concentrations: 20, 10, 5, 2.5, 1.25, and 0.625 $\mu\text{g ml}^{-1}$. Calibration curves were constructed by plotting the peak areas of the standards against their respective concentrations. Analysis was carried out in triplicate at each concentration and linear regression analysis was used to produce the calibration curve shown in Figure 4-24.

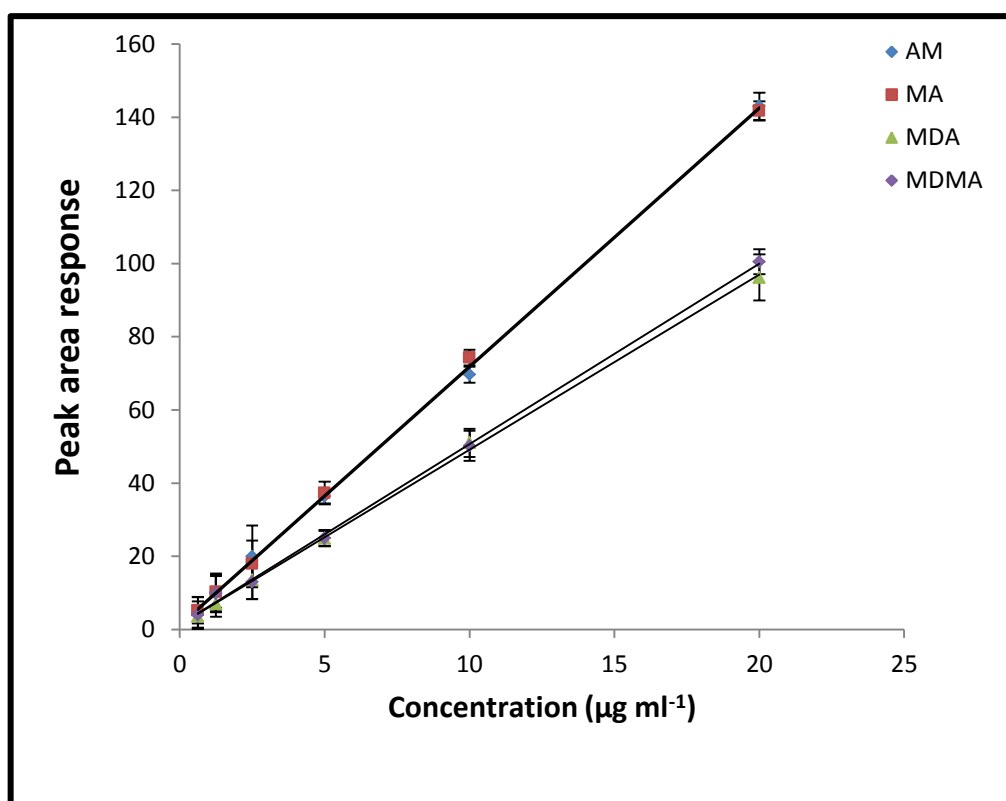


Figure 4-24: Calibration curve for the extraction of the mixed amphetamine standard in the range of 0.625 to 20 $\mu\text{g ml}^{-1}$ using an HPLC system with UV-visible detection.

Calibration curves for the target analytes showed linearity over the chosen concentration range and produced a correlation coefficient (R) ≥ 0.9988 . LOD and LLOQ were statistically determined during the evaluation of the linear range of the calibration curve using Equations 2.2, 2.3 and 2.4, 2.5, respectively. The lowest amount of analytes in a sample that can be detected and quantified using HPLC with UV detection are summarised in Table 4.2.

Table 4.2: Analytical figures of merit.

Drug	LOD ($\mu\text{g ml}^{-1}$)	LLOQ ($\mu\text{g ml}^{-1}$)	Range of linearity ($\mu\text{g ml}^{-1}$)	Linearity	Correlation coefficient
AM	0.56	1.88	0.625-20	$y = 7.0676x + 0.872$	0.9995
MA	0.59	1.98	0.625-20	$y = 7.0704x + 1.3841$	0.9994
MDA	0.69	2.30	0.625-20	$y = 4.7877x + 1.2773$	0.9992
MDMA	0.82	2.82	0.625-20	$y = 4.9332x + 1.3539$	0.9988

The performance of the modified silica beads in extracting the mixed target molecules was evaluated in terms of repeatability (within-day precision) and reproducibility (between-day precision) from the results of the peak areas of each reference standard. In this study, low ($3 \mu\text{g ml}^{-1}$), medium ($10 \mu\text{g ml}^{-1}$) and high ($20 \mu\text{g ml}^{-1}$) concentrations of the mixed drugs standard were used to express precision as a percentage RSD of the test results. Each concentration was extracted three times on a single day to perform intra-day precision analysis and over five consecutive days in triplicate using the same modified silica beads patch to obtain inter-day precision analysis, as shown in Table 4.3.

Table 4.3: Intra-day and inter-day recoveries for the drugs of interest and relative standard deviations of the extraction method.

Drug ($\mu\text{g ml}^{-1}$)	Intra-day (n = 3)		Inter-day (n = 15)	
	Recovery (%)	RSD (%)	Recovery (%)	RSD (%)
AM				
3	87.7	3.8	80.5	9.4
10	80.3	4.7	79.1	6.3
20	84.1	1.8	76.3	6.8
MA				
3	83.8	2.4	78.6	11.4
10	81.6	4.9	77.3	9.3
20	88.4	3.5	79.3	8.6
MDA				
3	90.6	2.4	79.43	9.7
10	88.0	3.3	83.6	9.7
20	87.2	3.3	83.7	8.4
MDMA				
3	80.4	2.5	70.8	12.6
10	81.4	1.3	73.3	8.0
20	78.2	3.7	73.2	8.3

As shown in Table 4.3, the intra-day %RSDs were in the range from 1.3 to 4.9% whereas the inter-day %RSDs were in the range from 6.3 to 12.6% for the examined concentrations which may due to degradation of amphetamines during storage at 4 °C for five days. These results indicate that the proposed extraction method using modified silica beads has both good reliability and applicability, as the %RSD values were within the bioanalysis acceptable limit of 15%.²⁴⁸

4.2.5.6 Pre-concentration performance

SPE has been successfully reported to have extracted and pre-concentrated different compounds of interest from different sample matrices.^{52, 169, 311, 312} The principle of the pre-concentration method is to load a low concentration of analyte in a large sample volume and then elute the analyte in small volume. The pre-concentration capability of C₁₈ silica beads was investigated in this study for AM, MA, MDA and MDMA from a large sample volume in order to improve the sensitivity of the method and the detection limit. Pre-concentration was achieved by loading 1 ml of 20 µg ml⁻¹ mixed drugs standard onto the C₁₈-modified beads and then washing with 1 ml ultra-pure water at 20 µl min⁻¹. In order to establish the minimum elution volume required to elute all the introduced analytes from the modified solid stationary phase, different amounts of mobile phase were used as an eluent (25, 50, and 100 µl) at a flow rate of 10 µl min⁻¹. Each eluted fraction was directly injected into the HPLC system and the peak area of each extracted analyte was compared with the peak area of directly injected mixed drugs standard. The results are presented in Table 4.4.

Table 4.4: The average concentrations of 1 ml mixed drugs standard (20 µg ml⁻¹) pre-concentrated using C₁₈ silica beads and then eluted with various amounts of mobile phase (n = 3).

Elution volume (µl)	Pre-concentration factor			
	AM	MA	MDA	MDMA
25	0.2	0.5	0.5	0.6
50	0.7	2	2.5	3.5
100	0.1	0.3	0.4	0.6

As can be seen from Table 4.4, an elution volume of 25 μl was not sufficient to elute all the loaded amount of the target analytes from the hydrophobic monolith. However, significant improvements in the recovery of the analytes of interest were then achieved by increasing the elution volume to 50 μl . In comparison with the direct injection chromatogram (see Figure 4-25), the peak sizes of the eluted analytes using a 50 μl mobile phase showed considerable improvement in UV sensitivity for MA, MDA, and MDMA by 2, 2.5 and 3.5 times, respectively. Using the same elution volume (50 μl), however, the proposed method cannot pre-concentrate AM, as the peak size was decreased 30% compared to the direct injection chromatogram of AM. That means the other analytes (MA, MDA, and MDMA) absorb the UV light more than the AM.

In order to increase AM recovery, the elution volume was increased to 100 μl . This elution volume (100 μl) resulted, however, in dilution of the pre-concentrated analytes and a correspondingly significant reduction in the sensitivity of all the drugs of interest. These results indicated that 50 μl was the optimum volume for completely filling the packed modified silica beads in the female luer lock adaptor. As shown in the previous section (4.2.5.5), the LODs for MA, MDA, and MDMA were 0.59, 0.69, and 0.82 $\mu\text{g ml}^{-1}$, respectively. Therefore, the lowest concentrations of MA, MDA, and MDMA that can be detected from a 1 ml sample volume when eluted by the optimum minimum volume (50 μl) of mobile phase using HPLC with UV detection are 0.30, 0.28, and 0.25 $\mu\text{g ml}^{-1}$, respectively, because the sensitivity was increased by 2, 2.5 and 3.5 times for the corresponding drugs.

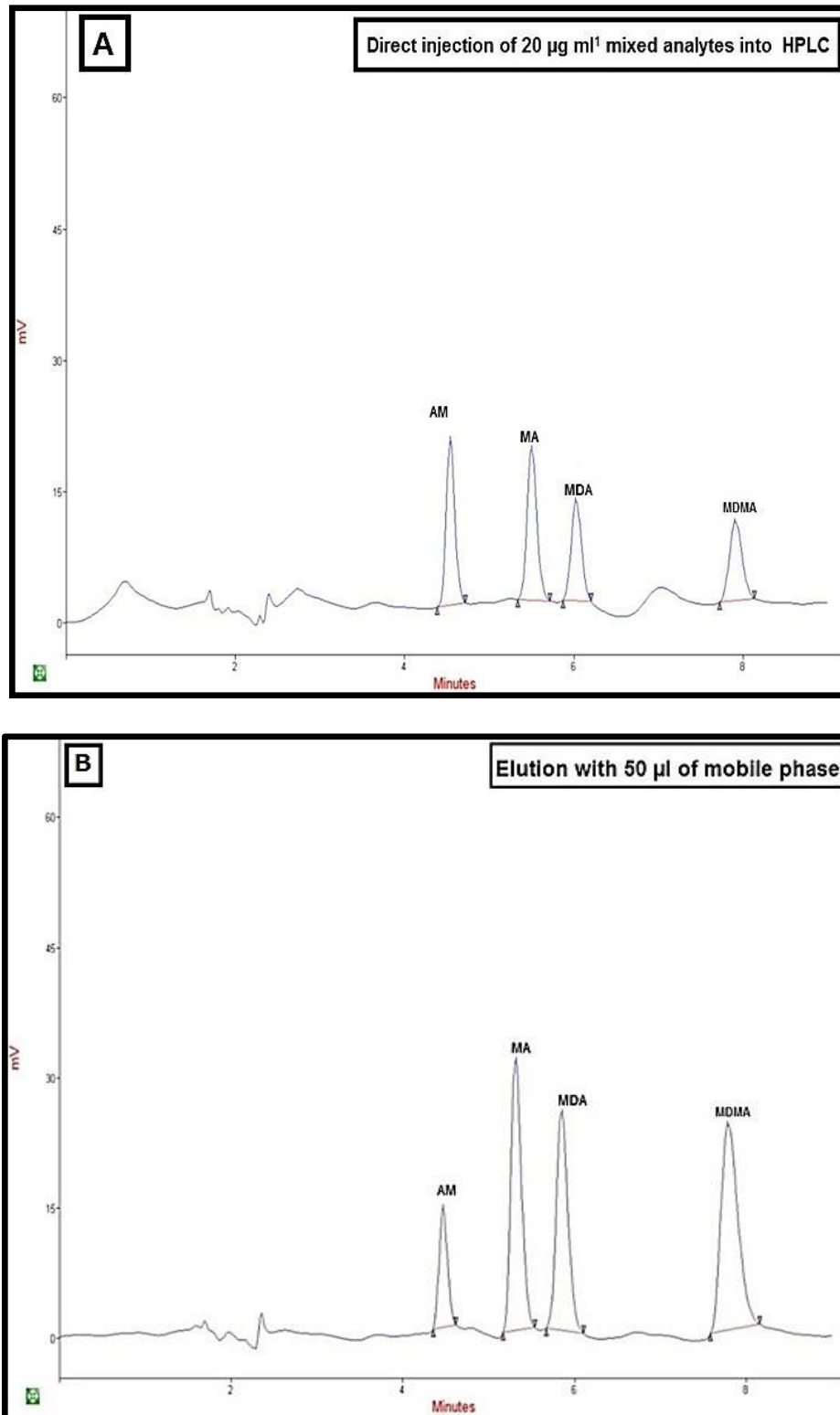


Figure 4-25: Comparison of chromatograms when 1 ml of 20 μg of mixed drugs standard was A) directly injected into the HPLC system and B) extracted using C_{18} -modified silica beads and eluted with a 50 μl mobile phase. The HPLC column was a 5 μm ProdigyTM C_{18} (150 x 4.6 mm); isocratic conditions of 10% acetonitrile:90% 50 mM phosphoric acid mobile phase (pH 4) at a flow rate of 1 ml min^{-1} . UV detection was obtained at 210 nm and the injection volume was 20 μl .

4.3 Combined DNA and Drug Extraction

In general, simultaneous extraction methods involve the extraction of analytes from the same group or those with a similar chemical characterisation. In this section, the target analytes (DNA and amphetamines) are from different chemical groups and thus have different structural and chemical characteristics. Combined extraction was carried out using two types of silica in tandem: octadecylated coated silica beads (packed inside a female luer lock connector) for drug isolation and thermally activated potassium silicate (a microfluidic device) for DNA purification. Sample loading, washing and elution of the target analytes was driven by hydrodynamic pumping, as shown in Figure 4-26.

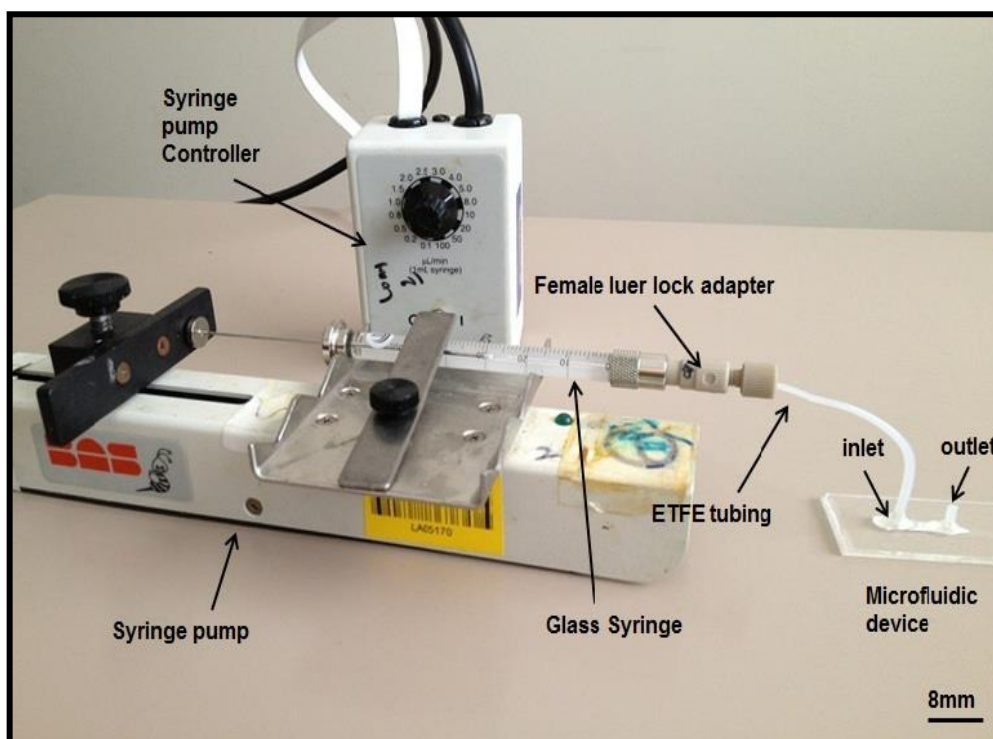


Figure 4-26: Photograph of the experimental set-up for combined genetic and drugs extraction. The C₁₈ silica beads were packed inside the luer lock adaptor where the drug extraction takes place. The DNA extraction was carried out within the microfluidic chip device.

This study has some similarity to the method reported by Landers *et al.* for protein capture in a commercial C₁₈ reversed phase and DNA extraction on a monolithic column within a microfluidic environment.¹⁹⁹ The aim of this current study, however, was to develop and validate an analytical procedure to extract drugs (amphetamines) and DNA using a single extraction procedure. A polar adsorbent (a thermally activated monolith) was used to retain polar analytes (DNA), and a non-polar adsorbent (C₁₈ beads) was used to retain non-polar analytes (amphetamines). It was important to investigate the compatibility of the DNA buffers and reagents in the extraction recovery of the drugs of interest. DNA extraction efficiency was calculated as the amount of eluted DNA expressed as a percentage of the total amount introduced to the system.²⁰³ In addition, drug recovery was evaluated by the ratio of peak areas for the extracted drug vs. the peak area for the corresponding non-extracted standard analyte, expressed as a percentage. In order to investigate the affinity of the DNA with the reversed phase, DNA extraction was carried out using packed C₁₈ silica beads only, as described in section 2.4.3. Figure 4-27 shows that the majority of the DNA passed through the modified phase unretained. The small amount of DNA retained (7%) was recovered during the elution stage, as DNA is thought to be adsorbed onto the residual non-modified or non-capped silanol group. The initial evaluation of the combined drugs and DNA method will discuss the DNA extraction first, because it was eluted before the four amphetamines to avoid organic solvent contamination (mobile phase) that may inhibit PCR.

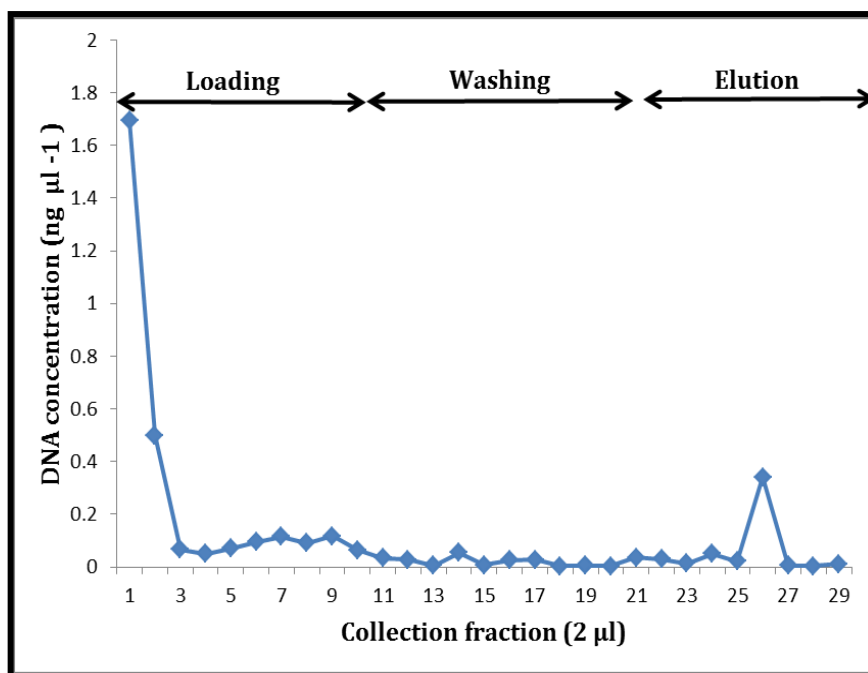


Figure 4-27: DNA extraction profile carried out on octadecylated silica beads packed inside a luer lock adaptor.

The method of extraction was a hybrid between DNA and drugs extractions described in sections 2.4.3 and 2.5.3. The surface of the silica was activated with 5 M GuHCl in a TE buffer (10 mM Tris, 1mM EDTA; pH 6.7) for 30 minutes at a flow rate of $5 \mu\text{l min}^{-1}$. For efficient DNA adsorption onto the silica-based monolith, the concentration of GuHCl should be 5 M in the final solution.¹⁵⁹ Therefore, 10 M GuHCl was prepared and then used to dilute the purified human DNA and stock standard solution to achieve a sample volume of $50 \mu\text{l}$, with 5 M GuHCl as the final concentration. A volume of $50 \mu\text{l}$ TE buffer or artificial urine spiked with DNA (13 ng) and the target amphetamines (final concentration of $5 \mu\text{g ml}^{-1}$) was loaded through the $50 \mu\text{l}$ glass syringe at a flow rate of $2.5 \mu\text{l min}^{-1}$. PCR inhibitors were then removed using 5 M GuHCl at a flow rate of $5 \mu\text{l min}^{-1}$. DNA was eluted prior to the amphetamines using 10 mM TE buffer at pH 8.5 at a flow rate of $1 \mu\text{l min}^{-1}$.

All analyte fractions from loading, washing and elution were collected in 4 μl aliquots for DNA quantification and amplification.

As can be seen from Figure 4-28, once the DNA had passed through the reversed-phase support, it was retained on the thermally activated potassium silicate and then released under the influence of 10 mM TE buffer (pH 8.5) during the elution step. It was determined that the proposed system was able to extract the DNA from the TE buffer or artificial urine (36% and 30%, respectively) with almost a similar extraction to that obtained previously for a single extraction method (chapter 3) with no adverse effect on the C_{18} phase from the extraction of DNA. The extracted DNA was found to be of sufficient quantity and quality for PCR amplification of the D21 S11 locus, as determined by gel electrophoresis (Figure 4-29) due to amplification of the target base pair size (223 bp and 227 bp).

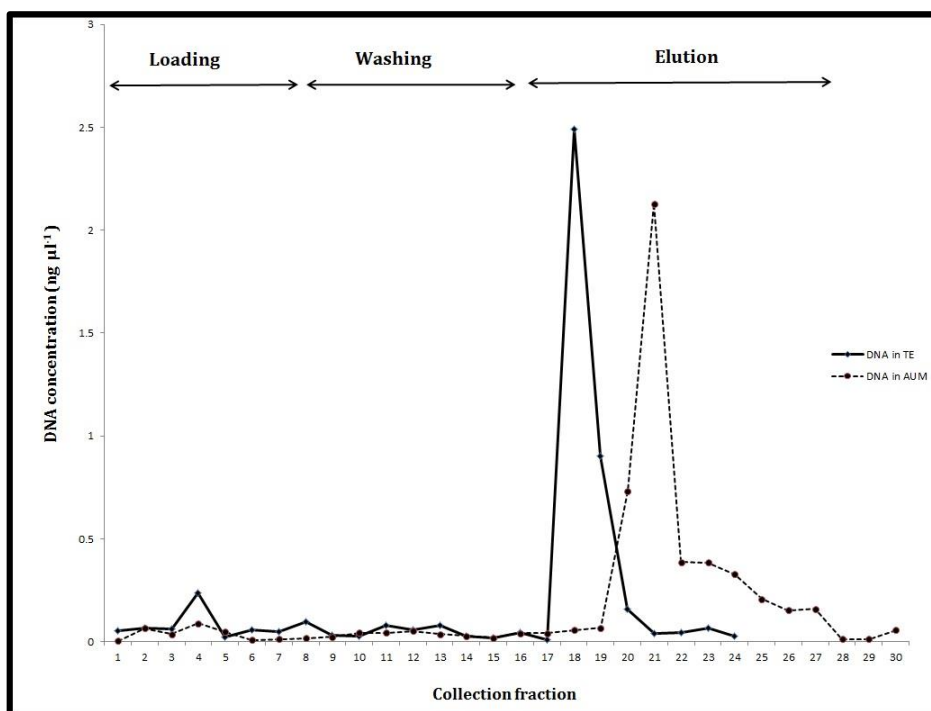


Figure 4-28: DNA elution profiles of 13 ng of purified DNA extracted from TE buffer (—) and from artificial urine (...) using the tandem silica extraction system (packed C_{18} silica beads inside a luer lock adaptor and a silica-based monolith within a microfluidic device).

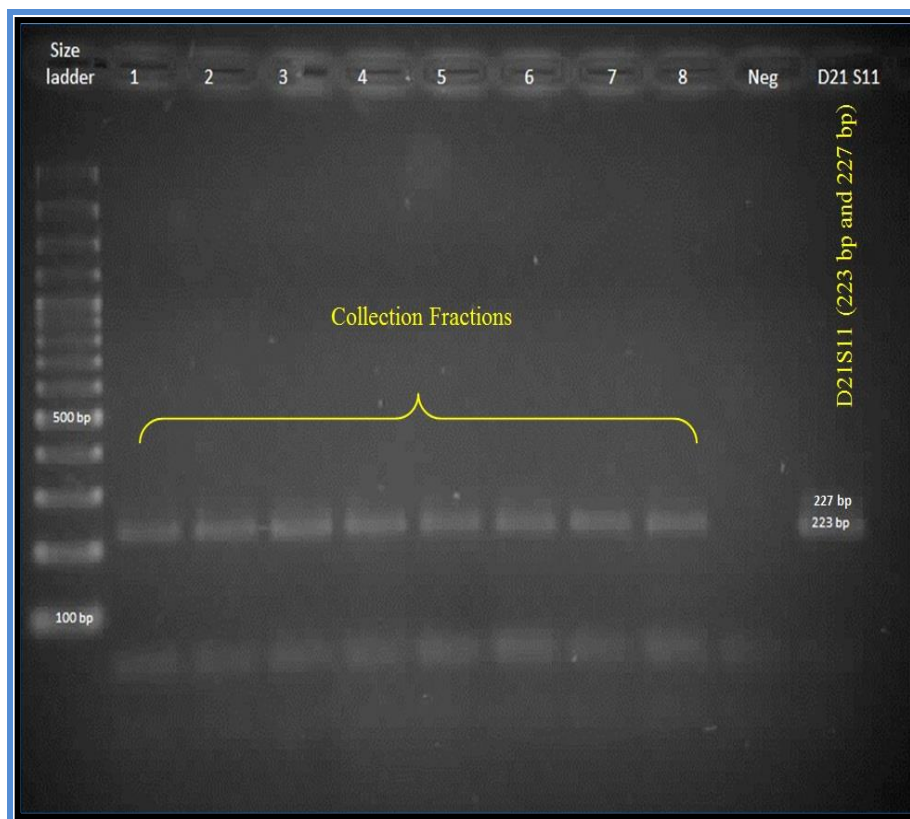


Figure 4-29: UV transilluminator image of slab-gel electrophoresis results from DNA eluted from an artificial urine sample using D21 S11 gene.

Next, the glass microfluidic chip was disconnected from the extraction set-up (Figure 4-26) by cutting the ETFE tube and then the packed C_{18} beads were washed with highly purified water at a flow rate of $10 \mu\text{l min}^{-1}$ to remove any previous buffer. Finally, the adsorbed target drugs were eluted using optimised HPLC mobile phase (10% acetonitrile:90% 50 mM phosphoric acid; pH adjusted at 4 by triethylamine) at a flow rate of $10 \mu\text{l min}^{-1}$. The eluted fractions from the spiked TE buffer and artificial urine were directly injected into the HPLC system and the peak areas obtained were compared with those of directly injected peak areas as shown in Figure 4-30.

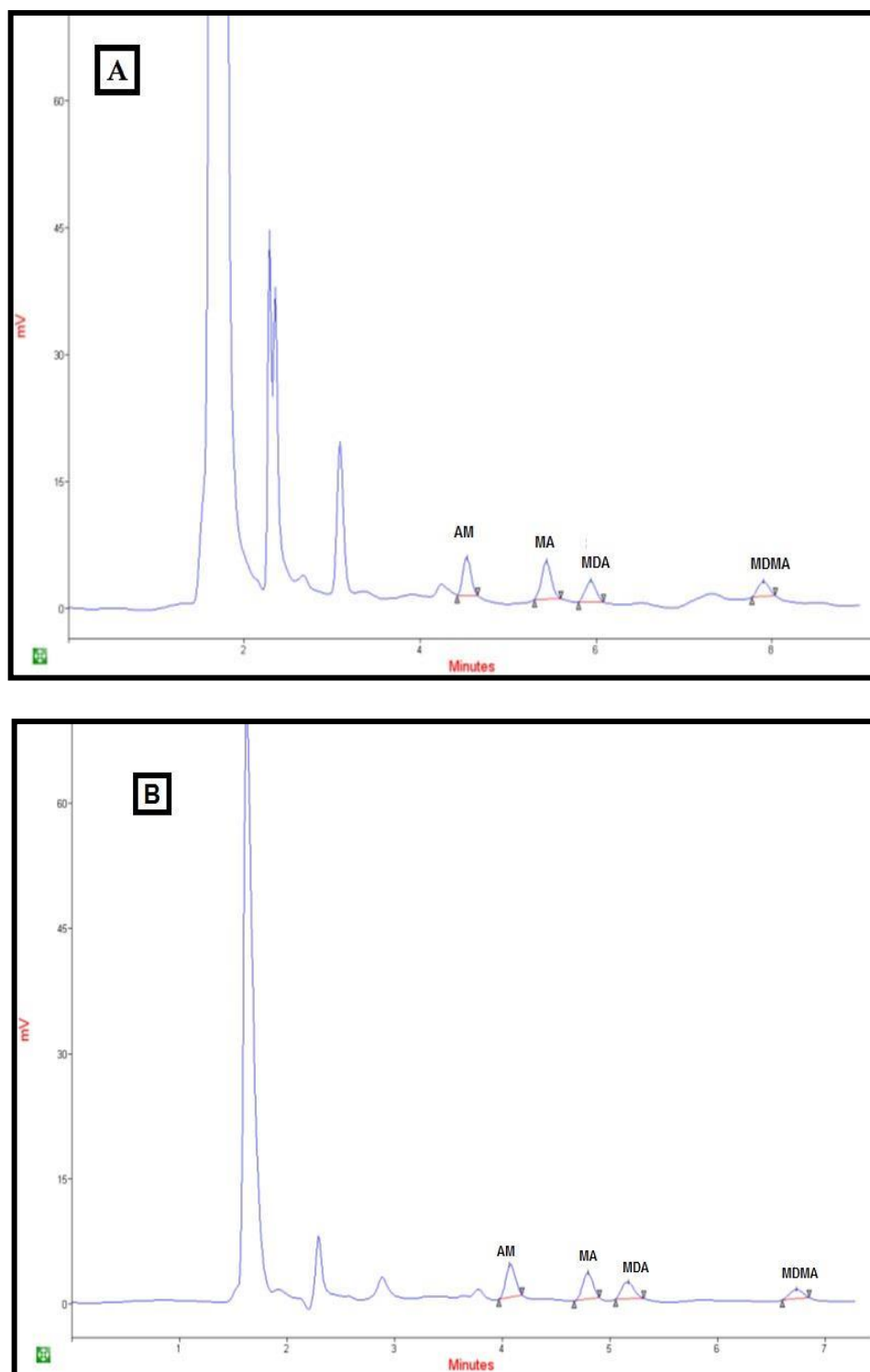


Figure 4-30: UV chromatogram of $5 \mu\text{g ml}^{-1}$ A) directly injected mixed amphetamines standard and B) elution fraction of extracted artificial urine using C_{18} silica beads after DNA extraction with a silica-based monolith. The chromatographic conditions were: ProdigyTM C_{18} (150 x 4.6 mm column, 5 μm); isocratic conditions of 10% acetonitrile:90% 50 mM phosphoric acid mobile phase (pH 4); flow rate of 1 ml min^{-1} . UV detection was obtained at 210 nm and the injection volume was 20 μl .

The four target amphetamines were successfully eluted from the reversed phase using the optimised mobile phase. Recoveries of amphetamines from spiked samples using the combined method of extraction are presented in Table 4.5. The recoveries obtained from the current method (tandem solid-phases; C₁₈ and normal phase) showed no significant differences from those obtained from previous extraction recoveries with a single extraction phase (C₁₈ phase, section 4.2.5) with an acceptable reproducibility (< 15%).

Table 4.5: The recoveries for the four target amphetamines extracted from TE buffer and artificial urine using octadecylated silica beads in a series silica system (n = 3).

Drug (5 µg ml ⁻¹)	TE buffer		Artificial urine	
	Recovery (%)	RSD (%)	Recovery (%)	RSD (%)
AMP	87	7	78	10.2
MA	82	11	62	8.9
MDA	73	6	68	11.6
MDMA	78	6	52	13

4.4 Summary

The selectivity of the drugs of interest towards different silica materials was investigated. The non-modified silica-based monolith that exhibited a normal phase extraction due to surface silanol groups was found not to be efficient in retaining the compounds of interest. In particular, SPE can be designed to be highly selective to the analyte of interest through surface functionalisation.³¹³ Silica-based matrices such as monoliths or silica beads were successfully modified for the desired solid-phase extraction. Lysine was covalently introduced into the silica-based monolith by treating the epoxy monolith with hydrochloric acid in order to open the epoxy ring in the γ -glycidoxypropyltrimethoxysilane, which allowed the lysine to bond covalently with the diol monolith. Infrared (IR) analysis confirmed the modification of the silica-based monolith. For example, the bending vibrations of CH_2 and NH_2 functional groups were observed with the modified monolith at wavelengths of 2980 and 1630 cm^{-1} , respectively. The zwitterionic properties of lysine were evaluated for simultaneous adsorption of DNA and the drugs of interest.

The lysine-modified monolith showed high selectivity towards DNA at pH 5 (MES buffer) with reasonable desorption of 77% extraction efficiency at pH 9 (carbonate buffer) at a low flow rate ($1\text{ }\mu\text{l min}^{-1}$) without any adverse effect on PCR amplification. In addition, the lysine-modified silica-based monolith had greater binding capacity, 1.7 mg DNA g^{-1} , compared to $0.823\text{ mg DNA g}^{-1}$ for the silica monolith. However, the lysine-modified monolith was unable to achieve the cation-exchange required for the four amphetamines of interest. Therefore, lysine-modified monoliths are not suitable for the simultaneous adsorption of DNA and the four drugs of interest.

To overcome the inability of the lysine-modified monolith to extract the drugs of interest, silica was modified with chloro(dimethyl)octadecylsilane (C_{18}). Silica beads were successfully modified with C_{18} because it can functionalise the outer surface of silica beads, whereas the thermally activated monolith cured within a glass capillary was blocked by large C_{18} molecules. The IR spectrum of the modified silica beads showed no water absorbance band at 3000 to 4000 cm^{-1} . For the extraction of the drugs of interest, the modified silica beads were packed inside a female luer lock adaptor to avoid the requirement of multiple steps such as stirring,^{219, 314} centrifugation^{108, 233, 315} or aspiration and dispensing¹⁰⁸ of samples that are associated with most of the current methods. The octadecylated silica beads were effective in retaining the target amphetamines from authentic working solutions and an artificial urine sample with extraction recoveries between 90% and 50%, respectively. The proposed method was not only useful for small volumes of sample (50 μl), but was found to offer pre-concentration for the four compounds from larger volumes (1 ml). Extraction using the modified C_{18} silica beads required about 12 minutes, compared with 25 minutes for a conventional SPE cartridge.²⁴⁰ The validation data are indicative of excellent linearity in the range from 20 to 0.625 $\mu g ml^{-1}$; acceptable precision < 15%; and correlation coefficients > 0.99. Using HPLC with UV detection, the lowest amount of analytes in the sample that can be detected and quantified were within the range from 0.56 to 0.82 $\mu g ml^{-1}$ and between 1.88 and 2.8 $\mu g ml^{-1}$, respectively.

For combined DNA and drugs of interest analysis using a single experimental work, two solid-phase extractions were arranged in tandem (phase 1 and phase 2). The C_{18} silica beads for drugs extraction (phase 1) were packed inside a female luer lock adaptor and then connected via ETFE tubing to a glass microfluidic chip that

contained a thermally activated monolith (phase 2) for DNA extraction. All the extraction procedures, such as sample loading, washing, and elution were performed using hydrodynamic pumping. For low sample volumes (50 μl), the proposed method was efficient at extracting both DNA and the four target compounds simultaneously with minimal sample handling. DNA extraction efficiencies from the spiked TE buffer and urine sample were 36% and 30%, respectively. In addition, the recoveries for the four amphetamines were in the range between 93% and 52% with acceptable precision ($< 15\%$). In this study, an HPLC instrument with UV detection obtained at 210 nm was used to calculate the extraction recovery of the drugs of interest. The separation of the drugs was carried out on a 5 μm ProdigyTM C₁₈ (Phenomenex, Torrance, CA, USA) 150 x 4.6 mm column under isocratic conditions for the mobile phase (10% acetonitrile:90% 50 mM phosphoric acid, at pH 4 using triethylamine), and a flow rate of 1 ml min⁻¹.

5 Conclusions

Analyses in the field of forensic toxicology can suffer from limited sample size, particularly when multiple investigations are required. In response to that challenge, this PhD project focused on developing a single extraction method that can be used for combined DNA and drugs of abuse analysis using silica material coupled with microfluidics to obtain more information from a low-volume single sample with minimal sample handling and within a short amount of time. In order to achieve this, the research work was divided into three sections:

- 1) Extraction and pre-concentration of DNA from limited cell numbers, which may include DNA from different species, using a solid-phase monolith structure.
- 2) Selection of suitable solid-phase extraction methods for four drugs of interest: amphetamine (AM), methamphetamine (MA), 3,4-methylenedioxyamphetamine (MDA) and 3,4-methylenedioxymethamphetamine hydrochloride (MDMA).
- 3) Optimisation of a combined solid-phase extraction methodology for DNA and the drugs of interest from the same sample.

This study has focused on the use of silica-based matrices for the extraction of DNA and drugs of interest using hydrodynamic pumping to generate controlled flow rates. The conclusions from this work are summarised and discussed in the following sections.

5.1 DNA Extraction

Based on the reported literature,^{58, 72, 316-318} the adsorption of DNA on silica-based monoliths was more efficient with the presence of a GuHCl loading buffer at pH 6.7 and accomplished desorption with solutions of low ionic strength or ultra-pure water. The performances of both solutions in eluting DNA from a potassium silicate monolith were investigated. The results of this investigation showed that high DNA extraction recovery (45.6%) could be obtained with 10 mM TE at pH 8.5 compared with 22.6% using purified water (pH 5.5). This indicates that elution depends on the pH of the elution buffer, which should be slightly alkaline and contain a sufficient number of counter-ions to break down the hydrogen bonding between the silica surfaces and the DNA and enable the free DNA to return back into the solution. Based on low cell numbers (i.e., limited biological samples), high DNA extraction efficiencies were achieved without the need for additional carrier RNA¹⁵⁸ due to the high surface area and preferential use of DNA reversible binding sites afforded by silica monoliths. Although other studies have shown that the commercial EZ1 DNA Tissue extraction Kit is not suitable for samples that contain less than 10 ng of DNA,²⁶⁶ this relatively closed system showed robust performance with regard to pre-concentrated limited samples containing 4 ng total DNA and subsequently eluted with high extraction efficiency (84%) within a microfluidic environment device. Given the low cell numbers that can be successfully extracted, this system lends itself to the examination of clinical or forensic specimens where samples are often limited, such as DNA profiling from crime scene samples. Although a silica-based monolith was efficient at extracting low DNA quantity, it was not found to offer species-specific extraction. This particular investigation is important in cases of mixed DNA, such as sexual assault or contamination of human DNA with DNA from other species.

5.2 Drugs Extraction

Initially, the performance of a silica-based monolith in extracting the drugs of interest was evaluated according to three different chemical properties of the stationary phase (hydrophilic, hydrophobic, and ion-exchange) in order to determine the most suitable extraction technique for amphetamines. Normal-phase extraction of the four amphetamines showed low extraction recoveries (< 10%), which is in good agreement with the results of a previous study where amphetamines showed low recoveries with a common hydrophilic balance (Oasis HLB[®]) sorbent.³¹⁹

A lysine-modified monolith that showed zwitterionic ion-exchange also exhibited a low retention affinity for the four positively charged amphetamines (< 5%), which indicated that the weak cation-exchanger had a low retention for compounds with aliphatic amines, such as amphetamines, when compared with a strong cation-exchanger as predicted by Kuwayama *et al.*³²⁰ However, DNA was preferentially adsorbed on a modified amino support due to electrostatic interactions between the cationic solid support (NH₃⁺) and the negatively charged DNA and was eluted in good quantity (77%) and of a quality that was useful for subsequent polymerase chain reaction (PCR) analysis. DNA capturing using the lysine-modified monolith was highly effective in terms of binding capacity (1.7 mg DNA g⁻¹ of monolith) when compared to a non-modified monolith (823 μg DNA g⁻¹ of monolith).

High extraction recoveries (between 90% and 75%) from the TE buffer and artificial urine spiked with the four drugs of interest were obtained using a chemically modified silica-bead monolith with octadecyl groups. This proposed method, which involves packed C₁₈ beads inside a female luer lock adaptor, has several advantages: it is simple and fast to extract target drugs within a short amount of time (12 minutes) compared to conventional SPE cartridges (25 minutes) which require filtration, high-

level skills and special equipment such as a vacuum or centrifuge.³²¹ In addition, the method is useful for the simultaneous extraction of the four amphetamine drugs from low-volume samples (50 µl), such as those associated with biological forensic samples. The method was able to pre-concentrate MA, MDA and MDMA from a large sample volume (1 ml) with improvement in the LOD by 2, 2.5 and 3.3 times for the corresponding drugs when eluted using a small volume of mobile phase (50 µl of 10% acetonitrile and 90% 50 mM phosphoric acid; pH 4 adjusted by triethylamine) but with 65% recovery for AM. In this study, the HPLC mobile phase was optimised to separate the four drugs of interest in less than 10 minutes, which offers considerable advantages.

5.3 Combined DNA and Drugs Extraction

Although DNA and amphetamine analyses are individually well established, no combined extraction has been reported especially for forensic work, where often only a limited sample is available in terms of quantity and quality. In this study, a tandem reversed- and normal-phase system for independent purification of DNA and the extraction of four amphetamines was successfully developed based on a single experiment. The development of the two-phase extraction method will reduce the possibility of sample loss and contamination due to minimal sample handling, which will facilitate the ability to manipulate low-volume samples (50 µl). In addition, with complex samples (such as blood), the proposed method is hypothesised to reduce the competition of proteins for DNA active sites in the normal phase, as indicated in the literature.^{168, 199}

6 Further Work

This work has demonstrated a novel application of a two-phase monolith for the combined extraction of genetic material and drugs of interest within a single extraction method. Further works are proposed to improve the work presented here:

- 1) This study has worked well with TE buffer and artificial urine analysis, but further work is required in its application to a wide variety of real biological sample types such as blood, urine, saliva and hair which might be collected from a suspect in a police custody suite or found at the scene of a crime.
- 2) The proposed method simultaneously extracted four amphetamines using octadecylated silica beads. There is a wide variety of drugs that can potentially be abused; therefore, further work would require additional investigation of different types of drugs, especially those containing amine groups such as lidocaine, morphine and nicotine.
- 3) The current system involved the extraction of four target drugs using C₁₈-modified beads packed inside a female luer lock adaptor and DNA extraction using a thermally activated monolith cured inside a glass microfluidic chip. Future work could involve complete integration of a closed system that would allow extraction and detection of both DNA and drugs analysis within a single microfluidic chip device.
- 4) The developed system is suitable for combination with immunochemical techniques by immobilising a specific antibody on a monolith in order to reduce the effect of endogenous matrix components and pre-concentrate the target molecules to obtain a more sensitive immunoassay for a complete screening and detection method.

7 References

1. Budowle, B., van Daal, A., Extracting evidence from forensic DNA analyses: future molecular biology directions. *Biotechniques*, 2009, **46**(5): 339-40, 342-350.
2. Min, J., Kim, J.-H., Lee, Y., Namkoong, K., Im, H.-C., Kim, H.-N., Kim, H.-Y., Huh, N., Kim, Y.-R., Functional integration of DNA purification and concentration into a real time micro-PCR chip. *Lab on a Chip*, 2011, **11**(2): 259-265.
3. Kataoka, H., Ishizaki, A., Nonaka, Y., Saito, K., Developments and applications of capillary microextraction techniques: a review. *Analytica Chimica Acta*, 2009, **655**(1-2): 8-29.
4. Delaunay, N., Pichon, V., Hennion, M.-C., Immunoaffinity solid-phase extraction for the trace-analysis of low-molecular-mass analytes in complex sample matrices. *Journal of Chromatography B: Biomedical Sciences and Applications*, 2000, **745**(1): 15-37.
5. Fu, X., Liao, Y., Liu, H., Sample preparation for pharmaceutical analysis. *Analytical and Bioanalytical Chemistry*, 2005, **381**(1): 75-77.
6. Saunders, K. C., Ghanem, A., Boon Hon, W., Hilder, E. F., Haddad, P. R., Separation and sample pre-treatment in bioanalysis using monolithic phases: a review. *Analytica Chimica Acta*, 2009, **652**(1-2): 22-31.
7. Rodrigues, E. P., Torres, A. R., Batista, J. S. d. S., Huergo, L., Hungria, M., A simple, economical and reproducible protein extraction protocol for proteomics studies of soybean roots. *Genetics and Molecular Biology*, 2012, **35**: 348-352.
8. Bader, N. R., Sample preparation for flame atomic absorption spectroscopy: an overview. *Rasayan Journal of Chemistry*, 2011, **4**(1): 49-55.
9. Stanaszek, R., Piekoszewski, W., Simultaneous determination of eight underivatized amphetamines in hair by high-performance liquid chromatography-atmospheric pressure chemical ionization mass spectrometry (HPLC-APCI-MS). *Journal of Analytical Toxicology*, 2004, **28**(2): 77-85.
10. Richter, B. E., Jones, B. A., Ezzell, J. L., Porter, N. L., Avdalovic, N., Pohl, C., Accelerated solvent extraction: A technique for sample preparation. *Analytical Chemistry*, 1996, **68**(6): 1033-1039.
11. Kabir, A., Holness, H., Furton, K. G., Almirall, J. R., Recent advances in micro-sample preparation with forensic applications. *TrAC Trends in Analytical Chemistry*, 2013, **45**(0): 264-279.
12. Bayne, S., Carlin, M., *Forensic applications of high performance liquid chromatography*. CRC Press: Boca Raton, 2010.

13. Thessalonikeos, E., Tsoukali, H., Spagou, K., Vlachou, M., Pouliopoulos, A., Raikos, N., Development of a liquid-liquid extraction procedure for the analysis of amphetamine in biological specimens by GC-FID. *The Open Forensic Science Journal*, 2009, **2**(1): 12-15.
14. Huang, Z. P., Chen, X. H., Wijsbeek, J., Franke, J. P., de Zeeuw, R. A., An enzymic digestion and solid-phase extraction procedure for the screening for acidic, neutral, and basic drugs in liver using gas chromatography for analysis. *Journal of Analytical Toxicology*, 1996, **20**(4): 248-254.
15. Atapattu, S. N., Rosenfeld, J. M., Solid phase analytical derivatization as a sample preparation method. *Journal of Chromatography A*, 2013, **1296**(0): 204-213.
16. Fan, Y., Feng, Y.-Q., Zhang, J.-T., Da, S.-L., Zhang, M., Poly(methacrylic acid-ethylene glycol dimethacrylate) monolith in-tube solid phase microextraction coupled to high performance liquid chromatography and analysis of amphetamines in urine samples. *Journal of Chromatography A*, 2005, **1074**(1-2): 9-16.
17. Dasgupta, A., *Beating drug tests and defending positive results: a toxicologist's perspective*. Springer: Dordrecht, 2010.
18. Nováková, L., Vlčková, H., A review of current trends and advances in modern bio-analytical methods: chromatography and sample preparation. *Analytica Chimica Acta*, 2009, **656**(1-2): 8-35.
19. Hyötyläinen, T., Critical evaluation of sample pretreatment techniques. *Analytical and Bioanalytical Chemistry*, 2009, **394**(3): 743-758.
20. Kole, P. L., Venkatesh, G., Kotecha, J., Sheshala, R., Recent advances in sample preparation techniques for effective bioanalytical methods. *Biomedical Chromatography*, 2011, **25**(1-2): 199-217.
21. Namera, A., Nakamoto, A., Saito, T., Miyazaki, S., Monolith as a new sample preparation material: recent devices and applications. *Journal of Separation Science*, 2011, **34**(8): 901-924.
22. Namera, A., Saito, T., Advances in monolithic materials for sample preparation in drug and pharmaceutical analysis. *TrAC Trends in Analytical Chemistry*, 2013, **45**(0): 182-196.
23. Vas, G., Vékey, K., Solid-phase microextraction: a powerful sample preparation tool prior to mass spectrometric analysis. *Journal of Mass Spectrometry*, 2004, **39**(3): 233-254.
24. Schwenke, K. D., Rieman, W., Walton, H. F., Ion exchange in analytical chemistry. *Food/Nahrung*, 1974, **18**(3): 334-335.
25. Mitra, S., *Sample preparation techniques in analytical chemistry*. John Wiley & Sons: New Jersey, 2003.

26. Zief, M., Kakodkar, S. V., Solid phase extraction for sample preparation. In *Pharmaceutical and biomedical applications of liquid chromatography*, eds. Riley, C. M., Lough, W. J., Wainer, I. W., Pergamon: New York, 1994, Vol. 1, pp. 127-143.
27. Khayoon, W. S., Saad, B., Salleh, B., Manaf, N. H. A., Latiff, A. A., Micro-solid phase extraction with liquid chromatography-tandem mass spectrometry for the determination of aflatoxins in coffee and malt beverage. *Food Chemistry*, 2014, **147**(0): 287-294.
28. Barciela-Alonso, M. C., Plata-García, V., Rouco-López, A., Moreda-Piñeiro, A., Bermejo-Barrera, P., Ionic imprinted polymer based solid phase extraction for cadmium and lead pre-concentration/determination in seafood. *Microchemical Journal*, 2014, **114**(0): 106-110.
29. Miskam, M., Abu Bakar, N. K., Mohamad, S., Determination of polar aromatic amines using newly synthesized sol-gel titanium (IV) butoxide cyanopropyltriethoxysilane as solid phase extraction sorbent. *Talanta*, 2014, **120**(0): 450-455.
30. Sun, N., Han, Y., Yan, H., Song, Y., A self-assembly pipette tip graphene solid-phase extraction coupled with liquid chromatography for the determination of three sulfonamides in environmental water. *Analytica Chimica Acta*, 2014, **810**(0): 25-31.
31. Zwir-Ferenc, A. B., M, Solid phase extraction technique - trends, opportunities and applications. *Polish Journal of Environmental Studies*, 2006, **15**(5): 677-690.
32. Thurman, E. M., Mills, M. S., *Solid-phase extraction: principles and practice*. John Wiley & Sons: New York, 1998.
33. Haupt, K., Molecularly imprinted polymers in analytical chemistry. *Analyst*, 2001, **126**(6): 747-756.
34. Logan, B. K., Stafford, D. T., Tebbett, I. R., Moore, C. M., Rapid screening for 100 basic drugs and metabolites in urine using cation exchange solid-phase extraction and high-performance liquid chromatography with diode array detection. *Journal of Analytical Toxicology*, 1990, **14**(3): 154-159.
35. Simpson, N. J. K., *Solid-phase extraction: principles, techniques, and applications*. Taylor & Francis, Abingdon: 2000.
36. Shen, G., Hian Kee, L., Hollow fiber-protected liquid-phase microextraction of triazine herbicides. *Analytical Chemistry*, 2002, **74**(3): 648-654.
37. Lingeman, H., Hoekstra-Oussoren, S. J. F., Particle-loaded membranes for sample concentration and/or clean-up in bioanalysis. *Journal of Chromatography B: Biomedical Sciences and Applications*, 1997, **689**(1): 221-237.
38. Ulrich, S., Solid-phase microextraction in biomedical analysis. *Journal of Chromatography A*, 2000, **902**(1): 167-194.

39. Hansen, S., Pedersen-Bjergaard, S., Rasmussen, K., *Introduction to pharmaceutical chemical analysis*. John Wiley & Sons: Chichester, England, 2011.
40. Camel, V., Solid phase extraction of trace elements. *Spectrochimica Acta Part B: Atomic Spectroscopy*, 2003, **58**(7): 1177-1233.
41. Pawliszyn, J., Sample preparation: quo vadis? *Analytical Chemistry*, 2003, **75**(11): 2543-2558.
42. Oleschuk, R. D., Shultz-Lockyear, L. L., Ning, Y., Harrison, D. J., Trapping of bead-based reagents within microfluidic systems: on-chip solid-phase extraction and electrochromatography. *Analytical Chemistry*, 1999, **72**(3): 585-590.
43. Calderon, L. d. A., *Chromatography - the most versatile method of chemical analysis*. InTech: Croatia, 2012.
44. Hennion, M.-C., Solid-phase extraction: method development, sorbents, and coupling with liquid chromatography. *Journal of Chromatography A*, 1999, **856**(1-2): 3-54.
45. Sabik, H., Jeannot, R., Rondeau, B., Multiresidue methods using solid-phase extraction techniques for monitoring priority pesticides, including triazines and degradation products, in ground and surface waters. *Journal of Chromatography A*, 2000, **885**(1-2): 217-236.
46. Bagheri, H., Piri-Moghadam, H., Naderi, M., Towards greater mechanical, thermal and chemical stability in solid-phase microextraction. *TrAC Trends in Analytical Chemistry*, 2012, **34**(0): 126-139.
47. Augusto, F., Hantao, L. W., Mogollón, N. G. S., Braga, S. C. G. N., New materials and trends in sorbents for solid-phase extraction. *TrAC Trends in Analytical Chemistry*, 2013, **43**(0): 14-23.
48. Ettre, L. S., Sakodynskii, K. I., M.S. Tswett and the discovery of chromatography II: completion of the development of chromatography (1903-1910). *Chromatographia*, 1993, **35**(5-6): 329-338.
49. Abel, E. W., Pollard, F. H., Uden, P. C., Nickless, G., A new gas-liquid chromatographic phase. *Journal of Chromatography A*, 1966, **22**(0): 23-28.
50. Mallik, R., Xuan, H., Hage, D. S., Development of an affinity silica monolith containing alpha1-acid glycoprotein for chiral separations. *Journal of Chromatography A*, 2007, **1149**(2): 294-304.
51. Allen, D., El Rassi, Z., Silica-based monoliths for capillary electrochromatography: methods of fabrication and their applications in analytical separations. *Electrophoresis*, 2003, **24**(22-23): 3962-3976.
52. Jal, P. K., Patel, S., Mishra, B. K., Chemical modification of silica surface by immobilization of functional groups for extractive concentration of metal ions. *Talanta*, 2004, **62**(5): 1005-1028.

53. Nawrocki, J., The silanol group and its role in liquid chromatography. *Journal of Chromatography A*, 1997, **779**(1-2): 29-71.
54. Zhuravlev, L. T., The surface chemistry of amorphous silica. Zhuravlev model. *Colloids and Surfaces A: Physicochemical and Engineering Aspects*, 2000, **173**(1-3): 1-38.
55. Ong, S., Zhao, X., Eisenthal, K. B., Polarization of water molecules at a charged interface: second harmonic studies of the silica/water interface. *Chemical Physics Letters*, 1992, **191**(3-4): 327-335.
56. Kabir, A., Furton, K. G., Malik, A., Innovations in sol-gel microextraction phases for solvent-free sample preparation in analytical chemistry. *TrAC Trends in Analytical Chemistry*, 2013, **45**(0): 197-218.
57. Zief, M., Kiser, R., *Solid phase extraction for sample preparation, a technical guide to theory, method development and use*. J.T. Baker: Phillipsburg, USA, 1994.
58. Tian, H., Hühmer, A. F. R., Landers, J. P., Evaluation of silica resins for direct and efficient extraction of DNA from complex biological matrices in a miniaturized format. *Analytical Biochemistry*, 2000, **283**(2): 175-191.
59. Wen, J., Guillo, C., Ferrance, J. P., Landers, J. P., DNA extraction using a tetramethyl orthosilicate-grafted photopolymerized monolithic solid phase. *Analytical Chemistry*, 2006, **78**(5): 1673-1681.
60. Minakuchi, H., Nakanishi, K., Soga, N., Ishizuka, N., Tanaka, N., Effect of domain size on the performance of octadecylsilylated continuous porous silica columns in reversed-phase liquid chromatography. *Journal of Chromatography A*, 1998, **797**(1-2): 121-131.
61. Yu, S., Geng, J., Zhou, P., Wang, J., Feng, A., Chen, X., Tong, H., Hu, J., Application of a new hybrid organic-inorganic monolithic column for efficient deoxyribonucleic acid purification. *Analytica Chimica Acta*, 2008, **611**(2): 173-181.
62. Hjertén, S., Liao, J.-L., Zhang, R., High-performance liquid chromatography on continuous polymer beds. *Journal of Chromatography A*, 1989, **473**(0): 273-275.
63. Svec, F., Frechet, J. M. J., Continuous rods of macroporous polymer as high-performance liquid chromatography separation media. *Analytical Chemistry*, 1992, **64**(7): 820-822.
64. Guiochon, G., Monolithic columns in high-performance liquid chromatography. *Journal of Chromatography A*, 2007, **1168**(1-2): 101-168.
65. Švec, F., Tennikova, T. B., Deyl, Z. *Monolithic materials: preparation, properties, and applications*. Elsevier Science & Technology Books: Amsterdam, 2003.

66. Ueki, Y., Umemura, T., Li, J., Odake, T., Tsunoda, K.-i., Preparation and application of methacrylate-based cation-exchange monolithic columns for capillary ion chromatography. *Analytical Chemistry*, 2004, **76**(23): 7007-7012.
67. Nema, T., Chan, E. C. Y., Ho, P. C., Applications of monolithic materials for sample preparation. *Journal of Pharmaceutical and Biomedical Analysis*, 2014, **87**(0): 130-141.
68. Silva, R. G. C., Bottoli, C. B. G., Collins, C. H., New silica gel-based monolithic column for nano-liquid chromatography, used in the HILIC mode. *Journal of Chromatographic Science*, 2012, **50**(8): 649-657.
69. Minakuchi, H., Nakanishi, K., Soga, N., Ishizuka, N., Tanaka, N., Octadecylsilylated porous silica rods as separation media for reversed-phase liquid chromatography. *Analytical Chemistry*, 1996, **68**(19): 3498-3501.
70. Fields, S. M., Silica xerogel as a continuous column support for high-performance liquid chromatography. *Analytical Chemistry*, 1996, **68**(15): 2709-2712.
71. Kennedy, J. F., Phillips, G. O., Williams, P. A., *Cellulosics: materials for selective separations and other technologies*. Ellis Horwood: New York, 1993.
72. Chen, X., Cui, D.-F., Liu, C.-C., Li, H., Fabrication of DNA purification microchip integrated with mesoporous matrix based on MEMS technology. *Microsystem Technologies*, 2007, **14**(1): 51-57.
73. Wu, Q., Bienvenue, J. M., Hassan, B. J., Kwok, Y. C., Giordano, B. C., Norris, P. M., Landers, J. P., Ferrance, J. P., Microchip-based macroporous silica sol-gel monolith for efficient isolation of DNA from clinical samples. *Analytical Chemistry*, 2006, **78**(16): 5704-5710.
74. Kirkland, J. J., Truszkowski, F. A., Ricker, R. D., Atypical silica-based column packings for high-performance liquid chromatography. *Journal of Chromatography A*, 2002, **965**(1-2): 25-34.
75. Urban, J., Jandera, P., Polymethacrylate monolithic columns for capillary liquid chromatography. *Journal of Separation Science*, 2008, **31**(14): 2521-2540.
76. Nema, T., Chan, E. C. Y., Ho, P. C., Application of silica-based monolith as solid phase extraction cartridge for extracting polar compounds from urine. *Talanta*, 2010, **82**(2): 488-494.
77. Nakanishi, K., Minakuchi, H., Soga, N., Tanaka, N., Structure design of double-pore silica and its application to HPLC. *Journal of Sol-Gel Science and Technology*, 1998, **13**(1-3): 163-169.
78. Unger, K. K., Skudas, R., Schulte, M. M., Particle packed columns and monolithic columns in high-performance liquid chromatography-comparison and critical appraisal. *Journal of Chromatography A*, 2008, **1184**(1-2): 393-415.

79. Nakanishi, K., Pore structure control of silica gels based on phase separation. *Journal of Porous Materials*, 1997, **4**(2): 67-112.
80. Cabrera, K., Applications of silica-based monolithic HPLC columns. *Journal of Separation Science*, 2004, **27**(10-11): 843-852.
81. Nakanishi, K., Soga, N., Phase separation in gelling silica-organic polymer solution: systems containing poly(sodium styrenesulfonate). *Journal of the American Ceramic Society*, 1991, **74**(10): 2518-2530.
82. Nakanishi, K., Soga, N., Phase separation in silica sol-gel system containing polyacrylic acid I. Gel formation behavior and effect of solvent composition. *Journal of Non-Crystalline Solids*, 1992, **139**(0): 1-13.
83. Nakanishi, K., Soga, N., Phase separation in silica sol-gel system containing polyacrylic acid II. Effects of molecular weight and temperature. *Journal of Non-Crystalline Solids*, 1992, **139**(0): 14-24.
84. Siouffi, A. M., Silica gel-based monoliths prepared by the sol-gel method: facts and figures. *Journal of Chromatography A*, 2003, **1000**(1-2): 801-818.
85. Fricke, J., Tillotson, T., Aerogels: production, characterization, and applications. *Thin Solid Films*, 1997, **297**(1-2): 212-223.
86. Schubert, U., Hüsing, N., *Synthesis of inorganic materials*. Third edition. Bergstr Wiley-VCH: Weinheim, 2012.
87. Kato, M., Sakai-Kato, K., Toyo'oka, T., Silica sol-gel monolithic materials and their use in a variety of applications. *Journal of Separation Science*, 2005, **28**(15): 1893-1908.
88. Folgar, C. E., Structural evolution of silica aerogel under a microwave field, Blacksburg, *Materials Science and Engineering*, 2010.
89. Núñez, O., Nakanishi, K., Tanaka, N., Preparation of monolithic silica columns for high-performance liquid chromatography. *Journal of Chromatography A*, 2008, **1191**(1-2): 231-252.
90. Ishizuka, N., Minakuchi, H., Nakanishi, K., Soga, N., Nagayama, H., Hosoya, K., Tanaka, N., Performance of a monolithic silica column in a capillary under pressure-driven and electrodriven conditions. *Analytical Chemistry*, 2000, **72**(6): 1275-1280.
91. Frolova, A., Chukhlieb, M., Drobot, A., Kryshstal, A., Loginova, L., Boichenko, A., Producing of monolithic layers of silica for thin-layer chromatography by sol-gel synthesis. *The Open Surface Science Journal*, 2009, **1**: 40-45.
92. Wu, N., Thompson, R., Fast and efficient separations using reversed phase liquid chromatography. *Journal of Liquid Chromatography & Related Technologies*, 2006, **29**(7-8): 949-988.
93. Keeling-Tucker, T., Rakic, M., Spong, C., Brennan, J. D., Controlling the material properties and biological activity of lipase within sol-gel derived

- bioglasses via organosilane and polymer doping. *Chemistry of Materials*, 2000, **12**(12): 3695-3704.
94. Gharagozlou, M., Influence of calcination temperature on structural and magnetic properties of nanocomposites formed by co-ferrite dispersed in sol-gel silica matrix using tetrakis(2-hydroxyethyl) orthosilicate as precursor. *Chemistry Central Journal*, 2011, **5**(1): 19.
 95. Fletcher, P. I., Haswell, S., He, P., Kelly, S., Mansfield, A., Permeability of silica monoliths containing micro- and nano-pores. *Journal of Porous Materials*, 2011, **18**(4): 501-508.
 96. Qu, Q.-S., Wang, S., Mangelings, D., Wang, C.-Y., Yang, G.-J., Hu, X.-Y., Yan, C., Monolithic silica xerogel capillary column for separations in capillary LC and pressurized CEC. *Electrophoresis*, 2009, **30**(6): 1071-1076.
 97. Tanaka, N., Kobayashi, H., Ishizuka, N., Minakuchi, H., Nakanishi, K., Hosoya, K., Ikegami, T., Monolithic silica columns for high-efficiency chromatographic separations. *Journal of Chromatography A*, 2002, **965**(1-2): 35-49.
 98. Ghanem, A., Ikegami, T., Recent advances in silica-based monoliths: preparations, characterizations and applications. *Journal of Separation Science*, 2011, **34**(16-17): 1945-1957.
 99. Wu, R. a., Hu, L., Wang, F., Ye, M., Zou, H., Recent development of monolithic stationary phases with emphasis on microscale chromatographic separation. *Journal of Chromatography A*, 2008, **1184**(1-2): 369-392.
 100. Zou, H., Huang, X., Ye, M., Luo, Q., Monolithic stationary phases for liquid chromatography and capillary electrochromatography. *Journal of Chromatography A*, 2002, **954**(1-2): 5-32.
 101. Wang, R., Zhang, F., Yang, B., Liang, X., A fast way to make a monolithic column for a high pressure electroosmotic pump. *Analytical Sciences*, 2010, **26**(8): 921-923.
 102. Christensen, P., Johnson, S., McCreedy, T., Skelton, V., Wilson, N., The fabrication of micro-porous silica structures for micro-reactor technology. *Analytical Communications*, 1998, **35**(10): 341-343.
 103. Shaw, K. J., Joyce, D. A., Docker, P. T., Dyer, C. E., Greenman, J., Greenway, G. M., Haswell, S. J., Simple practical approach for sample loading prior to DNA extraction using a silica monolith in a microfluidic device. *Lab on a Chip*, 2009, **9**(23): 3430-3432.
 104. Yuan, H., Zhang, L., Zhang, Y., Monoliths, fundamentals for sample preparation. In *Comprehensive sampling and sample preparation*, ed. Pawliszyn, J., Academic Press: Oxford, 2012, Vol. 2, pp. 345-358.
 105. Wong, S. Y., Sood, N., Putnam, D., Combinatorial evaluation of cations, pH-sensitive and hydrophobic moieties for polymeric vector design. *Molecular*

- Therapy: The Journal of the American Society of Gene Therapy*, 2009, **17**(3): 480-490.
106. Chen, Y., Guo, Z., Wang, X., Qiu, C., Sample preparation. *Journal of Chromatography A*, 2008, **1184**(1-2): 191-219.
 107. Qiu, H., Liang, X., Sun, M., Jiang, S., Development of silica-based stationary phases for high-performance liquid chromatography. *Analytical and Bioanalytical Chemistry*, 2011, **399**(10): 3307-3322.
 108. Namera, A., Nakamoto, A., Nishida, M., Saito, T., Kishiyama, I., Miyazaki, S., Yahata, M., Yashiki, M., Nagao, M., Extraction of amphetamines and methylenedioxyamphetamines from urine using a monolithic silica disk-packed spin column and high-performance liquid chromatography-diode array detection. *Journal of Chromatography A*, 2008, **1208**(1-2): 71-75.
 109. Rudaz, S., Haerdi, W., Veuthey, J. L., Evaluation of procedures for solid-phase extraction of [125I]-methadone from serum on to discs and cartridges. *Chromatographia*, 1997, **44**(5-6): 283-288.
 110. van Hout, M. W. J., de Zeeuw, R. A., de Jong, G. J., Coupling device for desorption of drugs from solid-phase extraction-pipette tips and on-line gas chromatographic analysis. *Journal of Chromatography A*, 1999, **858**(1): 117-122.
 111. Buchmeiser, M. R., Polymeric monolithic materials: syntheses, properties, functionalization and applications. *Polymer*, 2007, **48**(8): 2187-2198.
 112. Kumazawa, T., Hasegawa, C., Lee, X.-P., Sato, K., New and unique methods of solid-phase extraction for use before instrumental analysis of xenobiotics in human specimens. *Forensic Toxicology*, 2010, **28**(2): 61-68.
 113. Weibel, D. B., Whitesides, G. M., Applications of microfluidics in chemical biology. *Current Opinion in Chemical Biology*, 2006, **10**(6): 584-591.
 114. Whitesides, G. M., The origins and the future of microfluidics. *Nature*, 2006, **442**(7101): 368-373.
 115. McDonald, J. C., Duffy, D. C., Anderson, J. R., Chiu, D. T., Wu, H., Schueller, O. J., Whitesides, G. M., Fabrication of microfluidic systems in poly(dimethylsiloxane). *Electrophoresis*, 2000, **21**(1): 27-40.
 116. Sia, S., Whitesides G. M., Microfluidic devices fabricated in poly (dimethylsiloxane) for biological studies. *Electrophoresis*, 2003, **24**(21): 3563-3576.
 117. Price, C. W., Leslie, D. C., Landers, J. P., Nucleic acid extraction techniques and application to the microchip. *Lab on a Chip*, 2009, **9**(17): 2484-2494.
 118. Dittrich, P. S., Manz, A., Lab-on-a-chip: microfluidics in drug discovery. *Nature Reviews Drug Discovery*, 2006, **5**(3): 210-218.

119. Manz, A., Graber, N., Widmer, H. M., Miniaturized total chemical analysis systems: a novel concept for chemical sensing. *Sensors and Actuators B: Chemical*, 1990, **1**(1-6): 244-248.
120. Zhang, X., Haswell, S. J., Micro-fluidic and lab-on-a-chip technology. In *New avenues to efficient chemical synthesis*, eds. Seeberger, P. H., Blume, T., Springer: Berlin, 2007, Vol. 2006/3, pp. 21-37.
121. Cady, N. C., Stelick, S., Batt, C. A., Nucleic acid purification using microfabricated silicon structures. *Biosensors and Bioelectronics*, 2003, **19**(1): 59-66.
122. Zhang, C., Xu, J., Ma, W., Zheng, W., PCR microfluidic devices for DNA amplification. *Biotechnology Advances*, 2006, **24**(3): 243-284.
123. Ong S., Zhang, S., Du, H., Fu, Y., Fundamental principles and applications of microfluidic systems. *Frontiers in Bioscience*, 2008, **13**(1): 2757-2773.
124. Haswell, S. J., Watts, P., Green chemistry: synthesis in micro reactors. *Green Chemistry*, 2003, **5**(2): 240-249.
125. Beebe, D., Wheeler, M., Zeringue, H., Walters, E., Raty, S., Microfluidic technology for assisted reproduction. *Theriogenology*, 2002, **57**(1): 125-135.
126. Ligler, F. S., Taitt, C. A. R., *Optical biosensors: today and tomorrow*. Elsevier: Amsterdam, 2008.
127. Rhodes, M. J., *Introduction to particle technology*. Second edition. John Wiley and Sons: Chippenham, 2008.
128. Stone, H. A., Stroock, A. D., Ajdari, A., Engineering flows in small devices. *Annual Review of Fluid Mechanics*, 2004, **36**(1): 381-411.
129. Urbanski, J. P., Thies, W., Rhodes, C., Amarasinghe, S., Thorsen, T., Digital microfluidics using soft lithography. *Lab on a Chip*, 2006, **6**(1): 96-104.
130. Watts, P., Haswell, S. J., Microfluidic combinatorial chemistry. *Current Opinion in Chemical Biology*, 2003, **7**(3): 380-387.
131. Marle, L., *Miniaturised analytical systems with chemiluminescence detection for environmental application*. PhD thesis: University of Hull, 2006.
132. McCreedy, T., Fabrication techniques and materials commonly used for the production of microreactors and micro total analytical systems. *TrAC Trends in Analytical Chemistry*, 2000, **19**(6): 396-401.
133. Manz, A., Pamme, N., Iossifidis, D., *Bioanalytical chemistry*. Imperial College Press: London, 2004.
134. Haeberle, S., Zengerle, R., Microfluidic platforms for lab-on-a-chip applications. *Lab on a Chip*, 2007, **7**(9): 1094-1110.

135. Tarn, M. D., Pamme, N., Microfluidics. In *Reference module in chemistry, molecular sciences and chemical engineering*, Elsevier: 2014.
136. Peeni, B. A., Lee, M. L., Hawkins, A. R., Woolley, A. T., Sacrificial layer microfluidic device fabrication methods. *Electrophoresis*, 2006, **27**(24): 4888-4895.
137. Erill, I., Campoy, S., Erill, N., Barbé, J., Aguiló, J., Biochemical analysis and optimization of inhibition and adsorption phenomena in glass-silicon PCR-chips. *Sensors and Actuators B: Chemical*, 2003, **96**(3): 685-692.
138. Ashley, J. F., Cramer, N. B., Davis, R. H., Bowman, C. N., Soft-lithography fabrication of microfluidic features using thiol-ene formulations. *Lab on a Chip*, 2011, **11**(16): 2772-2778.
139. Becker, H., Locascio, L. E., Polymer microfluidic devices. *Talanta*, 2002, **56**(2): 267-287.
140. McDonald, J. C., Duffy, D. C., Anderson, J. R., Chiu, D. T., Wu, H., Schueller, O. J. A., Whitesides, G. M., Fabrication of microfluidic systems in poly(dimethylsiloxane). *Electrophoresis*, 2000, **21**(1): 27-40.
141. McCormick, R. M., Nelson, R. J., Alonso-Amigo, M. G., Benvegna, D. J., Hooper, H. H., Microchannel electrophoretic separations of DNA in injection-molded plastic substrates. *Analytical Chemistry*, 1997, **69**(14): 2626-2630.
142. Kolari, K., Satokari, R., Kataja, K., Stenman, J., Hokkanen, A., Real-time analysis of PCR inhibition on microfluidic materials. *Sensors and Actuators B: Chemical*, 2008, **128**(2): 442-449.
143. Zhang, C. S., Xing, D., Miniaturized PCR chips for nucleic acid amplification and analysis: latest advances and future trends. *Nucleic Acids Research*, 2007, **35**(13): 4223-4237.
144. Jeffreys, A. J., Wilson, V., Thein, S. L., Hypervariable 'minisatellite' regions in human DNA. *Nature*, 1985, **314**(6006): 67-73.
145. Dale, J., Schantz, M. V., *From genes to genomes: concepts and applications of DNA technology*. John Wiley & Sons: London, 2002.
146. Goodwin, W., Linacre, A., Hadi, S., *An introduction to forensic genetics*. John Wiley & Sons: Chichester, England, 2007.
147. Dietrich, W., Katz, H., Lincoln, S. E., Shin, H. S., Friedman, J., Dracopoli, N. C., Lander, E. S., A genetic map of the mouse suitable for typing intraspecific crosses. *Genetics*, 1992, **131**(2): 423-447.
148. Butler, J. M., *Forensic DNA typing: biology, technology, and genetics of STR markers*. Elsevier Academic Press: London, 2005.
149. Kimpton, C., Fisher, D., Watson, S., Adams, M., Urquhart, A., Lygo, J., Gill, P., Evaluation of an automated DNA profiling system employing multiplex

- amplification of four tetrameric STR loci. *International Journal of Legal Medicine*, 1994, **106**(6): 302-11.
150. Sparkes, R., Kimpton, C., Watson, S., Oldroyd, N., Barnett, L., Arnold, J., Thompson, C., Hale, R., Chapman, J., Urquhart, A., Gill, P., Clayton, T., The validation of a 7-locus multiplex STIR test for use in forensic casework. *International Journal of Legal Medicine*, 1996, **109**(4): 186-194.
151. AmpFISTR[®] SGM Plus[®] PCR Amplification Kitt User's Manual. In Biosystems, A., Ed. 2006.
152. Benecke, M., DNA typing in forensic medicine and in criminal investigations: a current survey. *Naturwissenschaften*, 1997, **84**(5) 181-188.
153. Sgueglia, J., Geiger, S., Davis, J., Precision studies using the ABI Prism 3100 Genetic Analyzer for forensic DNA analysis. *Analytical and Bioanalytical Chemistry*, 2003, **376**(8): 1247-1254.
154. DeMaria, A. N., A structure for deoxyribose nucleic acid. *Journal of the American College of Cardiology*, 2003, **42**(2): 373-374.
155. Detlev, G., Ruckpaul, K., DNA Structure. In *Encyclopedic Reference of Genomics and Proteomics in Molecular Medicine*. First edition. Springer Berlin Heidelberg: New York, 2006; pp 449-450.
156. Dickerson, R. E., The DNA helix and how it is read. *Scientific American*, 1983, **249**: 94-111.
157. Reedy, C. R., Hagan, K. A., Strachan, B. C., Higginson, J. J., Bienvenue, J. M., Greenspoon, S. A., Ferrance, J. P., Landers, J. P., Dual-domain microchip-based process for volume reduction solid phase extraction of nucleic acids from dilute, large volume biological samples. *Analytical Chemistry*, 2010, **82**(13): 5669-5678.
158. Shaw, K. J., Thain, L., Docker, P. T., Dyer, C. E., Greenman, J., Greenway, G. M., Haswell, S. J., The use of carrier RNA to enhance DNA extraction from microfluidic-based silica monoliths. *Analytica Chimica Acta*, 2009, **652**(1-2): 231-233.
159. Shaw, K. J., *Integrated DNA extraction and amplification on a microfluidic device*. PhD thesis: University of Hull, 2009.
160. Garrett, P. E., Tao, F., Lawrence, N., Ji, J., Schumacher, R. T., Manak, M. M., Tired of the same old grind in the new genomics and proteomics era? *Targets*, 2002, **1**(5): 156-162.
161. Huang, Y., Mather, E., Bell, J., Madou, M., MEMS-based sample preparation for molecular diagnostics. *Analytical and Bioanalytical Chemistry*, 2002, **372**(1): 49-65.
162. Lee, H. J., Kim, J.-H., Lim, H. K., Cho, E. C., Huh, N., Ko, C., Chan Park, J., Choi, J.-W., Lee, S. S., Electrochemical cell lysis device for DNA extraction. *Lab on a Chip*, 2010, **10**(5): 626-633.

163. Horsman, K. M., Bienvenue, J. M., Blasier, K. R., Landers, J. P., Forensic DNA analysis on microfluidic devices: a review. *Journal of Forensic Sciences*, 2007, **52**(4): 784-799.
164. Meacle, F. J., Lander, R., Ayazi Shamlou, P., Titchener-Hooker, N. J., Impact of engineering flow conditions on plasmid DNA yield and purity in chemical cell lysis operations. *Biotechnology and Bioengineering*, 2004, **87**(3): 293-302.
165. Bielawski, J., Two types of haemolytic activity of detergents. *Biochimica et Biophysica Acta (BBA) - General Subjects*, 1990, **1035**(2): 214-217.
166. Berkelman, T., Brubacher, M. G., Chang, H., Important factors influencing protein solubility for 2-D electrophoresis. *Bio Rad Laboratories*, 2004, **114**: 30-32.
167. Miller, D. N., Bryant, J. E., Madsen, E. L., Ghiorse, W. C., Evaluation and optimization of DNA extraction and purification procedures for soil and sediment samples. *Applied and Environmental Microbiology*, 1999, **65**(11): 4715-4724.
168. Wen, J., Guillo, C., Ferrance, J. P., Landers, J. P., Microfluidic chip-based protein capture from human whole blood using octadecyl (C18) silica beads for nucleic acid analysis from large volume samples. *Journal of Chromatography A*, 2007, **1171**(1-2): 29-36.
169. Witek, M. A., Llopis, S. D., Wheatley, A., McCarley, R. L., Soper, S. A., Purification and preconcentration of genomic DNA from whole cell lysates using photoactivated polycarbonate (PPC) microfluidic chips. *Nucleic Acids Research*, 2006, **34**(10): 74.
170. Boom, R., Sol, C. J., Salimans, M. M., Jansen, C. L., Wertheim-van Dillen, P. M., van der Noordaa, J., Rapid and simple method for purification of nucleic acids. *Journal of Clinical Microbiology*, 1990, **28**(3): 495-503.
171. Larson, R. G., Poeckh, T., Lopez, S., Fuller, A. O., Solomon, M. J., Adsorption and elution characteristics of nucleic acids on silica surfaces and their use in designing a miniaturized purification unit. *Analytical Biochemistry*, 2008, **373**(2): 253-262.
172. Wolfe, K. A., Breadmore, M. C., Ferrance, J. P., Power, M. E., Conroy, J. F., Norris, P. M., Landers, J. P., Toward a microchip-based solid-phase extraction method for isolation of nucleic acids. *Electrophoresis*, 2002, **23**(5): 727-733.
173. Melzak, K. A., Sherwood, C. S., Turner, R. F. B., Haynes, C. A., Driving forces for DNA adsorption to silica in perchlorate solutions. *Journal of Colloid and Interface Science*, 1996, **181**(2): 635-644.
174. Landers, J. P., Wen, J., Legendre, L. A., Bienvenue, J. M., Purification of nucleic acids in microfluidic devices. *Analytical Chemistry*, 2008, **80**(17): 6472-6479.
175. Mason, P. E., Neilson, G. W., Enderby, J. E., Saboungi, M. L., Dempsey, C. E., MacKerell, A. D., Jr., Brady, J. W., The structure of aqueous guanidinium

- chloride solutions. *Journal of the American Chemical Society*, 2004, **126**(37): 11462-11470.
176. Nicklas, J. A., Buel, E., Quantification of DNA in forensic samples. *Analytical and Bioanalytical Chemistry*, 2003, **376**(8): 1160-1167.
177. Ji, H. M., Samper, V., Chen, Y., Hui, W. C., Lye, H. J., Mustafa, F. B., Lee, A. C., Cong, L., Heng, C. K., Lim, T. M., DNA purification silicon chip. *Sensors and Actuators A: Physical*, 2007, **139**(1-2): 139-144.
178. Singer, V. L., Jones, L. J., Yue, S. T., Haugland, R. P., Characterization of PicoGreen reagent and development of a fluorescence-based solution assay for double-stranded DNA quantitation. *Analytical Biochemistry*, 1997, **249**(2): 228-238.
179. Dragan, A. I., Casas-Finet, J. R., Bishop, E. S., Strouse, R. J., Schenerman, M. A., Geddes, C. D., Characterization of PicoGreen interaction with dsDNA and the origin of its fluorescence enhancement upon binding. *Biophysical Journal*, 2010, **99**(9): 3010-3019.
180. Zhang, Y., Ozdemir, P., Microfluidic DNA amplification - a review. *Analytica Chimica Acta*, 2009, **638**(2): 115-125.
181. Li, H., Cui, X., Arnheim, N., Direct electrophoretic detection of the allelic state of single DNA molecules in human sperm by using the polymerase chain reaction. *Proceedings of the National Academy of Sciences of the United States of America*, 1990, **87**(12): 4580-4584.
182. deMello, A. J., Microfluidics: DNA amplification moves on. *Nature*, 2003, **422**(6927): 28-29.
183. *Polymerase chain reaction*. Science Info World.
<http://scienceinfoworld.blogspot.co.uk/2012/11/polymerase-chain-reaction-pcr.html> [Accessed: 30/01/2014]
184. Findlay, I., Quirke, P., Fluorescent polymerase chain reaction: part I. A new method allowing genetic diagnosis and DNA fingerprinting of single cells. *Human Reproduction Update*, 1996, **2**(2): 137-152.
185. Abu Al-Soud, W., Radstrom, P., Capacity of nine thermostable DNA polymerases to mediate DNA amplification in the presence of PCR-inhibiting samples. *Applied and Environmental Microbiology*, 1998, **64**(10): 3748-3753.
186. Kreader, C. A., Relief of amplification inhibition in PCR with bovine serum albumin or T4 gene 32 protein. *Applied and Environmental Microbiology*, 1996, **62**(3): 1102-1106.
187. Gill, P., Ghaemi, A., Nucleic acid isothermal amplification technologies - a review. *Nucleosides, Nucleotides and Nucleic Acids*, 2008, **27**(3): 224-243.
188. Notomi, T., Okayama, H., Masubuchi, H., Yonekawa, T., Watanabe, K., Amino, N., Hase, T., Loop-mediated isothermal amplification of DNA. *Nucleic Acids Research*, 2000, **28**(12): 63.

189. Morabito, K., Wiske, C., Tripathi, A., Engineering insights for multiplexed real-time nucleic acid sequence-based amplification (NASBA): implications for design of point-of-care diagnostics. *Molecular Diagnosis and Therapy*, 2013, **17**(3): 185-192.
190. Guatelli, J. C., Whitfield, K. M., Kwoh, D. Y., Barringer, K. J., Richman, D. D., Gingeras, T. R., Isothermal, in vitro amplification of nucleic acids by a multienzyme reaction modeled after retroviral replication. *Proceedings of the National Academy of Sciences*, 1990, **87**(5): 1874-1878.
191. Walker, G. T., Fraiser, M. S., Schram, J. L., Little, M. C., Nadeau, J. G., Malinowski, D. P., Strand displacement amplification - an isothermal, in vitro DNA amplification technique. *Nucleic Acids Research*, 1992, **20**(7): 1691-1696.
192. Walker, G. T., Little, M. C., Nadeau, J. G., Shank, D. D., Isothermal in vitro amplification of DNA by a restriction enzyme/DNA polymerase system. *Proceedings of the National Academy of Sciences*, 1992, **89**(1): 392-396.
193. Liu, D., Daubendiek, S. L., Zillman, M. A., Ryan, K., Kool, E. T., Rolling circle DNA synthesis: small circular oligonucleotides as efficient templates for DNA polymerases. *Journal of the American Chemical Society*, 1996, **118**(7): 1587-1594.
194. Asiello, P. J., Baeumner, A. J., Miniaturized isothermal nucleic acid amplification, a review. *Lab on a Chip*, 2011, **11**(8): 1420-1430.
195. Demidov, V. V., A new use for old stuff: DNA hairpins in DNA amplification. *Trends in Biotechnology*, 2002, **20**(15): 189-190.
196. Auroux, P. A., Koc, Y., deMello, A., Manz, A., Day, P. J. R., Miniaturised nucleic acid analysis. *Lab on a Chip*, 2004, **4**(6): 534-546.
197. Hopwood, A. J., Hurth, C., Yang, J., Cai, Z., Moran, N., Lee-Edghill, J. G., Nordquist, A., Lenigk, R., Estes, M. D., Haley, J. P., McAlister, C. R., Chen, X., Brooks, C., Smith, S., Elliott, K., Koumi, P., Zenhausem, F., Tully, G., Integrated microfluidic system for rapid forensic DNA analysis: sample collection to DNA profile. *Analytical Chemistry*, 2010, **82**(16): 6991-6999.
198. Nge, P. N., Rogers, C. I., Woolley, A. T., Advances in microfluidic materials, functions, integration, and applications. *Chemical Reviews*, 2013, **113**(4): 2550-2583.
199. Wen, J., Guillo, C., Ferrance, J. P., Landers, J. P., Microfluidic-based DNA purification in a two-stage, dual-phase microchip containing a reversed-phase and a photopolymerized monolith. *Analytical Chemistry*, 2007, **79**(16): 6135-6142.
200. Reedy, C. R., Price, C. W., Sniegowski, J., Ferrance, J. P., Begley, M., Landers, J. P., Solid phase extraction of DNA from biological samples in a post-based, high surface area poly(methyl methacrylate) (PMMA) microdevice. *Lab on a Chip*, 2011, **11**(9): 1603-1611.

201. Nakagawa, T., Tanaka, T., Niwa, D., Osaka, T., Takeyama, H., Matsunaga, T., Fabrication of amino silane-coated microchip for DNA extraction from whole blood. *Journal of Biotechnology*, 2005, **116**(2): 105-111.
202. Cao, W., Easley, C. J., Ferrance, J. P., Landers, J. P., Chitosan as a polymer for pH-induced DNA capture in a totally aqueous system. *Analytical Chemistry*, 2006, **78**(20): 7222-7228.
203. Parton, J., Birch, C., Kemp, C., Haswell, S. J., Pamme, N., Shaw, K. J., Integrated DNA extraction and amplification using electrokinetic pumping in a microfluidic device. *Analytical Methods*, 2012, **4**(1): 96-100.
204. Mao, H.-Q., Roy, K., Troung-Le, V. L., Janes, K. A., Lin, K. Y., Wang, Y., August, J. T., Leong, K. W., Chitosan-DNA nanoparticles as gene carriers: synthesis, characterization and transfection efficiency. *Journal of Controlled Release*, 2001, **70**(3): 399-421.
205. Bozkir, A., Saka, O. M., Chitosan nanoparticles for plasmid DNA delivery: effect of chitosan molecular structure on formulation and release characteristics. *Drug Delivery*, 2004, **11**(2): 107-112.
206. Wang, K., Liu, Q., Chemical structure analyses of phosphorylated chitosan. *Carbohydrate Research*, 2014, **386**(0): 48-56.
207. Nakashima, K., High-performance liquid chromatographic analysis of drugs of abuse in biologic samples. *Journal of Health Science*, 2005, **51**(3): 272-277.
208. *United Nations Office on Drugs and Crime (UNODC)*. United Nations Publications: New York, 2012.
209. Kintz, P., Villain, M., Dumestre-Toulet, V., Capolaghi, B., Cirimele, V., Methadone as a chemical weapon: two fatal cases involving babies. *Therapeutic Drug Monitoring*, 2005, **27**(6): 741-743.
210. Trujols, J., Solà, I., Iraurgi, I., de los Cobos, J. P., Contextualizing methadone-related deaths: failure to contextualize may be considered a weapon against public health. *Therapeutic Drug Monitoring*, 2006, **28**(5): 712-713.
211. *Terminology and Information on Drugs*. United Nations Publications: New York, 2003.
212. Moffat, A. C., Osselton, D., Widdop, B., Clarke, E. G. C., *Clarke's analysis of drugs and poisons: in pharmaceuticals, body fluids and postmortem material*. Third edition. Pharmaceutical Press: London, 2004.
213. Nakahara, Y., Detection and diagnostic interpretation of amphetamines in hair. *Forensic Science International*, 1995, **70**(1-3): 135-153.
214. Chung, L.-W., Liu, G.-J., Li, Z.-G., Chang, Y.-Z., Lee, M.-R., Solvent-enhanced microwave-assisted derivatization following solid-phase extraction combined with gas chromatography-mass spectrometry for determination of amphetamines in urine. *Journal of Chromatography B*, 2008, **874**(1-2): 115-118.

215. Oyler, J. M., Cone, E. J., Joseph, R. E., Jr., Moolchan, E. T., Huestis, M. A., Duration of detectable methamphetamine and amphetamine excretion in urine after controlled oral administration of methamphetamine to humans. *Clinical Chemistry*, 2002, **48**(10): 1703-1714.
216. Lledo-Fernandez, C., Banks, C. E., An overview of quantifying and screening drugs of abuse in biological samples: past and present. *Analytical Methods*, 2011, **3**(6): 1227-1245.
217. *European Monitoring Centre for Drugs and Drug Addiction. Annual Report*. Publications Office of the European Union, Luxembourg, 2013.
218. Beckett, A. H., Rowland, M., Urinary excretion kinetics of methylamphetamine in man. *Journal of Pharmacy and Pharmacology*, 1965, **17**(S1): 109-114.
219. Okajima, K., Namera, A., Yashiki, M., Tsukue, I., Kojima, T., Highly sensitive analysis of methamphetamine and amphetamine in human whole blood using headspace solid-phase microextraction and gas chromatography-mass spectrometry. *Forensic Science International*, 2001, **116**(1): 15-22.
220. Brecht, M.-L., Herbeck, D. M., Methamphetamine use and violent behavior: user perceptions and predictors. *Journal of Drug Issues*, 2013, **43**(4): 468-482.
221. Lin, Y. H., Lee, M. R., Lee, R. J., Ko, W. K., Wu, S. M., Hair analysis for methamphetamine, ketamine, morphine and codeine by cation-selective exhaustive injection and sweeping micellar electrokinetic chromatography. *Journal of Chromatography A*, 2007, **1145**(1-2): 234-240.
222. Verstraete, A. G., Detection times of drugs of abuse in blood, urine, and oral fluid. *Therapeutic Drug Monitoring*, 2004, **26**(2): 200-205.
223. Schepers, R. J. F., Oyler, J. M., Joseph, R. E., Cone, E. J., Moolchan, E. T., Huestis, M. A., Methamphetamine and amphetamine pharmacokinetics in oral fluid and plasma after controlled oral methamphetamine administration to human volunteers. *Clinical Chemistry*, 2003, **49**(1): 121-132.
224. Ray, E., *Immunodiagnosics: a practical approach*. Oxford University Press: New York, 1999.
225. Xiang, Y., Lu, Y., Portable and quantitative detection of protein biomarkers and small molecular toxins using antibodies and ubiquitous personal glucose meters. *Analytical Chemistry*, 2012, **84**(9): 4174-4178.
226. Botchkareva, A. E., Eremin, S. A., Montoya, A., Manclús, J. J., Mickova, B., Rauch, P., Fini, F., Girotti, S., Development of chemiluminescent ELISAs to DDT and its metabolites in food and environmental samples. *Journal of Immunological Methods*, 2003, **283**(1-2): 45-57.
227. Sun, J. W., Zhang, Y., Wang, S., Development of chemiluminescence enzyme-linked immunosorbent assay for the screening of metolcarb and carbaryl in orange juice, cabbage and cucumber. *Food Additives and Contaminants*, 2010, **27**(3): 338-346.

228. Greenway, G. M., Nelstrop, L. J., Port, S. N., Tris(2,2-bipyridyl)ruthenium (II) chemiluminescence in a microflow injection system for codeine determination. *Analytica Chimica Acta*, 2000, **405**(1-2): 43-50.
229. Far, H. R. M., Torabi, F., Danielsson, B., Khayyami, M., ELISA on a microchip with a photodiode for detection of amphetamine in plasma and urine. *Journal of Analytical Toxicology*, 2005, **29**(8): 790-793.
230. Jones, A. W., Karlsson, L., Relation between blood- and urine-amphetamine concentrations in impaired drivers as influenced by urinary pH and creatinine. *Human & Experimental Toxicology*, 2005, **24**(12): 615-622.
231. Drummer, O. H., Requirements for bioanalytical procedures in postmortem toxicology. *Analytical and Bioanalytical Chemistry*, 2007, **388**(7): 1495-1503.
232. Kokosa, J. M., Advances in solvent-microextraction techniques. *TrAC Trends in Analytical Chemistry*, 2013, **43**(0): 2-13.
233. Nakamoto, A., Nishida, M., Saito, T., Kishiyama, I., Miyazaki, S., Murakami, K., Nagao, M., Namura, A., Monolithic silica spin column extraction and simultaneous derivatization of amphetamines and 3,4-methylenedioxyamphetamines in human urine for gas chromatographic-mass spectrometric detection. *Analytica Chimica Acta*, 2010, **661**(1): 42-46.
234. Zhang, Y., Xie, W., Chen, C., Lin, L., Rapid screening for 61 central nervous system drugs in plasma using weak cation exchange solid-phase extraction and high performance liquid chromatography with diode array detection. *African Journal of Pharmacy and Pharmacology*, 2011, **5**(6): 706-720.
235. Nema, T., Chan, E. C. Y., Ho, P. C., Efficiency of a miniaturized silica monolithic cartridge in reducing matrix ions as demonstrated in the simultaneous extraction of morphine and codeine from urine samples for quantification with liquid chromatography-tandem mass spectrometry (LC-MS/MS). *Journal of Mass Spectrometry*, 2011, **46**(9): 891-900.
236. Nema, T., Chan, E. C. Y., Ho, P. C., Extraction of ketamine from urine using a miniature silica monolithic cartridge followed by quantification with liquid chromatography tandem mass spectrometry (LC-MS/MS). *Journal of Separation Science*, 2011, **34**(9): 1041-1046.
237. Lee, M.-R., Yu, S.-C., Lin, C.-L., Yeh, Y.-C., Chen, Y.-L., Hu, S.-H., Solid-phase extraction in amphetamine and methamphetamine analysis of urine. *Journal of Analytical Toxicology*, 1997, **21**(4): 278-282.
238. Berlardi, R., Pawliszyn, J., The application of chemically modified fused silica fibers in the extraction of organics from water matrix samples and their rapid transfer to capillary columns. *Water Pollution Research Journal of Canada*, 1989, **24**(1): 179.
239. Namera, A., Nakamoto, A., Nishida, M., Yashiki, M., Kuramoto, T., Takei, Y., Furuno, M., Minakuchi, H., Nakanishi, K., Kimura, K., Monolithic silica capillary column as a new tool for extraction of methamphetamine in urine. *Japanese Journal of Forensic Toxicology*, 2004, **22**(3): 200-204.

240. Kumazawa, T., Hasegawa, C., Lee, X.-P., Hara, K., Seno, H., Suzuki, O., Sato, K., Simultaneous determination of methamphetamine and amphetamine in human urine using pipette tip solid-phase extraction and gas chromatography-mass spectrometry. *Journal of Pharmaceutical and Biomedical Analysis*, 2007, **44**(2): 602-607.
241. Watts, P., Haswell, S. J., The application of micro reactors for organic synthesis. *Chemical Society Reviews*, 2005, **34**(3): 235-246.
242. Qiagen, QIAamp[®] DNA mini and blood mini handbook. Third edition. 2010.
243. Breadmore, M. C., Wolfe, K. A., Arcibal, I. G., Leung, W. K., Dickson, D., Giordano, B. C., Power, M. E., Ferrance, J. P., Feldman, S. H., Norris, P. M., Landers, J. P., Microchip-based purification of DNA from biological samples. *Analytical Chemistry*, 2003, **75**(8): 1880-1886.
244. Ahn, S. J., Costa, J., Rettig Emanuel, J., PicoGreen quantitation of DNA: effective evaluation of samples pre- or post-PCR. *Nucleic Acids Research*, 1996, **24**(13): 2623-2625.
245. Huang, G., Lian, Q., Zeng, W., Xie, Z., Preparation and evaluation of a lysine-bonded silica monolith as polar stationary phase for hydrophilic interaction pressurized capillary electrochromatography. *Electrophoresis*, 2008, **29**(18): 3896-3904.
246. Cheong, G. W. K. a. W. J., Open tubular monolith formation and C18 ligand immobilization in silica capillary by microwave heating for capillary electrochromatography. *Bulletin of the Korean Chemical Society*, 2006, **27**(9): 1459-1462.
247. Musshoff, F., Madea, B., New trends in hair analysis and scientific demands on validation and technical notes. *Forensic Science International*, 2007, **165**(2-3): 204-215.
248. Peters, F. T., Drummer, O. H., Musshoff, F., Validation of new methods. *Forensic Science International*, 2007, **165**(2-3): 216-224.
249. *Guidance for the validation of analytical methodology and calibration of equipment used for testing of illicit drugs in seized materials and biological specimens*. United Nations Office on Drugs and Crime: New York, 2009.
250. Peters, F. T., Stability of analytes in biosamples - an important issue in clinical and forensic toxicology? *Analytical and Bioanalytical Chemistry*, 2007, **388**(7): 1505-1519.
251. *Validation of analytical methods: definitions and terminology ICH Q2 A*. International Conference on Harmonization (ICH): London, 1994.
252. Taverniers, I., De Loose, M., Van Bockstaele, E., Trends in quality in the analytical laboratory. II. Analytical method validation and quality assurance. *TrAC Trends in Analytical Chemistry*, 2004, **23**(8): 535-552.

253. Miller, J., Miller, J. C., *Statistics and chemometrics for analytical chemistry*. Pearson Prentice Hall: Harlow, England, 2010.
254. Peters, F. T., Maurer, H. H., Bioanalytical method validation and its implications for forensic and clinical toxicology - a review. *Accreditation and Quality Assurance*, 2002, **7**(11): 441-449.
255. Wille, S. R., Peters, F., Fazio, V., Samyn, N., Practical aspects concerning validation and quality control for forensic and clinical bioanalytical quantitative methods. *Accreditation and Quality Assurance*, 2011, **16**(6): 279-292.
256. Cao, W., Gerhardt, R., Wachtman, J. B., Preparation and sintering of colloidal silica-potassium silicate gels. *Journal of the American Ceramic Society*, 1988, **71**(12): 1108-1113.
257. Qu, Q., Tang, X., Wang, C., Yang, G., Hu, X., Lu, X., Liu, Y., Yan, C., Preparation of particle-fixed silica monoliths used in capillary electrochromatography. *Journal of Separation Science*, 2006, **29**(13): 2098-2102.
258. Yun, S.-S., Yoon, S. Y., Song, M.-K., Im, S.-H., Kim, S., Lee, J.-H., Yang, S., Handheld mechanical cell lysis chip with ultra-sharp silicon nano-blade arrays for rapid intracellular protein extraction. *Lab on a Chip*, 2010, **10**(11): 1442-1446.
259. Ramadan, Q., Samper, V., Poenar, D., Liang, Z., Yu, C., Lim, T. M., Simultaneous cell lysis and bead trapping in a continuous flow microfluidic device. *Sensors and Actuators B: Chemical*, 2006, **113**(2): 944-955.
260. Chen, X., Cui, D., Liu, C., Cai, H., Microfluidic biochip for blood cell lysis. *Chinese Journal of Analytical Chemistry*, 2006, **34**(11): 1656-1660.
261. Carlo, D. D., Jeong, K.-H., Lee, L. P., Reagentless mechanical cell lysis by nanoscale barbs in microchannels for sample preparation. *Lab on a Chip*, 2003, **3**(4): 287-291.
262. Schiffner, L. A., Bajda, E. J., Prinz, M., Sebestyén, J., Shaler, R., Caragine, T. A., Optimization of a simple, automatable extraction method to recover sufficient DNA from low copy number DNA samples for generation of short tandem repeat profiles. *Croatian Medical Journal.*, 2005, **46**(4): 578-586.
263. Heath, E. M., Morken, N. W., Campbell, K. A., Tkach, D., Boyd, E. A., Strom, D. A., Use of buccal cells collected in mouthwash as a source of DNA for clinical testing. *Archives of Pathology & Laboratory Medicine*, 2001, **125**(1): 127-133.
264. Kashkary, L., Kemp, C., Shaw, K. J., Greenway, G. M., Haswell, S. J., Improved DNA extraction efficiency from low level cell numbers using a silica monolith based micro fluidic device. *Analytica Chimica Acta*, 2012, **750**(0): 127-131.

265. Reedy, C. R., Bienvenue, J. M., Coletta, L., Strachan, B. C., Bhatni, N., Greenspoon, S., Landers, J. P., Volume reduction solid phase extraction of DNA from dilute, large-volume biological samples. *Forensic Science International: Genetics*, 2010, **4**(3): 206-212.
266. Kishore, R., Reef Hardy, W., Anderson, V. J., Sanchez, N. A., Buoncristiani, M. R., Optimization of DNA extraction from low-yield and degraded samples using the BioRobot® EZ1 and BioRobot® M48. *Journal of Forensic Sciences*, 2006, **51**(5): 1055-1061.
267. Parton, J., Abu-Mandil Hassan, N., Brown, T. A., Haswell, S. J., Brown, K. A., Shaw, K. J., Sex identification of ancient DNA samples using a microfluidic device. *Journal of Archaeological Science*, 2013, **40**(1): 705-711.
268. Alonso, A., DNA extraction and quantification. In *Encyclopedia of forensic sciences*, Second edition. Siegel, J. A., Saukko, P. J., Houck, M. M., Academic Press: Waltham, 2013, pp. 214-218.
269. Kim, J., Hilton, J. P., Yang, K.-A., Pei, R., Stojanovic, M., Lin, Q., Nucleic acid isolation and enrichment on a microchip. *Sensors and Actuators A: Physical*, 2013, **195**(0): 183-190.
270. Yeung, S. W., Hsing, I. M., Manipulation and extraction of genomic DNA from cell lysate by functionalized magnetic particles for lab on a chip applications. *Biosensors and Bioelectronics*, 2006, **21**(7): 989-997.
271. Legler, T. J., Liu, Z., Heermann, K.-H., Hempel, M., Gutensohn, K., Kiesewetter, H., Pruss, A., Specific magnetic bead-based capture of free fetal DNA from maternal plasma. *Transfusion and Apheresis Science*, 2009, **40**(3): 153-157.
272. Teixeira, H., Verstraete, A., Proença, P., Corte-Real, F., Monsanto, P., Vieira, D. N., Validated method for the simultaneous determination of Δ^9 -THC and Δ^9 -THC-COOH in oral fluid, urine and whole blood using solid-phase extraction and liquid chromatography-mass spectrometry with electrospray ionization. *Forensic Science International*, 2007, **170**(2-3): 148-155.
273. Nestić, M., Babić, S., Pavlović, D. M., Sutlović, D., Molecularly imprinted solid phase extraction for simultaneous determination of Δ^9 -tetrahydrocannabinol and its main metabolites by gas chromatography-mass spectrometry in urine samples. *Forensic Science International*, 2013, **231**(1-3): 317-324.
274. Antelo-Domínguez, Á., Ángel Cocho, J., Jesús Tabernero, M., María Bermejo, A., Bermejo-Barrera, P., Moreda-Piñeiro, A., Simultaneous determination of cocaine and opiates in dried blood spots by electrospray ionization tandem mass spectrometry. *Talanta*, 2013, **117**(0): 235-241.
275. Wang, R., Wang, X., Liang, C., Ni, C., Xiong, L., Rao, Y., Zhang, Y., Direct determination of diazepam and its glucuronide metabolites in human whole blood by μ Elution solid-phase extraction and liquid chromatography-tandem mass spectrometry. *Forensic Science International*, 2013, **233**(1-3): 304-311.

276. Kaddoumi, A., Kikura-Hanajiri, R., Nakashima, K., High-performance liquid chromatography with fluorescence detection for the simultaneous determination of 3,4-methylenedioxymethamphetamine, methamphetamine and their metabolites in human hair using DIB-Cl as a label. *Biomedical Chromatography*, 2004, **18**(3): 202-204.
277. Seidi, S., Yamini, Y., Baheri, T., Feizbakhsh, R., Electrokinetic extraction on artificial liquid membranes of amphetamine-type stimulants from urine samples followed by high performance liquid chromatography analysis. *Journal of Chromatography A*, 2011, **1218**(26): 3958-3965.
278. Elliott, S. P., Hale, K. A., Applications of an HPLC-DAD drug-screening system based on retention indices and UV spectra. *Journal of Analytical Toxicology*, 1998, **22**(4): 279-289.
279. Moeller, M. R., Steinmeyer, S., Kraemer, T., Determination of drugs of abuse in blood. *Journal of Chromatography B: Biomedical Sciences and Applications*, 1998, **713**(1): 91-109.
280. Lee, M. R., Yu, S. C., Lin, C. L., Yeh, Y. C., Chen, Y. L., Hu, S. H., Solid-phase extraction in amphetamine and methamphetamine analysis of urine. *Journal of Analytical Toxicology*, 1997, **21**(4): 278-282.
281. Sadeghipour, F., Giroud, C., Rivier, L., Veuthey, J. L., Rapid determination of amphetamines by high-performance liquid chromatography with UV detection. *Journal of Chromatography A*, 1997, **761**(1-2): 71-78.
282. Vervoort, R. J. M., Maris, F. A., Hindriks, H., Comparison of high-performance liquid chromatographic methods for the analysis of basic drugs. *Journal of Chromatography A*, 1992, **623**(2): 207-220.
283. Cooper, G., Negrusz, A., *Clarke's analysis of drugs and poisons*. Second edition Pharmaceutical Press: London, 2013.
284. United Nations, *Recommended methods for the identification and analysis of amphetamine, methamphetamine and their ring-substituted analogues in seized materials*. United Nations Office on Drugs and Crime: New York, 2006.
285. Buckenmaier, S. M. C., McCalley, D. V., Euerby, M. R., Overloading study of bases using polymeric RP-HPLC columns as an aid to rationalization of overloading on silica-ODS phases. *Analytical Chemistry*, 2002, **74**(18): 4672-4681.
286. Naidong, W., Bioanalytical liquid chromatography tandem mass spectrometry methods on underivatized silica columns with aqueous/organic mobile phases. *Journal of Chromatography B*, 2003, **796**(2): 209-224.
287. Xiong, J., Chen, J., He, M., Hu, B., Simultaneous quantification of amphetamines, caffeine and ketamine in urine by hollow fiber liquid phase microextraction combined with gas chromatography-flame ionization detector. *Talanta*, 2010, **82**(3): 969-975.

288. Nesterenko, E. P., Nesterenko, P. N., Paull, B., Zwitterionic ion-exchangers in ion chromatography: a review of recent developments. *Analytica Chimica Acta*, 2009, **652** (1-2): 3-21.
289. Nesterenko, P. N., Elefterov, A. I., Tarasenko, D. A., Shpigun, O. A., Selectivity of chemically bonded zwitterion-exchange stationary phases in ion chromatography. *Journal of Chromatography A*, 1995, **706**(1-2): 59-68.
290. Dong, X., Dong, J., Ou, J., Zhu, Y., Zou, H., Capillary electrochromatography with zwitterionic stationary phase on the lysine-bonded poly(glycidyl methacrylate-co-ethylene dimethacrylate) monolithic capillary column. *Electrophoresis*, 2006, **27**(12): 2518-2525.
291. Wade, L. G., *Organic chemistry*. Eighth edition. Pearson Education: London, 2013.
292. Lenza, R. F. S., Vasconcelos, W. L., Preparation of silica by sol-gel method using formamide. *Materials Research*, 2001, **4**: 189-194.
293. White, L. D., Tripp, C. P., Reaction of (3-Aminopropyl)dimethylethoxysilane with amine catalysts on silica surfaces. *Journal of Colloid and Interface Science*, 2000, **232**(2): 400-407.
294. Ma, M., Zhang, Y., Yu, W., Shen, H.-y., Zhang, H.-q., Gu, N., Preparation and characterization of magnetite nanoparticles coated by amino silane. *Colloids and Surfaces A: Physicochemical and Engineering Aspects*, 2003, **212**(2-3): 219-226.
295. Tanaka, T., Sakai, R., Kobayashi, R., Hatakeyama, K., Matsunaga, T., Contributions of phosphate to DNA adsorption/desorption behaviors on aminosilane-modified magnetic nanoparticles. *Langmuir*, 2009, **25**(5): 2956-2961.
296. Yoza, B., Matsumoto, M., Matsunaga, T., DNA extraction using modified bacterial magnetic particles in the presence of amino silane compound. *Journal of Biotechnology*, 2002, **94** (3), 217-224.
297. Nakagawa, T., Hashimoto, R., Maruyama, K., Tanaka, T., Takeyama, H., Matsunaga, T., Capture and release of DNA using aminosilane-modified bacterial magnetic particles for automated detection system of single nucleotide polymorphisms. *Biotechnology and Bioengineering*, 2006, **94**(5): 862-868.
298. Nesterenko, P. N., Kebets, P. A., Ion-exchange properties of silica gel with covalently bonded histidine. *Journal of Analytical Chemistry*, 2007, **62**(1): 2-7.
299. Stoscheck, C. M., Quantitation of protein. In *Methods in enzymology*, First edition. Deutscher, M. P., Academic Press: 1990, Vol. 182, pp. 50-68.
300. Sugrue, E., Nesterenko, P. N., Paull, B., Fast ion chromatography of inorganic anions and cations on a lysine bonded porous silica monolith. *Journal of Chromatography A*, 2005, **1075**(1-2): 167-175.

301. Marko, V., Šoltés, L., Novák, I., Selective solid-phase extraction of basic drugs by C8-silica. Discussion of possible interactions. *Journal of Pharmaceutical and Biomedical Analysis*, 1990, **8**(3): 297-301.
302. Nagae, N., Itoh, H., Nimura, N., Kinoshita, T., Takeuchi, T., Rapid separation of proteins and peptides by reversed-phase microcolumn liquid chromatography. *Journal of Microcolumn Separations*, 1991, **3**(1): 5-9.
303. Huang, T., Geng, T., Sturgis, J., Li, H., Gomez, R., Bashir, R., Bhunia, A. K., Robinson, J. P., Ladisch, M. R., Lysozyme for capture of microorganisms on protein biochips. *Enzyme and Microbial Technology*, 2003, **33**(7): 958-966.
304. Jianzhi, L., Zong, G., Zhang, H. C., *Plug and play information sharing architecture and its application in green supply chain management*. Proceedings of the IEEE International Symposium on Electronics and Environment, May 2002, pp. 157-162.
305. Nakamoto, A., Namera, A., Nishida, M., Yashiki, M., Kuramoto, T., Takei, Y., Furuno, M., Minakuchi, H., Nakanishi, K., Kimura, K., Monolithic silica capillary column extraction of methamphetamine and amphetamine in urine coupled with thin-layer chromatographic detection. *Forensic Toxicology*, 2006, **24**(2): 75-79.
306. Miyazaki, S., Morisato, K., Ishizuka, N., Minakuchi, H., Shintani, Y., Furuno, M., Nakanishi, K., Development of a monolithic silica extraction tip for the analysis of proteins. *Journal of Chromatography A*, 2004, **1043**(1): 19-25.
307. Kuraoka, K., Chujo, Y., Yazawa, T., Hydrocarbon separation via porous glass membranes surface-modified using organosilane compounds. *Journal of Membrane Science*, 2001, **182**(1-2): 139-149.
308. Wang, X., Lin, K. S. K., Chan, J. C. C., Cheng, S., Direct synthesis and catalytic applications of ordered large pore aminopropyl-functionalized SBA-15 mesoporous materials. *The Journal of Physical Chemistry B*, 2005, **109**(5): 1763-1769.
309. Ma, X., Sun, H., Yu, P., A novel way for preparing high surface area silica monolith with bimodal pore structure. *Journal of Materials Science*, 2008, **43**(3): 887-891.
310. Gan, B. K., Baugh, D., Liu, R. H., Walia, A. S., Simultaneous analysis of amphetamine, methamphetamine, and 3, 4-methylenedioxymethamphetamine (MDMA) in urine samples by solid-phase extraction, derivatization, and gas chromatography/mass spectrometry. *Journal of Forensic Sciences*, 1991, **36**(5): 1331-1341.
311. Giordano, B. C., Burgi, D. S., Hart, S. J., Terray, A., On-line sample pre-concentration in microfluidic devices: a review. *Analytica Chimica Acta*, 2012, **718**: 11-24.
312. Khandurina, J., Jacobson, S. C., Waters, L. C., Foote, R. S., Ramsey, J. M., Microfabricated porous membrane structure for sample concentration and electrophoretic analysis. *Analytical Chemistry*, 1999, **71**(9): 1815-1819.

313. Chen, X. H., Wijsbeek, J., Franke, J. P., de Zeeuw, R. A., A single-column procedure on Bond Elut Certify for systematic toxicological analysis of drugs in plasma and urine. *Journal of Forensic Sciences*, 1992, **37**(1): 61-71.
314. Myung, S.-W., Min, H.-K., Kim, S., Kim, M., Cho, J.-B., Taek-Jae, K., Determination of amphetamine, methamphetamine and dimethamphetamine in human urine by solid-phase microextraction (SPME)-gas chromatography/mass spectrometry. *Journal of Chromatography B: Biomedical Sciences and Applications*, 1998, **716**(1-2): 359-365.
315. Namera, A., Yamamoto, S., Saito, T., Miyazaki, S., Oikawa, H., Nakamoto, A., Nagao, M., Simultaneous extraction of acidic and basic drugs from urine using mixed-mode monolithic silica spin column bonded with octadecyl and cation-exchange group. *Journal of Separation Science*, 2011, **34**(16-17): 2232-2239.
316. Chen, X., Cui, D. F., Liu, C. C., On-line cell lysis and DNA extraction on a microfluidic biochip fabricated by microelectromechanical system technology. *Electrophoresis*, 2008, **29**(9): 1844-1851.
317. Kemp, C., Birch, C., Shaw, K. J., Nixon, G. J., Docker, P. T., Greenman, J., Huggett, J. F., Haswell, S. J., Foy, C. A., Dyer, C. E., Direct processing of clinically relevant large volume samples for the detection of sexually transmitted infectious agents from urine on a microfluidic device. *Analytical Methods*, 2012, **4**(7): 2141-2144.
318. Shaw, K. J., Joyce, D. A., Docker, P. T., Dyer, C. E., Greenway, G. M., Greenman, J., Haswell, S. J., Development of a real-world direct interface for integrated DNA extraction and amplification in a microfluidic device. *Lab on a Chip*, 2011, **11**(3): 443-448.
319. Gonzalez-Marino, I., Quintana, J. B., Rodriguez, I., Rodil, R., Gonzalez-Penas, J., Cela, R., Comparison of molecularly imprinted, mixed-mode and hydrophilic balance sorbents performance in the solid-phase extraction of amphetamine drugs from wastewater samples for liquid chromatography-tandem mass spectrometry determination. *Journal of Chromatography. A*, 2009, **1216**(48): 8435-8441.
320. Kuwayama, K., Inoue, H., Kanamori, T., Tsujikawa, K., Miyaguchi, H., Iwata, Y. T., Miyauchi, S., Kamo, N., Analysis of amphetamine-type stimulants and their metabolites in plasma, urine and bile by liquid chromatography with a strong cation-exchange column-tandem mass spectrometry. *Journal of Chromatography B*, 2008, **867**(1): 78-83.
321. Huang, Z., Zhang, S., Confirmation of amphetamine, methamphetamine, MDA and MDMA in urine samples using disk solid-phase extraction and gas chromatography-mass spectrometry after immunoassay screening. *Journal of Chromatography B*, 2003, **792**(2): 241-247.

8 Publications and Presentations

8.1 Journal Articles

L. Kashkary, C. Kemp, K. Shaw, G. M. Greenway and S. J. Haswell, “Improved DNA extraction efficiency from low level cell numbers using a silica monolith based micro fluidic device”, *Analytica Chimica Acta* 2012, **750**, (0), 127-131, doi: 10.1016/j.aca.2012.05.019.

8.2 Oral Presentations

L. Kashkary, G. M. Greenway and S. J. Haswell, “Development of combined drug and DNA extraction methodology for forensic toxicology application”, *Chemistry Colloquium*, University of Hull, UK (2013).

8.3 Poster Presentations

L. Kashkary, G. M. Greenway and S. J. Haswell, “Development of a rapid amphetamines extraction method for low sample volume using a monolithic packed-connector and HPLC with UV detector”, *1st Regional TIAFT Meeting*, Izmir, Turkey (2014).

Poster presentation prize awarded.

L. Kashkary, C. Kemp, K. Shaw, G. M. Greenway and S. J. Haswell, “Improved DNA extraction efficiency from low level cell numbers using a silica monolith based micro fluidic device”, *Analytical Research Forum*, University of Durham, Durham, UK (2012).

L. Kashkary, K. Shaw, G. M. Greenway and S. J. Haswell, “Microfluidic device integrated for DNA extraction and PCR amplification from mixed samples”, *Analytical Research Forum*, University of Loughborough, Loughborough, UK (2010).